

WHEN IS  $2+2 \neq 4$ ? INTERACTIVE PRIMING OF PYROGENIC ORGANIC  
MATTER, SOIL ORGANIC CARBON, AND PLANT ROOTS IN NATURAL AND  
MANAGED ECOSYSTEMS

A Dissertation

Presented to the Faculty of the Graduate School

of Cornell University

In Partial Fulfillment of the Requirements for the Degree of

Doctor of Philosophy

by

Thea Leslie Whitman

August 2014

© 2014 Thea Leslie Whitman

WHEN IS  $2+2 \neq 4$ ? INTERACTIVE PRIMING OF PYROGENIC ORGANIC  
MATTER, SOIL ORGANIC CARBON, AND PLANT ROOTS IN NATURAL AND  
MANAGED ECOSYSTEMS

Thea Leslie Whitman, Ph. D.

Cornell University

Soils hold a globally important stock of carbon (C) and can act as both a C source and sink, depending on management and environmental conditions. Pyrogenic organic matter (PyOM) is produced naturally during fires, and contains relatively stable forms of C. Its intentional production has also been proposed as a mechanism for C management (in such cases PyOM is often referred to as “biochar”). However, the impact of natural or anthropogenic PyOM production on soils is complex and depends on many factors. In particular, the effects of PyOM on existing soil organic C (SOC) dynamics is poorly characterized or understood. Understanding the mechanisms behind these interactions, often referred to as “priming”, is essential to predict the impact of PyOM additions to soils. In a greenhouse study, PyOM additions counteracted positive priming of SOC by corn plants, almost completely eliminating net C losses either by decreasing SOC decomposition or increasing corn C additions to soil. This highlights the importance of including plants in studies of PyOM-SOC interactions. In an incubation trial, the relative mineralizability of PyOM as compared to SOC predicted priming interactions, where the soil with lower SOC mineralization was more susceptible to short-term increases in SOC mineralization with PyOM

additions, which were proportional to the C mineralization in the added PyOM. Soils also experienced net long-term decreases in SOC mineralization with PyOM additions, possibly due to stabilization of SOC on PyOM surfaces, an example of which we imaged using nanoscale secondary ion mass spectrometry. In a field trial, PyOM additions temporarily increased total soil CO<sub>2</sub> fluxes, dramatically less than the addition of fresh corn stover, which likely increased SOC mineralization. Three-part stable isotopic partitioning revealed significantly greater root-derived CO<sub>2</sub> fluxes with PyOM additions than without, and significantly lower PyOM-C derived CO<sub>2</sub> fluxes when plants were present. PyOM additions only resulted in significant changes to the soil microbial community on day 79, while stover additions induced shifts by day 11. This work informs our understanding of PyOM-soil-plant-microbe interactions and contributes to progress toward a comprehensive predictive framework of PyOM effects on C cycling in soils.

## BIOGRAPHICAL SKETCH

Thea Leslie Whitman grew up in White Rock, Nova Scotia, Canada with her mother and father, brother, and two sisters. She attended Gaspereau Elementary School, Wolfville Junior High, and Horton High School. She earned a B.Sc. in Environmental Biology at Queen's University in Kingston, Ontario, where she spent one year abroad studying at Leeds University in the U.K. and earned the subject medal in Environmental Studies. She began her studies at Cornell in 2008, during which she was awarded the Barbara McClintock, Macdonald-Musgrave, and Outstanding TA awards. She completed an M.S. in Soil Science in 2010 and attended the Marine Biological Laboratory's Microbial Diversity training course in Woods Hole in 2012. Upon completing her Ph.D., she will take up a postdoctoral position at the University of California, Berkeley, after which she will join the University of Wisconsin-Madison Soil Science department as a tenure-track assistant professor of soil ecology.

## ACKNOWLEDGMENTS

I would like to thank the Natural Sciences and Engineering Research Council of Canada for financial support throughout this research. I would also like to thank Cornell's Atkinson Center for a Sustainable Future and the various forms of the Biogeochemistry and Environmental Biocomplexity / Biogeochemistry, Environmental Science, and Sustainability / Cross-Scale Biogeochemistry and Climate group, for providing both a vibrant intellectual community and also key grants for the research in each chapter of this dissertation. I am grateful to the Toward Sustainability Foundation, which supported my first foray into microbial community analyses. Additionally, funding from the Cornell Graduate School, NSF, Sigma Xi Cornell, and Cornell Mellon grants helped to make this work possible. The Crop and Soil Science department has also been a key supporter during my time at Cornell, both financially and as a community, for which I am thankful. Thanks to the Canadian Soil Science Society, the Soil Science Society of America, the American Geophysical Union, the American Society of Microbiology, the International Biochar Initiative, and the Soil Ecology Society for providing robust intellectual communities and many opportunities and funding to present my research findings.

My major advisor, Dr. Johannes Lehmann, and minor advisors, Dr. Daniel Buckley and Dr. Christine Goodale, were invaluable for their support and inspiration throughout this work and I thank them wholeheartedly for their encouragement and advice. Many thanks go to my lab group, particularly Akio Enders and Kelly Handley for their endless assistance in the lab, greenhouse, and field. Thanks to Joe Yavitt and Tim Fahey for generously allowing access to the  $^{13}\text{C}$ -labelled maple twigs which made much of this research possible, and to Alexis Heinz for laboratory support with  $\text{CO}_2$

analyses. Kim and Jed Sparks and the Cornell Stable Isotope Laboratory were very helpful assisting with methods development, sample analyses, and generously loaned CO<sub>2</sub> measuring equipment for the field trial. Thanks also to Nick Nickerson of Forerunner Research for helpful advice and suggestions about chamber and <sup>13</sup>CO<sub>2</sub> sampling design in the greenhouse and field trials. Thanks to Dr. Daniel Buckley, Dr. Janice Thies, Dr. Charles Pepe-Ranney, Ashley Campbell, and Chantal Koechli for their support with microbial lab and bioinformatics work. Thanks to Dr. Zihua Zhu at the Pacific Northwest National Lab's Environmental Molecular Sciences Laboratory for collaborating on the nanoSIMS analyses. Thanks also to a number of anonymous reviewers whose comments on the published portions of this dissertation helped improve the manuscript. Finally, I would like to thank my friends and family for their support throughout my dissertation and time here in Ithaca.

## TABLE OF CONTENTS

BIOGRAPHICAL SKETCH	v
ACKNOWLEDGEMENTS	vi
LIST OF FIGURES	x
LIST OF TABLES	xi
CHAPTER 1. PRIMING EFFECTS IN BIOCHAR-AMENDED SOILS: IMPLICATIONS OF BIOCHAR-SOIL ORGANIC MATTER INTERACTIONS FOR CARBON STORAGE	1
1.1 <i>Introduction to biochar - soil organic matter cycling interactions</i>	1
1.2 <i>“Priming”: biochar interactions with SOM</i>	2
1.3 <i>Trends and mechanisms for changes in native SOC mineralization with biochar additions</i>	4
1.4 <i>Mechanisms by which soil organic matter may affect biochar C turnover</i>	26
1.5 <i>Effect of plant roots on SOC-biochar interactions</i>	30
1.6 <i>Multiple mechanisms likely act simultaneously and may affect microbial communities</i>	32
1.7 <i>Methods and approaches to studying biochar-SOM interactions</i>	33
1.8 <i>Implications of SOC-biochar interactions for soil C and fertility management</i>	39
1.9 <i>Future directions</i>	41
<i>Supplementary information for Chapter One</i>	44
1.S1 <i>Notes on the properties of biochars</i>	44
1.S2 <i>Notes on using C isotopes to partition three-part systems</i>	44
1.S3 <i>Notes on C debt-credit ratio in different “priming” scenarios</i>	47
<i>References</i>	50
CHAPTER 2. PYROGENIC CARBON ADDITIONS TO SOIL COUNTERACT POSITIVE PRIMING OF SOIL CARBON DECOMPOSITION BY PLANTS	40
2.1 <i>Introduction</i>	57
2.2 <i>Materials and methods</i>	61
2.3 <i>Results</i>	70
2.4 <i>Discussion</i>	78
<i>Supplementary information for Chapter Two</i>	87
2.S1 <i>Details on isotopic partitioning</i>	87
2.S2 <i>Notes on the challenges of applying isotopic partitioning</i>	88
<i>References</i>	92
CHAPTER 3. RELATIVE CARBON MINERALIZABILITY DETERMINES INTERACTIVE PRIMING BETWEEN PYROGENIC ORGANIC MATTER AND SOIL ORGANIC CARBON	96
3.1 <i>Introduction</i>	97
3.2 <i>Materials and methods</i>	100
3.3 <i>Results</i>	110
3.4 <i>Discussion</i>	118
<i>Supplementary information for Chapter Three</i>	126
3.S1 <i>Notes on standard curve application</i>	126

3.S2 Nutrient addition experiment	126
3.S3 Determining $\delta^{13}\text{C}$ values of PyOM and SOC end-members	127
References	137
CHAPTER 4. PYROGENIC ORGANIC MATTER, SOIL ORGANIC MATTER, AND PLANT ROOT INTERACTIONS DETERMINED USING THREE-PART PARTITIONING WITH STABLE C ISOTOPES AND MICROBIAL COMMUNITY ANALYSIS	139
4.1 Introduction	140
4.2 Materials and methods	143
4.3 Results	156
4.4 Discussion	165
Supplementary information for Chapter Four	173
4.S1 Iso-FD chambers	173
References	177
APPENDIX 1.1 PRIMARY DATA FOR CHAPTER 2	
APPENDIX 1.2 PRIMARY DATA FOR CHAPTER 3	
APPENDIX 1.3 PRIMARY DATA FOR CHAPTER 4	

## LIST OF FIGURES

Figure 1.1. Schematic of positive and negative priming of soil organic matter by biochar	3
Figure 1.2. Net biochar effect on native SOC mineralization vs. total duration of study	6
Figure 1.3 Net biochar effect on native SOC mineralization vs. total fraction of added biochar mineralized	12
Figure 1.4 Illustration of two ways by which biochar additions could increase SOC mineralization or induce “apparent priming”	14
Figure 1.5 Illustration of three mechanisms by which biochar additions may decrease SOC mineralization	20
Figure 1.6 Illustration of two possible effects of root-derived C on SOC and biochar-C mineralization	31
Figure 1.S1 Graphic concept of multiple isotopic partitioning solutions to a hypothetical three-part system	46
Figure 1.S2 Conceptualization of the comparative effects of biochar characteristics and priming on total C sequestered in the soil over time	48
Figure 2.1. Emissions rate over time	71
Figure 2.2. Fraction of CO <sub>2</sub> emissions from SOC in soils with PyOM predicted under a no-priming scenario and actual fraction on days 1 and 8	75
Figure 2.3. $\delta^{13}\text{C}$ values of DOC and SOC at the end of the experiment	76
Figure 2.4 Total final C stocks after $^{13}\text{C}$ partitioning	77
Figure 2.S1 Pot and chamber design	89
Figure 2.S2 Biomass production with and without PyOM additions	89
Figure 2.S3 Comparison of $\delta^{13}\text{C}$ values for labelled and unlabelled sugar maple PyOM and sub-components, including original materials	90
Figure 3.1 Cumulative mean C mineralization over time	111
Figure 3.2 Mean cumulative relative effect of PyOM additions on SOC mineralization over time	112
Figure 3.3 Cumulative mean relative effect of SOC on PyOM-C mineralization	114
Figure 3.4 Relationships between SOC mineralized and PyOM-C mineralized over the first day of incubation	115
Figure 3.5 Relationship between SOC mineralized and PyOM-C mineralized in the first two days across soil pre-incubations of 1, 10, 20 and 180 d	116
Figure 3.6 Effect of pre-incubation duration on relative effect of PyOM on SOC mineralization	117
Figure 3.7 Calculated image of $^{15}\text{N}/^{14}\text{N}$ ratio across a 30 x 30 $\mu\text{m}$ region of selected incubated PyOM particle	118
Figure 3.S1 Gleying in aggregates within the 6-month pre-incubated soil	131
Figure 3.S2 Iterative adjustments of $\delta^{13}\text{C}$ of mineralized PyOM to calculate the correct $\delta^{13}\text{C}$ value for a mineralized mass of PyOM	132
Figure 3.S3 Effect of mineral N additions on 24-hour SOC mineralization	133
Figure 3.S4 Mean 48-hour SOC mineralization in soils with and without equivalent to those added with the PyOM	134
Figure 3.S5 Increase in Mehlich-III-extractable nutrients with PyOM additions	135

Figure 3.S6 Mean impact of $\text{NH}_4\text{NO}_3$ additions on PyOM-C mineralization rates	136
Figure 4.1 Daily precipitation over duration of experiment and mean soil temperature on measurement days	144
Figure 4.2 Mean $\text{CO}_2$ flux rates	156
Figure 4.3 Rough estimate of cumulative evolved $\text{CO}_2$ , assuming constant flux rates between sampling intervals	157
Figure 4.4 Partitioned $\text{CO}_2$ fluxes on days 12 and 66	158
Figure 4.5 Partitioned final soil C stocks near the beginning (Day 12) and end (Day 82) of trial	159
Figure 4.6 Final mean above-ground dry biomass	160
Figure 4.7 Soil pH at the start and end of the trial with PyOM and stover amendments	161
Figure 4.8 PCoA components 1 (x-axis) and 3 (y-axis) from weighted UniFrac distances between bacterial communities on days 1, 12, and 82	163
Figure 4.9 Fraction of total taxa for top 10 phyla on Day 12	164
Figure 4.10 Fraction of total taxa for top 10 phyla on Day 82	165
Figure 4.S1 Sketch of isotopic forced diffusion chambers from above and below	173
Figure 4.S2 Relative abundance of the top 8 orders in the Acidobacteria phylum on day 12	174
Figure 4.S3 Relative abundance of the top 8 orders in the Acidobacteria phylum on day 82	175

## LIST OF TABLES

Table 1.1. Summary of studies of biochar-soil organic carbon mineralization interactions	7
Table 2.1. Initial soil properties	62
Table 2.2 Initial properties and production conditions of PyOM	63
Table 2.3 Mean $\delta^{13}\text{C}$ signature of SOC proxies.	72
Table 2.4 $\delta^{13}\text{C}$ signature of PyOM components	72
Table 2.5 Mean $\delta^{13}\text{C}$ signature of <i>Zea mays</i> L. components	73
Table 2.S1 Total elemental analysis of Mehlich III extraction	90
Table 2.S2 Modified Hoagland's solution	91
Table 2.S3 Measured $\delta^{13}\text{C}$ proxies for PyOM	91
Table 3.1 Initial soil properties	101
Table 3.2 Production conditions and initial properties for PyOM and after removal and additions of water-extractable compounds	102
Table 3.S1 Nutrient solution for nutrient effect experiment	128
Table 3.S2 Isotopic $\delta^{13}\text{C}$ signatures for PyOM-C for each timepoint and soil-PyOM combination	128
Table 3.S3 Cumulative $\text{CO}_2$ fluxes from soils	129
Table 3.S4 Cumulative $\text{CO}_2$ fluxes from PyOM	130
Table 4.1 Initial PyOM and corn stover properties	148
Table 4.2 Initial soil properties	146
Table 4.3 Percent variation explained by each component for PCoA of weighted UniFrac matrices	162
Table 4.S1 Mean total DNA extracted from soils	176
Table 4.S2 Forward primer (full) sequences	176
Table 4.S3 Reverse primer (full) sequences	176
Table A1.1.1 Final Total Soil C Stocks	180
Table A1.1.2 Final Total Biomass Stocks	181
Table A1.1.3.1 $\text{CO}_2$ flux rates over the course of the trial and mean temperature (Days 1-21)	182
Table A1.1.3.2 $\text{CO}_2$ flux rates over the course of the trial and mean temperature (Days 28-94)	183
Table A1.1.4 Gas samples and information for $^{13}\text{CO}_2$ determination of fluxes, Day 1	184
Table A1.1.5 Gas samples and information for $^{13}\text{CO}_2$ determination of fluxes, Day 8	185
Table A1.2.1 Partitioned $\text{CO}_2$ emissions: SOC-derived $\text{CO}_2$	186
Table A1.2.2 Partitioned $\text{CO}_2$ emissions: PyOM-derived $\text{CO}_2$	187
Table A1.2.3 Total $\text{CO}_2$ emissions	189
Table A1.2.4 $\delta^{13}\text{C}$ values corresponding to total $\text{CO}_2$ emissions in Table A1.2.3	191
Table A1.3.1 $\text{CO}_2$ Fluxes for "A" plots - no amendments - over time ( $\mu\text{mol CO}_2 \text{ m}^{-2} \text{ s}^{-1}$ )	193
Table A1.3.2 $\text{CO}_2$ Fluxes for "B" plots - PyOM additions - over time ( $\mu\text{mol CO}_2 \text{ m}^{-2} \text{ s}^{-1}$ )	194
Table A1.3.3 $\text{CO}_2$ Fluxes for "C" plots - sorghum-sudangrass - over time ( $\mu\text{mol CO}_2 \text{ m}^{-2} \text{ s}^{-1}$ )	195

CO <sub>2</sub> m <sup>-2</sup> s <sup>-1</sup> )	
Table A1.3.4 CO <sub>2</sub> Fluxes for “D” plots - PyOM+sorghum-sudangrass - over time (μmol CO <sub>2</sub> m <sup>-2</sup> s <sup>-1</sup> )	196
Table A1.3.5 CO <sub>2</sub> Fluxes for “E” plots - PyOM+sorghum-sudangrass - over time (μmol CO <sub>2</sub> m <sup>-2</sup> s <sup>-1</sup> )	197
Table A1.3.6 CO <sub>2</sub> Fluxes for “F” plots - fresh corn stover additions - over time (μmol CO <sub>2</sub> m <sup>-2</sup> s <sup>-1</sup> )	198
Table A1.3.7 <sup>13</sup> C signature of fluxes on selected days	199
Table A1.3.8 Final biomass	200
Table A1.3.9 Early and late soil C stocks and associated <sup>13</sup> C	200

## CHAPTER 1

# PRIMING EFFECTS IN BIOCHAR-AMENDED SOILS: IMPLICATIONS OF BIOCHAR-SOIL ORGANIC MATTER INTERACTIONS FOR CARBON STORAGE<sup>1</sup>

### **1.1 Introduction to biochar - soil organic matter cycling interactions**

While understanding of biochar persistence in soil has improved in recent years, the ways in which biochar interacts with non-biochar (native) soil organic matter (SOM) are only beginning to be understood. Research within the last decade has revealed that biochar additions to soil can affect the mineralization of soil organic carbon (SOC). Conversely, the mineralization of biochar in the environment has also been shown to vary with soil type, likely due to the effects of native SOM and other soil properties on the mineralization of biochar. It is important to recognize and study biochar-SOM interactions for a number of reasons. First, these interactions must be understood and quantified so that biochar users or land managers can predict future soil C stocks following biochar amendments, which is particularly important in scenarios where the C impact of biochar application must be properly determined for climate change mitigation purposes. Second, many important properties of soil depend upon the quantity of organic matter (OM) present, including fertility, water holding capacity, and aggregation. Third, any changes in SOC cycling following the addition of biochar will have effects on the cycling of other nutrients

---

<sup>1</sup> Reviewed and accepted for publication as Whitman, T., Singh, B.P., Zimmerman, A., 2014, Chapter 17: Priming Effects in Biochar-Amended Soils: Implications of Biochar-Soil Organic Matter Interactions for Carbon Storage, in: Lehmann, J., Joseph, S. (Eds.) Biochar for Environmental Management: Science, Technology, and Implementation/Adaptation, Second Edition, Earthscan, Sterling, VA.

associated with SOM, including nitrogen (N) and phosphorus (P), possibly altering nutrient availability to soil microbes or plants, nutrient leaching, or gaseous emission rates. Thus, the interactions between biochar and SOM could have a critical effect on most or all of the very benefits one hopes to gain through the application of biochar to soil. Research on biochar-SOM interactions is still growing (*e.g.*, this chapter and its subject are a new addition to the first, 2009, edition of this book). This chapter reviews what is known about biochar-SOM interactions, proposes possible mechanisms for these interactions, and suggests future research directions and approaches.

## **1.2 “Priming”: biochar interactions with SOM**

The term “priming” is commonly used to describe an increase or decrease in mineralization of one source of OM (*e.g.*, native SOM) due to the addition of a new OM source (*e.g.*, biochar, Figure 1.1). The “priming” phenomenon was first identified by Löhnis in 1926, who observed that additions of fresh organic matter, or “green manure”, to soils resulted in the stimulation of N mineralization in existing SOM (Löhnis, 1926). About 30 years later, Bingeman *et al.* (1953) introduced the idea that priming effects could be both positive (mineralization increases) or negative (mineralization decreases). While positive (or negative) priming is most commonly used to refer to the faster (or slower) turnover of SOM in a soil receiving an organic amendment as compared to the turnover of SOM in an untreated soil, in recent years, the term has been applied to extremely diverse phenomena. For example, Kuzyakov *et al.* (2000) defined priming effects as, “[...] strong short-term changes in the turnover of soil organic matter caused by comparatively moderate treatments of the soil. Such treatments might be input of organic or

mineral fertilizer to the soil, exudation of organic substances by roots, mere mechanical treatment of soil, or its drying and rewetting.” Clearly, under such a broad definition, priming almost becomes a synonym for any change in SOM turnover rate induced by an external forcing.

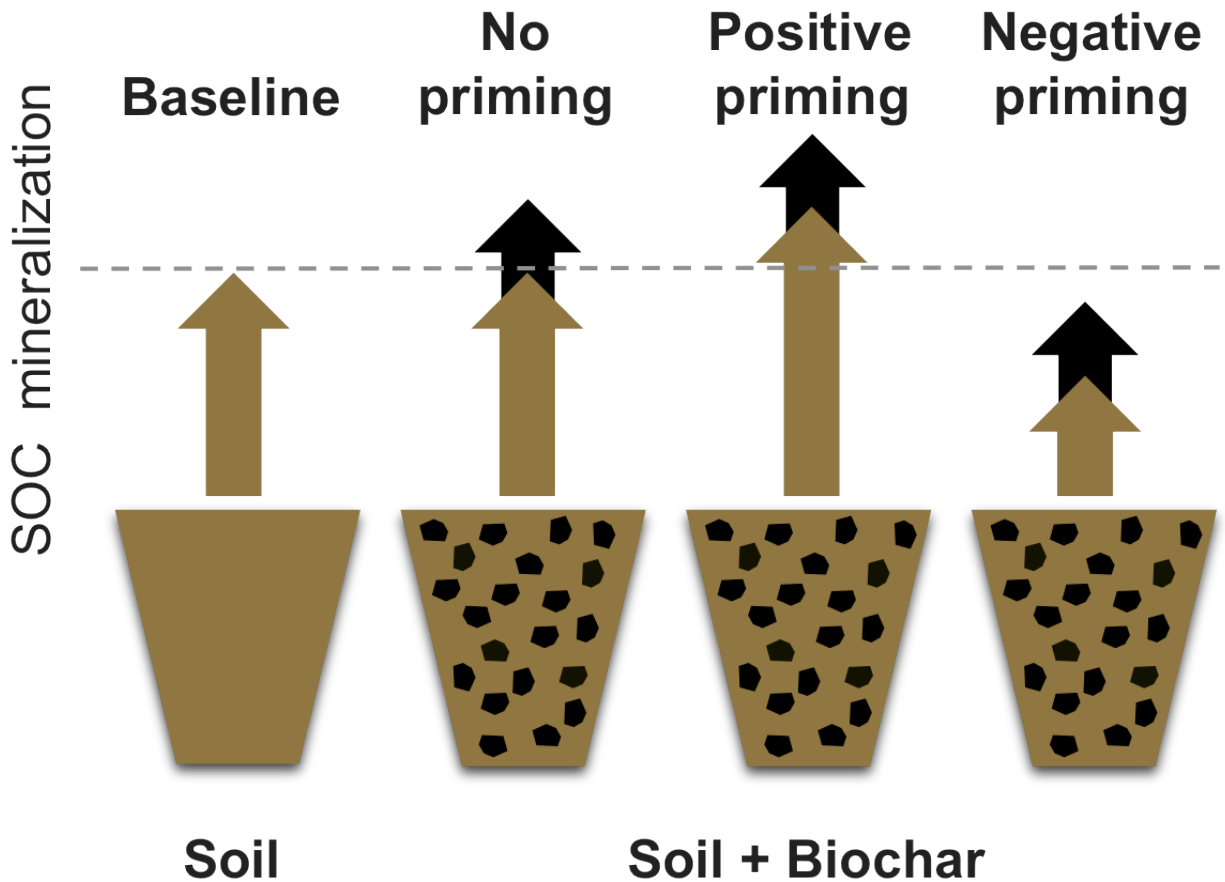


**Figure 1.1** Schematic of positive and negative priming of soil organic matter (SOM) by biochar. The size of the arrows represent the magnitude of C mineralized from SOM (brown) and biochar (black) in soils without (far left) and with (three scenarios on right) biochar additions.

In systems that include biochar, it is now recognized that priming can be interactive - *i.e.*, each C source - biochar and SOM - affects the mineralization of the other (Keith *et al.*, 2011; Zimmerman *et al.*, 2011). Furthermore, both positive and negative priming can occur simultaneously, but may change in relative importance over time (Zimmerman and Gao, 2013),

as observed in laboratory incubation studies (Keith *et al.*, 2011; Zimmerman *et al.*, 2011; Singh and Cowie, 2014). While all the systems discussed in this chapter include native SOM and biochar, systems with other OM inputs, such as fresh plant residues, root exudates or root litter, will also be discussed. Because of the broad and varied meanings assigned to the term “priming” across the literature, for clarity, the terms “increased or decreased decomposition or mineralization” (of SOM or SOC relative to a no-biochar treatment) will be used preferentially.

### **1.3 Trends and mechanisms for changes in native SOC mineralization with biochar additions**

There are diverse mechanisms that may account for increased or decreased mineralization of native SOC following biochar additions. Before discussing these and other effects, the phenomenon known as “apparent priming” should be understood. Blagodatskaya and Kuzyakov (2008) describe apparent priming as an increase in CO<sub>2</sub> evolution from soils due to acceleration of microbial metabolism (or “maintenance respiration”), such as that which might be caused by the addition of nutrients or organic substrates to a system (Figure 1.4). Thus, while microbial C turnover may increase, non-microbial biomass SOC mineralization does not. However, they note that this increased microbial activity may still be accompanied by greater SOC mineralization through increased enzyme production and sustained co-metabolic effects, which would be defined as a “true” priming effect. A coarse indicator of the presence of true priming is that the amount of CO<sub>2</sub> respired is greater than the amount of C present as microbial biomass (Kuzyakov, 2010). By measuring the effect of a substrate on microbial biomass and its contribution to the

microbial C pool, apparent priming can be distinguished from true priming (Paterson and Sim, 2013).

Due to the still limited number of studies and the wide range of systems in terms of soil and biochar types and experimental conditions, it is difficult to conduct a meaningful meta-analysis on the effects of biochar on native SOC mineralization at this point. However, it is possible to point to some broad trends in the results of studies conducted to date. The final timepoint data from 13 biochar-SOM interaction studies were combined to produce figures 1.2 and 1.3, with the criteria for inclusion being that studies conclusively partition SOM and biochar-derived C and have a baseline, no-biochar control treatment. The studies that found the greatest increases in SOC mineralization with biochar additions usually detected these increases during short laboratory incubation periods or during early portions of longer term studies (Luo *et al.*, 2011; Zimmerman *et al.*, 2011; Singh and Cowie, 2014; Farrell *et al.*, 2013) (Figure 1.2).

Some studies have found that increases in native SOC mineralization observed initially diminish with time (Keith *et al.*, 2011; Zimmerman *et al.*, 2011; Singh and Cowie 2014). Still other studies have observed decreases in SOC mineralization with biochar additions (Kuzyakov *et al.*, 2009; Dempster *et al.*, 2011; Keith *et al.*, 2011; Jones *et al.*, 2012; Stewart *et al.*, 2012; Prayogo *et al.*, 2014), and there are some studies that have found that biochar additions decreased SOC mineralization immediately (Cross and Sohi, 2011; Whitman *et al.*, 2014). These immediate decreases may be transient effects, due to a number of possible mechanisms that decrease SOC mineralization discussed below, such as substrate switching or the dilution effect (Singh and Cowie, 2014; Whitman *et al.*, 2014). Finally, many studies have found no significant effect of

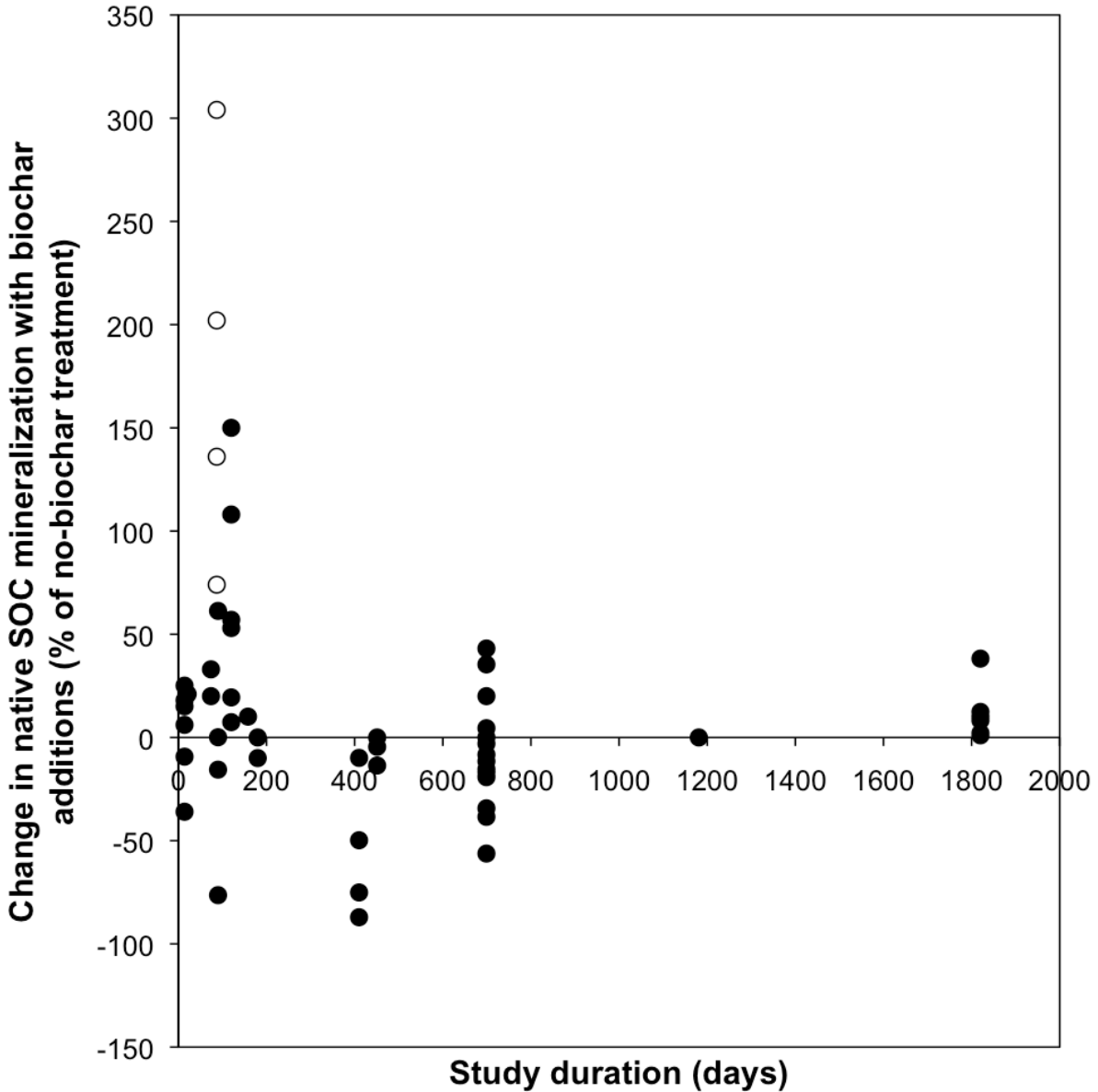


**Figure 1.2** Net biochar effect on native SOC mineralization (relative to the no-biochar control) vs. total duration of study. Data from 13 studies (Kuzyakov *et al.*, 2009; Steinbeiss *et al.*, 2009; Cross and Sohi, 2011; Jones *et al.*, 2011; Keith *et al.*, 2011; Luo *et al.*, 2011; Zimmerman *et al.*, 2011; Bruun and El-Zehery 2012; Santos *et al.*, 2012; Stewart *et al.*, 2012; Farrell *et al.*, 2013; Maestrini *et al.*, 2013; Singh and Cowie, 2014). Open circles indicate data from Luo *et al.*, 2011.

biochar additions on native SOC mineralization (Kuzyakov *et al.*, 2009; Cross and Sohi, 2011; Dempster *et al.*, 2011; Mukome *et al.*, 2013; Prayogo *et al.*, 2014). The widely-ranging results of these previous studies are not necessarily surprising, given the diversity of systems which have been studied. These differences may be due to variations in the proportion of labile C in biochars

(Luo *et al.*, 2011), amount and type of labile OM in soil (Keith *et al.*, 2011), the extent of biochar ageing in soil (Liang *et al.*, 2010; Cross and Sohi, 2011; Zimmerman *et al.*, 2011), and soil type among other factors (see supplementary information on biochar properties 1.S1). This chapter covers the mechanisms that may be driving these diverse effects, with more details from specific studies summarized in Table 1.1. The following discussion of mechanisms of biochar-SOM interactions is organized by the overarching effect of biochar additions (increased vs. decreased SOC mineralization) and whether the added biochar is metabolized by microbes (direct effects) or simply affects microbial activity by altering chemical or physical properties of the soil (indirect effects).

**Table 1.1** Summary of studies of biochar-soil organic carbon mineralization interactions. Modified from Zimmerman and Gao (2013).

Source	Biochar feedstock and production conditions	Soil	Incubation duration (days)	Biochar C mineralized (% of total added)	Soil C mineralized (% change from no-biochar control)	Initial BC-C / Initial SOC-C (m/m)
Kuzyakov <i>et al.</i> (2009)	<sup>14</sup> C-labeled ryegrass, 400°C, 13h	Haplic Luvisol	1181	4.0	0.0	0.1
"	<sup>14</sup> C-labeled ryegrass, 400°C, 13h	loess arable	1181	4.0	decrease	1.1
Steinbeiss <i>et al.</i> (2009)	<sup>13</sup> C-labeled glucose, hydrothermal pyrolysis	Eutric Fluvisol arable	120	8.0	53.0	0.3
"	<sup>13</sup> C-labelled yeast, hydrothermal pyrolysis	Eutric Fluvisol	120	9.0	150.0	0.3
"	<sup>13</sup> C-labeled glucose, hydrothermal pyrolysis	forest Cambisol	120	3.0	57.0	0.3
"	<sup>13</sup> C-labelled yeast, hydrothermal pyrolysis	forest Cambisol Colombia	120	6.0	108.0	0.3
Major <i>et al.</i> (2010)	mango prunings charred in kiln, 400-600°C, 48h	savanna Oxisol	730	2.2	38.5	~5 in top 0.1m
Zimmerman	grass, 250°C under N <sub>2</sub>	forest	90	2.9	61.3	3.8

<i>et al.</i> (2011)		Alfisol forest				
"	grass, 650°C under N <sub>2</sub>	Alfisol wetland	90	0.9	-15.6	4.7
"	grass, 250°C under N <sub>2</sub>	Mollisol wetland	90	6.8	0.1	1.0
"	grass, 650°C under N <sub>2</sub>	Mollisol forest	90	0.2	-76.4	1.2
"	grass, 250°C under N <sub>2</sub>	Alfisol forest	90-500	1.9	-75.1	3.8
"	grass, 650°C under N <sub>2</sub>	Alfisol wetland	90-500	0.1	-87.1	4.7
"	grass, 250°C under N <sub>2</sub>	Mollisol wetland	90-500	3.8	-9.9	1.0
"	grass, 650°C under N <sub>2</sub>	Mollisol fallow	90-500	2.6	-49.8	1.2
Cross and Sohi (2011)	Sugarcane bagasse, 350°C, 40min	silty-clay loam	14	1.1	15.1	1.7
"	Sugarcane bagasse, 550°C, 40min	silty-clay loam	14	0.2	18.0	1.8
"	Sugarcane bagasse, 350°C, 40min	arable loam	14	0.7	25.1	0.9
"	Sugarcane bagasse, 550°C, 40min	arable loam	14	0.0	6.1	1.0
"	Sugarcane bagasse, 350°C, 40min	grassland loam	14	0.4	-9.3	0.5
"	Sugarcane bagasse, 550°C, 40min	grassland loam	14	0.0	-36.0	0.5
Keith <i>et al.</i> (2011)	<sup>13</sup> C-depleted eucalyptus, 450°C, 40min	Vertisol	120	0.8	7.4	3.0
"	<sup>13</sup> C-depleted eucalyptus, 550°C, 40min	Vertisol	120	0.4	19.4	3.3
Luo <i>et al.</i> (2011)	straw, 350°C, 30min under Ar	Aquic Paleudalf, low pH	87	0.6	304.0	5.7
"	straw, 350°C, 30min under Ar	Aquic Paleudalf, high pH	87	0.8	202.0	5.1
"	straw 700°C, 30min under Ar	Aquic Paleudalf, low pH	87	0.1	136.0	5.7
"	straw 700°C, 30min under Ar	Aquic Paleudalf, high pH	87	0.2	74.0	5.1
Jones <i>et al.</i>	mixed hardwood, 450°C,	grazed	21	~0.045	21 average	2.2

(2011)	48h	grassland Eutric Cambisol				
Bruun <i>et al.</i> (2012)						
	Barley straw, 400°C	Luvisol	451	1.7	0	0.06
“	Barley straw, 400°C	Luvisol	451	1.7	-4.5	0.28
“	Barley straw, 400°C	Luvisol	451	1.7	-13.6	0.57
Santos <i>et al.</i> (2012)	<sup>13</sup> C-enriched pine, 450°C, 5h under N <sub>2</sub>	Forest - andesitic parent material	180	0.4	-10.0	0.1
"	<sup>13</sup> C-enriched pine, 450°C, 5h under N <sub>2</sub>	Forest - granitic parent material	180	0.4	0.0	0.1
Stewart <i>et al.</i> (2012)	Oak, 550°C fast pyrolysis	Aridic Argiustoll	699	4.9	-18.8	0.8
"	Oak, 550°C fast pyrolysis	Aridic Argiustoll	699	2.5	-16.7	4.1
"	Oak, 550°C fast pyrolysis	Aridic Argiustoll	699	1.7	-8.3	8.2
"	Oak, 550°C fast pyrolysis	Aridic Argiustoll	699	2.8	-56.3	16.5
"	Oak, 550°C fast pyrolysis	Aquic Haplustoll	699	7.6	0.0	0.5
"	Oak, 550°C fast pyrolysis	Aquic Haplustoll	699	4.7	20.0	2.5
"	Oak, 550°C fast pyrolysis	Aquic Haplustoll	699	6.0	35.4	4.9
"	Oak, 550°C fast pyrolysis	Aquic Haplustoll	699	7.9	43.1	9.8
"	Oak, 550°C fast pyrolysis	Aeric Haplaquept	699	6.9	-3.0	0.4
"	Oak, 550°C fast pyrolysis	Aeric Haplaquept	699	3.7	4.5	1.9
"	Oak, 550°C fast pyrolysis	Aeric Haplaquept	699	4.4	4.5	3.8
"	Oak, 550°C fast pyrolysis	Aeric Haplaquept	699	7.7	-34.3	7.6
"	Oak, 550°C fast pyrolysis	Oxyaquic Halpudalf	699	2.1	-11.5	0.3
"	Oak, 550°C fast pyrolysis	Oxyaquic Halpudalf	699	0.7	-19.2	1.4
"	Oak, 550°C fast pyrolysis	Oxyaquic Halpudalf	699	0.7	-15.4	2.8

"	Oak, 550°C fast pyrolysis	Oxyaquic Halpudalf	699	1.0	-38.5	5.7
Farrell <i>et al.</i> (2013)	<sup>13</sup> C-labelled wheat, 450°C, 40min under N <sub>2</sub>	Aridic Arenosol	74	0.3	20.0	0.2
"	<sup>13</sup> C labelled blue gum, 450°C, 40min under N <sub>2</sub>	Aridic Arenosol	74	0.2	33.0	0.3
Maestrini <i>et al.</i> (2013)	<sup>13</sup> C-labelled ryegrass, 450°C, 4h under N <sub>2</sub>	Cambisol	158	4.3	10.1	0.1
Singh and Cowie (2014)	Eucalyptus 400°C, 40min	grassland Vertisol	1820	2.0	8.3	1.4
"	Eucalyptus leaves 400°C, steam activated	grassland Vertisol	1820	2.5	12.4	1.3
"	Poultry Litter 400°C, 40min	grassland Vertisol	1820	6.9	38.2	0.8
"	Cow Manure 400°C, 40min	grassland Vertisol	1820	7.3	10.3	0.3
"	Eucalyptus 550°C, 40min	grassland Vertisol	1820	0.5	2.1	1.6
"	Eucalyptus leaves 550°C, steam activated	grassland Vertisol	1820	1.2	9.3	1.4
"	Poultry Litter 550°C, 40min, steam activated	grassland Vertisol	1820	2.1	8.3	0.8
"	Cow Manure 550°C, 40min	grassland Vertisol	1820	2.2	1.0	0.3

### 1.3.1 Mechanisms by which biochar additions may increase SOC mineralization: Direct effects

#### 1.3.1.1 Increased microbial activity and enzyme production stimulated by labile C additions

Biochar may provide energy-rich organic compounds that stimulate microbial growth and activity (Luo *et al.*, 2013; Singh and Cowie, 2014), leading to increased degradation of all OM types, including SOM. Evidence for this mechanism has been found in the greater increases in native SOC mineralization observed both earlier in incubation experiments and with the addition of biochars that are relatively rich in labile compounds (Zimmerman *et al.*, 2011; Singh and Cowie, 2014). This could possibly sustain increased SOC mineralization over several years

(Singh and Cowie, 2014). For example, Luo *et al.* (2011) observed greater short-term SOC mineralization following biochar addition to soil for a low-temperature (350°C) *Miscanthus* biochar, which had higher levels of water-extractable (and thus likely microbially available) biochar-C, compared to a high-temperature (700°C) *Miscanthus* biochar. Similarly, Singh and Cowie (2014) showed that the increased mineralization of native SOC, relative to a control, was greater in the presence of manure-based or 400°C biochars than that of plant-based or 550°C biochars, and this pattern was consistent with the lability of the tested biochars (Singh *et al.*, 2012). Finally, Zimmerman *et al.* (2011) found a greater increase in SOC mineralization during the early period of soil-biochar incubations (first 3 months), and in biochars made from grass (*vs.* oak) and those made at 250 and 400°C (*vs.* 535 and 650°C). Again, this pattern mirrored the lability of the tested biochars. Those biochars associated with greater increases in native SOC mineralization corresponded to those with greater volatile matter content (Deenik *et al.*, 2010; Zimmerman, 2010), and those yielding greater dissolved C leachate (Mukherjee and Zimmerman, 2013). The release of a portion of this water-soluble fraction from biochar surfaces may occur immediately, followed by a slower diffusion-limited release of water-soluble C fraction held within biochar pores (Jones *et al.*, 2011), determining to some extent the timescale over which this process might occur. Because this explanation is based on the premise that the soil is limited in energy-rich organic compounds, it could be predicted that its effects would be predominantly found in soils with less labile SOM or added OM, which is consistent with the findings of a number of studies (*e.g.*, Keith *et al.*, 2011; Zimmerman *et al.*, 2011). Similarly, the amount of easily mineralizable biochar-C present could be expected to predict the duration and magnitude of this effect. This expectation is supported by a significant correlation between the increase in native SOC mineralization with biochar additions and the fraction of biochar C

mineralized during each experiment (Figure 1.3). Possible reasons the data points from Luo *et al.* (2011) have comparatively large increases in SOC mineralization with biochar additions may include a relatively short incubation duration (87 d) with a majority of the increases in native SOC mineralization observed in the first 3 days, and/or a pH effect in the acidic soil resulting in the release of any inorganic C in biochar (Farrell *et al.*, 2013).

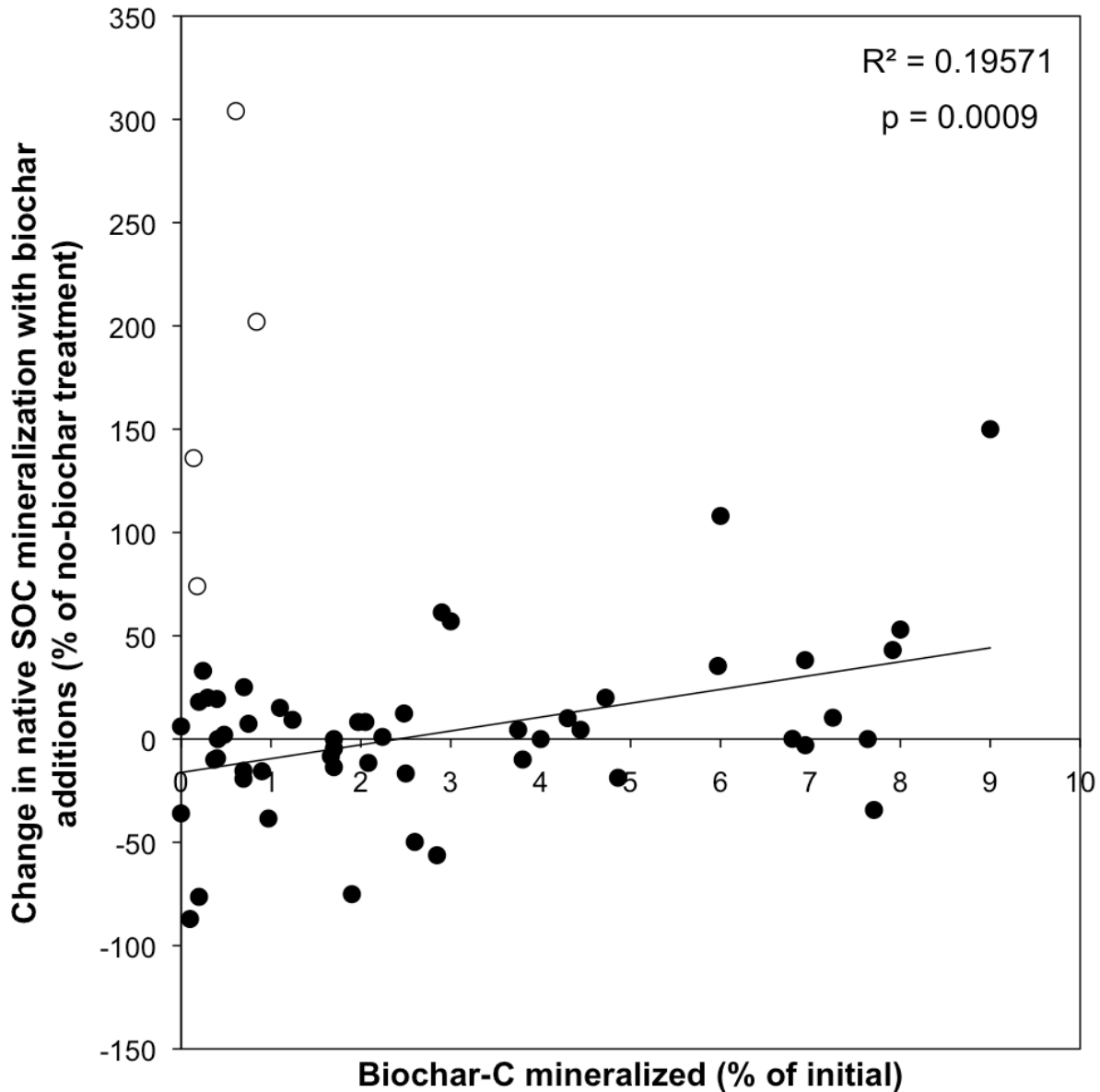


**Figure 1.3** Net (end-of-study) biochar effect on native SOC mineralization (relative to the no-biochar control) vs. total fraction of added biochar mineralized. Line indicates linear regression,  $R^2=0.19$ ,  $p=0.0009$ . Data from 13 studies listed in the caption of Figure 1.2. Open circles indicate data points from Luo *et al.* (2011), which were not included in the regression analysis.

The term “co-metabolism” is used to refer to the situations in which additions of more labile compounds are explicitly required for the production of enzymes to cause decomposition of more complex SOM compounds, rather than just causing increased microbial activity (Figure 1.4). *I.e.*, the decomposition of these complex compounds is not energetically favourable or possible without the presence of an additional organic substrate. The small amounts of low molecular weight organic compounds found in biochars (Lin *et al.*, 2012) could provide the labile compounds that drive this mechanism. However, more targeted experiments are needed to distinguish between the occurrence of co-metabolism and more general microbial stimulation, under different biochar and soil combinations and experimental conditions.

#### 1.3.1.2 SOM “mining” for N or P

Nutrient mining refers to the effect when OM is decomposed by microbes in search of nutrients, resulting in the incidental mineralization of C. Although biochar is rich in relatively stable organic C, it also contains some soluble and relatively easily decomposable organic substrates that could induce microbial scavenging of soil N or P, as they are needed for microbial growth and activity. These changes could then drive microbial “mining” of SOM for its N (Ramirez *et al.*, 2012) or P. This could result in increased C mineralization as N- or P-limited microbes decompose SOM through the release of OM-degrading enzymes. Simultaneously, biochar may directly and temporarily stabilize N or P species through SOM or mineral N or P sorption on surfaces and within pore spaces of biochar particles, further reducing N or P availability. This mechanism has not been investigated in detail and could be easily conflated with increased

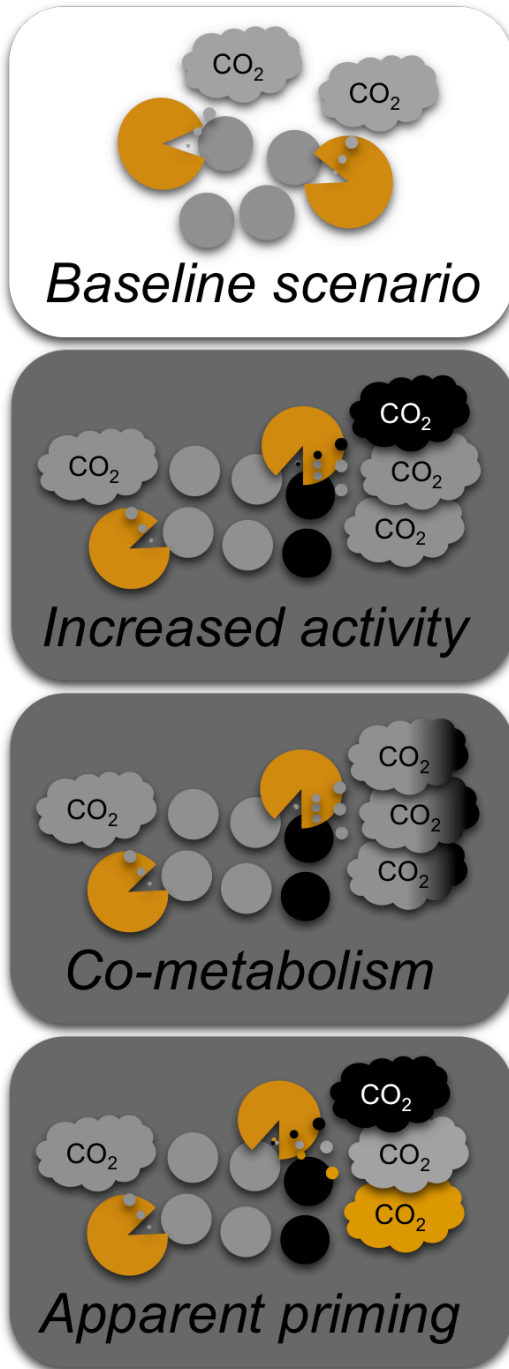


**Figure 1.4** Illustration of two ways by which biochar additions could increase SOC mineralization or induce “apparent priming”. Orange “Pac-men” represent microbes, circles represent SOC (grey) and biochar (black), and bubbles represent CO<sub>2</sub> emissions from microbial mineralization of SOC (grey), biochar (black), and maintenance respiration or “apparent priming” (orange).

microbial activity due to labile substrate addition. Designing experiments with varying levels and types of available N or P in soil and varying levels of labile versus stable organic matter in biochar could help to distinguish these mechanisms.

### *1.3.2 Mechanisms by which biochar additions may increase SOC mineralization: Indirect effects*

#### *1.3.2.1 pH effects*

Biochar additions may change soil pH (Chapter 16) favourably for microbes and enzymes, increasing their activity. For example, Luo *et al.* (2011) attributed a greater relative increase in SOC mineralization from a lower pH soil (3.7) than from a higher pH soil (7.6), with both 350°C and 700°C *Miscanthus giganteus* biochar additions to a liming effect. It is important to distinguish between the effects of mechanisms related to changes in soil pH and the simple release of inorganic C from (usually alkaline) biochar when it is mixed into an acidic soil (Dempster *et al.*, 2011; Jones *et al.*, 2011; Farrell *et al.*, 2013; Bruun *et al.*, 2014) or upon dissolution of carbonates (*e.g.*, in a sludge biochar), possibly caused by the acidity generated during biochar oxidation even in a higher pH soil (Singh *et al.* 2012). Stewart *et al.* (2012) observed predominantly increased native SOC mineralization relative to a soil-only control with 550°C fast pyrolysis oak pellet biochar additions only in an acidic soil (which became more basic with biochar additions), while the already basic soils experienced decreased native SOC mineralization.

#### *1.3.2.2 Alleviation of nutrient constraints*

Biochar can contain significant levels of nutrients and a proportion of the total nutrients in biochar may be present in readily bioavailable forms (Chapter 8). The addition of these nutrients could relieve constraints, increasing microbial activity. Cumulative losses during successive batch extractions of grass and oak biochars accounted for about 0.5-8 and 5-100% of the total N and P initially present, respectively (Mukherjee and Zimmerman, 2013). In this study, ammonium was usually the most abundant N form in leachates, but nitrate was also released by some biochars, while organic N and P represented as much as 61% and 93% of the total N and P lost, respectively. In another study, 15-20% of Ca, 10-60% of P, and about 2% of N in mallee wood biochar was readily leachable (Wu *et al.*, 2011). Because many of these nutrient forms were released very quickly, while others were leached gradually over longer time periods (Mukherjee and Zimmerman, 2013), they may also play a role in the variation in the extent and direction of biochar's effects on native SOC mineralization over time.

#### *1.3.2.3 Improved microbial habitat and soil faunal stimulation*

As a highly porous material, biochar may provide a preferred site for microbial colonization (Pietikäinen *et al.*, 2000), enhancing microbial activity and thus, C utilization. Possible reasons for microbial colonization of biochar include (1) protection of microbes from predation within pores, and (2) presence of sorbed OM and nutrients that are relatively more available to surface-colonizing microbes. For example, Wright *et al.* (1995) found that small (< 6 µm neck diameter) soil pore sizes afforded protection to *Pseudomonas fluorescens* from the soil ciliate *Colpoda steinii*. Hamer *et al.* (2004) suggested that the increased mineralization of glucose in a sand

incubation with additions of 350°C maize (*Zea mays* L.) and rye (*Secale cereale* L.) straw biochar could be due to the provision of more surfaces for microbial growth, although they did not test for this directly. However, this mechanism, if important, likely acts simultaneously with other mechanisms, because while biochars produced at lower temperatures tend to have lower surface area and pore volume than those made at higher temperatures, they also tend to result in greater increases in SOC mineralization than high temperature biochars (Zimmerman, 2011; Singh and Cowie, 2014). Further, Quilliam *et al.* (2013) reported limited microbial colonization of a mixed hardwood 450°C biochar after three years of burial in a Eutric Cambisol (although they did not compare colonization rates to that of adjacent soil).

Besides being inhabited directly by microbes, biochar may also affect microbial habitat by changing soil physical conditions. For example, biochar additions to soil could change soil temperature (due to an albedo effect) or water holding capacity (Chapter 20). This could, of course, increase microbial activity if the changes result in a more optimal moisture or temperature regime for microbes. Just as biochar additions to soil may affect the soil's water-holding capacity, its porous structure may increase soil aeration, which could increase soil oxygen levels, promoting aerobic respiration. While Jones *et al.* (2011) determined improved soil aeration was likely not the cause of increased native SOC mineralization with biochar additions in their incubation study using 450°C hardwood biochar and a grassland soil, they suggest this was because their soil already had relatively good structure, and do not rule it out for other biochar-soil systems. Whether and how soil physical factors such as the ratio of soil air-to-water pore space, water-holding capacity, or water potential are controlled in experimental studies is challenging and could have an important impact on soil microbial biomass and activity

and, consequently, on biochar-SOM interactions. For example, should water content be normalized by gravimetric water content, water-filled pore space, or water pressure potential across samples of different soil-biochar mixtures? Each choice might produce different results.

Other, less easily mineralizable, components of biochar may also stimulate microbial activity. During oxidative aging, biochar surfaces gain substituted aromatic functional groups including phenols and quinones and lactones (Cheng *et al.*, 2008; 2009), which have been found to increase numbers of active soil microbes (Visser, 1985). In addition, these compounds can act as electron shuttles, serving as electron acceptors during microbial respiration (Scott *et al.*, 1998).

Soil fauna tend to promote SOM decomposition, commonly ascribed to their comminution of organic matter, increasing its surface area for microbial attack, but also, perhaps, through a number of other mechanisms, such as faunal grazing effects on fungal decomposers (Bradford *et al.*, 2002) or soil fauna-driven N mineralization (Osler and Sommerkorn, 2007). Thus, if biochar additions stimulate soil fauna activity or populations (Chapter 14), SOM decomposition could be accelerated. There are few studies on the effects of biochar on soil fauna to date (Lehmann *et al.*, 2011), but, for example, earthworms have been found to prefer some biochar-soil combinations over soil alone (Chan *et al.*, 2008).

### *1.3.3 Mechanisms by which biochar additions may decrease SOC mineralization: Direct effects*

#### *1.3.3.1 Substrate switching*

According to this phenomenon (described generally by Kuzyakov *et al.* (2000) and in the context of biochar additions to soil by Singh and Cowie (2014)), the most labile organic fraction of biochar may be preferentially used by microbes to temporarily replace the use of native SOC, thus decreasing native SOC mineralization (Figure 1.5). This phenomenon may be of relatively greater importance in C-poor soils that receive an external supply of labile organic matter. Both Gontikaki *et al.* (2013) and Guenet *et al.* (2010) suggested this mechanism to explain their findings in systems with labile OM additions to soils. Because it is dependent on the presence of very labile biochar components, it may be expected to persist only until these compounds are used up by microbes (Whitman *et al.*, 2014).

#### *1.3.3.2 Dilution effect*

The dilution effect (Figure 1.5) is similar to substrate switching, except that labile biochar is not used preferentially by microbes - rather, there is just temporarily more total labile C in soil (from both biochar and native SOC) following biochar amendment than microbes can use, resulting in a temporary decrease in SOC mineralization. A combination of this effect and substrate switching may be responsible for the short-term (< 1 week) decrease in native SOC mineralization following 350°C sugar maple (*Acer saccharum*) biochar additions to a Typic Fragiudept (Whitman *et al.*, 2014).

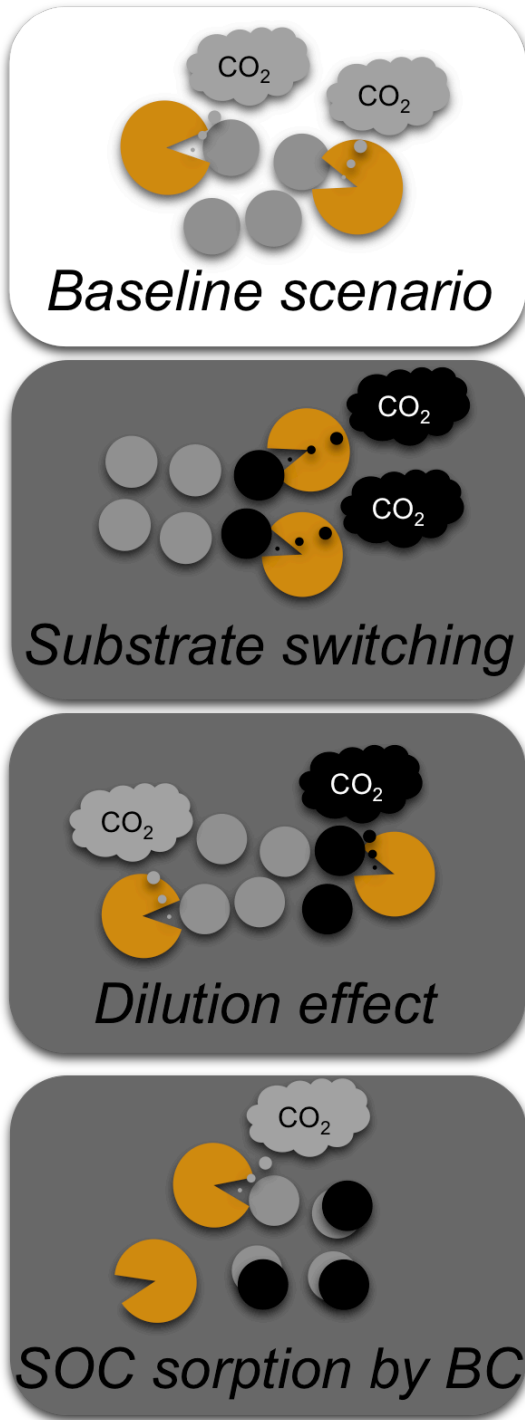


**Figure 1.5** Illustration of three mechanisms by which biochar additions may decrease SOC mineralization. Orange “Pac-men” represent microbes, circles represent SOC (grey) and biochar (black), and bubbles represent CO<sub>2</sub> emissions from microbial mineralization of SOC (grey) and biochar (black).

### 1.3.4 Mechanisms by which biochar additions may decrease SOC mineralization: Indirect effects

#### 1.3.4.1 Sorption of labile SOC

Pyrogenic materials have demonstrated a high sorption affinity for a wide range of natural organic compounds including recalcitrant OM (Kasozi *et al.*, 2010; Li *et al.*, 2002) and labile and water-soluble fractions of SOM, making them less available to microbes. This could take the form of encapsulation - SOM is absorbed within pores in biochar particles and becomes physically unavailable to microbes - or sorptive protection - SOM is sorbed on biochar surfaces and becomes less easily accessible to microbes (Figure 1.5). Both of these mechanisms have been found to be operative for organic compounds of a range of molecular sizes on mineral surfaces (Zimmerman *et al.*, 2004). In support of this mechanism, biochars with greater sorptive capacities (higher temperature biochars and hardwood biochars) have generally been found to result in the greatest long-term decreases in SOC mineralization (Zimmerman *et al.* 2011). Cross and Sohi (2011) found that the highest temperature sugarcane bagasse biochar that they studied provoked the greatest decrease in grassland soil respiration in an incubation study. Kuzyakov *et al.* (2009) also postulated this may partly explain the decreased SOC mineralization that they observed in a loess soil with 400°C ryegrass (*Lolium perenne*) biochar additions in an incubation trial. This sorption may be kinetically limited by the slow speed of diffusion into biochar pores (Kasozi *et al.*, 2010), delaying the onset of the effects of this mechanism. Furthermore, the surfaces and pore networks of biochar may get clogged by high molecular weight organic substances in soil (Pignatello *et al.*, 2006), which could limit biochar's sorption capacity for dissolved organic matter over time. It might be predicted that decreased SOC

mineralization due to the sorptive properties of biochar would be associated with more recalcitrant biochar or its more recalcitrant fractions. This is consistent with the positive linear relationship between increased SOC mineralization and BC mineralization shown in Figure 1.3.

#### *1.3.4.2 Sorption of microbial enzymes or signalling molecules*

Like other organic compounds, enzymes likely have a high affinity for biochar surfaces. Enzymes sorbed by biochar particles may be deactivated or inhibited, due to changes in pH or ionic strength at or near the biochar surface, conformational changes to the enzyme upon sorption, or steric hindrance, as can occur with enzyme-mineral interactions (Quiquampoix and Burns, 2007; Zimmerman and Ahn, 2010). When the enzyme laccase was sorbed to grass and oak biochars pyrolyzed at 650°C, its activity was reduced by 60-99%. However, the enzyme retained greater than 80% of its activity when sorbed to oak and grass biochars produced at 250 and 400°C (Zimmerman and Gao, 2013). Possible reasons for these variations include differences in the morphology and the chemistry of different biochar surfaces. Recent work by Masiello *et al.* (2013) indicates that biochar can also sorb microbial quorum-sensing signal compounds. Removal or inactivation of these compounds by biochar could interfere with processes such as biofilm formation, nitrogen fixation symbioses, and pest attack of root crops.

#### *1.3.4.3 Increased organomineral interactions and stable aggregate formation*

Biochar may mediate organomineral interactions between native or added organic matter and soil minerals, possibly through ligand exchange or cation bridging mechanisms (Liang *et al.* 2009;

Keith *et al.* 2011; Fang *et al.* 2014a, 2014b). Dissolved OM released by biochar, as well as colloidal biochar particles, may facilitate the formation of stable soil aggregates in which SOC is less accessible to microbes (Brodowski *et al.*, 2006; Liang *et al.*, 2010). Supporting this, Liang *et al.* (2009) found that labile OM amendments were incorporated into physically protected soil fractions more quickly in a highly aged biochar-rich Anthrosol as compared to biochar-poor adjacent soils. Singh and Cowie (2014) hypothesized that increased organomineral interactions during biochar ageing was a possible reason for the reduced native SOC mineralization in a biochar-amended clayey soil (relative to the non-amended control) in the later stages of their 5-year long incubation study. Although Mukherjee *et al.* (2014) found no significant change in water stable aggregates or the geometric mean diameter of aggregates in a Crosby silt-loam soil incubated over a growing season with additions of 650°C oak biochar, this may indicate that aggregate formation takes longer than a single growing season, or requires interactions with plants and soil fauna. These biochar-mediated organomineral interactions may be enhanced when additional labile organic matter is supplied (*e.g.*, Keith *et al.*, 2011) or by increased plant root activity and exudation in the presence of biochar (Major *et al.*, 2010; Slavich *et al.*, 2012). Keith *et al.* (2011) found rapid stabilization of labile OM (sugarcane residue) applied to a clayey soil in the presence of relatively young wood biochar. Thus, it could be hypothesized that higher organic matter content in a biochar-amended mineral soil would favour increased microbial biomass and activity, facilitating stable aggregate formation and soil structure development, possibly through organomineral interactions enhanced by microbiota (Young *et al.*, 1998). Similarly, Herath *et al.* (2014) found greater formation of stable aggregates in an OM rich mineral soil (Andisol) amended with a 350°C corn stover biochar than in an Alfisol containing

relatively low native SOM, but opposite trends for stable aggregate formation in the Andisol vs. the Alfisol were observed for the 550°C biochar.

#### *1.3.4.4 Decreased nutrient availability*

Biochar may decrease nutrient availability in soil through direct sorption ( Mukherjee and Zimmerman, 2013; Chintala *et al.*, 2014). Kuzyakov *et al.* (2009) postulated that sorption of nutrients by biochar may partly explain the decreased C mineralization they observed in a nutrient-poor loess soil with 400°C ryegrass (*Lolium perenne*) biochar, although they did not explicitly measure nutrient availability. Biochar addition may also cause the precipitation of nutrients, converting them into unavailable forms (due to pH shifts (Chapter 16) or interactions with biochar-derived mineral nutrients (Chapter 8)), thus decreasing availability of native nutrients in soil. Furthermore, biochar presence may increase immobilisation of mineral nutrients by microbes, particularly when they are promoted in their growth and activity in the presence of biochar, thus resulting in the incorporation of mineral nutrients into microbial biomass, making the nutrients less readily accessible, decreasing native SOM mineralization (Novak *et al.*, 2010; Chapter 16). Additionally, Prommer *et al.* (2014) showed in a field study that wood biochar addition slowed the cycling of soil organic N, possibly through the sorption of various forms of soil organic N and enzymes on biochar surfaces and in pore network, and hypothesized that this phenomenon may enhance soil C sequestration due to increases in non-biochar derived SOM.

#### *1.3.4.5 Nutrient “mining” inhibition*

If substantial levels of available nutrients, such as available N or P, are added with biochar, this could result in decreased “mining” of older SOM for nutrients by microbes (Ramirez *et al.*, 2012; Chintala *et al.*, 2013). This would, in turn, reduce the SOC mineralization associated with microbial decomposition of SOM. However, although “black N” may play an important role in SOM cycling (Knicker, 2007), biochar does tend to have low available N (Chapter 8), particularly when produced at higher temperatures (>500° C) or from woody, low-N feedstocks. Thus, the inhibition of nutrient mining due to the addition of available nutrients in biochar is not expected to be a common mechanism for decreased SOC mineralization for most biochars, although lower-temperature biochars produced from high N or P feedstocks such as manure or biosolids could be an exception. For example, a significant proportion of P in biochar may be present in readily available forms, depending on biochar type (Singh *et al.* 2010; Chapter 8), which could have implications for reduced P mining of SOM following the addition of biochar.

#### *1.3.4.6 Microbial or soil fauna inhibition due to pH effects, toxicity, or oxygen limitation*

Biochar additions could also change soil pH (Chapter 16) unfavourably for microbes, decreasing their activity. This would depend heavily on the specific soil and biochar combination and their individual characteristics (Enders *et al.*, 2013). Oxidation of biochar occurs both by abiotic and microbially-mediated processes (Zimmerman, 2010; Chapter 6). If this consumption of oxygen through oxidation occurs very rapidly, it could inhibit the activity of aerobic microbes and extracellular OM decomposing enzymes that require oxygen, such as oxidases. Since biochars are predominantly aromatic and have relatively low levels of labile C, this mechanism might only be likely in soils that are already nearly anaerobic. Additionally, biochar may be associated

with toxic compounds, such as polycyclic aromatic hydrocarbons (Chapter 22) or ethylene (Spokas *et al.*, 2010), which could inhibit microbial activity. The presence of these compounds varies widely from one biochar to the next and depends on the production mechanism, conditions, and feedstock used (Hale *et al.*, 2012). If these or other changes inhibit soil fauna (Chapter 14), their stimulation of SOM decomposition (Bradford *et al.*, 2002) could be inhibited.

#### **1.4 Mechanisms by which soil organic matter may affect biochar C turnover**

Many of the mechanisms discussed in the previous section for explaining biochar effects on SOM decomposition could also apply in the reverse direction. To understand these interactions, it is important to continue to think of biochar as a heterogeneous material, with different sub-components within any single biochar sample, and one biochar being different from the next, depending on its feedstock, production temperature, and production conditions. In general, one would expect native SOM to alter the C mineralization of easily mineralizable components of biochar (*e.g.*, water-extractable, volatile, or aliphatic compounds) through different mechanisms than it might alter the C mineralization of less easily mineralizable components of biochar (*e.g.*, aromatic compounds).

##### *1.4.1 Increased biochar C mineralization by labile SOM*

Zimmerman *et al.* (2011) found that soils with greater easily mineralizable SOM had increased rates of biochar C mineralization. In addition, adding a source of easily mineralizable OM to biochar-soil or biochar-sand mixtures has been found to increase biochar C mineralization

(Hamer *et al.*, 2004; Nocentini *et al.*, 2010; Keith *et al.*, 2011; Luo *et al.*, 2011). One of the most likely explanations for this finding is that the presence of or additions of easily mineralizable OM increases microbial activity and enzyme production, which stimulate the decomposition of biochar through co-metabolic effects. This is analogous to the increased activity mechanism for biochar's effects on SOC mineralization.

Most studies have not been designed to explicitly differentiate between mechanisms that may lead to an increase in biochar C mineralization, but the form and quantity of SOC or OM additions is likely important. For example, Hamer *et al.* (2004) found an increase in 350°C wood and maize biochar C mineralization with (highly labile) glucose additions in a sand incubation study. However, Nocentini *et al.* (2010) observed that while mineralization of 350°C pine needle and wood biochar was stimulated by additions of glucose, it was not stimulated by cellulose (a sugar polymer), in a sand incubation medium. Keith *et al.* (2011) found that 450°C and 550°C *Eucalyptus saligna* biochar mineralization increased with increasing additions of relatively easily mineralizable sugar cane residues in a soil incubation trial, although this effect decreased over time. This suggests that biochar mineralization is stimulated by easily available added organic C added to the soil and the subsequent increase in microbial activity. Once this added C source is depleted, the effects on biochar C may also disappear. Similarly to the findings of Hamer *et al.*, (2004), Kuzyakov *et al.* (2009) observed an increase in biochar mineralization with glucose additions in an incubation study, but they also noted that while glucose additions increased mineralization of 400°C perennial ryegrass (*Lolium perenne*) biochar in two soil types, there was a greater effect of glucose addition on biochar C mineralization in the low-C loess soil than the higher-C soil of the same parent material. This may indicate that the native soil C also interacts

with the added organic matter, with different effects depending on the level of native soil C and the relative mineralizability of the added OM, SOM, and biochar.

#### *1.4.2 Decreased biochar C mineralization by labile SOM*

Easily mineralizable OM additions or higher SOC contents may not always lead to higher biochar C mineralization. Liang *et al.* (2010) did not find evidence for any stimulation of CO<sub>2</sub> emissions from biochar-rich Anthrosols with additions of organic matter (sugar cane leaves) as compared to low-biochar adjacent soils, in an incubation study. However, these soils had received biochar additions centuries ago, and thus any effects driven by easily mineralizable components in biochar would likely no longer be active, as these components would disappear over time. Fang *et al.* (2014) found the greatest mineralization of 450 and 550°C *Eucalyptus saligna* biochar C when mixed with a low-C, quartz-rich Inceptisol, less when mixed with a medium-C, smectite-rich, Vertisol, and even less in a high-C, sesquioxide-rich, Oxisol. In addition to the possible effects of soil mineralogy or organomineral interactions on decreasing biochar C mineralisation, a mechanism similar to substrate switching might also explain why increasing native SOM or labile OM additions could result in decreased biochar C mineralization. This could explain the observation that mineralization of sugarcane bagasse biochar produced at a range of temperatures was greater in a soil previously kept fallow than in high-C agricultural or grassland soils (Cross and Sohi, 2011). In this study, labile C in biochar may have been a more readily available substrate than the native SOC in the fallow soil, which had the lowest CO<sub>2</sub> emissions on its own of all the soils. Zavalloni *et al.* (2011) observed lower total CO<sub>2</sub> emissions from a mixture of 500°C hardwood biochar and wheat straw in a Cambisol

than when the biochar and straw were added individually to soil, which could be partially explained by a substrate switching or a dilution effect. However it was not possible to tell whether the biochar “replaced” wheat straw mineralization or vice-versa, or how SOC mineralization changed.

#### *1.4.3 Effects of soil texture, mineralogy and structure on biochar mineralization*

Soil texture and mineralogy have been shown to directly affect biochar C dynamics. For example, Bruun *et al.* (2014) found a small but significant effect of soil clay content on biochar mineralization, with slightly lower biochar C mineralization in soils with higher clay contents. This is consistent with our understanding of clay content and clay minerals often being associated with increased SOM stabilization (Six *et al.*, 2002). Clay may also have an indirect effect on biochar mineralization, through interactions with native SOC, added labile OM and/or biochar C mineralization (Fang *et al.*, 2014a,b; Zavalloni *et al.*, 2011). For example, the decrease in biochar C mineralization with increasing levels of added labile OM in a clayey soil observed by Keith *et al.* (2011) may suggest that the labile OM additions increased organomineral interactions between biochar and soil particles, protecting biochar C from mineralization. Soil structure could also play a role in biochar-SOC interactions. For example, Kuzyakov *et al.* (2009) observed that soil mixing increased the mineralization of biochar, which could simply indicate disruption of physical protection of biochar by soil, but could also be due to stimulation by labile organic matter released during soil mixing.

## 1.5 Effect of plant roots on SOC-biochar interactions

There is a large body of research showing that the presence of roots and their relatively labile exudates often results in increased SOC mineralization (Cheng *et al.*, 2003; Kuzyakov, 2010). However, little study has been done on biochar-SOC interactions in systems with plants. This is problematic, both because many systems - natural and managed - contain plants, and also because it is to be expected that biochar-SOC interactions will differ in planted systems. Biochar additions could drive changes to belowground C inputs via roots, root exudates, and mycorrhizae (Chapter 15). In turn, the presence of roots and these changes in root C input dynamics could alter SOC and biochar C cycling. Many questions remain - would root-derived C add to the general stimulation of the microbial community, increasing SOC and biochar mineralization, or would this C source be used preferentially over the other two sources, decreasing SOC and biochar mineralization (Figure 1.6)? These effects are largely uncharacterized, as there have been very few studies of biochar-SOC interactions that include plants.

Ventura *et al.* (2014) found that a 500°C biochar made from fruit tree prunings did not change total soil CO<sub>2</sub> emission rates in an apple orchard on a Haplic Calcisol, but did increase total soil CO<sub>2</sub> emission rates when the tree roots were excluded by trenching. This may indicate that biochar applications decreased root respiration, that the presence of roots inhibited biochar and/or SOC mineralization, or some combination of interactions between the three CO<sub>2</sub> sources. However, trenching introduces a number of complicating factors, particularly, a high one-time input of C from roots killed during trenching, which could cause a transient increase in soil CO<sub>2</sub>

emissions. In a field study, Major *et al.* (2010) found net increases in soil CO<sub>2</sub> emissions with additions of mango wood biochar to a savannah soil, with this effect decreasing in the second

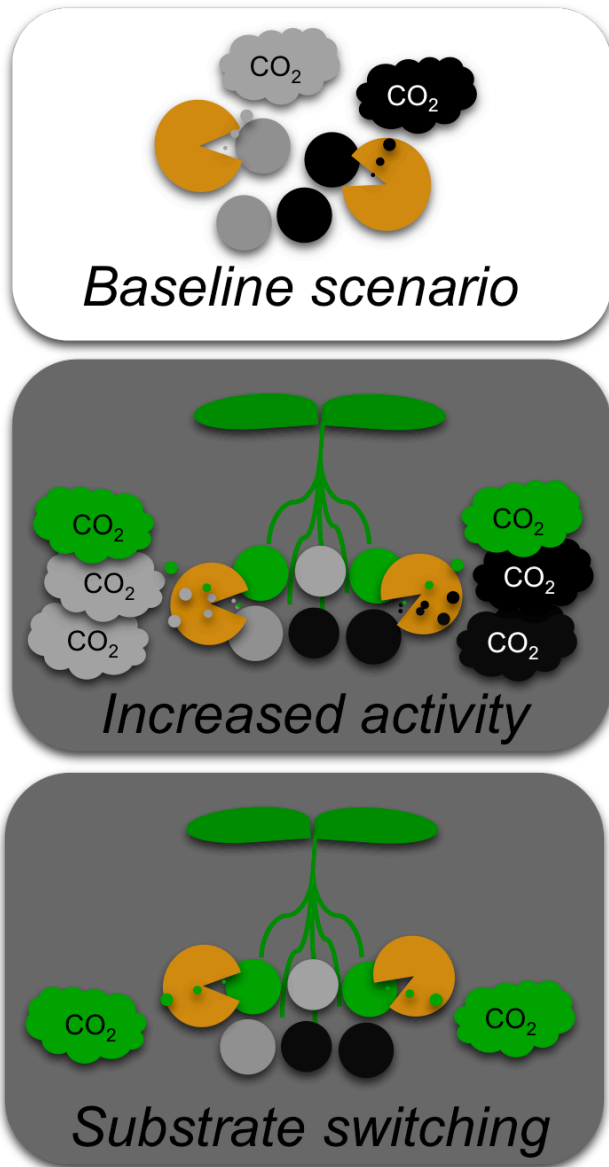


**Figure 1.6** Illustration of two possible effects of root-derived C on SOC and biochar-C mineralization. Orange “Pac-men” represent microbes, circles represent SOC (grey), biochar (black), and root-derived C (green) and bubbles represent CO<sub>2</sub> emissions from microbial mineralization of SOC (grey), biochar (black), and root-derived C (green).

year of the trial. They also observed increased aboveground biomass in the plots with biochar additions, leading them to suggest that these increases in CO<sub>2</sub> emissions could be attributed to

greater belowground growth and activity by plants. Slavich *et al.* (2013) found that 550°C feedlot manure and greenwaste biochar applications to a Ferralsol that was planted with a forage peanut (*Arachis pintoi* cv. Amarillo) and ryegrass (*Lolium multiflorum*) rotation increased total soil C more than could be explained by biochar C additions alone. Whitman *et al.* (2014) found that 350°C sugar maple (*Acer saccharum*) biochar additions to soil counteracted increased SOC mineralization induced by corn (*Zea mays* L.) plants. This counteractive effect may be due to an increased contribution of roots to total belowground C that decreased or offset the SOC losses induced by roots. It could also be caused by increased stabilization of SOC or root-derived C by biochar and possibly by enhanced organomineral interactions in the presence of roots and biochar. While the effects of including plants in the system are largely uncharacterized, they are likely important, making greenhouse, field, and laboratory experiments with plants a key area for future research.

### **1.6 Multiple mechanisms likely act simultaneously and may affect microbial communities**

Many of the mechanisms discussed in this chapter, both those enhancing and also those inhibiting SOM or biochar decomposition or mineralization, could, and most likely would, act simultaneously. For example, though net increased SOC mineralization may be observed, some stabilization of SOC may be taking place, and vice versa. This highlights the need to use diverse approaches and carefully designed experiments testing hypotheses and evaluating which mechanisms dominate, under which conditions, and during different stages of an experiment. Additionally, most or all of these effects will depend on the rates of biochar application to soils, which could vary widely in practice. Interestingly, many of these mechanisms would be expected

to induce shifts in the soil microbial community. For example, biochar additions may initially shift the community toward r-strategists (copiotrophs) due to the addition of a labile fraction of biochar-C. Then, over time, a shift toward K-strategists (oligotrophs) could be expected as the labile biochar-C fraction is consumed, leaving more recalcitrant OM (see discussion in Zimmerman *et al.*, 2011). Farrell *et al.* (2013) observed increased SOC mineralization with 450°C wheat (*Triticum aestivum* L. var. Ytpi) and blue gum eucalypt (*Eucalyptus globulus* Labill. ssp. *globulus*) biochars, and determined that biochar C was rapidly used by copiotrophic gram-positive bacteria initially, using compound specific isotopic analysis of phospholipid fatty acids. Fungal uptake of biochar C increased with time, and some of the biochar C was detected in actinomycetes by the end of 74-day incubation, which is consistent with our understanding of these organisms as being situated more to the oligotrophic end of the spectrum. Biochar has been shown to change soil microbial communities (Anderson *et al.*, 2011; Watzinger *et al.*, 2013), and such shifts in soil microbial communities could further entrench the induced changes in decomposition dynamics or could alter soil microbial activity in other ways, through inter-specific interactions, such as competition, adding another layer of complexity to the mechanisms described here.

### **1.7 Methods and approaches to studying biochar-SOM interactions**

In order to detect biochar-induced changes in the mineralization of C in SOM, it is necessary not only to measure C mineralization rates following a biochar addition, but also to distinguish C derived from each different C source (biochar and native SOM or other amended organic materials). An “additive” approach compares C mineralization of soil alone and biochar alone to

soil amended with biochar. The weighted sum of C mineralization rates of soil and biochar incubated separately are then compared to the C mineralization rate of the mixture of the two. This was the approach used by Wardle *et al.* (2008), in their litterbag study with organic surface horizon materials, biochar produced from *Empetrum hermaphroditum* at 450°C, and mixtures of the two. Likewise, Zimmerman *et al.* (2011) examined a range of biochars incubated, *in vitro*, separately and mixed with a number of soils. While useful as an indication of interactive effects, there are two limitations to the additive approach. The first is that it is not possible to determine whether the change in total C mineralization is due to changes in SOC mineralization, biochar C mineralization, or both. The second limitation is that the additive approach requires a baseline C mineralization rate for soil and biochar separately. While this is not an issue when incubating soil alone, biochar does not usually exist in isolation from the soil, and so this approach requires decisions such as whether and how to inoculate it with microbes, amend it with nutrients, control or account for pH effects, and/or mix it into some inert substrate, such as sand, and how to maintain “equivalent” moisture. Additionally, there are some issues with litterbag studies - particularly that they cannot distinguish losses due to comminution of organic matter, leaching, and mineralization.

Use of stable and radio-isotopes to distinguish CO<sub>2</sub> derived from SOM versus biochar can alleviate some of these limitations. Emitted CO<sub>2</sub> from two substrates can be distinguished if they have different <sup>13</sup>C:<sup>12</sup>C ratios, or <sup>14</sup>C contents. Differences in stable C isotope ratios can occur naturally, as with plants that use C<sub>4</sub> vs. C<sub>3</sub> photosynthetic pathways. For example, Cross and Sohi, (2011), Luo *et al.* (2011), Zimmerman *et al.* (2011) and Stewart *et al.* (2012) all applied such a “natural abundance” approach in their studies of biochar-SOC interactions by incubating

soils from C<sub>3</sub> vegetation systems (*e.g.*, temperate forest) with C<sub>4</sub> vegetation-derived biochar (*e.g.*, corn or sugarcane). Conversely, Singh and Cowie (2014) studied biochar-SOC interactions by incubating a soil from a C<sub>4</sub> vegetation system (treeless grassland dominated by tussock Mitchell grass) with biochars (*Eucalyptus* wood and leaves, poultry litter, or cow manure) that have <sup>13</sup>C:<sup>12</sup>C ratios characteristic of C<sub>3</sub>-vegetation. Differences in stable or radio-isotopic C contents can also be artificially generated by growing plants in an environment enriched in <sup>13</sup>CO<sub>2</sub> or <sup>14</sup>CO<sub>2</sub> or depleted in <sup>13</sup>CO<sub>2</sub> (compared to atmospheric CO<sub>2</sub>). For example, Keith *et al.* (2011), Farrell *et al.* (2013), Fang *et al.* (2014a,b), and Whitman *et al.* (2014) used this approach to distinguish SOC and biochar-C with stable C isotopes, and Hamer *et al.* (2004), Jones *et al.* (2011), and Kuzyakov *et al.* (2009) used this approach with the radioactive C isotope, <sup>14</sup>C. The advantage of using enriched C isotopes over the natural abundance approach is that a larger difference in C isotopic signatures or contents can be generated, allowing for smaller differences in C mineralization to be detected. This is particularly important when measuring biochar-derived CO<sub>2</sub> fluxes, which can be relatively low, and may fall below detection limits with time as the easily mineralizable fraction of biochar is lost. An enriched C isotope label may also help mitigate the errors created through isotopic fractionation, where biological or chemical processes could discriminate against the heavier C isotope, shifting the signature of, *e.g.*, the respired CO<sub>2</sub> from the bulk signature of the C substrate.

Whether using an additive or isotopic approach, all laboratory incubations can be criticized for their inability to truly simulate field conditions with regular plant inputs (Qiao *et al.*, 2014). Furthermore, most laboratory incubations do not account for stimulatory effects on biochar decomposition caused by environmental factors such as UV exposure, rainwater infiltration,

bioturbation, variability in climate parameters such as temperature, freeze and thaw cycles and saturation and desaturation, which have been shown to alter microbial activity and OM degradation processes (Sun *et al.*, 2002; Cravo-Laureau *et al.*, 2011). For example, oak biochar was shown to degrade most rapidly under alternating saturated–unsaturated conditions (Nguyen and Lehmann, 2009). Another issue is the possible decrease in microbial biomass over incubation time due to non-ideal conditions, such as nutrient limitation, depletion of labile SOC, and buildup of metabolic products (Spokas, 2010; Singh and Cowie, 2014). Also, laboratory incubations may select for certain groups of microbes (Lehmann *et al.*, 2011) that may not be representative of natural soil communities.

Modelling approaches have also been used to estimate the long-term effects of biochar-SOM interactions on soil C stocks and biochar C persistence in soil (Zimmerman *et al.*, 2011; Woolf and Lehmann, 2012). Although first-order kinetics, single or double pool exponential and power function mineralization models have been used to estimate biochar persistence, a double pool exponential model has most commonly been applied. In this model, organic C is represented as two pools - a relatively quickly cycling component and a relatively slowly cycling component, each mineralized with apparent first-order kinetics. For example, Zimmerman *et al.* (2011) compared the modelled additive mineralization of C in biochar alone and SOC alone with the modelled mineralization of C in biochar and soil mixtures in order to determine the direction and degree of soil-biochar interactions in a laboratory incubation of nearly 2 yr. However, it should be understood that these models are constrained by the assumptions of first order kinetics - *i.e.*, that there are no interactions between the mineralization of distinct substrates. A new generation of soil C cycling models may, in the future, provide better abilities to model soil C dynamics in

biochar-amended systems and, thus, add to our mechanistic understanding of biochar-SOM interactions. For example, Blagodatsky *et al.*, (2010) allowed for the simulation of such interactions by modelling decomposition as a sequential process where OM must be solubilized before it is available to microbes and the mineralization rate of SOC depends on the size of the microbial biomass pool, among other modifications. Bruun *et al.* (2010) propose developing fractionation methods to isolate fractions that could be used to parameterize models with continuous quality distributions of organic matter, rather than using fractionation methods and models with discrete pools. Other possible approaches include those of Neill and Guenet (2010), who compared two different models. The “extended mass action” model generalizes enzyme kinetics at the microbial scale. The “most probable dynamics” model determines the most probable fluxes of C, given a set of mass and energy constraints, while treating microbes and SOM particles essentially as individual components. Both of these models allowed for interactions between different types of OM to emerge, but Neill and Guenet (2010) found that the most probable dynamics model performed better than the extended mass action model at matching laboratory incubation data.

Future models should enable prediction of long-term (100 yr or greater) C persistence in biochar-amended soil using much shorter field or laboratory data (1-8.5 yr typically). Woolf and Lehmann (2012) altered the RothC soil turnover model to predict long-term SOC losses under biochar additions in three agroecological zones under maize and with and without yearly biochar additions to the soil. Their model predicted that increases in SOC mineralization induced by biochar would have a negligible long-term effect on SOC stocks (3-4% losses over 100 yr), while decreased SOC losses due to increased stabilization of SOC could increase total SOC

stocks by 30-60% over 100 yr. The main issue with this approach is that the outcomes depend, to some extent, on the assumptions about which mechanisms would drive these changes.

Depending on which underlying mechanism is at work, it may be more appropriate to model these changes as a modification to the rate constants (determining how quickly the different pools of SOC mineralize) or the partitioning constants (determining how relative amounts of SOC are partitioned between more stable or labile pools). For example, Woolf and Lehmann (2012) model increased SOC mineralization with biochar additions by increasing the SOC decomposition rate constant by a factor proportional to the total biochar in the soil, but model decreased SOC mineralization by increasing the proportion of SOC that is transferred to the stable organomineral fraction rather than being mineralized. Thus, the modelling effort is informed or constrained by our understanding of the underlying mechanisms. Another difficulty is that these interactions are likely dynamic, changing in extent or even direction over time (Keith *et al.*, 2011; Zimmerman *et al.*, 2011; Singh and Cowie, 2014) as biochar chemistry evolves with aging over time in the environment (Singh *et al.* 2013; Kuzyakov *et al.* 2014). The research community is still a long way from developing models that can incorporate this level of mechanistic complexity.

The majority of biochar-SOC interaction studies to date have been carried out in laboratory settings, with the notable exceptions of Wardle *et al.* (2008), Major *et al.* (2010), Slavich *et al.* (2013), and Ventura *et al.* (2014). Furthermore, there is a dearth of studies examining biochar-SOC interactions that include plants in the system, with the work by Major *et al.* (2010), Slavich *et al.* (2013), Ventura *et al.*, (2014) and Whitman *et al.* (2014) being notable exceptions. All of these studies have relied on either a combined dual C isotope and additive approach (Major *et*

*al.*, 2010, Whitman *et al.*, 2014) or only an additive approach (Slavich *et al.*, 2013) to distinguish biochar-C, SOC, and/or plant-derived C. Part of the reason for this lack of three-part studies is likely the challenges in distinguishing more than two sources of C (see supplementary information 1.S2).

Additionally, we are not aware of any studies that have used imaging approaches to observe *in-situ* biochar-SOC interactions directly. Key soil processes occur at micro- and nanometer scales (Mueller *et al.*, 2013), and may be central to understanding or providing conclusive evidence for specific mechanisms of biochar-SOC interactions, particularly SOC stabilization on or around biochar surfaces. Techniques such as nanoscale secondary ion mass spectrometry (nanoSIMS), which provide the elemental and isotopic composition of soil aggregates at a sub-micron scale, may prove to be a transformative tool in this area (Heister *et al.*, 2012; Mueller *et al.*, 2013).

### **1.8 Implications of SOC-biochar interactions for soil C and fertility management**

The soil and C management implications of biochar-SOM interactions will depend on (1) the specific soils and biochars in question, and (2) soil management practices and objectives. How different biochars may impact different soils is beginning to be better understood, but there remains much to be done before a robust predictive model can be developed. Currently, testing each biochar-soil combination individually, under environmentally relevant conditions, with plants present, is likely necessary to have confidence in predictions of a particular biochar's many effects on a soil in a real-world situation.

For soil C impacts in particular, the C debt-credit ratio (Whitman *et al.*, 2013), or a similar metric, could be very useful for predicting the impact of biochar on future C stocks, as our understanding of biochar-soil C interactions improves. The C debt-credit ratio quantifies the net C impact of biochar, including C lost during its production, application to soil and subsequent mineralization, as compared to the addition and mineralization of a mass of fresh, uncharred biomass equivalent to the amount required to produce the biochar (Whitman *et al.*, 2013). Herath *et al.* (2014) modified the C debt-credit ratio introduced by Whitman *et al.* (2013) to include the effects of biochar on native SOC mineralization (see supplementary information 1.S3).

The cycling of C and nutrients in SOM is a natural and essential part of soil ecology and, thus, it is not necessarily possible to place a value on changes to this cycling. For example, while slowing down the soil C cycle or increasing the relative amount of recalcitrant forms of C in soil is a key strategy for C sequestration and combating climate change, perturbations to the cycling of SOM may also have important effects on soil nutrient availability and management. If the primary management goal is to reduce overall SOC mineralization or increase relatively recalcitrant forms of C in soil, using higher-temperature biochars with lower levels of easily degradable C may reduce any interactive effects that are driven by the more labile organic C fractions of biochar. However, the production of higher temperature biochars will result in greater initial losses of C and some other elements, which could potentially reduce C savings and provide fewer available nutrients to the soil (Whitman *et al.*, 2013; Chapter 8). Additionally, slowing down SOM decomposition means that not only is C loss decreased, but also that N, P and other nutrients are released from SOM more slowly. If biochar-induced slowdown of SOM

decomposition is sustained in the long term, this could have implications for ecosystem functioning, resulting in nutrient limitations.

Better understanding of mechanisms of biochar-SOM interactions, at a molecular and microbial community level, will help us to identify and classify specific biochar-soil combinations that are more or less susceptible to increased or decreased SOC losses, and to predict long-term management implications. For example, if the relevant properties of biochar (*e.g.*, percent labile or stable fraction or ash content) and of soil (*e.g.*, total SOC and its quality, pH, mineralogy, or texture) that are responsible for the interactive C cycling responses of soil to biochar additions are determined, it will be possible to measure and use these properties in a modelling framework to predict and subsequently manage biochar-SOM decomposition interactions. This could reduce the need for specific biochar and soil testing for each unique system. Furthermore, this information may be used to predict whether the impacts will be long lasting (as with a persistent pH shift or SOC increase) or short-lived (as with interactions driven by easily mineralizable biochar-C). Clearly a better understanding of these interactions is needed to determine the net climate impact of biochar additions to soils.

## **1.9 Future directions**

Over the past few years, substantial progress has been made toward a better understanding of biochar-SOM interactions, but more research is warranted, particularly in planted systems and over longer timescales. Now that interactions between SOM and biochar are known to occur, and a number of strong hypotheses for the causes of these effects have been proposed, the next step is

to focus on understanding and quantifying the specific mechanisms at work for each general biochar-soil combination and understanding how these interactions may evolve over time. This will be necessary to determine how biochar-soil(-plant) interactions should be considered in C accounting of biochar-amended systems. Additionally, there are a number of ways that current research approaches to understanding biochar-SOM interactions could be expanded and improved. These include:

- Controlling studies to isolate and test for specific mechanisms, rather than general phenomena.
- Designing studies to determine how the different mechanisms are impacted by specific environmental conditions, over a range of timescales, and for specific biochar and soil types.
- Profiling microbial communities and activities to identify which taxa are responsible for or affected by various biochar-SOM interactions
- Using micro-scale investigations (*e.g.*, nanoscale secondary ion mass spectrometry) to provide support for or against various mechanisms, particularly those that elucidate microbiota-biochar interactions and stabilization of SOC on or around biochar surfaces and in aggregates.
- Addressing the artefacts or confounding factors present in many microcosm studies, particularly the lack of continuous inputs and outputs of C and nutrients. This may include carrying out column flow-through experiments and quantifying all fluxes.
- Establishing more and longer-term field studies designed to study biochar-soil interactions that include recurring OM or biochar inputs.

- Investigating dynamics of 3-part systems that include plants and their roots, as well as soil and biochar. Partitioning soil C stocks and fluxes into more than two components will require innovative approaches such as three C isotope systems or careful design of two C isotope systems in field or glasshouse settings.
- Developing dynamic models and identifying easily-measurable proxies for predicting soil C dynamics over a 100-year time frame that take into account biochar-soil interactions for modelling and policy applications.

Understanding biochar-SOC(-plant) interactions is necessary to predict how natural or anthropogenic additions of biochar to soils will change soil C stocks over time. With diverse mechanisms at work, these interactions could result in either increased or decreased SOC storage. A cross-disciplinary effort that will involve soil physics, biogeochemistry, soil microbial ecology, plant ecophysiology, agronomy, and mineralogy will be needed to carefully design future studies to determine which mechanisms are important, and when.

SUPPLEMENTARY INFORMATION FOR CHAPTER ONE -  
PRIMING EFFECTS IN BIOCHAR-AMENDED SOILS: IMPLICATIONS OF BIOCHAR-  
SOIL ORGANIC MATTER INTERACTIONS FOR CARBON STORAGE

*1.S1 Notes on the properties of biochars*

Certain properties of biochar are key to understanding the potential mechanisms of biochar-SOM interactions. As discussed in Chapter 11, biochar possesses a continuum of OM forms, from easily mineralizable to relatively refractory (Hilscher *et al.*, 2009; Nguyen *et al.*, 2010). While much of the C in biochar is predominantly aromatic (McBeath and Smernik, 2009; Singh *et al.*, 2012), it contains a small organic fraction that is water-extractable and relatively easily mineralizable (Farrell *et al.*, 2013; Whitman *et al.*, 2013; Lin *et al.*, 2012a; Zimmerman and Gao, 2013). There is a rich body of literature describing research on the effects of labile organic matter additions to soil (*e.g.*, in the form of simple sugars (Dalenberg and Jager, 1981), root exudates (Zhu and Cheng, 2010), or fresh organic matter (Fontaine *et al.*, 2004)), which might mirror the effects induced by the labile organic fractions in biochar. In addition, there are effects of biochar on SOM cycling that may be specific to biochar as compared with other organic soil amendments - particularly those associated with its more persistent organic fraction or its ash content - but distinguishing the effects of different forms of organic fractions or the ash fraction on SOC mineralization requires careful experimental design (Singh and Cowie, 2014).

*1.S2 Notes on using C isotopes to partition three-part systems*

One reason that field and greenhouse studies investigating biochar-SOM interactions in the presence of plants are relatively rare is likely that the interactive effect of three-plus part systems (including soil, biochar, and plants) makes it challenging to separate soil C or soil CO<sub>2</sub> emissions into their constituent parts using a standard two-pool C isotopic partitioning approach. Using all three C isotopes (stable <sup>12</sup>C and <sup>13</sup>C plus radioactive <sup>14</sup>C) could make this possible. For example, this could take the form of an experiment that distinguishes soil and plants using <sup>13</sup>C abundance levels (*e.g.*, a C<sub>3</sub> soil and a C<sub>4</sub> plant, or having one component highly labelled with <sup>13</sup>C), and distinguishes the biochar with a <sup>14</sup>C-enrichment. However, implementing these approaches could be relatively complex and expensive and the use of radioactive C will involve complex regulations, particularly in a field trial.

Alternatively, as a second approach, one could also employ enriched <sup>13</sup>C (instead of enriched <sup>14</sup>C) in two parallel experiments, where first the biochar and then the plants are labelled with <sup>13</sup>C, which could allow separation of root, biochar and soil contributions to total CO<sub>2</sub> evolved with a reasonable certainty. The challenge of using only the two stable isotopes for partitioning is that this approach will result in a range of possible solutions (as illustrated in Figure 1.S1). This approach would thus still require the application of a set of assumptions about the interactions between the three components (removing the possibility of conclusively detecting such interactions). However, with a very strong <sup>13</sup>C enrichment, one could make the argument that any shift in the <sup>13</sup>C of the control end members at natural abundance levels (*e.g.*, soil + root system in experiment-1 or soil + biochar system in experiment-2) due to the interactive effects of plant, soil and biochar would be small relative to the <sup>13</sup>C enriched signature from biochar and

plant in experiments-1 and -2, respectively. This would require very strong  $^{13}\text{C}$  enrichment beyond natural abundance levels, which can also get relatively expensive.

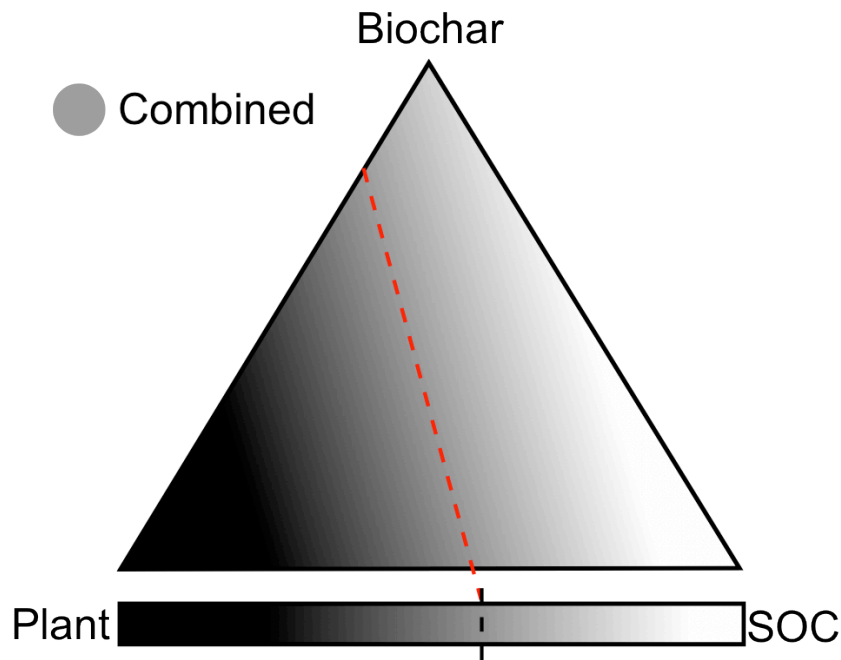


**Figure 1.S1** Graphic concept of multiple isotopic partitioning solutions to a hypothetical three-part system. Shading represents the  $^{13}\text{C}:^{12}\text{C}$  ratio of each end-member (biochar, SOC, and plant), while the grey circle indicates the combined  $^{13}\text{C}:^{12}\text{C}$  ratio for a given system. Dashed red and black lines represent possible partitioning solutions for the combined isotopic ratio. In a two-part system (rectangle between plant and SOC) there is only one solution (e.g. 57% from the plant and 43% from SOC), but for the three-part system (triangle of biochar, SOC, and plant), there are multiple solutions.

A third approach also allows for the application of just the two stable isotopes, but requires a doubled treatment, where one component is chemically and physically identical in the two treatments, except for having a different isotopic signature in each (e.g., biochar with two levels of  $^{13}\text{C}$ -enrichment) (Kuzyakov and Bol, 2004). It is essential that the component with two different isotopic signatures be otherwise functionally identical. This means biochar or plants are better candidates than soils, because plants could be grown in identical environments, only under

different  $^{13}\text{C}$  atmospheres (and then used to produce biochar). It would be challenging to produce two soils with different  $\delta^{13}\text{C}$  values without differences in their SOM content and composition.

In a fourth approach, if two of the three components can be ensured to have the same  $^{13}\text{C}:^{12}\text{C}$  ratio (e.g.,  $\text{C}_3$  soil and  $\text{C}_3$  plants), then the third (e.g.,  $^{13}\text{C}$ -labelled biochar) can be distinguished from the first two, but this would not allow for the first two to be distinguished from each other (e.g., we could not distinguish between changes in root respiration or SOC mineralization caused by biochar).

### *1.S3 Notes on C debt-credit ratio in different “priming” scenarios*

The C debt-credit ratio is the ratio of the C remaining in biochar to the C remaining in the original feedstock material (unpyrolyzed biomass) after biochar production and the application of both materials (biochar or feedstock) separately to the same soils. A value  $> 1$  indicates that more C remains in the biochar than in the original feedstock, while a value  $< 1$  indicates that less C remains – *i.e.*, C loss during biochar production outweighs the increased stability obtained through charring (Whitman *et al.*, 2013). This ratio will change over time, as the two materials mineralize at different rates.

This ratio was modified by Herath *et al.* (2014) as the  $\text{C}_{\text{Net}}$  debt-credit ratio, which incorporates the interactive effects of biochar and SOC to indicate the net C impact of biochar production and addition to a soil, including changes in SOC mineralization. This is done by adding or subtracting the change in SOC mineralization that results with the addition of the biochar or the

original feedstock material:

$$C_{\text{Net debt-credit ratio}} = \frac{\text{Biochar-C remaining} \pm \text{change in SOC mineralization}}{\text{Feedstock-C remaining} \pm \text{change in SOC mineralization}}$$

The C debt-credit ratio will depend on the characteristics of the original feedstock material and the resulting biochar (Figure 1.S2). The timescale over which the various characteristics (initial C loss during biochar production, relative mineralization rate of remaining biochar-C, and priming effects) would be important for the C debt-credit ratio would depend on the specific system.

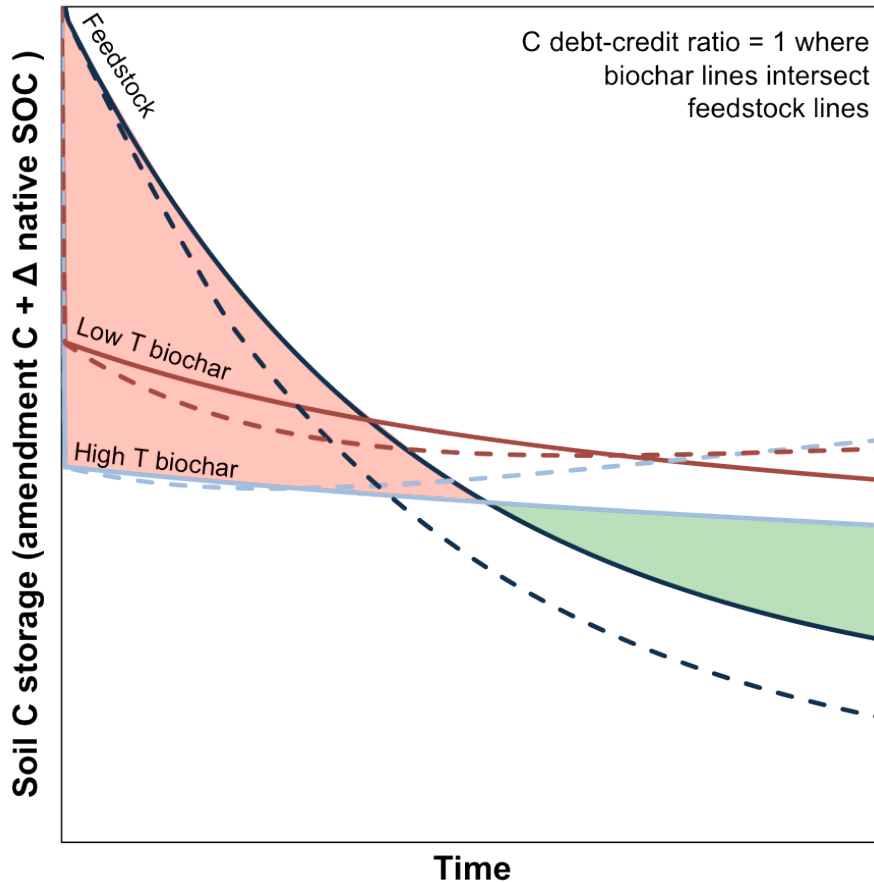


**Figure 1.S2** Conceptualization of the comparative effects of biochar characteristics and priming on total C sequestered in the soil over time (amended uncharred biomass, low temperature biochar, or high temperature biochar + change in native SOC). Solid and dashed lines indicate C remaining in soil over time without and with priming, respectively, and shaded areas indicate C debt (red) and C credit (green) for the high temperature biochar no-priming example. Specific

curve trajectories would vary with biomass C mineralization rate, C loss during pyrolysis, biochar C mineralization rate, and possible small effects of positive or negative priming, which may change over time.

## REFERENCES

- Anderson, C. R., Condon, L. M., Clough, T. J., Fiers, M., Stewart, A., Hill, R. A., Sherlock, R.R., 2011. Biochar induced soil microbial community change: Implications for biogeochemical cycling of carbon, nitrogen and phosphorus, *Pedobiologia* 54, 309-320.
- Bingeman, C. W., Varner, J. E., Martin, W. P., 1953. The effect of the addition of organic materials on the decomposition of an organic soil, *Soil Science Society of America Journal* 17, 34–38.
- Blagodatskaya, E., Kuzyakov, Y., 2008. Mechanisms of real and apparent priming effects and their dependence on soil microbial biomass and community structure: critical review, *Biology and Fertility of Soils* 45, 115–131.
- Blagodatsky, S., Blagodatskaya, E., Yuyukina, T., Kuzyakov, Y., 2010. Model of apparent and real priming effects: Linking microbial activity with soil organic matter decomposition, *Soil Biology and Biochemistry* 42, 1275-1283.
- Bradford, M. A. Tordoff, G. M., Eggers, T., Hefin Jones, T., Newington, J. E., 2002. Microbiota, fauna, and mesh size interactions in litter decomposition, *Oikos* 99, 317-323.
- Brodowski, S., John, B. Flesa, H., Amelung, W. A., 2006. Aggregate-occluded black carbon in soil, *European Journal of Soil Science* 57, 539-546.
- Bruun, S. Clauson-Kaas, S. Bobulská, L., Thomsen, I. K., 2014. Carbon dioxide emissions from biochar in soil: role of clay, microorganisms and carbonates, *European Journal of Soil Science* 65, 52-59.
- Bruun, S., El-Zehery, T., 2012. Biochar effect on the mineralization of soil organic matter, *Pesquisa Agropecuária Brasileira* 47, 665-671.
- Bruun, S., Ågren, G. I., Christensen, B. T., Jensen, L. S., 2010. Measuring and modeling continuous quality distributions of soil organic matter, *Biogeosciences* 7, 27-41.
- Chan, K. Y., Van Zwieten, L., Meszaros, I., Downie, A., Joseph, S., 2008. Using poultry litter biochars as soil amendments, *Soil, Land Care, and Environmental Research* 46, 437-444.
- Cheng, W., Johnson, D. W., Fu, S., 2003. Rhizosphere effects on decomposition, *Soil Science Society of America Journal* 67, 1418-1427.
- Cheng, C. H., Lehmann, J., Engelhard, M. H., 2008. Natural oxidation of black carbon in soils: Changes in molecular form and surface charge along a climosequence, *Geochimica et Cosmochimica Acta* 72, 1598-1610.
- Cheng, C. H., Lehmann, J., 2010. Ageing of black carbon along a temperature gradient, *Chemosphere* 75, 1021-1027.
- Chintala, R., Schumacher, T. E., McDonald, L. M., Clay, D. E., Malo, D. D., Papiernik, S. K., Clay, S. A., Julson, J. L., 2014. Phosphorus sorption and availability from biochars and soil/biochar mixtures, *CLEAN-Soil, Air, Water* 42, 626-634.
- Cravo-Laureau, C., Hernandez-Raquet, G., Vitte, I., Jézéquel, R., Bellet, V., Godon, J.-J., Caumette, P., Balaguer, P., Duran, R., 2011. Role of environmental fluctuations and microbial diversity in degradation of hydrocarbons in contaminated sludge, *Research in Microbiology* 162, 888-895.
- Cross, A., Sohi, S. P., 2011. The priming potential of biochar products in relation to labile carbon contents and soil organic matter status, *Soil Biology and Biochemistry* 43, 2127–2134.
- Dalenberg, J. W., Jager, G., 1981. Priming effect of small glucose additions to <sup>14</sup>C-labelled soil, *Soil Biology and Biochemistry* 13, 219–223.
- Dempster, D. N., Gleeson, D. B., Solaiman, Z. M., Jones, D. L., Murphy, D. V., 2011. Decreased

- soil microbial biomass and nitrogen mineralisation with Eucalyptus biochar addition to a coarse textured soil, *Plant and Soil* 354, 311–324.
- Enders, A., Hanley, K., Whitman, T., Lehmann, J. 2013. Characterization of biochars to evaluate recalcitrance and agronomic performance, *Bioresource Technology* 114, 64-653
- Fang Y., Singh B., Singh B. P., Krull E., 2014a. Biochar carbon stability in four contrasting soils, *European Journal of Soil Science* 65, 60–71.
- Fang Y., Singh B. P., Singh B., 2014b. Temperature sensitivity of biochar and native carbon mineralisation in biochar-amended soils, *Agriculture, Ecosystems and Environment*, published online.
- Farrell, M., Kuhn, T. K., Macdonald, L. M., Maddern, T. M., Murphy, D. V., Hall, P. A., Singh, B. P., Baumann, K., Krull, E. S., Baldock, J.A., 2013. Microbial utilisation of biochar-derived carbon, *Science of the Total Environment* 465, 288-297.
- Fontaine, S., Bardoux, G., Abbadie, L., Mariotti, A. 2004. Carbon input to soil may decrease soil carbon content, *Ecology Letters* 7, 314–320.
- Gontikaki, E., Thornton, B., Huvenne, V. A. I., Witte, U., 2013. Negative priming effect on organic matter mineralisation in NE Atlantic slope sediments, *PLoS One* vol 8, e67722.
- Guenet, B., Leloup, J., Raynaud, X., Bardoux, G., Abbadie, L., 2010. Negative priming effect on mineralization in a soil free of vegetation for 80 years. *European Journal of Soil Science* 61, 384–391.
- Hale, S. E., Lehmann, J., Rutherford, D., Zimmerman, A. R., Bachmann, R. T., Shitumbanuma, V., O’Toole, A., Sundqvist, K. L., Arp, H. P. H., Cornelissen, G., 2012. Quantifying the total and bioavailable polycyclic aromatic hydrocarbons and dioxins in biochars, *Environmental Science and Technology* 46, 2830–2838.
- Hamer, U., Marschner, B., Brodowski, S., Amelung, W., 2004. Interactive priming of black carbon and glucose mineralisation, *Organic Geochemistry* 35, 823–830.
- Heister, K., Höschel, C., Pronk, G. J., Mueller, C. W., Kögel-Knabner, I., 2012. NanoSIMS as a tool for characterizing soil model compounds and organomineral associations in artificial soils, *Journal of Soils and Sediments* 12, 35–47.
- Herath H. M. S. K., Camps-Arbestain, M., Hedley, M. J., Kirschbaum, M. U. F., Wang, T., Van Hale, R., 2014. Experimental evidence for sequestering C with biochar by avoidance of CO<sub>2</sub> emissions from original feedstock and protection of native soil organic matter, *Global Change Biology - Bioenergy*, published online.
- Hilscher, A. Heister, K., Siewert, C., Knicker, H., 2009. Mineralisation and structural changes during the initial phase of microbial degradation of pyrogenic plant residues in soil, *Organic Geochemistry* 40, 332-342.
- Jones, D. L., Murphy, D. V., Khalid, M., Ahmad, W., Edwards-Jones, G., DeLuca, T. H., 2011. Short-term biochar-induced increase in soil CO<sub>2</sub> release is both biotically and abiotically mediated, *Soil Biology and Biochemistry* 43, 1723–1731.
- Jones, D. L., Rousk, J., Edwards-Jones, G., DeLuca, T. H., Murphy, D. V., 2012. Biochar-mediated changes in soil quality and plant growth in a three year field trial, *Soil Biology and Biochemistry* 45, 113-124.
- Kasozi, G. N., Zimmerman, A. R., Nkedi-Kizza, P., Gao, B., 2010. Catechol and Humic Acid Sorption onto a Range of Laboratory-Produced Black Carbons (Biochars), *Environmental Science and Technology* 44, 6189–6195.
- Keith, A., Singh, B., Singh, B. P., 2011. Interactive priming of biochar and labile organic matter mineralization in a smectite-rich soil, *Environmental Science and Technology* 45, 9611–

9618.

- Knicker, H., 2007. How does fire affect the nature and stability of soil organic nitrogen and carbon? A review, *Biogeochemistry* 85, 91–118.
- Kuzyakov, Y., Friedel, J. K., Stahr, K., 2000. Review of mechanisms and quantification of priming effects, *Soil Biology and Biochemistry* 32, 1485–1498.
- Kuzyakov, Y., Bol, R., 2004. Using natural  $^{13}\text{C}$  abundances to differentiate between three  $\text{CO}_2$  sources during incubation of a grassland soil amended with slurry and sugar, *Journal of Plant Nutrition and Soil Science* 167, 669–677.
- Kuzyakov, Y., Subbotina, I., Chen, H., Bogomolova, I., Xu, X., 2009. Black carbon decomposition and incorporation into soil microbial biomass estimated by  $^{14}\text{C}$  labeling, *Soil Biology and Biochemistry* 41, 210–219.
- Kuzyakov, Y., 2010. Priming effects: Interactions between living and dead organic matter, *Soil Biology and Biochemistry* 42, 1363–1371.
- Kuzyakov, Y., Bogomolova, I., Glaser, B., 2014. Biochar stability in soil: Decomposition during eight years and transformation as assessed by compound-specific  $^{14}\text{C}$  analysis, *Soil Biology and Biochemistry* 70, 229–236.
- Lehmann, J., Rillig, M. C., Thies, J., Masiello, C. A., Hockaday, W. C., Crowley, D., 2011. Biochar effects on soil biota - A review, *Soil Biology and Biochemistry* 43, 1812–1836.
- Li, L., Quinlivan, P. A., Knappe, D. R. U., 2002. Effects of activated carbon surface chemistry and pore structure on the adsorption of organic contaminants from aqueous solution, *Carbon* 40, 2085–2100.
- Liang, B., Lehmann, J., Sohi, S. P., Thies, J. E., O'Neill, B., Trujillo, L., Gaunt, J., Solomon, D., Grossman, J., Neves, E. G., Luizão, F. J., 2009. Black carbon affects the cycling of non-black carbon in soil, *Organic Geochemistry* 41, 206–213.
- Lin, Y., Munroe, P., Joseph, S., Henderson, R., Ziolkowski, A., 2012a. Water extractable organic carbon in untreated and chemical treated biochars, *Chemosphere* 87, 151–157.
- Lin, Y., Munroe, P., Joseph, S. D., Kimber, S., Van Zwieten, L., 2012b. Nanoscale organo-mineral reactions of biochars in ferrosol: An investigation using microscopy, *Plant and Soil* 357, 369–380.
- Löhnis, F., 1926 Nitrogen availability of green manures, *Soil Science* 22, 253–290.
- Luo, Y., Durenkamp, M., De Nobili, M., Lin, Q., Brookes, P. C., 2011. Short term soil priming effects and the mineralisation of biochar following its incorporation to soils of different pH, *Soil Biology and Biochemistry* 43, 2304–2314.
- McBeath, A. V., Smernik, R. J., 2009. Variation in the degree of aromatic condensation of chars, *Organic Geochemistry* 40, 1161–1168.
- Major, J., Lehmann, J., Rondon, M., Goodale, C., 2010. Fate of soil-applied black carbon: downward migration, leaching and soil respiration, *Global Change Biology* 16, 1366–1379.
- Masiello, C. A., Chen, Y., Gao, X., Liu, S., Cheng, H.-Y., Bennett, M. R., Rudgers, J. A., Wagner, D. S., Zygourakis, K. and Silberg, J. J., 2013. Biochar and microbial signaling: production conditions determine effects on microbial communication, *Environmental Science & Technology* 47, 11496–11503.
- Mueller, C. W., Weber, P. K., Kilburn, M. R., Hoeschen, C., 2013. Advances in the analysis of biogeochemical interfaces: nanoSIMS to investigate soil microenvironments, *Advances in Agronomy* 121, 1–46.
- Mukome, F., Six, J., Parikh, S. J., 2013. The effects of walnut shell and wood feedstock biochar amendments on greenhouse gas emissions from a fertile soil, *Geoderma* 200, 90–98.

- Mukherjee, A., Zimmerman, A. R., 2013. Organic carbon and nutrient release from a range of laboratory-produced biochars and biochar-soil mixtures, *Geoderma* 193-194, 122-130.
- Mukherjee, A., Lal, R., Zimmerman, A. R., 2014. Effects of biochar and other amendments on the physical properties and greenhouse gas emissions of an artificially degraded soil, *Science of the Total Environment* 487, 26–36.
- Neill, C., Guenet, B., 2010. Comparing two mechanistic formalisms for soil organic matter dynamics: A test with in vitro priming effect observations, *Soil Biology and Biochemistry* 42, 1212-1221.
- Nguyen, B. T., Lehmann, J., 2009. Black carbon decomposition under varying water regimes, *Organic Geochemistry* 40, 846-853.
- Nocentini, C., Guenet, B., Di Mattia, E., Certini, G., Bardoux, G., Rumpel, C., 2010. Charcoal mineralisation potential of microbial inocula from burned and unburned forest soil with and without substrate addition, *Soil Biology and Biochemistry* 42, 1472–1478.
- Novak, J. M., Busscher, W. J., Watts, D. W., Laird, D.A., Ahmedna, M. A., Niandou, M. A. S., 2010. Short-term CO<sub>2</sub> mineralization after additions of biochar and switchgrass to a Typic Kandiudult, *Geoderma* 154, 281–288.
- Osler, G. H. R., Sommerkorn, M., 2007. Toward a complete soil C and N cycle: incorporating the soil fauna, *Ecology* 88, 1611-1621.
- Paterson, E., Sim, A., 2013. Soil-specific response functions of organic matter mineralization to the availability of labile carbon, *Global Change Biology* 19, 1562-1571.
- Pietikäinen, J., Kiikkilä, O., Fritze, H., 2000. Charcoal as a habitat for microbes and its effect on the microbial community of the underlying humus, *OIKOS* 89, 231-242.
- Pignatello, J. J., Kwon, S., Lu, Y., 2006. Effect of natural organic substances on the surface and adsorptive properties of environmental black carbon (char): attenuation of surface activity by humic and fulvic acids, *Environmental Science and Technology* 40, 7757–7763.
- Prayogo, C., Jones, J. E., Baeyens, J., 2014. Impact of biochar on mineralisation of C and N from soil and willow litter and its relationship with microbial community biomass and structure, *Biology and Fertility of Soils* 50, 695-702.
- Prommer, J., Wanek, W., Hofhansl, F., Trojan, D., Offre, P., Urich, T., Schleper, C., Sassmann, S., Kitzler, B., Soja, G., Hood-Nowotny, R. C., 2014. Biochar Decelerates Soil Organic Nitrogen Cycling but Stimulates Soil Nitrification in a Temperate Arable Field Trial, *PLoS ONE* vol 9, e86388.
- Qiao, N., Schaefer, D., Blagodatskaya, E., Zou, X., Xu, X., Kuzyakov, Y., 2014. Labile carbon retention compensates for CO<sub>2</sub> released by priming in forest soils, *Global Change Biology*, published online.
- Quillam, R. S., Glanville, H. C., Wade, S. C., 2013. Life in the ‘charosphere’- Does biochar in agricultural soil provide a significant habitat for microorganisms? *Soil Biology and Biochemistry* 65, 287-293.
- Quiquampoix, H., Burns, R. G., 2007. Interactions between proteins and soil mineral surfaces: environmental and health consequences, *Elements* 3, 401–406.
- Ramirez, K. S., Craine, J. M., Fierer, N., 2012. Consistent effects of nitrogen amendments on soil microbial communities across biomes, *Global Change Biology* 18, 1918-1927.
- Scott, D. T., McKnight, D. M., Blunt-Harris, E. L., Kolesar, S. E., Lovley, D. R., 1998. Quinone moieties act as electron acceptors in the reduction of humic substances by humics-reducing microorganisms, *Environmental Science and Technology* vol 32, 2984-2989.
- Singh, B., Singh, B. P., Cowie, A. L., 2010. Characterisation and evaluation of biochars for their

- application as a soil amendment, *Australian Journal of Soil Research* 48, 516–525.
- Singh, B. P., Cowie, A.L. 2014. Long-term influence of biochar on native organic carbon mineralisation in a low-carbon clayey soil, *Scientific Reports* 4, published online.
- Singh, N., Abiven, S., Maestrini, B., Bird, J. A., Torn, M. S., Schmidt, M. W. I., 2013. Transformation and stabilization of pyrogenic organic matter in a temperate forest field experiment, *Global Change Biology*, published online.
- Singh, B. P., Cowie, A. L., Smernik, R. J., 2012. Biochar carbon stability in a clayey soil as a function of feedstock and pyrolysis temperature, *Environmental Science and Technology* 46, 11770–11778.
- Six, J., Conant, R. T., Paul, E. A., Paustian, K., 2002. Stabilization mechanisms of soil organic matter: Implications for C-saturation of soils, *Plant and Soil* 241, 155-176.
- Slavich, P. G., Sinclair, K., Morris, S. G., Kimber, S. W. L., Downie, A., Zwieten, L., 2013. Contrasting effects of manure and green waste biochars on the properties of an acidic ferralsol and productivity of a subtropical pasture, *Plant and Soil* 366, 213–227.
- Spokas, K. A., 2010. Review of the stability of biochar in soils: predictability of O:C molar ratios, *Carbon Management* 1, 289-303.
- Stewart, C. E., Zheng, J., Botte, J., Cotrufo, M. F., 2012. Co-generated fast pyrolysis biochar mitigates green-house gas emissions and increases carbon sequestration in temperate soils, *GCB Bioenergy* 5, 153-164.
- Sun, M. Y., Aller, R. C., Lee, C., Wakeham, S. G., 2002. Effects of oxygen and redox oscillation on degradation of cell-associated lipids in surficial marine sediments, *Geochimica and Cosmochimica Acta* 66, 2003-2012.
- Ventura, M. Zhang, C. Baldi, E. Fornasier, F., Sorrenti, G., Panzacchi, P., Tonon, G., 2014. Effect of biochar addition on soil respiration partitioning and root dynamics in an apple orchard, *European Journal of Soil Science* 65, 186-195.
- Visser, S. A., 1985. Physiological action of humic substances on microbial cells, *Soil Biology and Biochemistry* 17, 457-462.
- Wardle, D. A., Nilsson, M. C., Zackrisson, O., 2008. Fire-derived charcoal causes loss of forest humus, *Science* 320, 629–629.
- Watzinger, A., Feichtmair, S., Kitzler, B., Zehetner, F., Kloss, S., Wimmer, B., Zechmeister-Boltenstern, S., Soja, G., 2014. Soil microbial communities responded to biochar application in temperate soils and slowly metabolized <sup>13</sup>C-labelled biochar as revealed by <sup>13</sup>C PLFA analyses: results from a short-term incubation and pot experiment, *European Journal of Soil Science* 65, 40-51.
- Whitman, T., Hanley, K., Enders, A., Lehmann, J., 2013. Predicting pyrogenic organic matter mineralization from its initial properties and implications for carbon management, *Organic Geochemistry* 64, 76-83.
- Whitman, T., Enders, A., Lehmann, J., 2014. Pyrogenic carbon additions to soil counteract positive priming of soil carbon decomposition by plants, *Soil Biology and Biochemistry* 73, 33-41.
- Woolf, D., Lehmann, J., 2012. Modelling the long-term response to positive and negative priming of soil organic carbon by black carbon, *Biogeochemistry* 111, 83–95.
- Wright, D. A., Killham, K., Glover, L. A., Prosser, J. I., 1995. Role of pore size location in determining bacterial activity during predation by protozoa in soil, *Applied and Environmental Microbiology* 61, 3537-3543.

- Young, I. M., Blanchart, E., Chenu, C., Dangerfield, M., Fragoso, C., Grimaldi, M., Ingram, J., Monrozier, L. J., 1998. The interaction of soil biota and soil structure under global change, *Global Change Biology* 4, 703-712.
- Zavalloni, C., Alberti, G., Biasiol, S., Vedove, G. D., Fornasier, F., Liu, J., Peressotti, A., 2011. Microbial mineralization of biochar and wheat straw mixture in soil: A short-term study, *Applied Soil Ecology* 50, 45–51.
- Zhu, B., Cheng, W., 2010. Rhizosphere priming effect increases the temperature sensitivity of soil organic matter decomposition, *Global Change Biology* 17, 2172–2183.
- Zimmerman, A. R., Gao, B., Ahn, M.-Y., 2011. Positive and negative carbon mineralization priming effects among a variety of biochar-amended soils, *Soil Biology and Biochemistry* 43, 1169–1179.
- Zimmerman, A. R., Ahn, M.Y., 2010. Organo-mineral enzyme interactions and influence on soil enzyme activity, in: Shukla, G., Varma, A. (eds), *Soil Enzymology, Soil Biology*, Springer-Verlag, Berlin Heidelberg, 271-292.
- Zimmerman, A. R., Goyne, K. W., Chorover, J., Komarneni, S., Brantley, S. L., 2004. Mineral mesopore effects on nitrogenous organic matter absorption, *Organic Geochemistry* 35, 355-375.
- Zimmerman, A. R., Gao, B., 2013. The stability of biochar in the environment, in: Ladygina, N., Rineau, F., (eds) *Biochar and Soil Biota*, CRC Press, Boca Raton, USA, 1-40.

## CHAPTER 2

### PYROGENIC CARBON ADDITIONS TO SOIL COUNTERACT POSITIVE PRIMING OF SOIL CARBON DECOMPOSITION BY PLANTS<sup>1</sup>

#### **Abstract**

Important due to both its role in fire-affected ecosystems, and also its proposed intentional production and application for carbon (C) management, pyrogenic organic matter (PyOM) is thought to contain very stable forms of C. However, the mechanisms behind its interactions with non-PyOM soil organic C (SOC) remain speculative, with studies often showing short-term positive and then long-term negative “priming effects” on SOC decomposition after PyOM applications. Furthermore, studies of these interactions to date have been limited to systems that do not include plants. This study describes results from a 12-week greenhouse experiment where PyOM-SOC priming effects with and without plants were investigated using stable isotope partitioning. In addition, we investigated the optimal  $\delta^{13}\text{C}$  end-members for sources of SOC, PyOM, and plant-derived  $\text{CO}_2$  emissions. The two-factorial experiment included the presence or absence of corn plants and of  $^{13}\text{C}$ -labelled PyOM. In order to control for pH and nutrient addition effects from PyOM, its pH was adjusted to that of the soil and optimal nutrient and water conditions were provided to the plants. We find that the  $\delta^{13}\text{C}$  of PyOM sub-components (DOC, tars C, mineralized C, and bulk C) were significantly different. Significant losses of 0.4% of the applied PyOM-C occurred in the first week. We find evidence for a “negative priming” effect of

---

<sup>1</sup> Published as Whitman, T., Enders, A., Lehmann, J., 2014. Pyrogenic carbon additions counteract positive priming of soil carbon mineralization by plants. *Soil Biology and Biochemistry* 73, 33-41.

PyOM on SOC in the system (SOC losses are 48% lower with PyOM present), which occurred primarily during the first week, indicating it may be due to transient effects driven by easily mineralizable PyOM. Additionally, while the presence of corn plants resulted in significantly increased SOC losses (“positive priming”), PyOM additions counteract this effect, almost completely eliminating net C losses either by decreasing SOC decomposition or increasing corn C additions to soil. This highlights the importance of including plants in studies of PyOM-SOC interactions.

## 2.1 Introduction

Pyrogenic organic matter (PyOM) plays a critical but poorly understood role in the global carbon (C) cycle. PyOM is the product of biomass heated to relatively high temperatures (< 700°C) under low or no oxygen, and includes a spectrum of materials from lightly charred biomass to soot (Masiello, 2004; Lehmann, 2007; Laird, 2008; Keiluweit *et al.*, 2010; Bird and Ascoug, 2012). On a global scale, 50-500 Tg of PyOM are produced through wildfires annually (Kuhlbusch and Crutzen, 1995; Forbes *et al.*, 2006), and data are emerging that PyOM is a more important natural pool of C in soils than previously thought (Skjemstad *et al.*, 2002; Krull *et al.*, 2006; Lehmann *et al.*, 2008; Mao *et al.*, 2012). Because PyOM is a more persistent form of C in comparison to the original biomass from which it is produced (Schmidt and Noack, 2000; Masiello, 2004; DeLuca and Aplet, 2008; Keiluweit *et al.*, 2010; Bird and Ascoug, 2012), its production and management have been proposed as a strategy for reducing atmospheric CO<sub>2</sub> stocks, in which case it is often referred to as “biochar” (Kuhlbusch and Crutzen, 1995; Forbes *et*

*al.*, 2006; Lehmann, 2007; Laird, 2008). However, interactions of PyOM with existing soil organic carbon (SOC) are still poorly understood.

PyOM additions have been shown to cause SOC to mineralize at a different rate than it would without the PyOM application, with the magnitude and direction of these interactions changing over time (Cross and Sohi, 2011; Jones *et al.*, 2011; Keith *et al.*, 2011; Luo *et al.*, 2011; Zimmerman *et al.*, 2011). Similarly, increased SOC mineralization in the presence of plant roots has been observed in many systems (*e.g.*, Cheng *et al.*, 2003; Dijkstra and Cheng, 2007; Pausch *et al.*, 2013). These interactions are often described as “priming”, where “positive priming” means a C pool (such as SOC) mineralizes more quickly when in the presence of another substrate (such as PyOM), while “negative priming” indicates it decomposes more slowly (Bingeman *et al.*, 1953). Recent papers on PyOM-SOC priming, examining different combinations of PyOM types and soils over different timescales, have shown mixed effects. For example, Luo *et al.* (2011) observed predominantly positive priming of SOC for different PyOM types in both low and high pH soils over 180 days, Cross and Sohi (2011) saw insignificant or negative priming over a range of soils and PyOM types over two weeks, while Zimmerman *et al.* (2011) observed initial positive (for low-temperature and grass PyOM) or neutral priming effects becoming negative (for higher-temperature and hardwood PyOM) over one year in a range of soils. However, we are aware of no published studies that have explicitly considered these effects in systems where plants are present. Since plant roots have been found to dramatically affect SOC cycling, it is likely that they also affect PyOM-SOC interactions, and PyOM additions may, in turn, affect plant root-SOC interactions (Major *et al.*, 2010; Slavich *et al.*, 2013). For example, Slavich *et al.* (2013) found that PyOM additions to soils planted with ryegrass increased total

SOC in the top 75 mm more than could be explained by the PyOM additions alone, after three years. However, they were not able to partition the soil C between the ryegrass, original SOC, and added PyOM, and so could not conclusively determine how much each component contributed to total SOC.

To explain positive priming of SOC by PyOM, at least three key mechanisms have been proposed (Blagodatskaya and Kuzyakov, 2008; Jones *et al.*, 2011; Zimmerman *et al.*, 2011): (1) Co-metabolism – microbial mineralization of the easily mineralizable fraction of PyOM allows for the direct simultaneous mineralization of SOC and increases active extracellular enzyme levels, resulting in additional SOC mineralization. This effect can also be understood in terms of classic Michaelis-Menten enzyme kinetics, where rate of reaction is not linearly proportional to substrate concentration. If the concentration of the substrate (here, C) is initially limiting, and is then increased, a non-linear increase in reaction rate could occur, resulting in positive priming; (2) N or other nutrient stimulation – the addition of N or other nutrients in PyOM alleviates some microbial constraint, resulting in generally increased activity; (3) General stimulation – PyOM additions result in a beneficial pH shift or alleviation of physical constraints, resulting in generally increased microbial activity. In addition, Blagodatskaya and Kuzyakov (2008) describe an “apparent [positive] priming effect”, where changes to the system result in increased microbial biomass turnover (appearing as increased CO<sub>2</sub> emissions), but do not affect the SOC mineralization rate. It can be challenging to distinguish this mechanism from the others, particularly since this increase in microbial activity may subsequently result in SOC mineralization, or “real” priming.

At least four general mechanisms have been proposed to explain the negative priming of SOC by PyOM (Blagodatskaya and Kuzyakov, 2008; Jones *et al.*, 2011; Zimmerman *et al.*, 2011): (1) Substrate switching - although much of the PyOM is highly stable, there is an easily mineralizable portion of PyOM (Cross and Sohi, 2011; Whitman *et al.*, 2013) which may be used preferentially by microbes as a C substrate, resulting in decreased SOC mineralization; (2) Stabilization - PyOM may adsorb or otherwise physically or chemically stabilise SOC in the soil, making it more difficult for microbes to decompose; (3) General inhibition - PyOM additions may have a general inhibitory effect on the microbial community, decreasing total mineralization rates. For example, this could occur if PyOM additions shift the soil pH out of the optimal range, added toxic chemicals, or if PyOM inactivates microbial enzymes necessary for mineralization. (4) N inhibition - the sometimes inhibitory effect of N on SOC mineralization has long been noted (Fog, 1988), and the reasons behind this phenomenon are still not settled (Ramirez *et al.*, 2012). However, although “black N” may play an important role in SOM cycling (Knicker, 2007), PyOM tends to have low available N. In fact, the high C:N ratio of PyOM could lead to the immobilization of N during PyOM mineralization, resulting in the opposite effect. In addition, we would add another potential mechanism, which is a variation on substrate switching: (5) “Dilution” - microbes may not use labile PyOM preferentially, but if it is used as readily as SOC, over very short timescales (hours to days), microbial populations are faced with a larger pool of C substrate, but have not yet grown to take full advantage of it - hence, a similar amount of total C is respired, but because a fraction of it is supplied by PyOM, less total SOC is respired. This mechanism would only be expected to be important over short timescales.

It is reasonable to expect that any or all of these mechanisms could take place given the right set of conditions, and many of the above mechanisms have analogues in plant root-SOC priming interactions. Thus, it is likely that the effects of plant roots and PyOM additions on SOC cycling could enhance, offset, or interact with each other. To investigate this gap in our knowledge, we ask how PyOM effects on SOC decomposition change with and without plants, hypothesizing that important interactions may occur among plants, PyOM, and SOC in these three-part systems. In addition, we investigated the optimal  $\delta^{13}\text{C}$  values to use as end-members for the isotopic end-members for sources of SOC, PyOM, and plant-derived  $\text{CO}_2$  emissions.

## **2.2 Materials and Methods**

### *2.2.1 Soil type and PyOM production*

Soil was collected from a mixed deciduous forest in Dryden, NY (42.461124, -76.386468), which has not been burned within recorded history. It is dominated by oaks (*Quercus sp.*), red maple (*Acer rubrum*), sugar maple (*Acer saccharum*), white ash (*Fraxinus Americana*), beech (*Fagus sp.*), basswood (*Tilia americana*), and hickories (*Carya sp.*), while understory species include hop hornbeam (*Ostrya virginiana*), musclewood (*Carpinus caroliniana*), and witch hazel (*Hamamelis virginiana*). The soil is a Mardin channery silt loam – a coarse-loamy, mixed, active, mesic Typic Fragiudept. It was collected from the top 0.5 m and was air-dried and sieved (< 10 mm). PyOM was produced from maple twigs grown under a labelled  $^{13}\text{C}$  atmosphere (see Horowitz *et al.*, 2009), milled < 2 mm and pyrolyzed at 325°C in a modified muffle furnace

under Ar gas. Initial soil and PyOM properties are listed in Tables 2.1 and 2.2, and Mehlich III-extractable nutrients in Table 2.S1.

<b>Table 2.1</b> Initial soil properties	
<b>Property (units)</b>	<b>Value</b>
Texture	(Channery) silt loam
Bulk density (packed at) (g cm <sup>-3</sup> )	1.28
60% WFPS (g water g <sup>-1</sup> dry soil)	0.28
Soil microbial biomass C (g kg <sup>-1</sup> dry soil)	0.01
Soil microbial biomass C (g kg <sup>-1</sup> SOC)	0.51
pH (0.01M CaCl <sub>2</sub> )	3.9
Total C (%)	1.1
Total N (%)	0.12
C:N	9.2
Water-extractable C (g kg <sup>-1</sup> total)	5.1
100% WFPS (g g <sup>-1</sup> dry soil)	0.45
Extractable NO <sub>3</sub> <sup>-</sup> and NO <sub>2</sub> <sup>-</sup> (mg kg <sup>-1</sup> )	3.73
Extractable NH <sub>4</sub> <sup>+</sup> (mg kg <sup>-1</sup> )	20.48
Available P (Mehlich III, mg kg <sup>-1</sup> )	1.0
Particle size (mm)	< 10
% sand	28.1
% silt	54.7
% clay	17.2

**Table 2.2** Initial properties and production conditions of PyOM

Property (units)	Value
pH (0.01M CaCl <sub>2</sub> )	Initial pH 8.95; Adjusted to soil pH (3.9)
Total C <sub>organic</sub> (%)	61
Total C <sub>inorganic</sub> (%)	none
Total N (%)	0.87
Total H (%)	3.55
Total O (%)	21.63
C:N (by mass)	69
H:C <sub>organic</sub> (molar)	0.69
O:C (molar)	0.26
Water-extractable C (g kg <sup>-1</sup> total)	0.61
Extractable NO <sub>3</sub> <sup>-</sup> and NO <sub>2</sub> <sup>-</sup> (mg kg <sup>-1</sup> )	0.4
Extractable NH <sub>4</sub> <sup>+</sup> (mg kg <sup>-1</sup> )	2.0
Available P (Mehlich III, mg kg <sup>-1</sup> )	360.1
Feedstock	Sugar maple twigs
Particle size (mm)	< 2
Heating rate (°C min <sup>-1</sup> )	2
Final temp (°C)	350
Residence time (hours)	2
Surface area (m <sup>2</sup> g <sup>-1</sup> )	50.5
Ash (%)	4.26
Volatiles (%)	40.12
Fixed carbon (%)	55.62

### 2.2.2 Treatments and experimental design

We used a 2 by 2 factorial design with corn (*Zea mays* (L.)) plants and PyOM as the two factors and 6 replicates for each of the 4 treatments. Pots were designed (Figure 2.S1) based on those

used by Yang and Cai (2006). Pots were constructed from 7.5-L white plastic buckets with a PVC tube fixed in the centre, extending 50 mm into the soil, into which the corn seeds were planted. This central tube was surrounded by an ethylene propylene diene monomer (EPDM) rubber cover, which could be stretched over the rim, sealing the chamber, or pulled back, leaving the chamber open to the air. In addition, a chamber vent 29 mm long with an internal diameter of 1.8 mm was installed to prevent pressure changes upon capping the chamber that could affect CO<sub>2</sub> evolution (Hutchinson and Mosier, 1981). Each pot received 7 kg soil. After bringing soil to 60% water-filled pore space (WFPS) with reverse osmosis water, pots were incubated in a greenhouse for 2 weeks, allowing for the flush of C made available through soil processing and the resulting microbial death to be respired. PyOM and corn seeds were added after this pre-incubation (day 0). 22 g PyOM was added (equivalent to ~3 t ha<sup>-1</sup>) and mixed by hand throughout the soil. Pots that did not receive PyOM additions were also mixed by hand. In planted pots, two corn seeds were sown per pot and thinned to one plant after 7 days. All pots received a modified Hoagland's nutrient solution (Table S2) every other day for the first 38 days, after which only pots with plants were fertilized, to reduce salt build-up in the unplanted soils. Pots of soil were maintained at 60% WFPS with reverse osmosis water over the course of the experiment by watering to weight every other day initially, and every day once plants had grown substantially.

### *2.2.3 Gas sampling*

Chambers were sealed for gas sampling by stretching the EPDM cover over the pot rim and sampling with a syringe through a rubber septum in the side. When sampling was not taking

place, the cover was retracted so the soil was exposed to the air and greenhouse light. CO<sub>2</sub> emitted from the soil was measured for each pot between 10 AM and 2 PM over a period of three months. After PyOM application and seed planting, measurement of CO<sub>2</sub> emission rates took place on days 1, 5, 9, and then every 7 days thereafter for the first month, after which sampling took place every 2 weeks. For each pot, 10 mL samples were taken every 11 to 15 min after sealing the chamber, depending on the rate of respiration, using syringes, which were sealed with rubber stoppers, for a total of 4 or 5 samples per pot. All samples were measured for CO<sub>2</sub> concentrations within 6 hours of collection in a LI-6200 portable photosynthesis system coupled to a LI-6200 infra-red CO<sub>2</sub> analyzer (LI-COR Biosciences, Lincoln, NE). Measurements for isotopic analysis were taken less frequently, on days 1, 7, and then every 2 weeks thereafter. All pots were capped at the same time, and then each pot within a given treatment was sampled once to represent a different time point for that treatment, giving 6 data points from which to construct the associated Keeling plot (Pataki, 2003). This approach was designed to reduce the impact of drawing CO<sub>2</sub> from soil pores by advection during sampling (Nick Nickerson, personal communication). 15 mL of sample were injected into 12.5 mL evacuated exetainers (Labco). Samples were analyzed for CO<sub>2</sub> concentrations and δ<sup>13</sup>C using a Gasbench II unit coupled with a Thermo Delta V Advantage Isotope Ratio Mass Spectrometer and a Temperature Conversion Elemental Analyzer (Thermo Scientific, West Palm Beach, FL). The δ<sup>13</sup>C signature of emitted CO<sub>2</sub> was calculated using a Keeling plot ([CO<sub>2</sub>]<sup>-1</sup> vs. δ<sup>13</sup>C) and extrapolating to the intercept. Only plots with an R<sup>2</sup> > 0.90 were interpreted.

#### *2.2.4 Biomass and soil sampling*

All pots were destructively sampled at the end of the experiment. Soil samples for microbial biomass measurements were taken by using a soil probe to collect 2 cores from the full depth of each pot, totaling about 100 g moist soil. These samples were sieved < 2 mm and stored at 4°C until analysis, which took place within 48 hours. Initial and final microbial biomass was measured using chloroform fumigation extraction (Vance *et al.*, 1987), with 0.5 M KCl used as the extractant. After extractions, samples were dried in a 60°C oven until only crystals remained, which were then ground with a mortar and pestle and weighed into tin capsules and analyzed for %C and  $\delta^{13}\text{C}$ . Soil sub-samples were sieved to < 2 mm and then ground in a Retsch mixer mill to a fine powder. The corn plants were divided into shoots and roots, washing soil from roots with water. Plant matter and soils were dried at 60°C and stored in the dark until analysis. Plant samples were progressively ground in a Viking hammer mill, a Wiley mill, and a Retsch mixer mill, until a fine and homogeneous sample remained. Root sugars were extracted, following Brugnoli *et al.* (1988), as modified by Richter *et al.* (2009).

#### 2.2.5 DOC and volatile PyOM analysis

DOC was extracted from soils and PyOM by shaking 100 g air-dried soil with 200 mL DIW or 7 g PyOM with 45 mL DIW for 10 min at 120 rpm, centrifuging for 15 minutes at 3000xg, filtering the supernatant using a 0.70  $\mu\text{m}$  glass fibre syringe filter, and then freeze-drying the filtrate for solid  $\delta^{13}\text{C}$  analysis (Zsolnay, 2003). Volatile PyOM (the collected condensate released as a gas during pyrolysis, henceforth referred to as “tar”) was collected and freeze-dried to remove any water before analysis for  $\delta^{13}\text{C}$ .

### 2.2.6 Solid sample $\delta^{13}\text{C}$ analysis

All dried and ground solid samples were weighed into tin capsules and analyzed in a Thermo Delta V Advantage Isotope Ratio Mass Spectrometer and a Temperature Conversion Elemental Analyzer (Thermo Scientific, West Palm Beach, FL) to determine  $\delta^{13}\text{C}$  values. For the PyOM tar samples, elemental analysis tins designed for liquid samples were used.

### 2.2.7 $\delta^{13}\text{C}$ of root-derived $\text{CO}_2$ and PyOM-derived $\text{CO}_2$

In order to determine the  $\delta^{13}\text{C}$  of root respiration alone, we grew corn plants in a “no-C soil”. We created the soil by ashing the same soil used for the greenhouse trial at  $550^\circ\text{C}$  for 2 hours, with the goal that this setup would best mimic the physical conditions of the soil. This resulted in a soil containing  $< 0.05\%$  C, which was negligible in relation to the magnitude of root respiration, allowing us to determine the  $\delta^{13}\text{C}$  of the root respiration using three pots and the same gas sampling approach as in the main experiment. However, a similar approach was not successful for PyOM additions, because the  $\text{CO}_2$  emissions from the  $< 0.05\%$  C of the ashed soil were not negligibly small in comparison to PyOM-derived emissions. (This was evident because the initial  $\delta^{13}\text{C}$  of the  $\text{CO}_2$  emissions from the pot with ashed soil and PyOM additions was calculated to be  $+16\pm 5\%$ . This value is substantially lower than we would expect it to be if the  $\text{CO}_2$  emissions were only derived from PyOM (see Tables 2.3 and 2.4), indicating that SOC, with a lower  $\delta^{13}\text{C}$ , is clearly a contributor).

In order to determine the  $\delta^{13}\text{C}$  of microbially-respired PyOM, we designed a PyOM-only incubation in a sand matrix. Six identical mixtures of 19.20 g quartz sand (ashed at 550°C for 2 h to remove any C) and 0.80 g PyOM were created in amber glass 50 mL vials, with Hoagland's nutrient solution (Table S2), a microbial inoculum, and deionized water added to bring the mixture to 60% WFPS. Vials were sealed, and each was sampled through a polytetrafluoroethylene silicone septum for  $^{13}\text{CO}_2$  analysis on the GC-MS at a different timepoint over the course of a day. Their  $[\text{CO}_2]$  and  $\delta^{13}\text{C}$  values were used to construct a Keeling plot in order to determine the  $\delta^{13}\text{C}$  of respired PyOM. In order to ensure that any C added in the microbial inoculum did not affect the  $\delta^{13}\text{C}$  values, the microbial inoculum was derived from a water extraction of a PyOM-sand incubation, which, in turn, had been inoculated with a water extract of another PyOM-sand incubation, which had originally been inoculated with a 1:50 (m:v) soil-water extraction from the pots with PyOM additions. Thus, we aimed to ensure that the  $\delta^{13}\text{C}$  of the microbial addition would resemble the  $\delta^{13}\text{C}$  of the PyOM.

### 2.2.8 Data analysis

Soil  $\text{CO}_2$  emission rates were calculated by fitting a quadratic curve to a  $[\text{CO}_2]$  vs. time plot, and using the slope of the first derivative (*i.e.*, slope at  $t=0$ ) to represent the emissions rate. Where possible, these emissions were partitioned between SOC-derived  $\text{CO}_2$  and PyOM-derived  $\text{CO}_2$  using stable isotopic partitioning (Werth and Kuzyakov, 2010):

$$f_{\text{PyOM}} = (\delta^{13}\text{C}_{\text{Total}} - \delta^{13}\text{C}_{\text{Soil}}) / (\delta^{13}\text{C}_{\text{PyOM}} - \delta^{13}\text{C}_{\text{Soil}}) \text{ and}$$

$$f_{\text{Soil}} = 1 - f_{\text{PyOM}},$$

where  $f_{\text{PyOM}}$  represents the fraction of total  $\text{CO}_2$  emissions attributable to PyOM,  $\delta^{13}\text{C}_{\text{Total}}$  is the measured  $\delta^{13}\text{C}$  signature of the combined sources,  $\delta^{13}\text{C}_{\text{Soil}}$  is the measured  $\delta^{13}\text{C}$  signature of the soil, and  $\delta^{13}\text{C}_{\text{PyOM}}$  is the  $\delta^{13}\text{C}$  signature of the PyOM. The end-member  $\delta^{13}\text{C}$  values chosen to represent SOC and PyOM were the  $\delta^{13}\text{C}$  signature of the emissions from the pots without PyOM on the corresponding day and the  $\delta^{13}\text{C}$  value measured during the PyOM-only incubation. (Further details and background on stable isotope partitioning are provided in the supplementary information.)

Final total belowground C was partitioned between SOC and either corn- or PyOM-derived C for the two-component pots, using the  $\delta^{13}\text{C}$  of the final soil-only pot, the corn roots, or the bulk PyOM, respectively, as the end-member  $\delta^{13}\text{C}$  values. We cannot conclusively partition the final C stocks in the pots with both plants and PyOM into three pools using only two isotopes. However, we can partition the total belowground C from these pots between (PyOM) and [SOC + corn-derived C] by making reasonable assumptions about the range of  $\delta^{13}\text{C}$  values expected for the [SOC + corn-derived C] pool. We might predict that it would lie between a lower value equivalent to that of the final soil-only pots and an upper value that represents some combination of the soil and the corn. We could use the final value from the soil+corn pots, but if the corn deposited more C in the soil in the three-component pots or those pots experienced greater SOC mineralization, corn-derived C would account for a larger fraction of the total belowground C and shift its  $\delta^{13}\text{C}$  signature to a higher value. To account for this fact, we also considered an extreme scenario where corn-derived C makes up 10% of the total [SOC + corn-derived C] (as compared to < 1% observed in the soil + corn only pots). We then partitioned the total C in the

three-component pots using both the upper and lower possible  $\delta^{13}\text{C}$  values to represent the  $\delta^{13}\text{C}$  of the [SOC + corn-derived C] fraction.

Where applicable, ANOVAs were used to detect significant treatment effects, after which Tukey's HSD was used to compare treatments. For paired or single comparisons, *t*-tests were used. Significance levels are  $p < 0.05$  unless otherwise stated. Statistical analyses were performed using JMP 9 software (SAS Institute Inc.).

## **2.3 Results**

### *2.3.1 CO<sub>2</sub> emission rates and plant growth*

Total CO<sub>2</sub> emission rates were significantly higher with PyOM additions at days 1 and 4 for all pots (Figure 2.1). CO<sub>2</sub> emission rates decreased over the first three weeks in all pots. Corn plants emerged on day 3, and after two weeks, the CO<sub>2</sub> emissions from pots with plants were significantly higher than without plants ( $p < 0.001$ ) as the corn plants grew larger, indicating a significant contribution from root respiration.

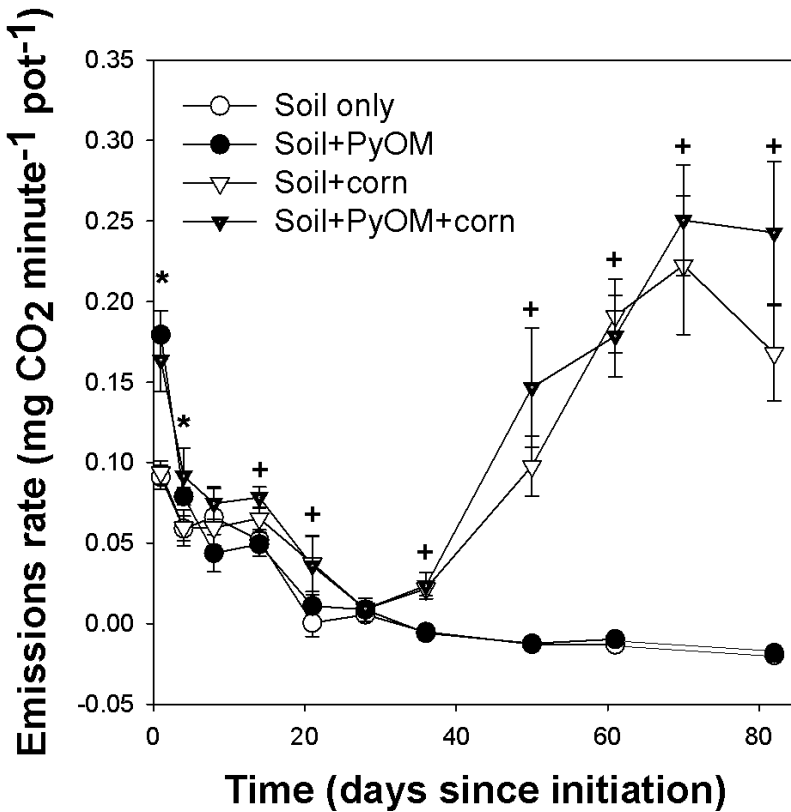


**Figure 2.1.** Emissions rate over time. Error bars are  $\pm 1SE$ . \* indicates significant differences between the +PyOM and -PyOM pots ( $t$ -test,  $p < 0.05$ ,  $n=12$ ), and + indicates significant differences between the +corn and -corn pots ( $t$ -test,  $p < 0.05$ ,  $n = 6$ ).

Although there seems to be a slight trend toward increased plant growth in soils that received PyOM, PyOM additions did not significantly increase above-ground ( $p=0.25$ ), below-ground ( $p=0.15$ ), or total ( $p=0.19$ ) plant biomass (Figure 2.S2).

### 2.3.2. $\delta^{13}C$ signature end-members for soil, PyOM, and corn respiration

Soil DOC was significantly enriched in  $^{13}C$  relative to the bulk SOC (Table 2.3). The final  $\delta^{13}C$  of the DOC in soil without plants or PyOM was significantly depleted in  $^{13}C$  compared to its

initial value. The CO<sub>2</sub> evolved from soil without plants or PyOM was depleted in <sup>13</sup>C relative to the bulk SOC on day 1, but was enriched in <sup>13</sup>C by day 8 (Table 2.3).

**Table 2.3** Mean  $\delta^{13}\text{C}$  signature of SOC end-members. Letters indicate significant differences (Tukey's HSD,  $p < 0.05$ ).

Component	$\delta^{13}\text{C}$ (SE) (‰)	n
Initial bulk SOC	-25.93 (0.10) c	4
Final bulk SOC	-25.98 (0.04) c	6
Initial DOC	-24.05 (0.04) a	6
Final DOC	-24.31 (0.04) b	6
Microbial biomass	Not significantly different from bulk SOC	3
CO <sub>2</sub> evolved from soil-only pots (Day 1; Day 8)	-26.73 (0.30) ( $R^2=0.99$ for Keeling plot); -24.80 (0.34) ( $R^2=0.99$ for Keeling plot)	6

The  $\delta^{13}\text{C}$  of the CO<sub>2</sub> evolved from the incubation of PyOM alone was not significantly different from the  $\delta^{13}\text{C}$  value of a bulk sample of PyOM (Table 2.4). However, the DOC from PyOM was significantly more enriched in <sup>13</sup>C, while the tars evolved and captured during PyOM production were significantly depleted in <sup>13</sup>C.

**Table 2.4**  $\delta^{13}\text{C}$  signature of PyOM components (*A. saccharum* pyrolyzed at 350°C). Different letters indicate significant differences (ANOVA, Tukey's HSD,  $p < 0.05$ ).

Component	$\delta^{13}\text{C}$ (SE) (‰)	n
Original material	+26.5 (1.0) b	3
DOC	+67.4 (1.7) a	5
Bulk PyOM	+27.2 (0.2) b	5
CO <sub>2</sub> evolved during PyOM-sand incubation ( $R^2=0.99$ )	+27.0 (0.6) b	6
Tars evolved and condensed during PyOM production	+22.4 (0.1) c	6

The  $\delta^{13}\text{C}$  values of bulk corn shoots or roots did not differ at the end of the trial within or between pots with or without PyOM. Therefore, the combined mean values for pots with and without PyOM are reported (Table 5). Root sugars were significantly enriched in  $^{13}\text{C}$  compared to bulk plant tissue. The sugars extracted from plant roots with PyOM additions were slightly enriched in  $^{13}\text{C}$  compared to the sugars from those without PyOM additions (by +0.42‰). However, because replicate root sugar samples had to be combined to achieve sufficient mass for analysis, it is not possible to determine whether these two values are significantly different. Because root respiration signatures are only reported from sampling dates where the  $R^2$  value of the Keeling plot was greater than 0.90, they are only available for later sampling dates, when the plants had reached relative maturity and substantially overwhelmed any trace emissions from remaining soil C in the ashed soil pots (initially 0.05% C). The  $\delta^{13}\text{C}$  of the  $\text{CO}_2$  evolved from the roots in the ashed soil was enriched in  $^{13}\text{C}$  relative to final bulk plant tissue on day 21 and depleted on day 36. However, because the plant tissue was not sampled until the end of the trial, it is not necessarily appropriate to compare these values directly.

**Table 2.5** Mean  $\delta^{13}\text{C}$  signature of *Zea mays* L. components, combined for plants grown with or without PyOM.

<b>Component</b>	<b><math>\delta^{13}\text{C}</math> (SE) (‰)</b>
Bulk shoots	-13.92 (0.05)
Bulk roots	-13.90 (0.05)
Root sugars	-12.81 (0.12)
$\text{CO}_2$ evolved from plant in	-13.50 (0.25) ( $R^2=0.99$ );
ashed soil (Day 21; Day 36)	-14.68 (0.37) ( $R^2=0.99$ )

### 2.3.3 $^{13}\text{C}$ partitioning of $\text{CO}_2$ emissions

SOC-derived  $\text{CO}_2$  emissions were lower with than without PyOM additions on day 1 ( $t$ -test,  $p < 0.05$ ) (Figure 2.2). However, SOC-derived  $\text{CO}_2$  emissions were not affected by PyOM additions by day 8. This indicates that short-term negative priming of SOC by PyOM occurred. Because emissions were partitioned between PyOM and SOC only on dates where the  $R^2$  values for the calculated Keeling plot were greater than 0.90, partitioning data are only presented for days 1 and 8. These were also the only two sampling days where PyOM additions significantly increased respiration rates, suggesting that results from these dates might capture the bulk of any short-term PyOM priming effects due to additions of easily mineralizable C.

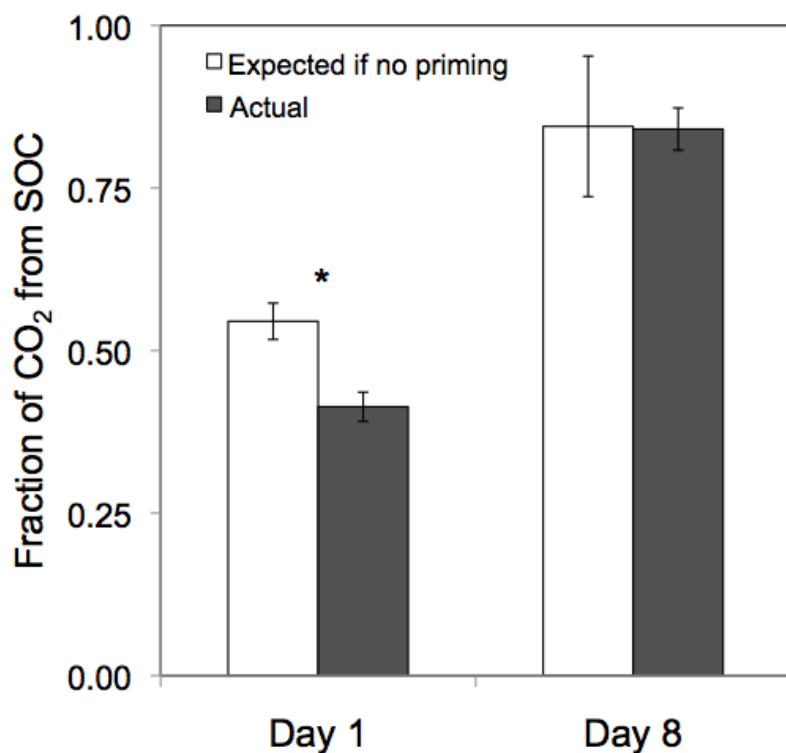


**Figure 2.2** Fraction of CO<sub>2</sub> emissions from SOC in soils with PyOM predicted under a no-priming scenario (white bars) and actual fraction, calculated using  $\delta^{13}\text{C}$  partitioning (grey bars), on days 1 (n=12) and 8 (n=6: emission rates from day 8 only include pots without corn plants). Error bars represent  $\pm 1$  SE. \* indicates a significant difference between the two treatments (*t*-test,  $p < 0.05$ ).

#### 2.3.4 $^{13}\text{C}$ Partitioning of Bulk Soil C

Only PyOM additions significantly shifted the final  $\delta^{13}\text{C}$  values of bulk SOC ( $p < 0.0001$ ), while for DOC, both PyOM additions ( $p=0.014$ ) and corn plants ( $p < 0.0001$ ) significantly changed the final  $\delta^{13}\text{C}$  values (Figure 2.3).

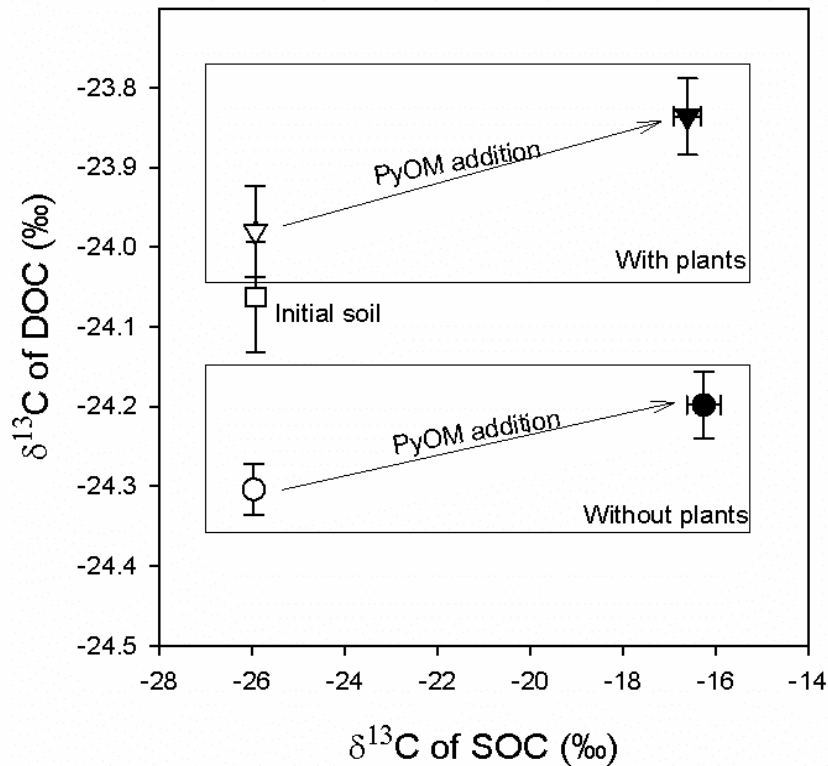


**Figure 2.3**  $\delta^{13}\text{C}$  values of DOC and SOC at the end of the experiment (black symbols = with PyOM; white symbols = without PyOM; circles = no corn; triangles = with corn; white square = initial soil). Error bars represent  $\pm 1\text{SE}$  ( $n =$  in Table 2.3).

Total C significantly decreased from initial values in pots without PyOM additions (paired  $t$ -test,  $p < 0.0001$ ), but did not decrease in pots with PyOM additions (paired  $t$ -test,  $p=0.21$ ).

Partitioning the final total C between SOC and corn-derived C or PyOM revealed significant SOC losses in the pots with no additions ( $t$ -test,  $p=0.006$ ) and with corn plants ( $t$ -test,  $p=0.0005$ ), while pots with PyOM additions experienced no significant SOC losses over the course of the experiment ( $t$ -test,  $p=0.57$ ). Significantly less SOC (3.09% less) remained in the pots with corn ( $t$ -test,  $p=0.04$ ) (Figure 2.4).

Partitioning the final soil C in the three-component pot yields a range of  $84.1 \pm 1.2$  to  $84.3 \pm 1.3$  g of [SOC + corn-derived C]. Both of these values are significantly higher ( $p=0.007$  and  $p=0.005$ ,

respectively) than the final total C measured in the pots with corn plants ( $79.3 \pm 0.8$  g) (Figure 2.4).

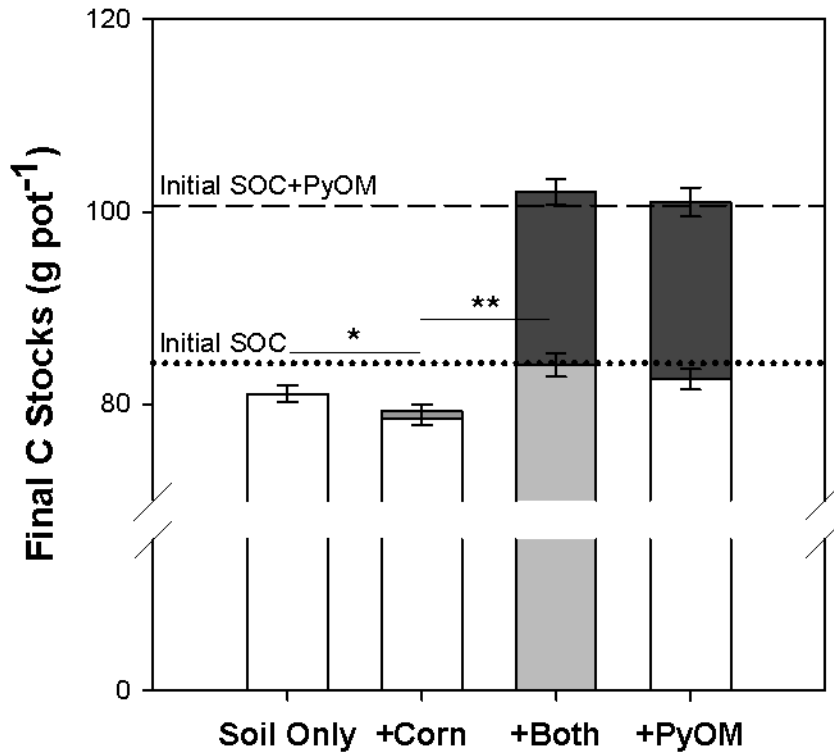


**Figure 2.4** Total final C stocks after  $^{13}\text{C}$  partitioning. SOC is represented by the white bars, corn and PyOM-derived C are represented by dark grey bars, and the unpartitioned [SOC + corn-derived C] in the +Both treatment is represented by the light grey bar. Dashed line represents initial SOC+PyOM-C stocks, while dotted line represents initial SOC stocks. Horizontal lines and stars indicate significant differences in SOC (\*) or [SOC + corn-derived C] stocks (\*\*). Error bars represent  $\pm\text{SE}$  ( $n = 6$ , except for the +PyOM+corn, for which  $n=5$ ). Note y-axis is broken to show detail.

## 2.4 Discussion

### 2.4.1 CO<sub>2</sub> emission rates

Our finding that a non-negligible fraction of PyOM is very labile and easily metabolized by microorganisms during the first week is consistent with other studies (Nguyen and Lehmann, 2009; Nocentini *et al.*, 2010; Jones *et al.*, 2011). This fraction was likely quickly depleted, mirroring the decrease in net respiration rate over time. This is a common pattern in incubated soils, where emissions decrease over time as easily mineralizable C - such as that released from protective aggregates during sieving and the drying-rewetting process - is depleted.

There was no detectable effect of PyOM on net emission rates by the time the corn was sufficiently large to contribute substantially to the soil CO<sub>2</sub> emissions, which supports the biomass data in showing that the PyOM did not have a significant effect on corn growth. However, this lack of an apparent PyOM effect on net soil CO<sub>2</sub> emissions in the pots with corn plants could also be the result of processes with opposite effects. *E.g.*, if PyOM additions increased plant growth, and, thus, root respiration, but at the same time exerted negative priming pressure on either SOC or root exudate-C, the net impact on CO<sub>2</sub> emissions could be unchanged. This highlights the need for three-part partitioning or other approaches (*e.g.*, Kuzyakov and Bol, 2004; Albanito *et al.*, 2012) to detect such complex effects in future studies.

The shift to negative net CO<sub>2</sub> emission rates in the pots without plants after 30 days could be explained by at least two factors. Initially, we speculated that this may have been a result of

microbial nitrification - an autotrophic, C-fixing process where microbes use  $\text{NH}_4^+$  as an electron donor for respiration, producing  $\text{NO}_3^-$ . The high nutrient levels in the pots from repeated fertilizer applications, without plants present to take up the nutrients, would have created favourable conditions for nitrification. Assuming a ratio of between 0.04-0.07 mol C fixed per mol  $\text{NO}_2$  or  $\text{NO}_3$  produced (Glover, 1985), this would predict nitrification rates of between 8-17 mg N consumed  $\text{kg dry soil}^{-1} \text{ day}^{-1}$ . While these values are 1.5-3x higher than measured rates in some natural systems (*e.g.*, Cheng *et al.*, 2011; Zhang *et al.*, 2011), they are of the same order of magnitude, and would be expected to be high in such a low-C high-N environment, which would strongly favour nitrification. The second explanatory hypothesis is that some degree of photosynthesis was taking place. Upon disassembly of the pots, small green patches of algae or cyanobacteria were discovered growing on the insides of the pots, which must have allowed some fraction of photosynthetically active radiation to reach the soils through their white plastic walls. If these photosynthesized at the same rate as the maximum observed by Su *et al.* (2012) for algal-cyanobacterial crusts, then only 2% of the pot's sides would need to be covered to account for the observed  $\text{CO}_2$  depletion. Even though the Su *et al.* (2012) rates are much higher than what would be expected on pot walls in this trial, it demonstrates that even a small amount of photosynthesis could also account for the observed net negative  $\text{CO}_2$  flux from the soil. Thus, either explanation - nitrification or photosynthesis - may be plausible. However, while this is an interesting finding, it does not impact our conclusions regarding short-term negative priming, as the net negative fluxes only occurred during the latter two months, and the fluxes were not significantly different between the pots with and without PyOM.

#### 2.4.2 $\delta^{13}\text{C}$ signature end-members for soil, PyOM, and corn respiration

During this study we determined which isotopic end-members were optimal to represent soil, PyOM, and plant root respiration. While DOC was significantly enriched in  $^{13}\text{C}$  relative to bulk SOC, the  $\delta^{13}\text{C}$  of the respired  $\text{CO}_2$  from the soil-only pots was initially depleted relative to both of these values (day 1), but was relatively enriched in  $^{13}\text{C}$  compared to bulk SOC by day 8. These findings are consistent with Werth and Kuzyakov's review (Werth and Kuzyakov, 2010), where they found that DOC tends to be marginally enriched in  $^{13}\text{C}$  relative to bulk SOC, but that  $\text{CO}_2$  emitted from soils ranges between being depleted and enriched. Thus, while for day 1, the bulk SOC would have been a more appropriate end-member, for day 8, DOC would have been a better end-member. However, no matter which end-member is used in the isotopic partitioning calculations, we still detect negative priming on day 1. Thus, while our data support the importance of directly measuring the  $\delta^{13}\text{C}$  values of soil respiration, they also indicate that if that is not possible, using either SOC or DOC as a end-member may not be a problem, depending on the system.

Similarly to soil respiration, we found that the  $\delta^{13}\text{C}$  of root-respired C changed significantly over the course of the study, becoming more depleted in  $^{13}\text{C}$  between days 21 and 36. This could represent shifting metabolic sources for the corn roots as the plants matured. The  $\delta^{13}\text{C}$  values of respired  $\text{CO}_2$  at these times were enriched and depleted in  $^{13}\text{C}$ , respectively, in relation to the final  $\delta^{13}\text{C}$  values of the corn shoots and roots (which were not significantly different from each other). This is consistent with previous studies, which have found a range of effects, with a number reporting both  $^{13}\text{C}$  depletion and enrichment in root-respired  $\text{CO}_2$  compared to root biomass (Werth and Kuzyakov, 2010). Contrary to our expectations, root sugars were not a good

end-member for the respired CO<sub>2</sub>, because they were significantly enriched in <sup>13</sup>C. This agrees with the observation of previous researchers that sugars tend to be enriched in <sup>13</sup>C compared to other plant tissues (Badeck *et al.*, 2005; Bowling *et al.*, 2008). Still, because the bulk roots and sugars were measured destructively only at the end of the experiment, some caution should be taken when comparing them to root respiration measurements taken during the experiment.

For PyOM end-members, we found that different sub-components had significantly different  $\delta^{13}\text{C}$  signatures, the most striking being strong <sup>13</sup>C enrichment in DOC from PyOM and a depletion in the condensed PyOM tars. Materials such as cellulose, starches, and sucrose tend to be enriched in <sup>13</sup>C (Ehleringer *et al.*, 2000), some of which would be expected to be extracted in the water-soluble PyOM fraction. Because lipids and lignins tend to be depleted in <sup>13</sup>C (Bowling *et al.*, 2008), this might indicate that the tars were derived more from one or both of these compound types. Additionally, fractionation could have occurred while the tars were being volatilized: during both chemical and physical fractionation, the heavier isotope is usually discriminated against (Hobbie and Werner, 2004), resulting in a product (here, tars) that is depleted in that isotope. These results are somewhat compatible with those of Czimeczik *et al.* (2002), who found that volatiles were depleted in <sup>13</sup>C relative to PyOM for lower-temperature PyOM materials, although their data show the opposite trend for chars created at temperatures within the range of those used in this experiment. What was surprising to us, given these differences in DOC from PyOM and tars, was that the  $\delta^{13}\text{C}$  of what was actually respired in the PyOM-only incubation was not significantly different from that of the bulk PyOM. We expect that this does not indicate that all portions of the bulk PyOM were respired proportionally to their abundance: Zimmerman *et al.* (2011) found that the  $\delta^{13}\text{C}$  signature of respired lower-temperature

PyOMs after 15-21 days tended to be depleted in comparison to the original bulk materials, but not by a consistent amount. In our case, we suggest that the combination of sub-components that were respired just happened to match the bulk signature of PyOM in this case (and would expect it to change over time, as was seen by Zimmerman *et al.* (2011)).

We considered the possibility that these differences in  $\delta^{13}\text{C}$  values of PyOM materials were an artifact of the isotopic labelling process. For example, if the  $^{13}\text{C}$  label was incorporated disproportionately into sugars and other water-soluble components, we might see these results. However, shifts of a proportional magnitude observed in PyOM produced from unlabelled *Acer saccharum* wood under the same production conditions indicate this is not the case (Figure 2.S3 and Table 2.S3). Thus, this effect of isotopic fractionation between PyOM sub-components does not seem to be simply an artifact of biomass labelling, and should be accounted for in all PyOM studies.

#### 2.4.3 Priming of SOC by PyOM without plant influence

The observed negative priming appears to have taken place primarily during the first few days after the experiment's initiation, since SOC-derived  $\text{CO}_2$  emissions were not affected by PyOM additions on day 8, and total emission rates declined in pots without plants over time. Indeed, by the end of the experiment, there was not a significant difference in total SOC remaining in pots with or without PyOM. The short-term negative priming in this system would be consistent with the model proposed by Blagodatskaya and Kuzyakov (2008), who find that when the easily available organic C added is in excess of 50% of the microbial biomass C, negative priming

effects may be observed. The DOC from PyOM additions was equal to 1.3 times the extracted initial microbial biomass C (Tables 2.1 and 2.2). Because this effect was seen so rapidly and transiently, it may give clues as to the mechanism responsible for this priming. Jones *et al.* (2011) and Zimmerman *et al.* (2011) suggest that PyOM sorption of SOM or enzymes may be the most likely explanation for their observations of negative priming, which occurred later in their incubation experiments. Depending on the mechanism through which direct PyOM stabilization of SOC takes place, we might not predict that this was the dominant mechanism observed in this experiment: if direct stabilization was the mechanism driving the negative priming effect seen here, it would indicate that the stabilization occurred within the first 24 hours (since negative priming was seen on day 1), but by day 8, this postulated sorption effect was no longer detectable in soil emissions. If this were the case, it would seem to indicate that the sorption capacity of the PyOM was rapidly filled, which is conceivable, although not consistent with the prolonged and later-appearing negative priming effects observed in previous studies. We suggest that a more likely candidate mechanism in this study would be a combination of substrate switching and the “dilution” effect. Because the soils were pre-incubated for two weeks before the corn seeds and PyOM were applied, in order to bring them to a relatively stable state, we might predict that the fraction of the PyOM additions that was readily accessible by microbes was either equivalent to (dilution effect) or “more appealing” than (substrate switching) the SOC. Because total emissions increased with the addition of PyOM, this indicates that the dilution effect could not be entirely responsible, and that some degree of true substrate switching would have occurred, should these mechanisms be the correct ones. Because these soils developed under forested conditions, we may expect that the potential microbial community would have been regularly exposed to relatively complex C substrates, such as tree litter-derived lignin. This

could lend support to both the substrate switching hypothesis - existing SOC may be less appealing than added PyOM - and the dilution effect hypothesis - dilution might occur even if the available PyOM were somewhat “unappealing”. We suggest that N inhibition of SOC mineralization is not a likely reason for the negative priming because (1) substantial levels of N were added to all pots as fertilizer and (2) PyOM additions would have had a negligible effect on available N levels (Tables 1 and 2).

#### *2.4.4 PyOM effects on priming with plants*

The positive priming of SOC by corn is consistent with previous studies (Dijkstra and Cheng, 2007; Bird *et al.*, 2011), where active plant roots increased SOC losses. However, when PyOM was present along with plants, there was no significant loss in total C, suggesting that the increased SOC losses with plants present were counteracted by the presence of PyOM. This is consistent with the findings of Slavich *et al.* (2013), who noted increases in total soil C with PyOM additions in a ryegrass system beyond the increase expected by the addition of the PyOM. However, because of their experimental design, they were not able to partition their total soil C between SOC, PyOM, and plant sources. Our findings further expand our understanding of these interactions, by conclusively revealing no significant losses of PyOM while confirming SOM losses under corn plants without PyOM additions. Partitioning the total C between PyOM and [SOC + corn-derived C] revealed that significantly more [SOC + corn-derived C] remained in the pots with PyOM than those without, indicating that PyOM additions counteracted the positive priming of SOC caused by corn. However, it is not possible to say conclusively whether (1) the addition of PyOM to the planted soil changed the effects of corn on SOC, (2) the positive

priming of SOC by corn remained the same but was offset by negative priming of SOC by PyOM, (3) the PyOM increased the contribution of corn C to total C (this is somewhat unlikely, as PyOM additions did not significantly increase plant root respiration or total biomass), or (4) some combination of the above occurred. We suggest that the presence of active plants in the system should be expected to alter priming dynamics between PyOM and SOC, but that more complex methodological approaches are needed to isolate the three different components.

#### *2.4.5 Conclusions*

PyOM additions to soil caused short-term negative priming of SOC, primarily occurring during the first week after PyOM additions. This negative priming of SOC by PyOM may be due to transient effects of labile PyOM additions to the system, through a combination of substrate switching and dilution. Additionally, PyOM additions counteracted the SOC losses incurred in the presence of corn plants, by decreasing SOC mineralization, increasing corn-derived C additions to the soil, or a combination of the two. These findings have important implications for future studies, since no PyOM-SOC priming studies of which we are aware to date that allowed partitioning between PyOM and SOC have included plants.

The  $\delta^{13}\text{C}$  values of different sub-components of PyOM are significantly different. While in this study, the best end-member for PyOM-derived  $\text{CO}_2$  emissions was simply the bulk PyOM  $\delta^{13}\text{C}$  signature, these findings highlight the need for further research into what fractions of PyOM are respired by microbes. An interesting direction of future study would be to further investigate this phenomenon, measuring the  $\delta^{13}\text{C}$  values of different sub-components of PyOM, developing a

fractionation process that is functionally meaningful, to identify which sub-components of PyOM contribute the most to respiration, over varying timescales. Systematically exchanging extractable fractions between PyOM samples that are identical except for their  $\delta^{13}\text{C}$  signatures, similar to a “reciprocal transplant” approach, and subsequently measuring the  $\delta^{13}\text{C}$  of respired  $\text{CO}_2$  would be an ideal approach.

SUPPLEMENTARY INFORMATION FOR CHAPTER TWO - PYROGENIC CARBON  
ADDITIONS TO SOIL COUNTERACT POSITIVE PRIMING OF SOIL CARBON  
DECOMPOSITION BY PLANTS

*2.S1 Details on isotopic partitioning*

A key tool for priming research is the use of stable C isotopes,  $^{12}\text{C}$  and  $^{13}\text{C}$ , to differentiate the original sources of a common product in a two-part system. Briefly, the use of  $^{13}\text{C}$  isotopic tracers for SOC studies derives from the contrasting metabolic pathways of  $\text{C}_3$  and  $\text{C}_4$  plants. During photosynthetic uptake of  $\text{CO}_2$ ,  $\text{C}_3$  plants discriminate more against the rare  $^{13}\text{C}$  stable C isotope than  $\text{C}_4$  plants (Farquhar *et al.*, 1989; O’Leary, 1988). Terrestrial plants with the  $\text{C}_3$  pathway have  $\delta^{13}\text{C}$  values (“ $\delta^{13}\text{C}$ ” ties the measured  $^{13}\text{C}/^{12}\text{C}$  to a standard  $^{13}\text{C}/^{12}\text{C}$  ratio) in the range of -32‰ to -22‰. Plants with  $\text{C}_4$  pathway have higher  $\delta^{13}\text{C}$  values, ranging from -17‰ to -9‰ (Boutton, 1991). Furthermore, over time, the isotopic composition of SOC grows to closely resemble the isotopic composition of the vegetation from which it has been derived (Ågren *et al.*, 1996). Thus, given a pool of C, such as soil  $\text{CO}_2$  emissions, and knowing the  $\delta^{13}\text{C}$  values of its two C sources, one can mathematically derive what fraction each source contributed to the whole (Werth and Kuzyakov, 2010). In an experiment where a  $\text{C}_4$  plant is grown on a soil developed under  $\text{C}_3$  vegetation, we could derive the fraction of total soil  $\text{CO}_2$  emissions that are from this plant as compared to those from the  $\text{C}_3$  soil using the equation:

$$f_{\text{C}_4\text{veg}} = \frac{\delta_T - \delta_{\text{C}_3\text{soil}}}{\delta_{\text{C}_4\text{veg}} - \delta_{\text{C}_3\text{soil}}},$$

where  $f_{\text{C}_4\text{veg}}$  is the fraction of  $\text{CO}_2$  contributed by the  $\text{C}_4$  plant,  $\delta$  is the  $\delta^{13}\text{C}$  signature of the total  $\text{CO}_2$  ( $\delta_T$ ), the  $\text{C}_3$  soil ( $\delta_{\text{C}_3\text{soil}}$ ), and the  $\text{C}_4$  vegetation ( $\delta_{\text{C}_4\text{veg}}$ ) (Werth and Kuzyakov, 2010).

## 2.S2 Notes on the challenges of applying isotopic partitioning

Although isotopic partitioning is an elegant concept, it can be challenging to apply, because a consistent approach does not exist for choosing what biomass (shoots, roots, or sugars in roots) or soil C (dissolved organic C [DOC], SOC, or microbial biomass) component is the best end-member for the  $\delta^{13}\text{C}$  of the  $\text{CO}_2$  emitted from the plant or the soil. If they all shared the same  $\delta^{13}\text{C}$ , this would not be a problem, but important isotopic fractionation can happen at coarse (roots *vs.* shoots) to fine (carbohydrates *vs.* lignin) levels. For example, the  $\delta^{13}\text{C}$  of roots and the  $\text{CO}_2$  they emit can differ by over 5‰ (Werth and Kuzyakov, 2010). We expect that PyOM also suffers from these issues. Czimczik *et al.* (2002) found that PyOM produced at lower charring temperatures was enriched in  $^{13}\text{C}$  relative to the initial biomass, while higher temperatures resulted in a  $^{13}\text{C}$  depletion. The volatiles released at each charring step ranged widely (by as much as 10‰ in softwood), likely due to the varied temperature ranges over which different compounds (characterized by different  $\delta^{13}\text{C}$  values) undergo thermal decomposition. Furthermore, Zimmerman *et al.* (2011) showed that the  $\delta^{13}\text{C}$  of  $\text{CO}_2$  evolved from a PyOM incubation varied substantially over the course of a >500-day incubation. Thus, it is clearly important to identify whether the  $\delta^{13}\text{C}$  of sub-components of PyOM serve as a better end-member for the  $\delta^{13}\text{C}$  of the  $\text{CO}_2$  derived from it than its bulk initial  $\delta^{13}\text{C}$  value.

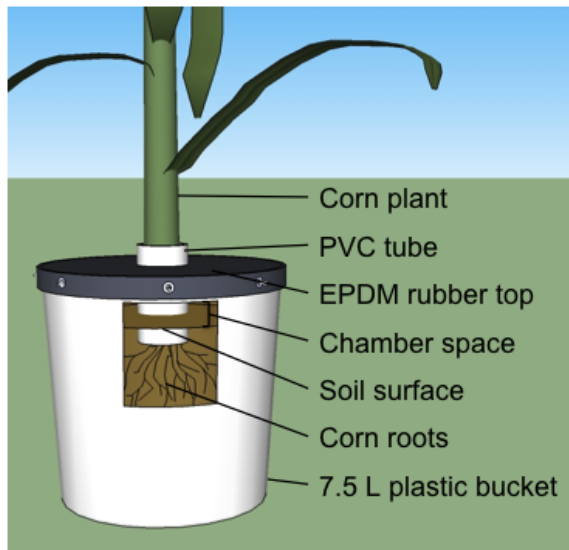


**Figure 2.S1** Pot and chamber design inspired by Yang and Cai (2006). Chamber is shown in closed (sampling) position. Sampling occurs through a rubber septum (not shown) and chamber includes a tube vent to prevent pressure changes (not shown).

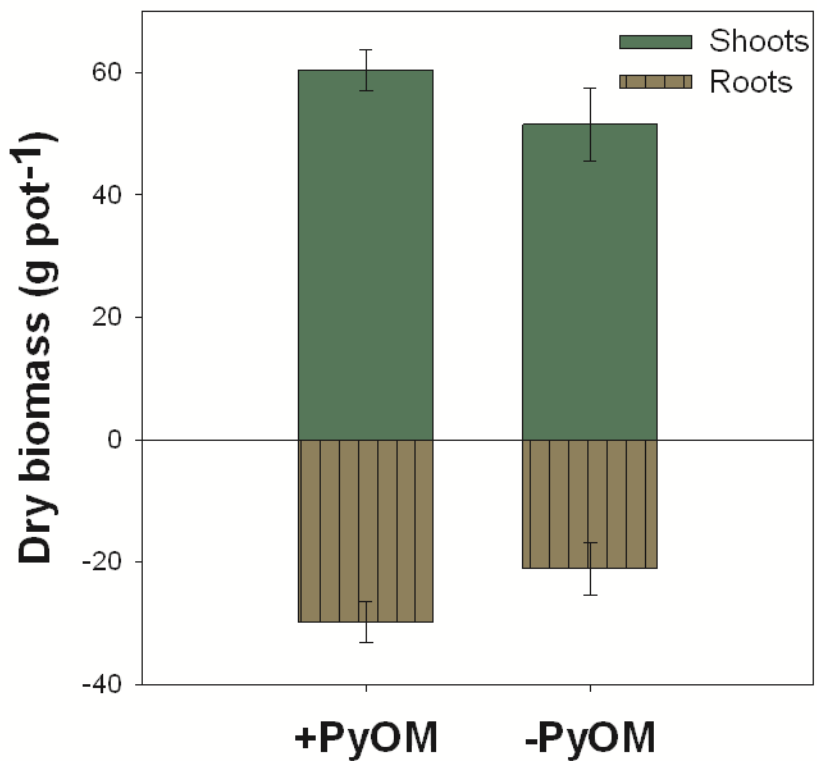


**Figure 2.S2** Biomass production with and without PyOM additions. Error bars represent  $\pm 1SE$  ( $n_{+PyOM}=5, n_{-PyOM}=6$ ).

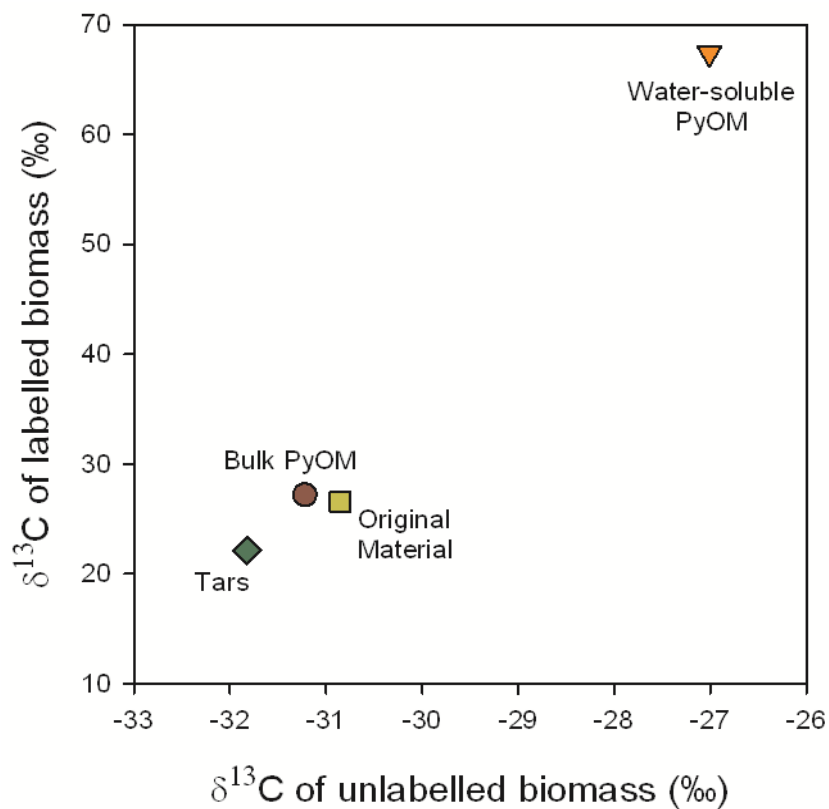


**Figure 2.S3** Comparison of  $\delta^{13}\text{C}$  values for labelled and unlabelled sugar maple PyOM and sub-components, including original materials. Water-soluble PyOM is consistently enriched in  $^{13}\text{C}$ , while tars are consistently depleted.

**Table 2.S1** Total elemental analysis of Mehlich III extraction ( $\text{mg kg}^{-1}$ )

Element	Initial soil	Wood feedstock	PyOM
B	19.3	6.6	6.3
Ca	104.8	3280.3	2344.6
Cu	6.9	3.2	0.8
Fe	257.8	20.6	9.1
K	40.4	2482.3	2434.1
Mg	27.8	500.1	230.9
Mn	88.1	502.3	265.1
P	1.0	479.7	360.1
S	21.3	59.6	33.1
Zn	52.1	23.3	8.5

<b>Table 2.S2</b> Modified Hoagland's solution					
<b>Stock</b>	<b>Chemical</b>	<b>Concentration</b>		<b>Final additions per pot</b>	
				<b>- plants</b>	<b>+ plants</b>
Macronutrients	KNO <sub>3</sub>	0.7755	M	54.5	91.8
	MgSO <sub>4</sub>	0.3	M	21.1	35.5
	NH <sub>4</sub> H <sub>2</sub> PO <sub>4</sub>	0.255	M	17.9	30.2
	NH <sub>4</sub> NO <sub>3</sub>	0.33	M	23.2	39.1
Ca	Ca(NO <sub>3</sub> ) <sub>2</sub>	3.75	M	52.3	88.0
Micronutrients	H <sub>3</sub> BO <sub>3</sub>	1.875	mM	0.132	0.222
	MnSO <sub>4</sub>	0.15	mM	0.011	0.018
	ZnSO <sub>4</sub>	0.0375	mM	0.003	0.004
	CuSO <sub>4</sub>	0.0375	mM	0.003	0.004
	Na <sub>2</sub> MoO <sub>4</sub>	0.0375	mM	0.003	0.004
	NiSO <sub>4</sub>	0.06	mM	0.004	0.007
Fe	FeEDTA	93.75	mM	1.306	2.200

<b>Table 2.S3</b> Measured <sup>13</sup> C end-members ( $\delta^{13}\text{C}$ relative to PDB standard $\pm$ SE (‰)) for PyOM		
<b>Sub-component</b>	<b>Unlabelled PyOM</b>	<b>Labelled PyOM</b>
Bulk	-31.22 $\pm$ 0.01 (n=3)	+27.21 $\pm$ 0.19 (n=7)
Dissolved PyOM	-27.01 (n=1)	+67.37 $\pm$ 1.67(n=5)
Tars / volatiles	-31.82 $\pm$ 0.04 (n=4)	+22.15 $\pm$ 0.19 (n=5)
Original wood	-30.85 $\pm$ 0.03 (n=3)	+26.53 $\pm$ 1.04 (n=3)
Respired PyOM	n.d.	+27.04 $\pm$ 0.64 (Keeling plot intercept, n=6)

## REFERENCES

- Ågren, G.I., Bosatta, E., Balesdent, J., 1996. Isotope discrimination during decomposition of organic matter: A theoretical analysis. *Soil Science Society of America Journal* 60, 1121-1126.
- Albanito, F., McAllister, J.L., Cescatti, A., Smith, P., Robinson, D., 2012. Dual-chamber measurements of  $\delta^{13}\text{C}$  of soil-respired  $\text{CO}_2$  partitioned using a field-based three end-member model. *Soil Biology and Biochemistry* 47, 106–115.
- Badeck, F.-W., Tcherkez, G., Nogués, S., Piel, C., Ghashghaie, J., 2005. Post-photosynthetic fractionation of stable carbon isotopes between plant organs--a widespread phenomenon. *Rapid Communications in Mass Spectrometry* 19, 1381–1391.
- Bingeman, C.W., Varner, J.E., Martin, W.P., 1953. The effect of the addition of organic materials on the decomposition of an organic soil. *Soil Science Society of America Journal* 17, 34–38.
- Bird, J.A., Herman, D.J., Firestone, M.K., 2011. Rhizosphere priming of soil organic matter by bacterial groups in a grassland soil. *Soil Biology and Biochemistry* 43, 718–725.
- Bird, M.I., Ascough, P.L., 2012. Isotopes in pyrogenic carbon: A review. *Organic Geochemistry* 42, 1529–1539.
- Blagodatskaya, E., Kuzyakov, Y., 2008. Mechanisms of real and apparent priming effects and their dependence on soil microbial biomass and community structure: critical review. *Biology and Fertility of Soils* 45, 115–131.
- Boutton, T.W., 1991. Stable carbon isotope ratios of natural materials I. Sample preparation and mass spectrometric analysis, in: Coleman, D.C., Fry, B. (Eds.), *Isotopic Techniques in Plant, Soil, and Aquatic Biology: Carbon Isotope Techniques*. Academic Press, Inc., San Diego, California, USA; London, England, UK, pp., 155-172.
- Bowling, D.R., Pataki, D.E., Randerson, J.T., 2008. Carbon isotopes in terrestrial ecosystem pools and  $\text{CO}_2$  fluxes. *New Phytologist* 178, 24–40.
- Brugnoli, E., Hubick, K.T., von Caemmerer, S., Wong, S.C., Farquhar, G.D., 1988. Correlation between the carbon isotope discrimination in leaf starch and sugars of  $\text{C}_3$  plants and the ratio of intercellular and atmospheric partial pressures of carbon dioxide. *Plant Physiology* 88, 1418–1424.
- Cheng, W., Johnson, D.W., Fu, S., 2003. Rhizosphere effects on decomposition. *Soil Science Society of America Journal* 67, 1418.
- Cheng, Y., Cai, Z.-C., Zhang, J.-B., Lang, M., Mary, B., Chang, S.X., 2011. Soil moisture effects on gross nitrification differ between adjacent grassland and forested soils in central Alberta, Canada. *Plant and Soil* 352, 289–301.
- Cross, A., Sohi, S.P., 2011. The priming potential of biochar products in relation to labile carbon contents and soil organic matter status. *Soil Biology and Biochemistry* 43, 2127–2134.
- Czimczik, C.I., Preston, C.M., Schmidt, M.W., Werner, R.A., Schulze, E.-D., 2002. Effects of charring on mass, organic carbon, and stable carbon isotope composition of wood. *Organic Geochemistry* 33, 1207–1223.
- DeLuca, T.H., Aplet, G.H., 2008. Charcoal and carbon storage in forest soils of the Rocky Mountain West. *Frontiers in Ecology and the Environment* 6, 18–24.
- Dijkstra, F.A., Cheng, W., 2007. Interactions between soil and tree roots accelerate long-term soil carbon decomposition. *Ecology Letters* 10, 1046–1053.
- Ehleringer, J.R., Buchmann, N., Flanagan, L.B., 2000. Carbon isotope ratios in belowground

- carbon cycle processes. *Ecological Applications* 10, 412–422.
- Farquhar, G.D., Ehleringer, J.R., Hubick, K.T., 1989. Carbon isotope discrimination and photosynthesis. *Annual Review of Plant Biology* 40, 503–537.
- Fog, K., 1988. The effect of added nitrogen on the rate of decomposition of organic matter. *Biological Reviews* 63, 433–462.
- Forbes, M.S., Raison, R.J., Skjemstad, J.O., 2006. Formation, transformation and transport of black carbon (charcoal) in terrestrial and aquatic ecosystems. *Science of the Total Environment* 370, 190–206.
- Glover, H.E., 1985. The relationship between inorganic nitrogen oxidation and organic carbon production in batch and chemostat cultures of marine nitrifying bacteria. *Archives of Microbiology* 142, 45–50.
- Hobbie, E., Werner, R.A., 2004. Intramolecular, compound - specific, and bulk carbon isotope patterns in C3 and C4 plants: a review and synthesis. *New Phytologist* 161, 371–385.
- Horowitz, M.E., Fahey, T.J., Yavitt, J.B., Feldpausch, T.R., Sherman, R.E., 2009. Patterns of late-season photosynthate movement in sugar maple saplings. *Canadian Journal of Forest Research* 39, 2294–2298.
- Hutchinson, G.L., Mosier, A.R., 1981. Improved soil cover method for field measurement of nitrous oxide fluxes. *Soil Science Society of America Journal* 45, 311–316.
- Jones, D.L., Murphy, D.V., Khalid, M., Ahmad, W., Edwards-Jones, G., DeLuca, T.H., 2011. Short-term biochar-induced increase in soil CO<sub>2</sub> release is both biotically and abiotically mediated. *Soil Biology and Biochemistry* 43, 1723–1731.
- Keiluweit, M., Nico, P.S., Johnson, M.G., Kleber, M., 2010. Dynamic molecular structure of plant biomass-derived black carbon (biochar). *Environmental Science and Technology* 44, 1247–1253.
- Keith, A., Singh, B., Singh, B.P., 2011. Interactive priming of biochar and labile organic matter mineralization in a smectite-rich soil. *Environmental Science and Technology* 45, 9611–9618.
- Knicker, H., 2007. How does fire affect the nature and stability of soil organic nitrogen and carbon? A review. *Biogeochemistry* 85, 91–118.
- Krull, E.S., Swanston, C.W., Skjemstad, J.O., McGowan, J.A., 2006. Importance of charcoal in determining the age and chemistry of organic carbon in surface soils. *Journal of Geophysical Research* 111, G04001.
- Kuhlbusch, T., Crutzen, P.J., 1995. Toward a global estimate of black carbon in residues of vegetation fires representing a sink of atmospheric CO<sub>2</sub> and a source of O<sub>2</sub>. *Global Biogeochemical Cycles* 9, 491–501.
- Kuzyakov, Y., Bol, R., 2004. Using natural <sup>13</sup>C abundances to differentiate between three CO<sub>2</sub> sources during incubation of a grassland soil amended with slurry and sugar. *Journal of Plant Nutrition and Soil Science* 167, 669–677.
- Laird, D.A., 2008. The charcoal vision: A win–win–win scenario for simultaneously producing bioenergy, permanently sequestering carbon, while improving soil and water quality. *Agronomy Journal* 100, 178–181.
- Lehmann, J., 2007. A handful of carbon. *Nature* 447, 143–144.
- Lehmann, J., Skjemstad, J., Sohi, S., Carter, J., Barson, M., Falloon, P., Coleman, K., Woodbury, P., Krull, E., 2008. Australian climate–carbon cycle feedback reduced by soil black carbon. *Nature Geoscience* 1, 832–835.
- Luo, Y., Durenkamp, M., De Nobili, M., Lin, Q., Brookes, P.C., 2011. Short term soil priming

- effects and the mineralisation of biochar following its incorporation to soils of different pH. *Soil Biology and Biochemistry* 43, 2304–2314.
- Major, J., Lehmann, J., Rondon, M., Goodale, C., 2010. Fate of soil-applied black carbon: downward migration, leaching and soil respiration. *Global Change Biology* 16, 1366–1379.
- Mao, J.-D., Johnson, R.L., Lehmann, J., Olk, D.C., Neves, E.G., Thompson, M.L., Schmidt-Rohr, K., 2012. Abundant and stable char residues in soils: implications for soil fertility and carbon sequestration. *Environmental Science and Technology* 46, 9571–9576.
- Masiello, C.A., 2004. New directions in black carbon organic geochemistry. *Marine Chemistry* 92, 201–213.
- Nguyen, B.T., Lehmann, J., 2009. Black carbon decomposition under varying water regimes. *Organic Geochemistry* 40, 846–853.
- Nocentini, C., Guenet, B., Di Mattia, E., Certini, G., Bardoux, G., Rumpel, C., 2010. Charcoal mineralisation potential of microbial inocula from burned and unburned forest soil with and without substrate addition. *Soil Biology and Biochemistry* 42, 1472–1478.
- O'Leary, M.H. 1988. Carbon isotopes in photosynthesis. *Bioscience* 38, 328–336.
- Pataki, D.E., 2003. The application and interpretation of Keeling plots in terrestrial carbon cycle research. *Global Biogeochemical Cycles* 17, 1022.
- Pausch, J., Zhu, B., Kuzyakov, Y., Cheng, W., 2013. Plant inter-species effects on rhizosphere priming of soil organic matter decomposition. *Soil Biology and Biochemistry* 57, 91–99.
- Ramirez, K.S., Craine, J.M., Fierer, N., 2012. Consistent effects of nitrogen amendments on soil microbial communities and processes across biomes. *Global Change Biology* 18, 1918–1927.
- Richter, A., Wanek, W., Werner, R.A., Ghashghaie, J., Jäggi, M., Gessler, A., Brugnoli, E., Hettmann, E., Göttlicher, S.G., Salmon, Y., Bathellier, C., Kodama, N., Nogués, S., Sørensen, A., Volders, F., Sörgel, K., Blöchl, A., Siegwolf, R.T.W., Buchmann, N., Gleixner, G., 2009. Preparation of starch and soluble sugars of plant material for the analysis of carbon isotope composition: a comparison of methods. *Rapid Communications in Mass Spectrometry* 23, 2476–2488.
- Schmidt, M.W., Noack, A.G., 2000. Black carbon in soils and sediments: analysis, distribution, implications, and current challenges. *Global Biogeochemical Cycles* 14, 777–793.
- Skjemstad, J.O., Reicosky, D.C., Wilts, A.R., McGowan, J.A., 2002. Charcoal carbon in US agricultural soils. *Soil Science Society of America Journal* 66, 1249–1255.
- Slavich, P.G., Sinclair, K., Morris, S.G., Kimber, S.W.L., Downie, A., Zwieten, L., 2013. Contrasting effects of manure and green waste biochars on the properties of an acidic ferralsol and productivity of a subtropical pasture. *Plant and Soil* 366, 213–227.
- Su, Y.-G., Li, X.-R., Qi, P.-C., Chen, Y.-W., 2012. Carbon exchange responses of cyanobacterial-algal crusts to dehydration, air temperature, and CO<sub>2</sub> concentration. *Arid Land Research and Management* 26, 44–58.
- Vance, E.D., Brookes, P.C., Jenkinson, D.S., 1987. An extraction method for measuring soil microbial biomass C. *Soil Biology and Biochemistry* 19, 703–707.
- Werth, M., Kuzyakov, Y., 2010. <sup>13</sup>C fractionation at the root-microorganisms-soil interface: A review and outlook for partitioning studies. *Soil Biology and Biochemistry* 42, 1372–1384.
- Whitman, T., Enders, A., Hanley, K., Lehmann, J., 2013. Predicting pyrogenic organic matter mineralization from its initial properties and implications for carbon management. *Organic Geochemistry* 64, 76–83.
- Yang, L.-F., Cai, Z.-C., 2006. Soil respiration during a soybean-growing season. *Pedosphere* 16,

192–200.

Zhang, L.-M., Hu, H.-W., Shen, J.-P., He, J.-Z., 2011. Ammonia-oxidizing archaea have more important role than ammonia-oxidizing bacteria in ammonia oxidation of strongly acidic soils. *The ISME Journal* 6, 1032–1045.

Zimmerman, A.R., Bin Gao, Ahn, M.-Y., 2011. Positive and negative carbon mineralization priming effects among a variety of biochar-amended soils. *Soil Biology and Biochemistry* 43, 1169–1179.

Zsolnay, Á., 2003. Dissolved organic matter: artefacts, definitions, and functions. *Geoderma* 113, 187–209.

## CHAPTER 3

### RELATIVE CARBON MINERALIZABILITY DETERMINES INTERACTIVE PRIMING BETWEEN PYROGENIC ORGANIC MATTER AND SOIL ORGANIC CARBON<sup>1</sup>

#### **Abstract**

Soil organic carbon (SOC) is a critical and active pool in the global C cycle, and the addition of pyrogenic organic matter (PyOM) has been shown to change SOC cycling, increasing or decreasing mineralization rates (often referred to as priming). The reasons for different soil responses to PyOM additions remain elusive. We conducted an incubation trial where we adjusted the amount of easily mineralizable C in the soil, through short (1 day) and long (6 months) pre-incubations, and in 350°C maple wood PyOM, through extraction. We investigated the impact of the relative C mineralizability of the two substances on C mineralization interactions, while excluding pH and nutrient effects and minimizing physical effects. We found greater short-term increases (+20-30%) in SOC mineralization with PyOM additions in the soil pre-incubated for 6 months. This increase in mineralization was proportional to the C mineralization in the added PyOM. Over the longer term, both the 6-month and 1-day pre-incubated soils experienced net ~10% decreases in SOC mineralization with PyOM additions. This was possibly due to stabilization of SOC on PyOM surfaces, an example of which we imaged using nanoscale secondary ion mass spectrometry. Additionally, we showed that increasing the duration of pre-incubation of soils from 1 day to 6 months resulted in a 9-fold

---

<sup>1</sup> To be submitted to Environmental Science and Technology as Whitman, T., Zhu, Z., and Lehmann, J., Relative carbon mineralizability determines interactive priming between pyrogenic organic matter and soil organic carbon.

increase in short-term SOC mineralization with PyOM additions, indicating that there may be no optimal duration of pre-incubation for SOC mineralization studies. We show conclusively that the relative mineralizability of SOC in relation to PyOM-C is an important determinant of the effect of PyOM additions of SOC mineralization.

### **3.1 Introduction**

Soil organic carbon (SOC) stocks are a globally important pool of C, holding more than twice as much C as the atmosphere. The addition of exogenous organic inputs, such as fresh organic matter, plant root exudates, or pyrogenic organic matter (PyOM) are known to affect the cycling of existing soil organic C stocks, sometimes increasing and at times decreasing SOC mineralization rates (Kuzyakov, 2010; Whitman *et al.*, 2014b). These changes in SOC mineralization rates are often referred to as “priming” (Bingeman *et al.*, 1953; Woolf and Lehmann, 2012; Zimmerman *et al.*, 2011), but we will use the specific terms “increased or decreased mineralization” here. Numerous mechanisms have been evoked to explain these observations, and these mechanisms have been revealed to be more complex than initially expected (Fontaine *et al.*, 2003; Kuzyakov, 2010). While the body of work that has focused on fresh organic matter or plant root inputs has certainly helped inform and form the basis for our understanding of PyOM-SOC interactions, PyOM as an input brings a suite of new complexities. These include: high heterogeneity within and between PyOM materials, possible effects of PyOM on soil physical properties, particularly when applied at high rates, chemical effects of PyOM on the soil, particularly pH shifts and mineral nutrient additions in PyOM-associated ash, and the sorptive capacity of PyOM materials. Isolating and controlling for these diverse factors

in order to understand what drives PyOM-SOC interactions is necessarily complex, and is one reason much study to date has focused primarily on identifying the phenomena, rather than systematically testing for specific mechanisms that may inform model building (Woolf and Lehmann, 2012). Still, within the past few years (particularly, since Wardle *et al.*, 2008), investigation into PyOM effects on SOC cycling has grown substantially, expanding our understanding of these dynamics. Reviewed recently by Maestrini *et al.* (2014b) and in Chapter 1, diverse mechanisms can explain both increased and decreased SOC mineralization with the addition of PyOM materials. In this study, we focus on whether and how the relative mineralizability of the PyOM and SOM can determine the impact of PyOM on SOC mineralization, and vice versa. We also consider the sorption of SOC on the surface of PyOM (Maestrini *et al.*, 2014b; Whitman *et al.*, 2014b) as a proposed mechanism for observations of decreased SOC mineralization in the presence of PyOM (Bruun and El-Zehery, 2012; Cross and Sohi, 2011; Stewart *et al.*, 2012; Zimmerman *et al.*, 2011).

PyOM is produced naturally during fires (Czimczik and Masiello, 2007), as well as intentionally for C management (Whitman *et al.*, 2010). Because of its heterogeneity, its interactions with SOC cycling are complex, and may depend on the properties of the specific combination of PyOM and soil. It has been postulated that the easily-decomposable components of PyOM function similarly to fresh organic matter additions (Maestrini *et al.*, 2014b; Whitman *et al.*, 2014b). Thus, the relative amount of easily mineralizable C compounds in PyOM vs. soil organic matter (SOM) could be an important predictor of these interactions. Specifically, if the addition of easily mineralizable PyOM alleviates an energy constraint for soil microbes, soils with less mineralizable SOM may be more prone to enhanced C mineralization (Fontaine *et al.*, 2007).

Similarly, the mineralizability of the SOM and the associated microbial activity of a given soil could influence the mineralization of added PyOM-C. However, achieving a gradient of mineralizability of PyOM-C or SOC is not straightforward. For example, Keith *et al.* (2011) used additions of fresh organic matter along with PyOM to investigate these effects. They found that increasing fresh organic matter additions to soils increased the decomposition of added PyOM, and that the soils with more fresh organic matter experienced decreased SOC mineralization rates with PyOM additions, while soils with no fresh organic matter additions experienced increased mineralization. However, fresh organic matter can be quite different from bulk SOM stocks, and this approach does not necessarily conclusively inform us how soils of different C composition would interact with PyOM additions. Another approach is to compare a diversity of soil types with PyOM produced from different feedstocks and temperatures (Zimmerman *et al.*, 2011). For example, Zimmerman *et al.* (2011) found a larger increase in SOC mineralization when easily mineralizable PyOM materials were added to soils. The complicating factor with this approach is that using different soils and PyOM materials, by necessity, means other key properties, such as pH or ash mineral contents, will differ as well, necessitating a very large sample set in order to control for all potential confounding variables. Therefore, we attempted to manipulate the mineralizability of SOC and PyOM while keeping as many other properties constant as possible, by using pre-incubations of varying lengths for the soil and altering the amount of water-dissolvable compounds in the PyOM (DPyOM).

Pre-incubations are often used to attempt to control for the disruptive effect of sampling, sieving, and/or drying and rewetting soils when investigating SOC mineralization dynamics, but there is no commonly accepted protocol. For example, across 12 recent studies of the effects of PyOM

additions to soil, seven studies did not report any pre-incubation, and those that did ranged from overnight to 23 days, with an average of 10 days (Cross and Sohi, 2011; Fang *et al.*, 2014; Farrell *et al.*, 2013; Jones *et al.*, 2012; Keith *et al.*, 2011; Kuzyakov *et al.*, 2009; Luo *et al.*, 2011; Maestrini *et al.*, 2014a; Singh and Cowie, 2014; Steinbeiss *et al.*, 2009; Stewart *et al.*, 2012; Zimmerman, 2010). If the amount of easily mineralizable SOC determines PyOM-induced changes to SOC mineralization, then the duration of pre-incubation may also affect the extent and direction of these effects.

We therefore studied the effects of PyOM additions on the mineralization of existing SOC as a function of the mineralizability of both PyOM and SOC. We hypothesized that (1) increased mineralizability of PyOM will result in greater increases in SOC mineralization, and soils with less mineralizable SOC will be more susceptible to increased mineralization with PyOM additions; (2) more PyOM-C will be mineralized in the soils with larger amounts of mineralizable SOC and greater microbial activity; and (3) pre-incubating soil for varying durations will alter the C status of the soil, thereby affecting its response to PyOM additions.

## **3.2 Materials and Methods**

### *3.2.1 Soil type and PyOM properties*

The soil (see Whitman *et al.*, 2014a) was collected from a mixed deciduous forest in Dryden, NY, which has not been burned within recorded history. It is dominated by oaks (*Quercus sp.*), red maple (*Acer rubrum*), sugar maple (*Acer saccharum*), white ash (*Fraxinus americana*), beech (*Fagus sp.*), basswood (*Tilia americana*), and hickories (*Carya sp.*), while understory

species include hop hornbeam (*Ostrya virginiana*), musclewood (*Carpinus caroliniana*), and witch hazel (*Hamamelis virginiana*). The soil is a Mardin channery silt loam – a coarse-loamy, mixed, active, mesic Typic Fragiudept. It was collected from the top 0.5 m and was air-dried and sieved (< 2 mm) (Table 3.1).

**Table 3.1** Initial soil properties

Property (units)	Value	
	6 months	24 hours
Texture	(Channery) silt loam	
100% WFPS (g water g <sup>-1</sup> dry soil)	47	
pH (0.01M CaCl <sub>2</sub> )	3.9	
Particle size (mm)	< 2	
% sand	28.1	
% silt	54.7	
% clay	17.2	
Total C (%)	1.07	1.16
Total N (%)	0.11	0.11
C:N (mass)	9.76	10.41
2M KCl extractable NO <sub>3</sub> <sup>-</sup> and NO <sub>2</sub> <sup>-</sup> (mg kg <sup>-1</sup> dry soil)	19.02	3.73
2M KCl extractable NH <sub>4</sub> <sup>+</sup> (mg kg <sup>-1</sup> dry soil)	35.37	20.48
Available P (Mehlich III, mg kg <sup>-1</sup> dry soil)	1.0	1.0
Microbial biomass C ± SE (mg kg <sup>-1</sup> dry soil)	18.7±10.4	17.6±14.8
Water-extractable C <2.5µm ± SE (mg kg <sup>-1</sup> dry soil)	68.7±9.3	171.3±7.7
Water-extractable N <2.5µm ± SE (mg kg <sup>-1</sup> dry soil)	60.4±4.8	37.6±1.1

The PyOM was produced from sugar maple (*Acer saccharum*) twigs grown under a labelled <sup>13</sup>C atmosphere and mineral <sup>15</sup>N additions (Horowitz *et al.*, 2009), milled < 2 mm and pyrolyzed at 325°C in a modified muffle furnace under Ar gas (Table 3.2).

**Table 3.2** Production conditions and initial properties for PyOM and after removal and additions of water-extractable compounds

Property (units)	PyOM treatment		
	High DPyOM	Medium DPyOM	Low DPyOM
Total C <sub>organic</sub> (%)	71	70	71
Total C <sub>inorganic</sub> (%)	0	0	0
Bulk $\delta^{13}\text{C}$ (‰)	+77.8	+77.0	+78.5
Total N (%)	0.9	0.9	0.9
Bulk $\delta^{15}\text{N}$ (‰)	+1038.4	+1027.1	+1050.6
Total H (%)	4.3	4.3	4.4
Total O (%)	20	21	21
C:N (by mass)	79	77	79
H:C <sub>organic</sub> (molar)	1.4	1.4	1.4
O:C <sub>organic</sub> (molar)	0.21	0.23	0.22
2M KCl extractable NO <sub>3</sub> <sup>-</sup> and NO <sub>2</sub> <sup>-</sup> (mg kg <sup>-1</sup> )	3.37	0.41	0.32
2M KCl extractable NH <sub>4</sub> <sup>+</sup> (mg kg <sup>-1</sup> )	0.96	1.46	0.70
Available P (Mehlich III, mg kg <sup>-1</sup> )	49.35	34.22	28.51
pH	Initial pH 8.9; Adjusted to soil pH (3.9)		
Feedstock	Sugar maple twigs		
Particle size (mm)	< 2		
Heating rate (°C min <sup>-1</sup> )	2		
Final pyrolysis temperature (°C)	325		
Residence time (hours)	2		
Surface area (m <sup>2</sup> g <sup>-1</sup> )	115	117	116
Ash (%)	4	4	3
Volatiles (%)	46	45	45
Fixed C (%)	50	51	52

### 3.2.2 Soil pre-incubations

To adjust the relative amount of easily mineralizable SOC without changing other soil properties such as pH, texture, or mineralogy, soils were pre-incubated for two different lengths of time - 6 months, leaving SOC with relatively lower mineralizability (“low easily mineralizable C soil”) and 24 hours, retaining the easily mineralizable SOC (“high easily mineralizable C soil”) - before initiating the experiment. The same air-dried, <2 mm sieved soil was divided into two equal portions. Both were hand-mixed with 27% (w/w<sub>dry</sub>) water (57% WFPS), sealed in an airtight bucket, and incubated at 30°C in the dark for either 6 months or 24 hours before beginning the experiment. The 6-month soil bucket was opened periodically to allow oxygen to be replenished, but likely developed some anaerobic pockets, as was indicated by gleying (Supplementary Figure 3.S1). Still, we did not note the characteristic odours of fermentation products when the bucket was opened, so expect that fully anaerobic zones were limited, and not distributed throughout the soil. Just before the initiation of the experiment, the water contents of both soils were determined and readjusted to be equal at 27% (w/w<sub>dry</sub>). Soils were sieved through a 4-mm sieve immediately before experimental initiation for optimal mixing.

Varying pre-incubation length to alter the characteristics of SOM has multiple implications. While pre-incubation effectively manipulates the SOM status, it would also be expected to affect the soil microbial community composition and activity, so it is difficult to separate or attribute the effects of one from those of the other. A strong benefit of this approach, though, is that it allows us to keep many variables as constant as possible, including pH, nutrients, management

history, texture and mineralogy. It would be challenging to find soils that contrast in organic matter status but not in one or many other ways.

### *3.2.3 Water-extractable PyOM and pH adjustment*

To alter the amount of easily mineralizable PyOM (Luo *et al.*, 2011), water-extractable compounds were removed from PyOM through a series of 3 sequential DIW extractions. PyOM (60 g) was shaken with DIW (300 mL), after which it was syringe filtered through a <0.45  $\mu\text{m}$  C-free glass filter. The resulting extracts were retained, and second and third DIW extractions were performed on the remaining PyOM, resulting in 2 mg dissolved C  $\text{g}^{-1}$  PyOM. The remaining PyOM was divided into three equal masses. The extract was then returned to the PyOM at rates of 2x (“high DPyOM”), 1x (“medium DPyOM”) or 0x (“low DPyOM”), with the remaining liquid made up with non-extract DIW, so each received an equivalent volume of liquid. Thus the three treatments received an addition of +1.3 mg DPyOM-C  $\text{g}^{-1}$  PyOM, no change, or a decrease of -1.3 mg DPyOM-C  $\text{g}^{-1}$  PyOM. Then, the pH of the resulting PyOM slurries was adjusted to match that of the soil (3.9 in 0.01M  $\text{CaCl}_2$ ) using HCl additions, in order to control for pH effects and potential release of inorganic C from the PyOM. The resulting PyOM materials were dried at 70°C.

### *3.2.4 Soil and PyOM incubations*

The incubations took place in 473 mL glass Mason jars. Each Mason jar received a 60 mL glass jar with the soil or soil-PyOM mixture and a 20 mL glass vial with 15 mL 0.09 M KOH made

with CO<sub>2</sub>-free DIW to trap CO<sub>2</sub> emissions, and 5 mL CO<sub>2</sub>-free DIW was added to the bottom of the jar to maintain a humid atmosphere. Each jar received 40 g moist (31.6 g dry) soil. The soils with PyOM additions received 200 mg PyOM. Jars were temporarily capped and rolled to mix soil and PyOM and then placed in the Mason jars. (Jars receiving no PyOM were also rolled.) KOH traps were added to the Mason jars immediately before sealing and incubating at 30°C in the dark. Eight replicates were established for each treatment, and eight blanks with no soil additions - only DIW and a KOH trap - were also established. At the same time, a standard curve was created by sealing KOH traps in a series of jars with rubber septa in their lids and injecting a range of volumes of CO<sub>2</sub> gas. After at least 24 h equilibration, the electrical conductivity (EC) of the traps was measured and linearly correlated with known CO<sub>2</sub> volumes to create a standard curve (Strotmann *et al.*, 2004).

A second incubation was run with PyOM alone in order to determine whether and how the  $\delta^{13}\text{C}$  signature of the mineralized PyOM-C changed over time. 200 mg of PyOM was mixed with 15.0 g ashed (550°C for 2 h) sand, with 8 replicates for each treatment. Samples were inoculated with 3.3 mL inoculum specific to the PyOM treatment. In order to ensure that the addition of the microbial inoculum did not affect the  $\delta^{13}\text{C}$  signature of the respired CO<sub>2</sub>, sequential pre-incubations and extractions were performed, where an initial soil extract was added to each type of PyOM-sand mixture and incubated for 48 hours. Then, these mixtures were extracted and used to inoculate subsequent PyOM-sand mixtures, etc., for a total of four times, before the final PyOM-sand mixtures were extracted and used as the microbial inocula for each type of PyOM.

A third incubation was run in order to answer two questions: (1) Are the effects of PyOM on SOC mineralization due to a nutrient subsidy? (2) Is there a short-term effect of soil pre-incubation on PyOM decomposition and its effect on SOC mineralization? This trial replicated the first, with the following exceptions. It was designed to elucidate the very short-term effects of experimental initiation, and so was only run for 48 hours. Soils were pre-incubated for 1 d, 10 d, or 20 d, and received one of three additions: PyOM, nutrients, or no additions. The added PyOM was the PyOM with increased water-extractable compounds described above for the main experiment. The nutrient treatment was added with a volume of 1 mL, and was designed to deliver a dose of nutrients equivalent to the plant-available (Mehlich III-extractable) nutrients quantified in the PyOM (Table 3.S1). Any nutrient for which PyOM additions would have resulted in a > 3% increase from initial soil levels was included in the nutrient solution (Supplementary Table 1 and Supplementary Figure 3.S4). Treatments that did not receive the nutrient solution received an equivalent amount of DIW.

### *3.2.5 Sampling protocol for determining C mineralization and $\delta^{13}C$ values*

On days 1, 2, 5, 10, 25, and 47, jars were opened and the electrical conductivity (EC) of the KOH traps was measured at a constant temperature of 23.0°C (EC is sensitive to temperature). The traps were then poured into 50-mL centrifuge tubes containing 5 mL 0.3 M BaCl<sub>2</sub>. Traps were replaced with fresh vials of KOH solution. DIW previously added to the bottom of the Mason jars was poured out and replaced with 5 mL fresh CO<sub>2</sub>-free DIW. Mason jars were resealed and returned to the incubation chamber. The BaCl<sub>2</sub> mixed with the KOH trap results in the precipitation of absorbed CO<sub>2</sub> as BaCO<sub>3</sub>. Precipitated solutions were centrifuged at 2500 rpm for

5 minutes. Supernatant solution was decanted, leaving the precipitate. The remaining precipitate was rinsed with 10 mL DIW, centrifuged again, and solution decanted, for a total of three rinses. The remaining precipitate was dried at 70°C. BaCO<sub>3</sub> samples were acidified using H<sub>3</sub>PO<sub>4</sub> and the released CO<sub>2</sub> was analyzed for δ<sup>13</sup>C on a Thermo Scientific DELTA V isotope ratio mass spectrometer interfaced with a Gasbench II (Thermo Scientific, West Palm Beach, FL).

### 3.2.6 Determining total CO<sub>2</sub> mineralization and δ<sup>13</sup>C values

To remove the effect of the small amount of CO<sub>2</sub> present in the air in the jar at the time of setup, measurements from “blank” jars with no soil additions were used. To determine total C mineralized by the sample, the average (n=8) blank EC value for the corresponding sampling day was subtracted from each jar’s EC measurement. This delta EC value was then converted into total CO<sub>2</sub> released by the sample, using the standard curve (more details provided in the supplementary information). To determine the δ<sup>13</sup>C signature (δ<sup>13</sup>C<sub>sample</sub>) of the C derived only from the sample (CO<sub>2sample</sub>), we used the following equation:

$$\delta^{13}C_{sample} = (\delta^{13}C_{total} \cdot CO_{2total} - \delta^{13}C_{blank} \cdot CO_{2blank}) / CO_{2sample},$$

where  $CO_{2total} = CO_{2blank} + CO_{2sample}$ .

To determine the amount of CO<sub>2</sub> sorbed by the blanks (CO<sub>2blank</sub>), we subtracted the average EC value of the blank KOH traps after 24 h under lab conditions from the initial EC of a CO<sub>2</sub>-free KOH solution and converted it to a mass of CO<sub>2</sub> using standard curves. (This is equivalent to 548 ppm CO<sub>2</sub> in the laboratory.) δ<sup>13</sup>C<sub>blank</sub> was calculated using the mean δ<sup>13</sup>C value of all blanks

generated throughout the incubation experiment. The  $\delta^{13}\text{C}$  values of PyOM and SOC end-members changed over time, and were determined through incubations of each component on its own (see supplementary information 3.S3 and supplementary Figure 3.S2 for details).

### *3.2.7 Nanoscale Secondary Ion Mass Spectrometry*

In order to investigate whether SOM is being stabilized on PyOM surfaces, we examined soil-incubated PyOM particles using nanoscale stable ion mass spectrometry (nanoSIMS). The final incubated soil-PyOM mixtures were flash-frozen in sterile Whirl-Paks in liquid  $\text{N}_2$  and stored at  $-80^\circ\text{C}$ . A sub-sample of one of the replicates from the 24-hour preincubated soil with increased water-extractable PyOM treatment was air-dried, and a set of PyOM particles were removed with tweezers. They were laid on the surface of indium foil and then pressed into the soft metal under a glass slide using a PanaPress. The resulting sample was coated with  $\sim 10$  nm Au to reduce any possible charging and imaged using a scanning electron microscope (Hitachi TM-1000, Krefeld, Germany) to find areas of interest. Then the sample was loaded into the Cameca NanoSIMS 50L spectrometer (AMETEK, Inc - CAMECA SAS, Paris, France). A  $\sim 2$  pA  $\text{Cs}^+$  beam (16 keV) was focused onto a  $\sim 150$  nm sized spot and rastered over a  $30\ \mu\text{m} \times 30\ \mu\text{m}$  area. Secondary ions of  $^{12}\text{C}^-$ ,  $^{13}\text{C}^-$ ,  $^{16}\text{O}^-$ ,  $^{12}\text{C}^{14}\text{N}^-$ ,  $^{12}\text{C}^{15}\text{N}^-$  and  $^{28}\text{Si}^-$  were simultaneously detected at high mass resolution ( $M/\Delta M > 7000$  for  $^{12}\text{C}^{14}\text{N}^-$ ).  $256 \times 256$  pixels were used for all images. Each measurement consists of 200 frames, and each frame was obtained over 131.072 s. Presputtering was required to remove surface contamination and Au-coating, as well as preparation of a mature crater with adequate Cs implantation. Presputtering was carried out on an area of  $\sim 35\ \mu\text{m} \times 35\ \mu\text{m}$  to avoid crater effects in the analysis area.

Image processing was performed using ImageJ software with MIMS plug-in (developed by Prof. Claude Lechene's group at Harvard Medical School). For each secondary ion, frames were aligned (shift correction), then all 200 frames were added together as a stack. To map the relative  $^{15}\text{N}$  enrichment of the samples, the stacked image for the  $^{12}\text{C}^{15}\text{N}^-$  ion was divided by the stacked image for the  $^{12}\text{C}^{14}\text{N}^-$  ion, returning a new calculated image of  $^{15}\text{N}/^{14}\text{N}$  ratios in the sample.

### 3.2.9 Statistics

If it was suspected that a jar leaked, because it was found to be a very strong outlier (11-21 standard deviations away from the mean of remaining samples), it was excluded from final analyses. This resulted in the exclusion of 8 samples out of 384, resulting in n values for each treatment at any given timepoint ranging from 6-8. All statistical analyses were performed in R (R Core Team, 2012). We fit a linear mixed effects model to the cumulative SOC-derived  $\text{CO}_2$  emissions and the PyOM-C-derived  $\text{CO}_2$  emissions, with PyOM addition, soil, day, and jar ID as a random effect as factors, an interaction between PyOM and day (does the effect of PyOM change over time?), an interaction between PyOM and soil (do the PyOM additions affect the two soils differently?), and an interaction between soil and day (does the effect of soil pre-incubation change over time?) using the R package lme4 (Bates *et al.*, 2014). To determine whether the interactions were significant, we performed a log-likelihood ratio comparison of a model with vs. without the interaction term. To make post-hoc comparisons within the models, we performed pairwise comparisons between the different PyOM additions or soils for a given day with a Tukey adjustment of p-values, using the lsmeans R package (Lenth, 2014).

### **3.3 Results**

#### *3.3.1 SOC mineralization*

SOC mineralization was significantly greater after the short-term than the long-term incubation (Figure 3.1, top; Supplementary Table 3.S3).

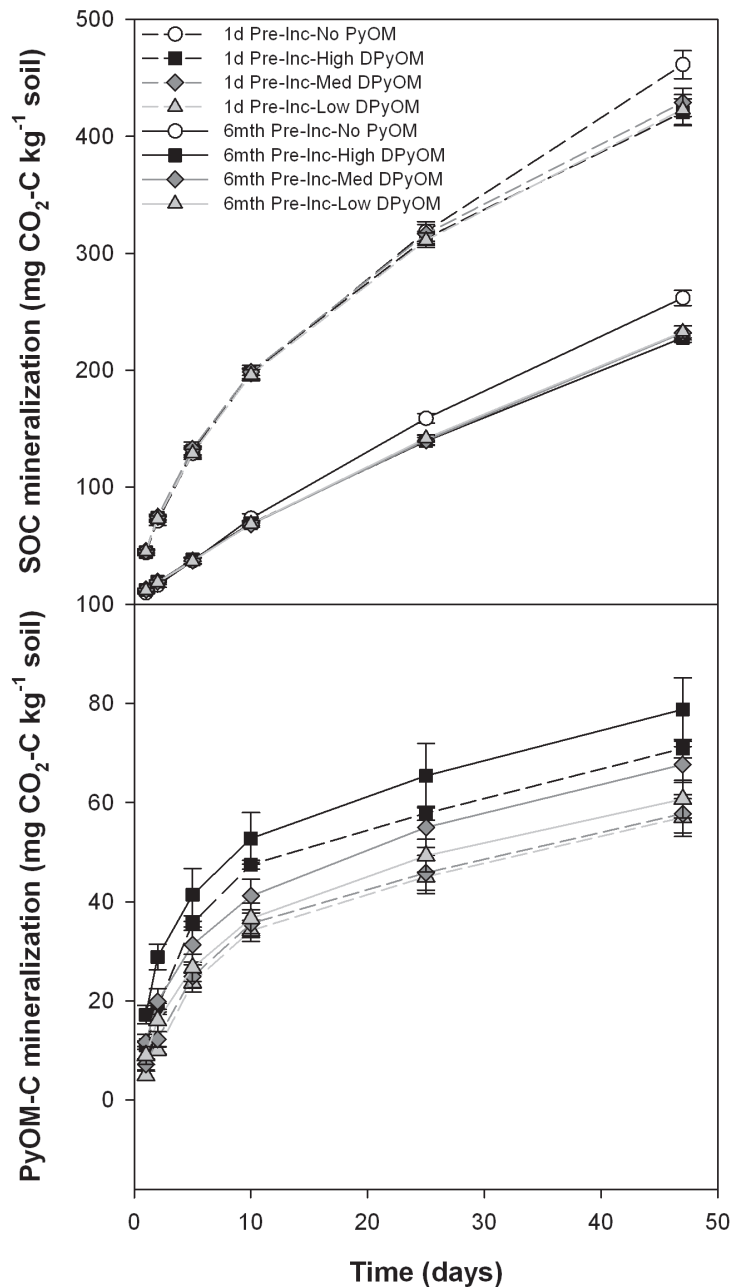


**Figure 3.1** Cumulative mean C mineralization over time for SOC (top) and PyOM-C (bottom) for different relative amounts of water-dissolvable PyOM (DPyOM) and pre-incubation durations. Dashed lines indicate 1-day pre-incubated soils; solid lines indicate 6-month pre-incubated soils. Black squares, dark grey diamonds, light grey triangles, and white circles indicate high DPyOM, medium DPyOM, low DPyOM, and no PyOM, respectively. Note different scales on y-axes, to show detail. Error bars  $\pm 1$ SE,  $n=6-8$ . Exact values and significant differences listed in Supplementary Tables 3.S3 and 3.S4.

Cumulative SOC mineralization was initially (days 1 and 2) greater in the soils that received PyOM additions in comparison to those that did not receive PyOM additions (Figure 3.3; Supplementary Table 3.S3). Over time this trend reversed, with significantly less cumulative SOC mineralized in the soils that received PyOM compared to soils with no additions by day 25 of the experiment for the 6-month pre-incubated soil and by day 49 for the 1-day pre-incubated soil (Figures 3.1 and 3.2; Supplementary Table 3.S3). The day by PyOM addition interaction term in the mixed effects model was significant ( $p < 0.0001$ ), indicating that this shift in the effect of PyOM on CO<sub>2</sub> emissions over time is significant. The soil by PyOM addition interaction had  $p = 0.052$ , indicating that the PyOM additions may have affected the two soils differently, although it is not significant.

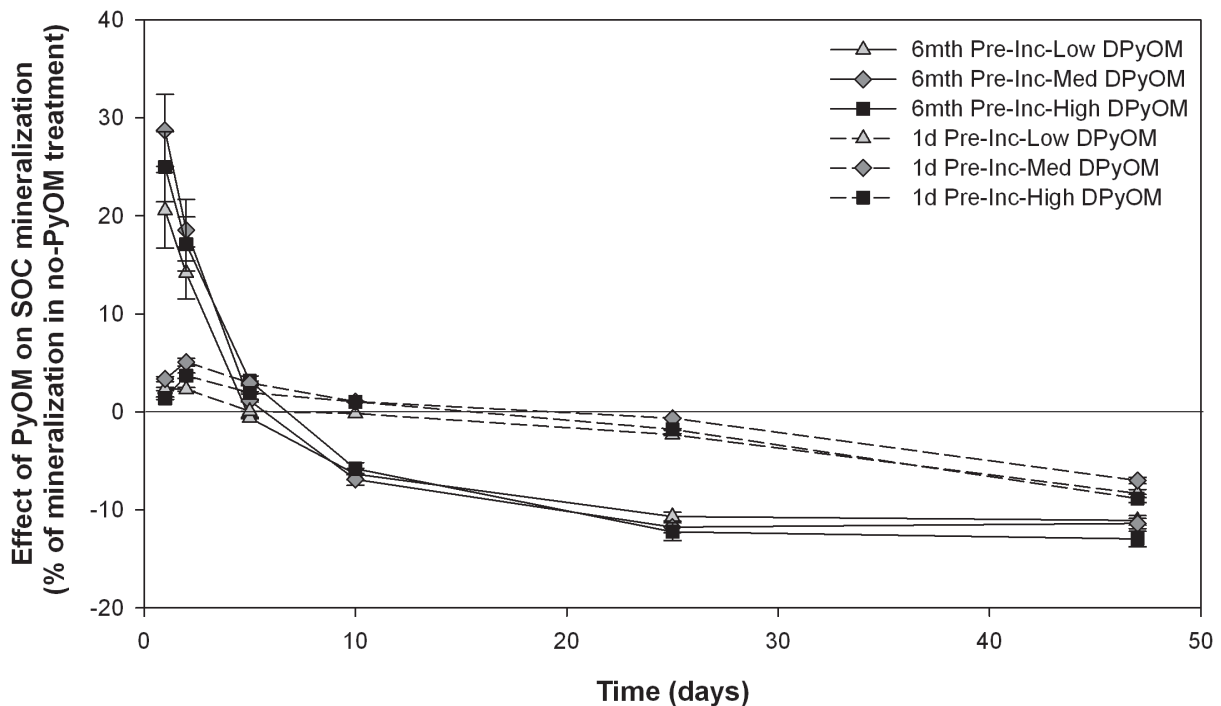


**Figure 3.2** Mean cumulative relative effect of PyOM additions on SOC mineralization over time:  $(SOC_{PyOM} - SOC_{no\ PyOM}) / SOC_{no\ PyOM}$ . Dashed lines indicate 1-day pre-incubated soils; solid lines indicate 6-month pre-incubated soils. Black squares, dark grey diamonds, and light grey

triangles indicate high DPyOM, medium DPyOM, and low DPyOM, respectively. Error bars  $\pm 1\text{SE}$ ,  $n=(6-8)$

### 3.3.2 *PyOM mineralization*

Cumulative PyOM-C mineralization was greatest with additions of more water-extractable PyOM and lowest with depleted water-extractable PyOM (Figure 3.1, bottom; Supplementary Table 3.S4). For a given level of water-extractable PyOM, cumulative PyOM-C mineralization was significantly greater in the 6-month pre-incubated soil mixtures, except for the PyOM with depleted water-extractable compounds, which were not significantly different between the two soils on days 1, 5, and 10 (Figure 3.3; Supplementary Table 3.S4). This effect was initially greatest for the PyOM with depleted water-extractable C and lowest for the PyOM with increased water-extractable C (although the absolute effect is greatest in the PyOM with greater water-extractable C), and decreased and stabilized at a positive value over time.

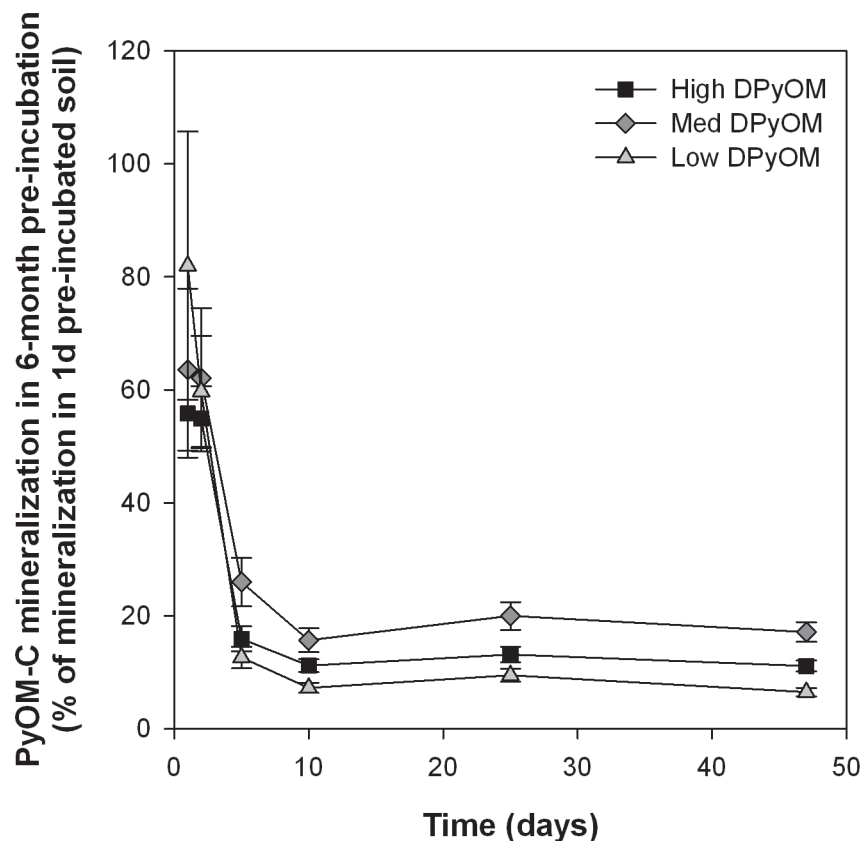


**Figure 3.3** Cumulative mean relative effect of SOC on PyOM-C mineralization ((PyOM-C mineralized in the 6-month pre-incubated soil - PyOM-C mineralized in the 1-day pre-incubated soil)/(PyOM-C mineralized in the 6-month pre-incubated soil) x 100) over time. Error bars  $\pm 1SE$ ,  $n=(6-8)$ .

### 3.3.3 PyOM-SOC mineralization correlations

Initial PyOM-C mineralization was positively correlated with SOC mineralization for the 6-month pre-incubated soil but not for the 1-day pre-incubated soil (Figure 3.4).

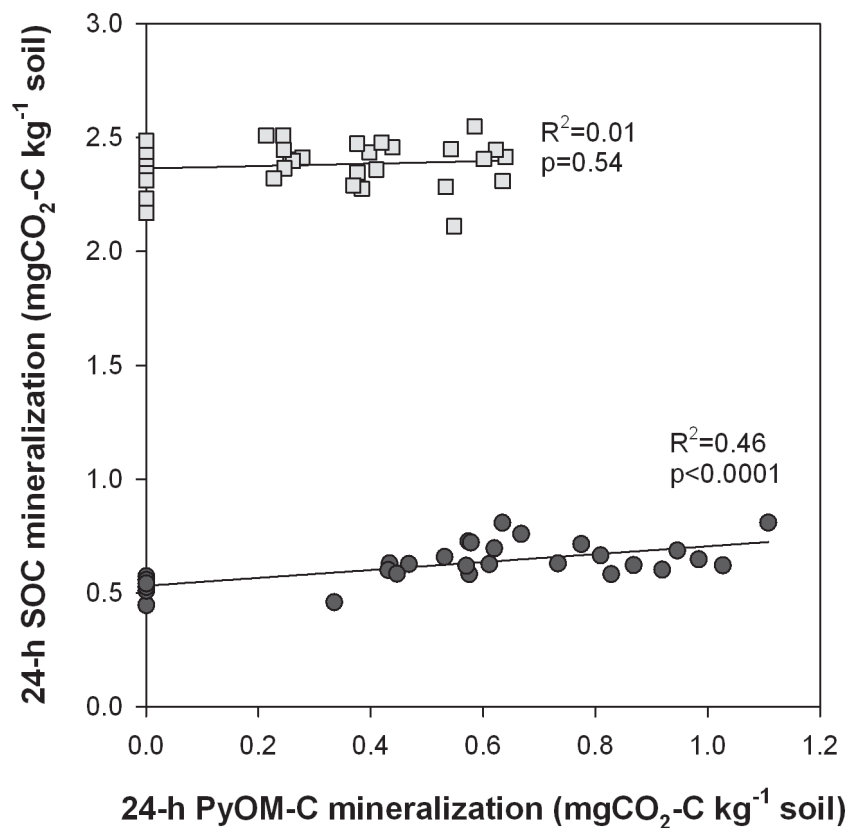


**Figure 3.4** Relationships between SOC mineralized and PyOM-C mineralized over the first day of incubation within soils after 6-month (dark circles) and 1-day (light squares) pre-incubation on Day 1. Lines indicate linear regressions: 1-day:  $y=2.36+0.05x$ ,  $p=0.54$ ,  $R^2=0.01$ ; 6-month:  $y=0.53+0.173x$ ,  $p<0.0001$ ,  $R^2=0.46$ .

Cumulative PyOM-C mineralization over the first two days was negatively correlated with SOC mineralization across the range of studies pre-incubation times (Figure 3.5).

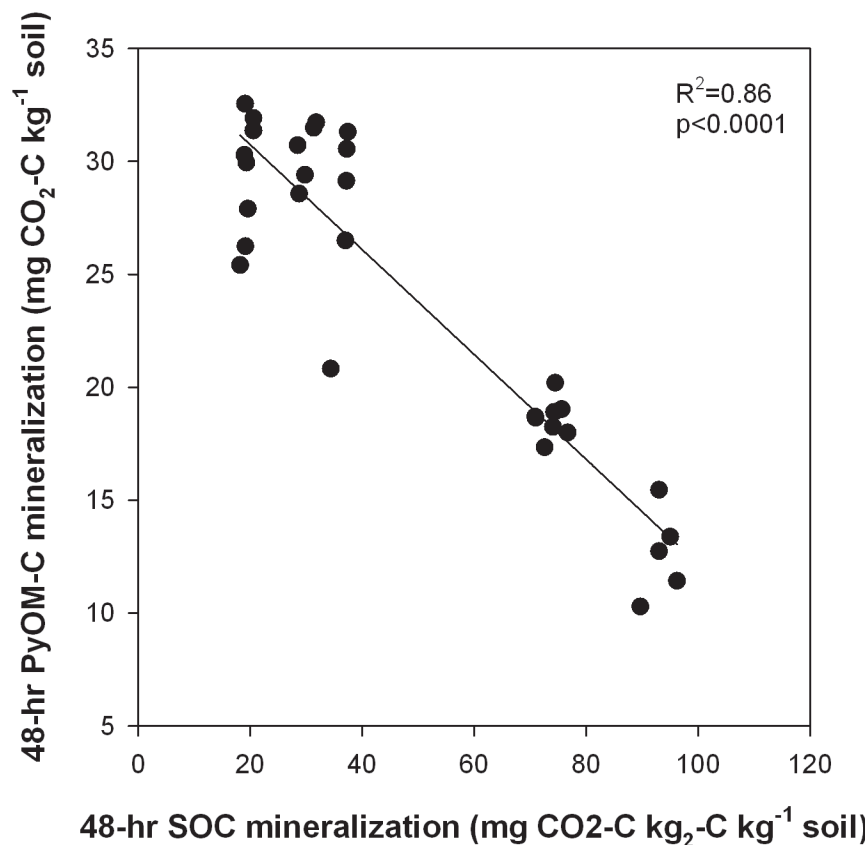


**Figure 3.5** Relationship between SOC mineralized and PyOM-C mineralized in the first two days across soil pre-incubations of 1, 10, 20 and 180 d and with high DPyOM additions. Line indicates linear regression,  $y=35.38-0.23x$ ,  $p<0.0001$ ,  $R^2=0.86$ .

The duration of pre-incubation affected the 48-hour change in SOC mineralization with PyOM additions, with longer pre-incubation times resulting in greater increases in SOC mineralization, while short pre-incubation times yielded negative or no changes to SOC mineralization (Figure 3.6). There is not a clear “levelling-off” effect over the 6-month range investigated here.

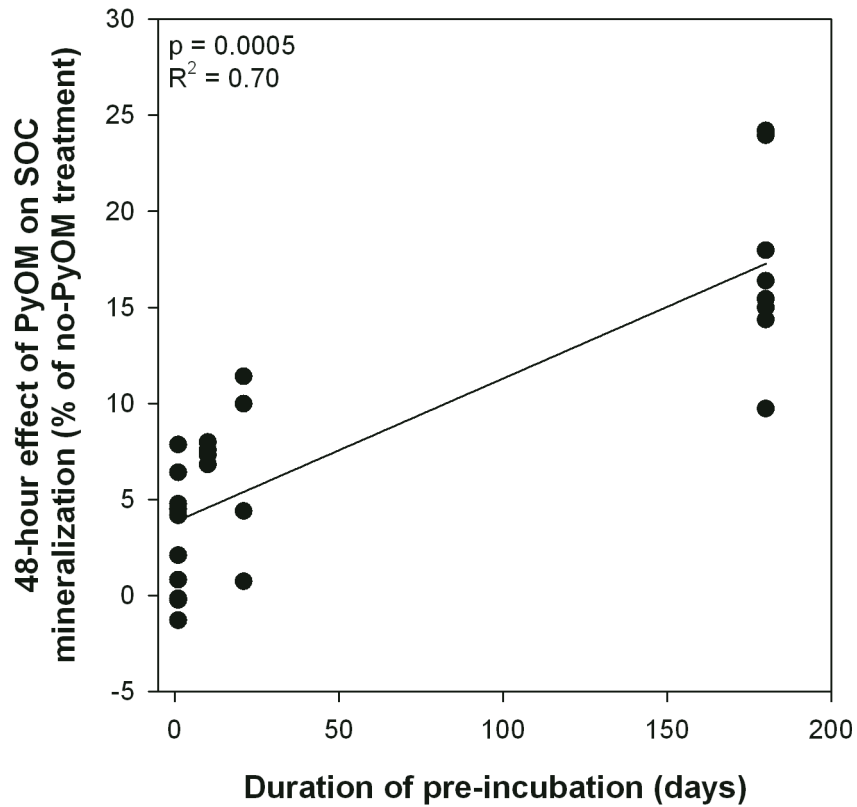


**Figure 3.6** Effect of pre-incubation duration on relative effect of PyOM (High DPyOM) on SOC mineralization. Line indicates linear regression,  $y=3.82+0.0747x$ ,  $p=0.0005$ ,  $R^2=0.70$ .

### 3.3.4 NanoSIMS

The nanoSIMS image map of the  $^{15}\text{N}/^{14}\text{N}$  ratios on the soil-incubated PyOM sample (Figure 3.7) indicates regions of relatively  $^{15}\text{N}$ -depleted regions on top of the relatively  $^{15}\text{N}$ -enriched PyOM.

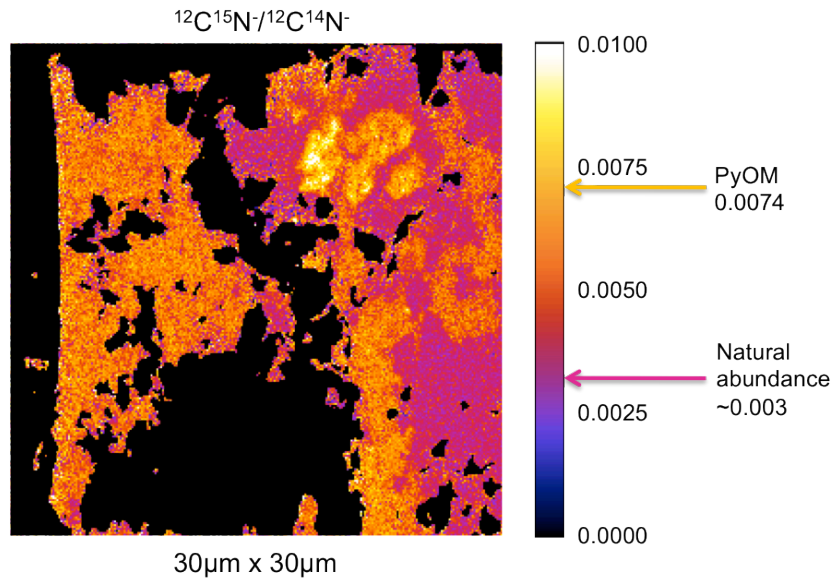


**Figure 3.7** Calculated image of  $^{15}\text{N}/^{14}\text{N}$  ratio (as  $^{12}\text{C}^{15}\text{N}^-$  and  $^{12}\text{C}^{14}\text{N}^-$  ions detected on 200 scans of nanoSIMS) across a  $30\mu\text{m} \times 30\mu\text{m}$  region of selected incubated PyOM particle. Note that the  $^{15}\text{N}/^{14}\text{N}$  ratio of naturally-occurring organic matter is about 0.0037, while labelled sample was 0.0074. Thus, orange (light) areas indicate PyOM, while pink (dark) areas indicate sorbed SOM. Black regions indicate non-OM regions (soil minerals) or regions with low-resolution data due to image shifting during scanning.

### 3.4 Discussion

#### 3.4.1 Short-term increase in SOC mineralization with PyOM additions in low-labile C soils

The observed short-term increases in SOC mineralization with PyOM additions are consistent with the growing array of PyOM-SOC mineralization studies that find that any increases in SOC mineralization with PyOM additions occur over relatively short timescales, with decreased SOC mineralization taking longer to emerge (*e.g.*, Cross and Sohi, 2011; Keith *et al.*, 2011; Luo *et al.*, 2011; Singh and Cowie, 2014). However, this study expands on previous studies in that it explicitly controlled for possible pH and nutrient addition effects of the PyOM additions on SOC, lending stronger support to the hypothesis that the short-term increased SOC

mineralization is driven largely by the more easily mineralizable fraction of PyOM. While this effect has largely been described in general terms by stimulation of the microbial community, resulting in increased enzyme production and metabolic activity, and shifts toward members of the microbial community that are best able to take advantage of the added substrate, there are certainly deeper mechanistic layers to this explanation. Outstanding questions include, among others: (1) What specific soil and PyOM properties lead to such a stimulation of the microbial community? (2) Which members of the soil microbial community are responsible for this response? While this experiment does not address the second question, we are able to make some inferences with regard to the first. The 6-month pre-incubated soil experienced greater increases in mineralization with PyOM additions. This could be explained in at least two ways: (1) In the 1-day pre-incubated soil, the microbial community is not C-limited. Thus, the addition of PyOM does not alleviate any constraint and does not result in increased SOC mineralization. (2) While SOC mineralization was actually inhibited by direct mineral N additions (Supplementary Figure 3.S3), the accumulated mineral N in the 6-month pre-incubated soil could have allowed for increased access to the added PyOM, which, in turn, stimulated the microbial community and increased SOC mineralization. These two explanations are not incompatible - increased mineral N in the 6-month pre-incubated soils could have alleviated the N constraint on PyOM-C mineralization (Supplementary Figure 3.S6), allowing access to the PyOM-C, which, in turn, alleviated the C limitation in the 6-month pre-incubated soils. This interpretation is further supported by the fact that short-term increased PyOM mineralization is positively correlated with increased SOC mineralization for the 6-month pre-incubated soil (Figure 3.4), while across soils, less PyOM was mineralized in the 1-day pre-incubated soil (Figure 3.5). These observations may indicate the mineralizability of the SOC determines whether PyOM-C is a more attractive

substrate (with less easily mineralizable SOM being more susceptible to increased mineralization by PyOM additions), since increasing the amount of easily mineralizable PyOM increases SOC mineralization over the short-term. This interpretation is consistent with the work of Fontaine *et al.*, (2007) who find that deep SOC decomposition is limited by available C. Thus, lower-temperature PyOM materials, which are more readily mineralized (Whitman *et al.*, 2013; Zimmerman, 2010), may be more likely to cause increased SOC mineralization. This is also consistent with the work of Keith *et al.* (2011), who found that the addition of fresh organic matter along with PyOM resulted in a net reduction in the (fresh organic matter + SOM) decomposition. Our results therefore extend prior research to unequivocally demonstrate the effects of the mineralizability of SOC on the magnitude and direction of changes to SOC mineralization induced by PyOM additions.

#### *3.4.2 Longer-term decrease in SOC mineralization with PyOM additions in both soils*

Over time, PyOM additions resulted in a net decrease in SOC mineralization for both soils. This decrease emerged later for the 1-day pre-incubated soil. There are at least five potential mechanisms (Jones *et al.*, 2011; Maestrini *et al.*, 2014b; Whitman *et al.*, 2014b) that we believe we can rule out. First, we suggest that in this case, the decrease in SOC mineralization was not caused by substrate-switching or dilution effects (Whitman *et al.*, 2014a). Both of these effects depend on a greater or equal “appeal” of the PyOM as compared to SOC as a substrate, and should be driven largely by the more available fractions of PyOM-C that are mineralized initially. Thus, under these mechanisms, the effects would likely be expected to occur in the first few days of the incubation, and would not be expected to emerge only after a week or more, as

was seen here. Second, because we adjusted the pH of the PyOM to match that of the soil, we do not expect that these changes reflect the release of inorganic C, or are due to the shift of the soil's pH to one more favourable for microbial activity. Third, because the PyOM was only added at a rate of 0.3% by mass, we would argue that changes to the physical properties of the soil are unlikely to be driving these effects, especially because the water contents were optimized. Fourth, while N inhibition is commonly observed in soils (Fog, 1988; Ramirez *et al.*, 2012), this is not likely the case in these soils - while SOC mineralization in the studied soils was also inhibited by N additions (Supplementary Figure 3.S3), the amount of mineral N added with the PyOM was marginal. Finally, it may be worth considering whether other nutrient additions could explain this inhibition of SOC mineralization. We did see some inhibition of the cumulative SOC mineralization over the first 2 days with the addition of nutrients equivalent to those added in the increased water-extractable PyOM treatment (Supplementary Figures 3.S4 and 3.S5). However, the Mehlich III-extractable nutrients varied almost twofold across the three PyOM treatments, and the effect of PyOM on the SOC mineralization did not change proportionally - indeed it was not significantly different across the three treatments. Thus, if we thought that nutrients were primarily responsible for this effect, we would likely also predict that the effect might be proportional to the relative level of nutrients in the PyOM and the soil (Supplementary Figure 3.S4). However, we see significant differences in changes to SOC mineralization between the soils, which had relatively similar levels of nutrients, but no significant differences between the types of PyOM additions, which had markedly different levels of nutrients. Thus, we would argue that this mechanism, while potentially active, is not primarily responsible for these effects.

We suggest that sorption of SOC by PyOM, making it less available to microbes, may play an important role in decreasing SOC mineralization over time. If we postulate that it is the bulk PyOM, and not the water-extractable PyOM that is largely responsible for any sorption of SOM, then we would not necessarily expect to see significant differences between the different PyOM additions, which is consistent with our findings. It might be more difficult to postulate how the SOC properties would be expected to affect PyOM sorption. We could predict that there is a limited quantity of sorption sites on the PyOM, and, once filled, stabilization would stop. The rate at which this would be expected to occur would depend on the kinetics of sorption - thus, we might predict that the SOC in the soil with a higher concentration of easily mineralizable SOC would be sorbed more quickly, which we cannot confirm from our data. However, it is also possible that this sorption is more limited by the rate of formation of sorption sites on the PyOM as it oxidises in the soil, and thus we would not necessarily predict that we should see differences in the two soil types. Zimmerman *et al.* (2011) consider sorption mechanisms in detail, citing sorption of SOC on PyOM surfaces and within pores as well as sorption and inactivation of enzymes on PyOM as mechanisms for reduced SOC mineralization with PyOM additions. While we did not test explicitly to differentiate between these mechanisms, we did confirm using nanoSIMS that SOM was located on PyOM surfaces. Still, it is important to interpret this image within the constraints of the technique: this is only a single 30 x 30  $\mu\text{m}$  region of a single sample of soil-incubated PyOM. Thus, while fine-scale observation techniques are inherently required to directly observe phenomena that occur at very small scales, we should not extrapolate these findings to make a statement about their importance at larger scales. What it does indicate is that PyOM surface-SOM interactions may be occurring in the soil, and are worth further investigation. For future nanoSIMS investigations, we would recommend that researchers take

care to design experiments using materials with high (*i.e.*, 10 atom% range) enrichments, which would allow for higher throughput analyses.

### 3.4.3 Soil C status effects on PyOM-C mineralization

Cumulative PyOM-C mineralization was greatest in the incubations that had increased DPyOM and lowest in the treatments that had depleted DPyOM (Figure 3.1, bottom; Supplementary Table 3.S4). This confirms that a substantial proportion of the easily mineralizable PyOM-C was in the form of water-extractable compounds, although a significant portion of rapidly mineralizable PyOM-C certainly remained post-extraction, as indicated by the PyOM mineralization in the DPyOM-depleted treatment. The finding that PyOM-C mineralization was lower in the 6-month pre-incubated soil is somewhat in opposition to the results of Keith *et al.* (2011), who found that increasing additions of fresh organic matter to soils along with PyOM resulted in increased mineralization of the PyOM. While we might have predicted that the more active soil would have generally higher microbial activity, and thus result in greater “incidental” PyOM mineralization, this did not occur. Because the bulk of this effect occurred over the first couple of days, one possible explanation is that the effect was driven by the relative appeal of the C substrates in the two soils. The relatively-easily mineralizable PyOM was used preferentially in the 6-month pre-incubated soil, but was relatively less appealing in the 1-day pre-incubated soil. This effect likely largely acted upon the DPyOM-C, and diminished after a few days as this source was depleted in both soils. Additionally, the 6-month incubated soil had relatively higher mineral N, which could have further facilitated the mineralization of the added PyOM-C, the decomposition of which is likely N-limited (Supplementary Figure 3.S6).

#### *3.4.4 Effects and implications of pre-incubation duration on SOC-PyOM interactions*

Pre-incubations are common practice in studies of SOM cycling, employed in order to allow C mineralization in the soils to stabilize to some extent after the liberation of fresh SOM during procedures that may include drying, re-wetting, sieving, and temperature changes. While the reasoning - that the changes induced temporarily by these manipulations are artificial and not germane to the processes we most want to study - is valid, the challenge is determining at what point of pre-incubation it is appropriate to initiate amendments or possibly any soil manipulation. The data in this study indicate that even if respiration rates seem to have levelled off, soils may still not have reached a meaningful sort of “steady state”. The change in short-term SOC mineralization in this experiment was 9 times greater in the 6-month compared to the 24-hour pre-incubation. Of course, it is impractical to recommend 6-month pre-incubations, and even then, no indication exists that a final point was reached, at which we could determine the “true” effect of PyOM on SOC mineralization. Perhaps it is best to (1) think of the state of the soil as a continuum, rather than imagining it possible to allow it “equilibrate” in a meaningful way, (2) discount or only carefully evaluate the practical importance of any very short-term effects, (3) attempt to design studies where soils are maintained in as natural conditions as possible, such as intact soil cores (challenging for studies involving the introduction of amendments), or (4) tie the manipulations or timescale to analogous real-world processes (*e.g.*, PyOM additions to agricultural systems while tilling or disking soils).

### *3.4.5 Conclusions*

In summary, we found that the 6-month pre-incubated soil, with overall lower SOC mineralization was more susceptible to short-term increases in SOC mineralization with PyOM additions, which were proportional to the mineralization in the added PyOM. Both soils experienced net long-term decreases in SOC mineralization with PyOM additions, possibly due to stabilization of SOC on PyOM surfaces. Additionally, we showed that the duration of pre-incubation of soils before PyOM additions between 1 day and 6 months resulted in a 9-fold increase in short-term SOC mineralization, indicating that there may be no optimal duration of pre-incubation for SOC mineralization studies.

SUPPLEMENTARY INFORMATION FOR CHAPTER THREE - RELATIVE CARBON  
MINERALIZABILITY DETERMINES INTERACTIVE PRIMING BETWEEN PYROGENIC  
ORGANIC MATTER AND SOIL ORGANIC CARBON

*3.S1 Notes on standard curve application*

While the standard curves produced for each sampling episode were consistently linear, we noticed that equilibration of the traps with the jar atmosphere over time led to small increases in the slope of the standard curve with increasing incubation times. Thus, we incubated traps for a standard curve over increasing lengths of time, up to 25 days, to create a linear regression for the slope of the standard curve. Over incubation lengths of 1-25 days, the slope (change in CO<sub>2</sub> (mL added) / change in EC ( $\mu\text{S cm}^{-1}$ )) ranged from 1.6 to 1.8. We used this adjusted slope equation to translate the measured EC values into CO<sub>2</sub> values. This does not significantly affect our general conclusions, but should increase the accuracy of the precise CO<sub>2</sub> measurements.

*3.S2 Nutrient addition experiment*

In order to determine whether an alleviation of nutrient constraints could be responsible for the short-term increase in SOC mineralization with PyOM additions, we conducted a trial where nutrients were added in an amount equal to that added with the PyOM with increased water-extractable compounds. We included any nutrient for which PyOM additions increased total concentrations in the soil by more than 5% (see Supplementary Figure 3.S4). Supplementary Figure 3.S3 shows the results from this short-term incubation.

### 3.S3 Determining $\delta^{13}\text{C}$ values of PyOM and SOC end-members

The procedure to subtract the effect of the blank jar on the  $\delta^{13}\text{C}$  values of the PyOM-only incubation was the same as that used for the soil+PyOM incubation. This generated a set of  $\delta^{13}\text{C}$  values for each PyOM treatment over time, corresponding to the mass of PyOM-C that had been mineralized over that interval. The  $\delta^{13}\text{C}$  values of the mineralized PyOM were initially relatively enriched in  $^{13}\text{C}$ , after which they all stabilized around +48‰. To account for this changing  $\delta^{13}\text{C}$  signature over time, we assumed that the  $\delta^{13}\text{C}$  signature changes consistently over the first period of the incubation and then stabilizes at +48‰. The challenge is that, in the PyOM-only incubation, larger masses of PyOM were respired per sampling interval than in the combined incubation. *I.e.*, while the average  $\delta^{13}\text{C}$  value of PyOM with added extractable PyOM respired over the first timepoint in the PyOM-only trial was +60.28‰, this included 1.70 mL of  $\text{CO}_2$ . We know that the amount of respired BC in the combined incubation was less than this, and so, if we expect that the  $\delta^{13}\text{C}$  of the PyOM decreased over time until it stabilized at +48‰, then we should predict that the average  $\delta^{13}\text{C}$  signature for this smaller initial mass of mineralized PyOM would be greater than +60.28‰. However, if we take a higher value, then this changes the mass of PyOM we calculate was respired in the incubation experiment. To calculate the correct average  $\delta^{13}\text{C}$  for the PyOM in each treatment at each sampling time, we assumed a linear decrease of  $\delta^{13}\text{C}$  of mineralized PyOM-C over the course of the PyOM incubation until it reaches 48‰, after which it stabilizes. To calculate the correct  $\delta^{13}\text{C}$  to use for each timepoint, we then iteratively adjusted the  $\delta^{13}\text{C}$  value to represent the mean amount of PyOM respired (for each treatment at each timepoint) until it stabilized at a value that yields a mass of PyOM respired that would generate this same mean  $\delta^{13}\text{C}$  value (Supplementary Figure 3.S2). This process was used to

generate the appropriate  $\delta^{13}\text{C}$  values for PyOM-C for each soil and PyOM combination at each timepoint (Supplementary Table 3.S2). Soil  $\delta^{13}\text{C}$  values in the no-PyOM soils did not show major shifts over time, but for each timepoint the corresponding mean  $\delta^{13}\text{C}$  value from the no-PyOM 24-hour or 6-month pre-incubated soils were used as the end-members for SOC mineralization.

**Table 3.S1** Nutrient solution for nutrient effect experiment

Nutrient	Form added	Amount added per jar ( $\mu\text{mol}$ )
Ca	$\text{CaCl}_2$	18.7
K	KCl	17.2
P	$\text{H}_2\text{KPO}_4$	0.3
Mg	$\text{MgCl}_2$	3.2
Sr	$\text{SrCl}_2$	2.9

**Table 3.S2** Isotopic  $\delta^{13}\text{C}$  signatures (‰) for PyOM-C for each timepoint and soil-PyOM combination

Pre-incubation	Water-extractable PyOM adjustment	Day 1	Day 2	Day 5	Days 11+
6-month	Increased	65.36	54.91	48.95	48.95
	No change	61.47	54.81	48.95	48.95
	Decreased	60.47	53.80	48.95	48.95
24-hour	Increased	67.68	61.07	52.33	48.95
	No change	63.05	58.85	52.76	48.95
	Decreased	62.20	57.88	48.95	48.95

**Table 3.S3** Cumulative CO<sub>2</sub> fluxes from soils (mg CO<sub>2</sub>-C kg<sup>-1</sup> soil). Different letters indicate significant differences between addition types for a given soil and day (ANOVA, Tukey's HSD with initial  $\alpha=0.00833$ , Bonferroni-corrected for 6 days' comparisons).

Soil	Addition	Day					
		1	2	5	10	25	47
6-month pre-incubated soil	High						
	DPyOM	12.05 b	19.04 b	38.05 b	69.03 b	139.38 d	227.80 e
	Med						
	DPyOM	12.41 b	19.27 b	37.31 b	68.23 b	140.13 d	231.92 e
	Low						
	DPyOM	11.62 b	18.56 b	36.66 b	68.64 b	141.83 d	232.73 e
1-day pre-incubated soil	No						
	PyOM	9.64 b	16.26 b	36.88 b	73.29 b	158.81 c	261.74 d
	High						
	DPyOM	44.54 a	73.71 a	131.34 a	198.39 a	312.87 b	420.53 c
	Med						
	DPyOM	45.40 a	74.70 a	132.63 a	198.43 a	316.51 b	428.96 b
1-day pre-incubated soil	Low						422.86
	DPyOM	44.95 a	72.72 a	128.91 a	196.02 a	311.15 b	bc
	No						
	PyOM	43.93 a	71.09 a	128.83 a	196.37 a	318.57 a	461.32 a

**Table 3.S4** Cumulative CO<sub>2</sub> fluxes from PyOM (mg CO<sub>2</sub>-C kg<sup>-1</sup> soil). Different letters indicate significant differences between soil-PyOM combinations for a given day (ANOVA, Tukey's HSD with initial  $\alpha=0.00833$ , Bonferroni-corrected for 6 days' comparisons).

PyOM	Soil	Day					
		1	2	5	10	25	47
High DPyOM	6-month pre- incubated soil	17.23 a	28.85 a	41.38 a	52.8 a	65.44 a	78.79 a
	1-day pre- incubated soil	11.06 b	18.63 bc	35.69 b	47.48 b	57.84 b	70.91 b
Med DPyOM	6-month pre- incubated soil	11.70 b	19.86 b	31.33 b	41.17 c	55.02 b	67.67 b
	1-day pre- incubated soil	7.15 c	12.25 d	24.87 c	35.59 d	45.85 cd	57.77 cd
Low DPyOM	6-month pre- incubated soil	8.96 bc	16.03 c	26.69 c	36.64 d	49.29 c	60.7 c
	1-day pre- incubated soil	4.93 c	10.03 d	23.7 c	34.16 d	45.02 d	56.99 d



**Figure 3.S1** Gleying in aggregates within the 6-month pre-incubated soil. Note grey, reduced core and band of oxidised  $\text{Fe}^{3+}$  minerals around oxygenated exterior.

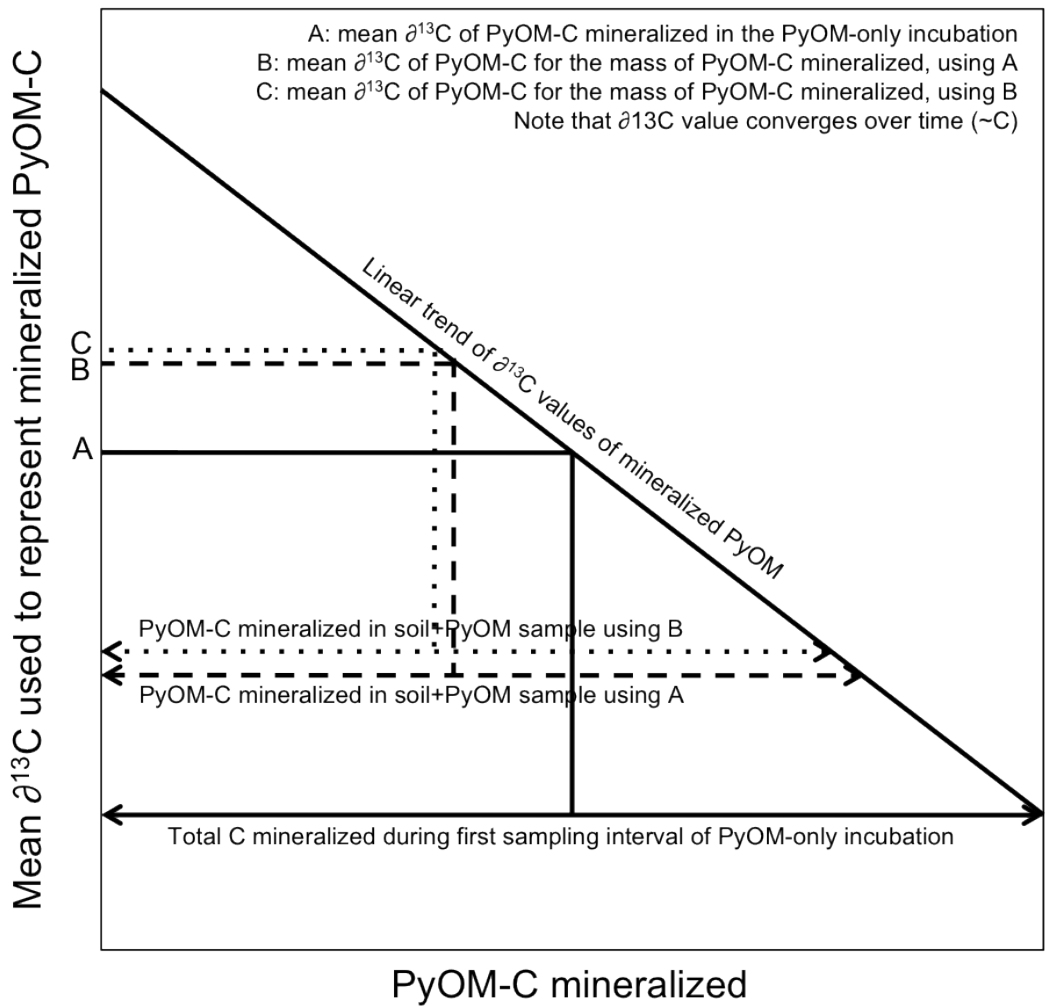


**Figure 3.S2** Iterative adjustments of  $\delta^{13}\text{C}$  of mineralized PyOM to calculate the correct  $\delta^{13}\text{C}$  value for a mineralized mass of PyOM in the soil+PyOM incubation that is less than that released in the first stage of the PyOM-only incubation.

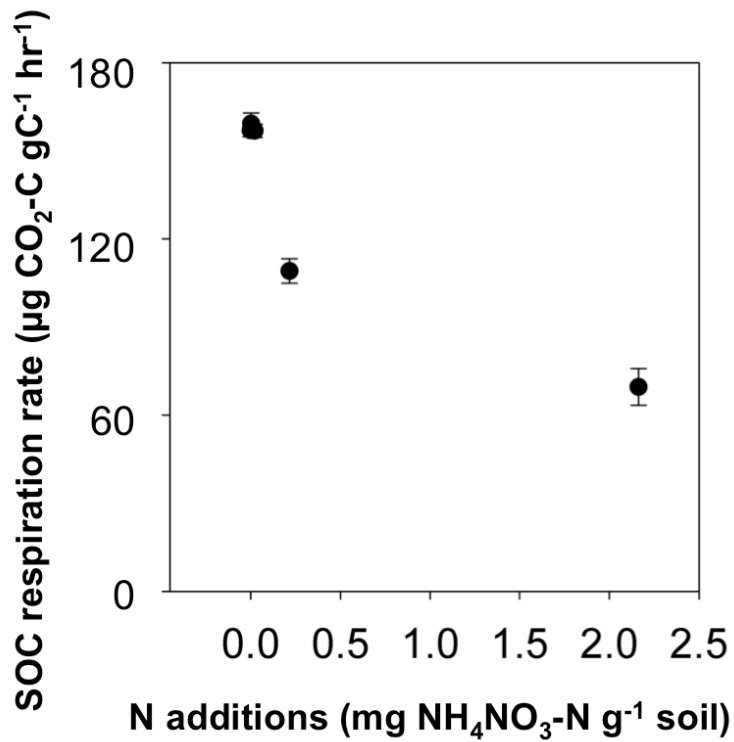


**Figure 3.S3** Effect of mineral N additions on 24-hour SOC mineralization. Between 0-2.2 mg NH<sub>4</sub>NO<sub>3</sub>-N g<sup>-1</sup> soil were added to 10 g < 2 mm sieved soil, incubated at 30°C at 55% WFPS. Error bars ±SE, n=3.

The addition of nutrients equivalent to those added with the high-water-extractable PyOM treatment resulted in a significant decrease (*t*-test, *p*<0.05) in 48-hour SOC mineralization for all durations of pre-incubation (Supplementary Figure 3.S3).

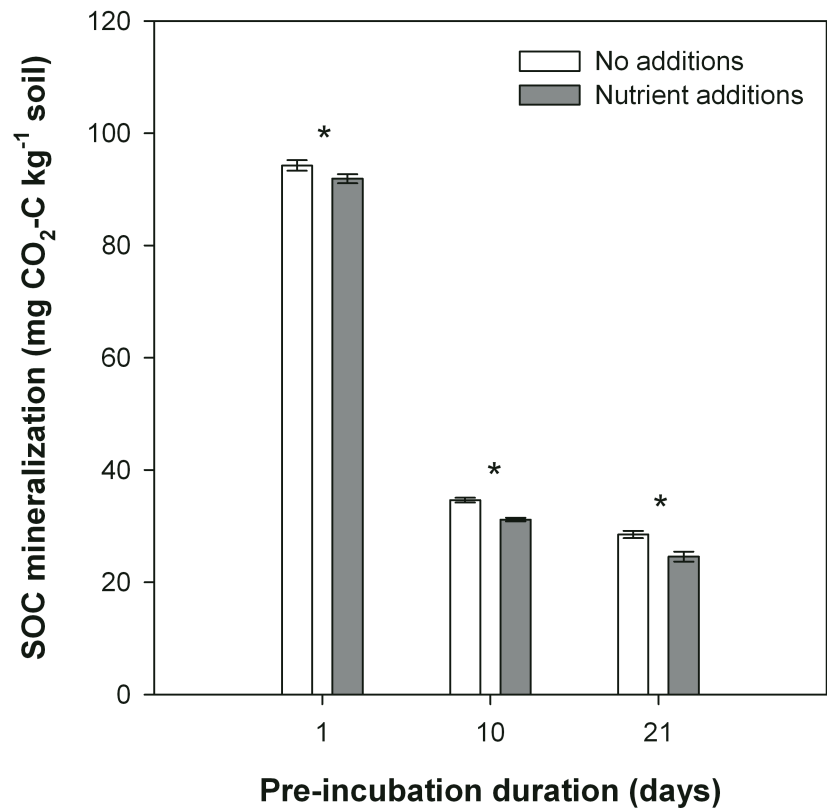


**Figure 3.S4** Mean 48-hour SOC mineralization in soils with (grey bars) and without (white bars) nutrient additions equivalent to those added with the PyOM. A \* indicates significantly lower mineralization in the soils which received nutrients. Error bars  $\pm 1$  SE, n=4-5.

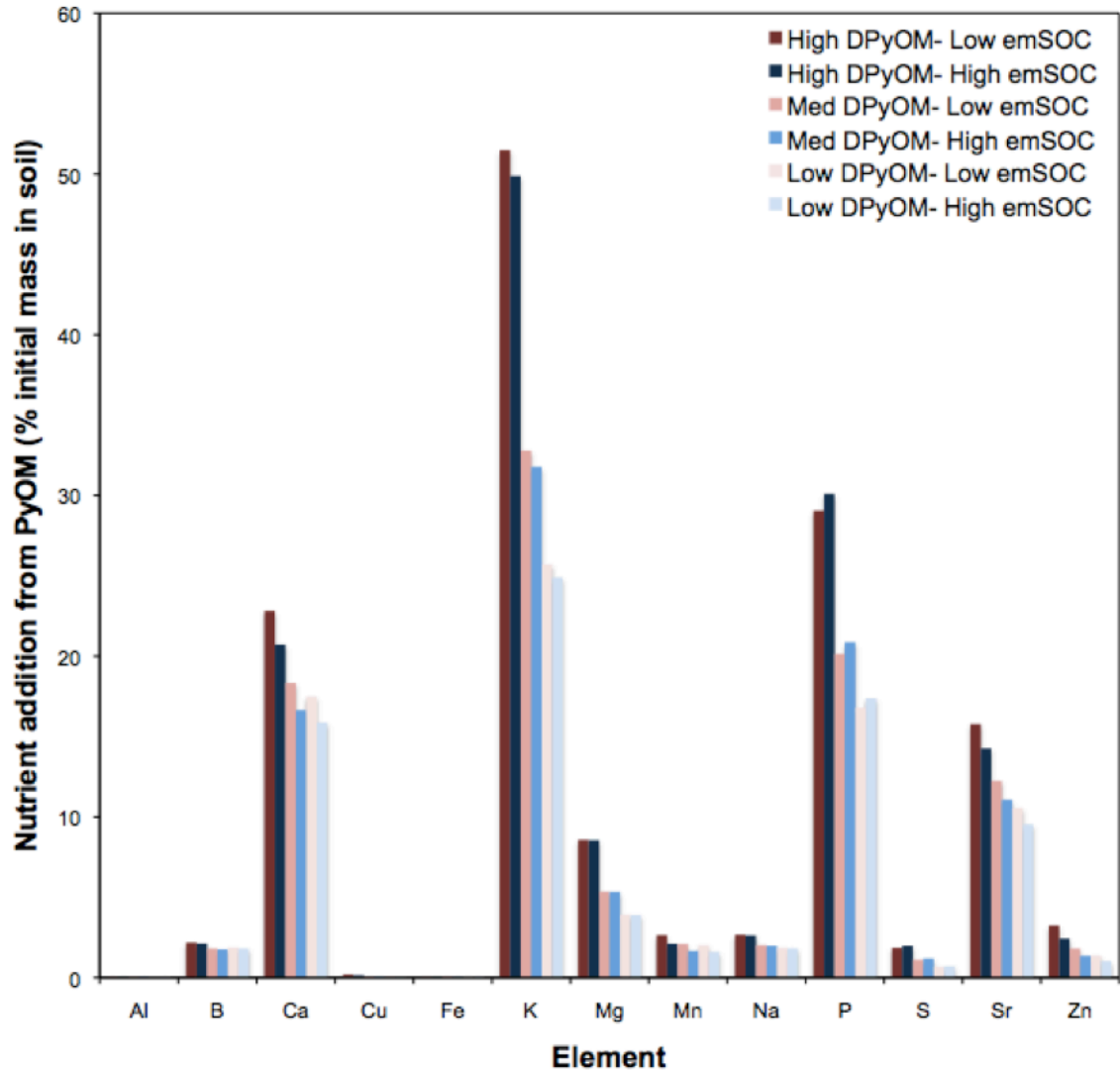


**Figure 3.S5** Increase in Mehlich-III-extractable nutrients with PyOM additions in relation to mass already present in soil.

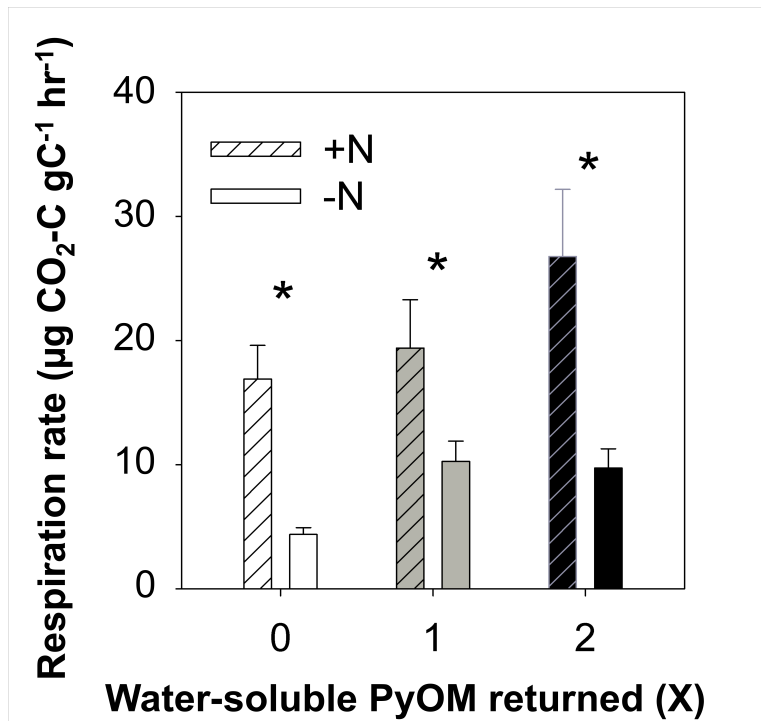


**Figure 3.S6** Mean impact of  $\text{NH}_4\text{NO}_3$  additions on PyOM-C mineralization rates.  $9.3 \text{ mg NH}_4\text{NO}_3\text{-N g}^{-1}$  PyOM were added to  $10 \text{ g}$  ashed sand +  $100 \text{ mg}$  PyOM and maintained at 55% WFPS, and incubated at  $30 \text{ }^\circ\text{C}$  for 24 hours. \* indicates significant differences between treatments with and with N additions ( $p < 0.05$ ),  $n=12$ .

## REFERENCES

- Bates, D., Maechler, M., Bolker, B., Walker, S., 2014. lme4: Linear mixed-effects models using Eigen and S4. R package version 1.1-6. <http://CRAN.R-project.org/package=lme4>
- Bingeman, C.W., Varner, J.E., Martin, W.P., 1953. The effect of the addition of organic materials on the decomposition of an organic soil. *Soil Science Society of America Journal* 17, 34–38.
- Bruun, S., El-Zehery, T., 2012. Biochar effect on the mineralization of soil organic matter. *Pesquisa Agropecuária Brasileira* 47, 665-671.
- Cross, A., Sohi, S.P., 2011. The priming potential of biochar products in relation to labile carbon contents and soil organic matter status. *Soil Biology and Biochemistry* 43, 2127–2134.
- Czimczik, C.I., Masiello, C.A., 2007. Controls on black carbon storage in soils. *Global Biogeochemical Cycles* 21, GB3005.
- de Mendiburu, F., 2013. agricolae: Statistical procedures for agricultural research. R package version 1.1-4. <http://CRAN.R-project.org/package=agricolae>
- Fang, Y., Singh, B., Singh, B.P., 2014. Biochar carbon stability in four contrasting soils. *European Journal of Soil Science* 65, 60–71.
- Farrell, M., Kuhn, T.K., Macdonald, L.M., Maddern, T.M., Murphy, D.V., Hall, P.A., Singh, B.P., Baumann, K., Krull, E.S., Baldock, J.A., 2013. Microbial utilisation of biochar-derived carbon. *Science of The Total Environment* 465, 288–297.
- Fog, K., 1988. The effect of added nitrogen on the rate of decomposition of organic matter. *Biological Reviews* 63, 433–462.
- Fontaine, S., Barot, S., Barré, P., Bdioui, N., Mary, B., Rumpel, C., 2007. Stability of organic carbon in deep soil layers controlled by fresh carbon supply. *Nature* 450, 277–280.
- Fontaine, S., Mariotti, A., Abbadie, L., 2003. The priming effect of organic matter: a question of microbial competition? *Soil Biology and Biochemistry* 35, 837–843.
- Horowitz, M.E., Fahey, T.J., Yavitt, J.B., Feldpausch, T.R., Sherman, R.E., 2009. Patterns of late-season photosynthate movement in sugar maple saplings. *Canadian Journal of Forest Research* 39, 2294–2298.
- Jones, D.L., Murphy, D.V., Khalid, M., Ahmad, W., Edwards-Jones, G., DeLuca, T.H., 2011. Short-term biochar-induced increase in soil CO<sub>2</sub> release is both biotically and abiotically mediated. *Soil Biology and Biochemistry* 43, 1723–1731.
- Jones, D.L., Rousk, J., Edwards-Jones, G., DeLuca, T.H., Murphy, D.V., 2012. Biochar-mediated changes in soil quality and plant growth in a three year field trial. *Soil Biology and Biochemistry* 45, 113–124.
- Keith, A., Singh, B., Singh, B.P., 2011. Interactive priming of biochar and labile organic matter mineralization in a smectite-rich soil. *Environmental Science & Technology* 45, 9611–9618.
- Kuzyakov, Y., 2010. Priming effects: Interactions between living and dead organic matter. *Soil Biology and Biochemistry* 42, 1363–1371.
- Kuzyakov, Y., Subbotina, I., Chen, H., Bogomolova, I., Xu, X., 2009. Black carbon decomposition and incorporation into soil microbial biomass estimated by <sup>14</sup>C labeling. *Soil Biology and Biochemistry* 41, 210–219.
- Lenth, R.V., 2014. lsmeans: Least-Squares Means. R package version 2.05. <http://CRAN.R-project.org/package=lsmeans>.
- Luo, Y., Durenkamp, M., De Nobili, M., Lin, Q., Brookes, P.C., 2011. Short term soil priming effects and the mineralisation of biochar following its incorporation to soils of different pH.

- Soil Biology and Biochemistry 43, 2304–2314.
- Maestrini, B., Herrmann, A.M., Nannipieri, P., Schmidt, M.W.I., Abiven, S., 2014a. Ryegrass-derived pyrogenic organic matter changes organic carbon and nitrogen mineralization in a temperate forest soil. *Soil Biology and Biochemistry* 69, 291–301.
- Maestrini, B., Nannipieri, P., Abiven, S., 2014b. A meta-analysis on pyrogenic organic matter induced priming effect. *GCB Bioenergy*.
- R Core Team, 2012. R: A language and environment for statistical computing. R Foundation for Statistical Computing, Vienna, Austria. ISBN 3-900051-07-0, URL <http://www.R-project.org>.
- Ramirez, K.S., Craine, J.M., Fierer, N., 2012. Consistent effects of nitrogen amendments on soil microbial communities and processes across biomes. *Global Change Biology* 18, 1918–1927.
- Singh, B.P., Cowie, A.L., 2014. Long-term influence of biochar on native organic carbon mineralisation in a low-carbon clayey soil. *Scientific Reports* 4, 1–9.
- Steinbeiss, S., Gleixner, G., Antonietti, M., 2009. Effect of biochar amendment on soil carbon balance and soil microbial activity. *Soil Biology and Biochemistry* 41, 1301–1310.
- Stewart, C.E., Zheng, J., Botte, J., Cotrufo, M.F., 2012. Co-generated fast pyrolysis biochar mitigates green-house gas emissions and increases carbon sequestration in temperate soils. *GCB Bioenergy* 5, 153–164.
- Strotmann, U., Reuschenbach, P., Schwarz, H., Pagga, U., 2004. Development and evaluation of an online CO<sub>2</sub> evolution test and a multicomponent biodegradation test system. *Applied and Environmental Microbiology* 70, 4621–4628.
- Wardle, D.A., Nilsson, M.C., Zackrisson, O., 2008. Fire-derived charcoal causes loss of forest humus. *Science* 320, 629–629.
- Whitman, T., Enders, A., Lehmann, J., 2014a. Pyrogenic carbon additions to soil counteract positive priming of soil carbon mineralization by plants. *Soil Biology and Biochemistry* 73, 33–41.
- Whitman, T., Hanley, K., Enders, A., Lehmann, J., 2013. Predicting pyrogenic organic matter mineralization from its initial properties and implications for carbon management. *Organic Geochemistry* 64, 76–83.
- Whitman, T., Scholz, S.M., Lehmann, J., 2010. Biochar projects for mitigating climate change: an investigation of critical methodology issues for carbon accounting. *Carbon Management* 1, 89–107.
- Whitman, T., Singh, B.P., Zimmerman, A.R., 2014b. Priming effects in biochar-amended soils: implications of biochar-soil organic matter interactions for carbon storage, in: Lehmann, J., Joseph, S. (Eds.), *Biochar for Environmental Management: Science and Technology*. Earthscan, London, UK.
- Woolf, D., Lehmann, J., 2012. Modelling the long-term response to positive and negative priming of soil organic carbon by black carbon. *Biogeochemistry* 111, 83–95.
- Zimmerman, A.R., 2010. Abiotic and microbial oxidation of laboratory-produced black carbon (biochar). *Environmental Science & Technology* 44, 1295–1301.
- Zimmerman, A.R., Bin Gao, Ahn, M.-Y., 2011. Positive and negative carbon mineralization priming effects among a variety of biochar-amended soils. *Soil Biology and Biochemistry* 43, 1169–1179.

## CHAPTER 4

### PYROGENIC ORGANIC MATTER, SOIL ORGANIC MATTER, AND PLANT ROOT INTERACTIONS DETERMINED USING THREE-PART PARTITIONING WITH STABLE C ISOTOPES AND MICROBIAL COMMUNITY ANALYSIS<sup>1</sup>

#### **Abstract**

The effects of pyrogenic organic matter (PyOM) additions to soils have been noted with respect to its effects on plant growth as well as its effects on soil C cycling. However, despite indications of complex three-way interactions among plant roots, soil organic carbon (SOC), and PyOM, few studies have been conducted to investigate C dynamics in all three components, partly because it is methodologically complex to conclusively distinguish the three components. Additionally, the response of the soil microbial community to PyOM additions is likely key to understanding these interactions, but remains poorly characterized. We studied soil C dynamics and soil microbial communities in a field study with 350°C PyOM from <sup>13</sup>C-labelled corn stover, a C<sub>3</sub>-derived soil, and C<sub>4</sub> plants (sudangrass). PyOM additions only temporarily increased total soil CO<sub>2</sub> fluxes, dramatically less than the increase associated with the addition of corn stover, which likely increased SOC losses. We used three-part stable isotopic partitioning after two months to distinguish 334% higher root-derived CO<sub>2</sub> fluxes in the plots with PyOM additions than those without, and 45% lower PyOM-C derived CO<sub>2</sub> fluxes in the plots with plants present. The 84% increase in estimated cumulative soil CO<sub>2</sub> emissions with stover additions was accompanied by a significant shift in the soil bacterial community on days 12 and 82, while the

---

<sup>1</sup> To be submitted to Agriculture Ecosystems and Environment

PyOM additions only resulted in significant changes to the overall community on day 82. Future progress toward a comprehensive predictive framework of PyOM effects on C cycling in soils could be enhanced by including the study of complex multi-component systems, possibly by applying approaches similar to the three-part partitioning method used here, and by investigating effects on the functional microbial community.

## **4.1 Introduction**

### *4.1.1 Carbon cycling interactions in soil-pyrogenic organic matter-plant systems*

Whether pyrogenic organic matter (PyOM) is produced naturally in fires (Czimczik and Masiello, 2007) or intentionally for carbon management and/or as an agricultural amendment (Lehmann, 2007; Laird, 2008), it is important to understand the effects of its production and addition to soils on the carbon (C) cycle (Whitman *et al.*, 2010). PyOM additions to soil can have significant effects on plant growth and crop yields (*e.g.*, Jeffery *et al.*, 2011). Additionally, it has been established that PyOM additions can affect soil C dynamics in a wide variety of ways (Maestrini *et al.*, 2014; Chapter 1). Despite strong expectations that complex three-way interactions could occur, C cycling in three-part systems with PyOM, plants, and soils have been scarcely published, with Whitman *et al.* (2014), Major *et al.* (2010), and Slavich *et al.* (2013) being the only exceptions of which we are currently aware. Whitman *et al.* (2014) found that PyOM additions to soil counteracted the increase in existing soil organic C (SOC) losses induced by the presence of roots. While they did not detect significant changes in above- or below-ground plant biomass, there was a trend toward increased plant growth in the pots with PyOM

additions. Slavich *et al.* (2013) measured net increases in soil C stocks beyond the C that was added with PyOM in a system with 550°C feedlot manure and greenwaste PyOM additions to a Ferralsol planted with a forage peanut (*Arachis pintoi* cv. Amarillo) and ryegrass (*Lolium multiflorum*) rotation. Additionally, they found that the feedlot manure increased total pasture productivity by 11%. Major *et al.* (2010) measured 189% increases in above-ground pasture biomass with additions of PyOM from mango (*Mangifera indica* L.) tree prunings, which increased total soil CO<sub>2</sub> emissions from non-PyOM sources. These three studies (Major *et al.*, 2010; Slavich *et al.*, 2013; Whitman *et al.*, 2014) support the prediction that there are likely complex three-way interactions between soils, plant roots, and PyOM, but none of them was designed in such a way that the three C sources could conclusively be partitioned. There are at least two major reasons that this area of study has remained largely overlooked. First, researchers often choose to isolate and control for as many factors as possible, in order to test for specific mechanisms (*e.g.*, the approach used in Chapter 3), rather than studying all possible components at once. This has led to many studies of PyOM in isolation or just with soil (as reviewed in Chapter 1). Second, separating the three sources of C is not straightforward. Classic stable C isotope partitioning techniques are generally only used to separate two different sources (or “end members”). Employing radioactive <sup>14</sup>C to add a third isotope can be expensive and require complicated regulations, including likely limited use in field settings. In this experiment, we hypothesize that there will be three-way interactions among the C dynamics of plant roots, PyOM, and SOC, and employ a stable C isotope partitioning approach to separate plant root respiration, SOC mineralization, and PyOM-C mineralization in a field setting. We also consider a treatment where plots receive a mass of fresh organic matter equivalent to the initial mass required to produce the amount of PyOM that is added. This treatment serves as a system-level

control that helps to answer the question, “What if a given mass of biomass were not used to produce PyOM, but were applied directly to the soil?” We hypothesize that there will be significant differences in C dynamics between the two systems, with fresh biomass decomposing faster, and having a greater effect on SOC mineralization.

#### *4.1.2 PyOM effects on soil microbial communities*

Understanding the effects of PyOM additions to soil on SOC stocks is bolstered by an understanding of the effects of PyOM on the soil microbial community. While PyOM additions to soils can alter inorganic C dynamics, particularly through changes to a soil’s pH, most mechanisms for increases in SOC losses with PyOM additions are related at some level to the microbes that are responsible for mineralizing SOC, whether the PyOM is used directly as a C substrate, or if its indirect effects on other soil properties affect microbial activities, and, potentially, communities. Just as the potential effects of PyOM on soils are diverse, there are many ways PyOM could affect soil microbes (Ameloot *et al.*, 2013; Lehmann *et al.*, 2011), including, but not limited to addition of OM substrates for energy or nutrients, pH shifts, provision of microbial habitat, changes to soil physical properties, impacts on plant growth, and interference with microbial signalling molecules (Masiello *et al.*, 2013). Recent research has only begun to identify PyOM effects on soil microbial communities, and it is clear that PyOM additions to soil can, indeed, induced changes in soil microbial communities. Most of the evidence for this to date has been gathered using “fingerprinting” types of approaches, such as T-RFLP (Chen *et al.*, 2013; Jin, 2010), PLFA (Gomez *et al.*, 2014; Jindo *et al.*, 2012; Watzinger *et al.*, 2013), or DGGE (Chen *et al.*, 2013) analyses. In a more natural setting, Taketani *et al.*

(2013) found significant differences between soil bacterial communities in Amazonian dark earth soils (amended with PyOM thousands of years ago), PyOM from the soils, and adjacent Acrisols, using 454 pyrosequencing. However, due to the low number of studies and the diversity of PyOM materials and addition rates, soils, and environmental conditions, it is difficult to make broad generalization about the effects of PyOM on soil microbial communities, particularly at the level of individual taxa. Here, we hypothesize that the addition of fresh biomass will induce the greatest shifts in the microbial community, with organisms that are able to quickly access easily-available and easily-decomposable C sources increasing initially, and the emergence of organisms that are able to decompose more complex substrates, such as cellulose, emerging later. PyOM-induced microbial community shifts may resemble the shifts in plots with fresh organic matter additions, but be less dramatic, since less of the PyOM-C is easily mineralizable.

## **4.2 Materials and methods**

### *4.2.1 Experimental design*

A 2 x 2 factor field trial was conducted, with <sup>13</sup>C-labelled 350°C corn PyOM additions and sudangrass plants as the two factors. In addition, a fifth treatment was added which also received PyOM amendments and plants, but where the PyOM had a higher <sup>13</sup>C label. A sixth treatment was added where a mass of the dried original feedstock biomass was applied that was equivalent to that which would have been required to produce the mass of PyOM that was applied to each plot (*i.e.*, 4.1 T ha<sup>-1</sup> corn-derived PyOM were applied, and with 0.365 mass fraction conserved during PyOM production, translate into 11.2 T ha<sup>-1</sup> corn stover.)

#### 4.2.2 Biomass production

Two sets of corn plants (*Zea mays* (L.)) were grown, one in an enriched  $^{13}\text{CO}_2$  atmosphere growth chamber and the other in an ambient  $^{13}\text{CO}_2$  greenhouse. While it would have been ideal to grow them in exactly the same conditions - *i.e.*, both sets in growth chambers - the mass of biomass needed for the field trial (hundreds of plants needed to produce 15 kg) was too great for this to be practical, and we do not expect potential variations in the initial biomass induced by the growing conditions to significantly alter our findings. The labelled plants were grown in potting mix in a Percival AR-100L3  $\text{CO}_2$ -controlled growth chamber (Percival, Perry, IA). The plants were exposed to cycles of 18 h light / 6 h darkness. During light cycles, the atmosphere was maintained at 400 ppm  $\text{CO}_2$ , while  $\text{CO}_2$  was allowed to accumulate during respiration during the dark cycle, and was then drawn down by photosynthesis during the next light cycle. This was done in order to reduce net respiratory losses of labelled  $^{13}\text{CO}_2$ . Plants were pulse-labelled with 13 L of 99%  $^{13}\text{CO}_2$  at regular intervals over the course of their growth in order to produce an even label. Pulse labels were delivered by opening the  $^{13}\text{CO}_2$  cylinder to fill a balloon with ~500 mL  $^{13}\text{CO}_2$ . The balloon remained attached to the cylinder so that the  $^{13}\text{CO}_2$  slowly diffused out of the balloon, delivering the pulse at a rate so that the total atmospheric concentration of  $\text{CO}_2$  was not affected. Plants in the growth chambers and the greenhouse were harvested just before they reached reproductive maturity and were oven-dried at 70°C.

#### 4.2.3 PyOM production and amendment mixing

Oven-dried corn plants were ground in a hammer mill to < 2 mm. The milled corn was pyrolyzed in a modified muffle furnace by ramping by 5°C min<sup>-1</sup> to 350°C, then holding at 350°C for 45 minutes, under Ar (Table 1). The <sup>13</sup>C-labelled and natural abundance corn PyOM materials were mixed together at masses of 12.5 g labelled PyOM + 187.5 g unlabelled PyOM for the lower label treatment and 31.35 g labelled PyOM + 168.7 g unlabelled PyOM for the higher label treatment. For the corn biomass-only plots, mixtures of 4.1 g labelled + 232.6 g unlabelled corn were created. Mixing was done in plot-level batches to ensure that each plot received exactly these proportions of labelled and unlabelled materials.

**Table 4.1** Initial PyOM and corn stover properties

Property (units)	Value	
	PyOM	Stover
Total C (%)	61.0	41.9
Total N (%)	2.7	1.96
C:N (by mass)	22	21
Total H (%)	3.9	
Total O (%)	15	
pH <sub>D1W</sub> (1:20 w/v)	10.0	
Feedstock	Corn	
Particle size (mm)	< 2	
Heating rate (°C min <sup>-1</sup> )	5	
Final temp (°C)	350	
Residence time (min)	45	
Surface area (m <sup>2</sup> g <sup>-1</sup> )	92.8	
ASTM Ash (%)	17	
ASTM Volatiles (%)	35	
ASTM Fixed C (%)	48	

#### 4.2.4 Field site and soil description

The field site is located in Cornell's research fields in Mt. Pleasant, N.Y., and is a Mardin soil (Coarse-loamy, mixed, active, mesic Typic Fragiudept) (Table 2). The soil has been historically planted to a potato, rye, clover rotation, for the past > 30 years, but was kept in rye-clover rotation for the past 5 years, with one planting of sudangrass 3 years ago. The plot was sprayed with Roundup (glyphosate) herbicide in the fall, ploughed on May 3, 2013, and kept weed-free using hand-weeding and water-permeable landscape fabric through the summer until trial initiation.

**Table 4.2** Initial soil properties

Property (units)	Value
Texture	(Channery) silt loam
pH <sub>DIW</sub>	6.0
% sand	28.1
% silt	54.7
% clay	17.2
Total C (%)	1.48
Total N (%)	0.16
C:N (mass)	9.39
Microbial biomass N* (mg kg <sup>-1</sup> dry soil) (Vance <i>et al.</i> , 1987)	8.5

\*Microbial biomass C data were compromised, but based on a measured C:N ratio of 10.2 in the DOM, we predict roughly 87 mg MB-C kg<sup>-1</sup> dry soil.

#### 4.2.5 Field trial setup and maintenance

The trial initiation date was August 16, 2013 (Day 0). Square plots (0.7 m x 0.7 m) were surrounded by 0.7-m wide weed-free borders maintained by hand weeding between every plot and along the edges. Treatments were organized using a spatially balanced complete block design (van Es *et al.*, 2007). 6.1 kg soil were removed from the top layer of soil at each plot, combined with biomass or PyOM additions, if needed, and mixed in a V-mixer. Amended plots received 4.1 T ha<sup>-1</sup> of PyOM or 11.2 T ha<sup>-1</sup> of dried original corn biomass. Mixed soils were then returned to their respective plots and evenly spread at the surface. Soil was gently tamped down using a flat piece of plywood. Soil respiration collars made from 194 mm diameter white polyvinylchloride pipes were installed at the centre of the plots with the collar protruding 30 mm and reaching 30 mm into the ground. The lower portion of the collar had holes drilled in it in order to allow roots to penetrate the soil-amendment mixtures belowground. Sudangrass seeds (*Sorghum bicolor x sudanese*) were planted in 6 groups of 3, evenly spaced around the centre of the plot and thinned to 6 plants 2 weeks after emergence. Plots were kept covered with water-permeable landscape fabric except during measurement until plant emergence, in order to keep weeds down. After plant emergence, plots were kept weed-free by hand-weeding multiple times a week. The plots were not fertilized or watered during the trial, but were exposed to natural rainfall (temperature and precipitation are plotted in Figure 4.1).

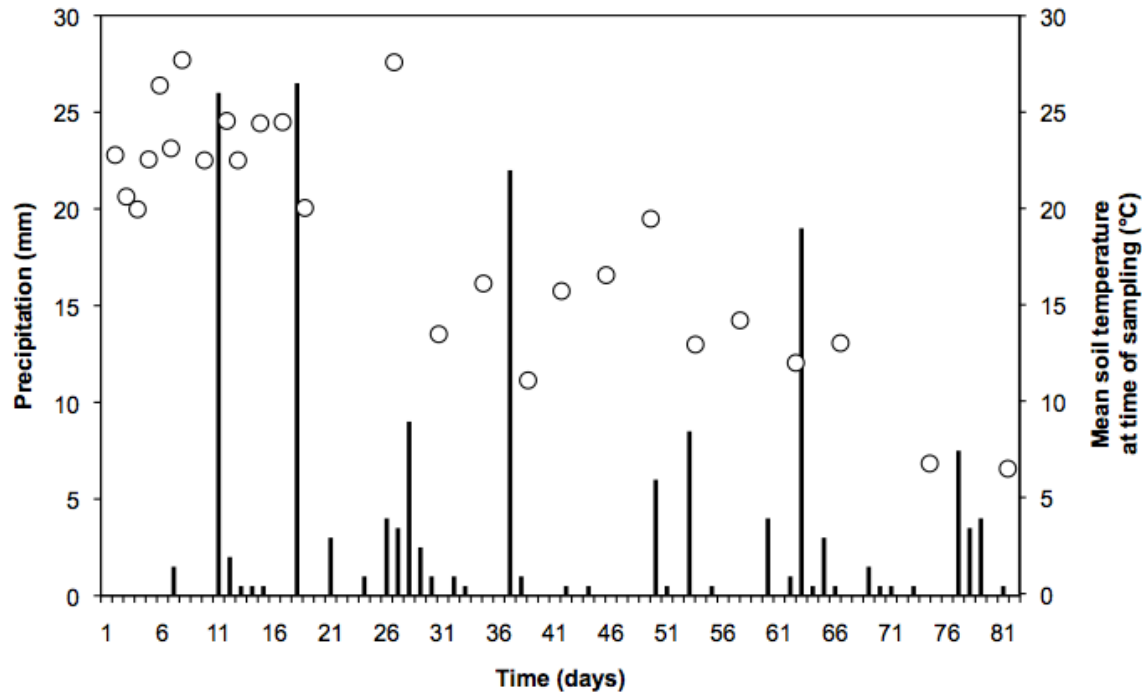


**Figure 4.1** Daily precipitation (bars) over duration of experiment and mean soil temperature (open circles) on measurement days.

#### 4.2.6 $CO_2$ flux and $^{13}CO_2$ measurements

Soil  $CO_2$  flux was measured using a LI-6400XT with a 6400-09 soil  $CO_2$  flux chamber attachment (LI-COR, Lincoln, Nebraska). Three flux measurements were taken in succession for each plot and averaged. Measurements were taken on days 0, 1, 2, 3, 4, 5, 6, 7, 9, 11, 12, 14, 16, 18, 26, 30, 34, 38, 41, 45, 49, 53, 57, 62, 66, 74, and 81. On days 12 and 66, samples were taken for  $^{13}CO_2$  analyses using modified static Iso-FD chambers (Nickerson *et al.*, 2013; see supplementary information in 4.S1 for more details). For each plot, collars were capped for 10-30 minutes with an adjacent atmospheric reference chamber capping a plugged collar. Samples of 20 mL air were then drawn from the sample and the reference chamber, and injected into 12.5

mL evacuated vials. Samples were analyzed for  $\delta^{13}\text{CO}_2$  and  $[\text{CO}_2]$  on a Thermo Scientific DELTA V isotope ratio mass spectrometer interfaced with a Gasbench II.

#### *4.2.7 Soil sampling and analysis for C*

On day 12, four 50-mm deep, 47-mm diameter cores were taken from each plot, pooled, sieved to  $< 2$  mm, sub-sampled for moisture determination, and then frozen until further analysis. On day 82, soil within the entire collar was destructively sampled and processed in the same way. All sample processing occurred within  $< 24$  hours from sampling. On days 1 and 12, two 25-mm deep soil probe samples were taken, pooled, sieved to  $< 2$  mm, and then immediately frozen in Whirl-Paks in liquid  $\text{N}_2$  and stored at  $-80^\circ\text{C}$  until further analysis. On day 82, the sieved destructive collar sample was sub-sampled for microbial community samples, which were frozen in Whirl-Paks in liquid  $\text{N}_2$  and stored at  $-80^\circ\text{C}$ .

In order to reduce issues associated with soil heterogeneity for  $\delta^{13}\text{C}$  analyses, sieved soil samples were sub-sampled to obtain about 50 g wet soil. These sub-samples were dried at  $60^\circ\text{C}$ , then the entire sub-sample was ground to a fine powder in a Retsch mixer mill. Ground samples were weighed into tin capsules and analyzed for C content and  $\delta^{13}\text{C}$  in a Thermo Delta V Advantage Isotope Ratio Mass Spectrometer and a Temperature Conversion Elemental Analyzer (Thermo Scientific, West Palm Beach, FL, at the Cornell University Stable Isotope Laboratory).

#### *4.2.8 Isotopic partitioning of solid and gas samples*

To determine the relative contribution from the two sources in the two-part systems, a standard isotope partitioning approach was applied. For example, for the plots with PyOM additions, the isotopic signature of the total emissions will be

$$(1) \delta_T = f_S * \delta_S + f_{PyOM} * \delta_{PyOM},$$

where  $\delta_X$  is the  $^{13}\text{C}$  signature of  $\text{CO}_2$  from soil ( $\delta_S$ ), PyOM ( $\delta_{PyOM}$ ), or total  $\text{CO}_2$  ( $\delta_T$ ), and  $f_S$  and  $f_{PyOM}$  represent the fraction of total emissions made up by soil and corn, respectively (Werth and Kuzyakov, 2010). Knowing that:

$$(2) f_S + f_{PyOM} = 1, \text{ or } f_S = 1 - f_{PyOM}$$

we can substitute, rearrange, and solve EQ 1 for  $f_S$ :

$$(3) f_S = (\delta_T - \delta_{PyOM}) / (\delta_S - \delta_{PyOM}).$$

In three-part systems, it is not so straightforward to separate out emission sources. However, with careful design, it is possible (Kuzyakov and Bol, 2004). The isotopic signature of the total emissions will now be:

$$(4) \delta_T = f_S * \delta_S + f_G * \delta_G + f_{PyOM} * \delta_{PyOM},$$

where  $f_G$  is the fraction of emissions from sudangrass and  $\delta_G$  is the  $\delta^{13}\text{C}$  signature of sudangrass. Initially, we will group soil and grass emissions together, calling this value  $X$ :

$$(5) X = f_S * \delta_S + f_G * \delta_G.$$

Substituting  $X$  into EQ 4, we get:

$$(6) \delta_T = X + f_{PyOM} * \delta_{PyOM}$$

This is where additional PyOM treatment is instrumental. Simply, the only difference between the two treatments with PyOM amendments and sudangrass is that their PyOM has different  $\delta^{13}\text{C}$  signatures. We know the  $\delta^{13}\text{C}$  values of each of these PyOM materials ( $\delta_{PyOM1}$  and  $\delta_{PyOM2}$ ), and measured the total  $\delta^{13}\text{C}$  from each treatment ( $\delta_{T1}$  and  $\delta_{T2}$ ) giving us two equations from EQ 6:

$$(7) \delta_{T1} = X + f_{PyOM} * \delta_{PyOM1} \text{ and } \delta_{T2} = X + f_{PyOM} * \delta_{PyOM2}.$$

With only two unknown variables,  $X$  and  $f_{PyOM}$ , and two equations, we solved EQ 7 for both values. Then, we solved EQ 5 ( $X = f_S * \delta_S + f_G * \delta_G$ ), using the approach of EQs 1-3. Thus, calculated the fraction of CO<sub>2</sub> emissions coming from PyOM, SOC, and sudangrass. To solve for the three fractions, we used each possible pairing of plots with higher and lower PyOM  $\delta^{13}C$  signatures, with the fluxes from the lower PyOM plots.

#### 4.2.9 Data processing and statistical analyses

On a small minority of occasions toward the end of the trial, we recorded negative fluxes, which we interpret as errors due to very low flux rates, and have excluded from analyses. In addition, we excluded two data points where recorded fluxes were 56 and 16 SD away from the mean of the remaining plots. All statistical analyses were performed in R (R Core Team, 2012). We fit linear mixed effects models to the CO<sub>2</sub> fluxes, with addition type, day, an interaction between PyOM and day, and plot ID as a random effect (a repeated measures approach) as factors, using the R package lme4 (Bates *et al.*, 2014). To make post-hoc comparisons, we performed pairwise comparisons between the different soil amendments for a given day with a Tukey adjustment of p-values, using the lsmeans R package (Lenth, 2014).

#### 4.2.10 Microbial community analyses

DNA was extracted from 0.250 g moist soil samples using the MoBio PowerLyzer PowerSoil kit, following the kit's directions. The DNA was quantified using the Quant-iT PicoGreen

dsDNA Assay Kit (Life Technologies) with a multimode microplate reader (Molecular Devices, Sunnyvale, CA). DNA results were normalized to a yield per gram of dry soil based on the soils' initial moisture contents. PCRs were performed for each sample in triplicate in order to yield sufficient sample without running too many reactions, which may increase the risk of PCR biases and chimera formation. PCR was conducted with 12.5  $\mu\text{L}$  Q5 Hot Start High Fidelity 2X mastermix (New England Biolabs), 5  $\mu\text{L}$  of DNA template diluted with water at a ratio of 1:50, 5  $\mu\text{L}$  water, and 2.5  $\mu\text{L}$  primer mixtures to a total volume of 25  $\mu\text{L}$ . Each PCR consisted of a 98°C hold for 30s, followed by 30 cycles of [5s at 98°C, 20s at 20°C, and 10s at 72°C], with a final extension for 2min at 72°C. Modified 515F and 907R primers were used to target the V4/V5 regions of the 16S ribosomal DNA. A different, unique, pair of barcoded forward and reverse primers were used for each sample so that they could be distinguished after pooling for sequencing (supplementary information Tables 4.S2 and 4.S3). Each PCR product was run on a 0.5% agarose gel, along with the negative control, to determine whether amplification was successful, with any unsuccessful reactions being re-run. Replicate PCRs were pooled, and DNA concentrations were normalized across all samples using SequalPrep normalization plates (Applied Biosystems) with 25  $\mu\text{L}$  of sample. The pooled sample was purified using a Wizard SV Gel and PCR Clean-Up System (Promega). The pooled sample was then dried in an evaporative centrifuge until there was < 100  $\mu\text{L}$  total sample. This sample was quantified using PicoGreen as above, and evaporated further until 23  $\mu\text{L}$  of sample at 4.75 ng DNA  $\mu\text{L}^{-1}$  remained. This sample was submitted with sequencing and indexing primers for paired ends 2 x300 bp sequencing on the Illumina MiSeq platform at Cornell's Biotech Core Facility.

## *4.2.11 Microbial community bioinformatics*

### *4.2.11.1 Data merging and demultiplexing*

The data, as returned from the sequencing facility, was in four sets - a forward and reverse sequence and two barcode reads. First, we merged the data from the forward and reverse reads together, using the Paired End reAd mergeR (PEAR) (Flouri and Zhang, 2013). From these merged reads, we created a database, using screed (Nolley and Brown, 2012). We also created databases for the forward and reverse barcode reads. Using these three databases, and a file with the sample identity of each primer combination, we used a custom Python script to associate the merged reads with their sample ID, resulting in a file with the sample sequences and quality scores (indicating the probability that the base was assigned incorrectly) along with their sample IDs.

### *4.2.11.2 Quality control*

We used the `fastq_maxee` command from USEARCH (Edgar, 2013) to remove any sequences with maximum expected error rates greater than 1. We also removed any sequences that had ambiguous base calls (represented by N's in the sequence). We used the `unique.seqs` command from `mothur` (Schloss *et al.*, 2013) to select the unique sequences (to pare down the mass of data we were working with for subsequent steps). We created a reference database by merging the Silva bacterial, archaeal, and eukaryal databases, which we then used to create a rough alignment for our sequences. We took our list of unique sequences, and aligned (considering both directions

in which the sequence could potentially be read) and filtered them to remove vertical gaps, using `align.seqs` and `filter.seqs`. This returned 10,612,808 sequences, 4,881,621 of which were unique. We then removed any sequences that were less than 370 bp or more than 376 bp long, and which had more than 8 homopolymers (runs of the same sequence in a row). This left us with 10,237,689 sequences, 4,697,703 of which were unique.

#### 4.2.11.3 Operational taxonomic unit (OTU) picking

We used the `usearch` command, `sortbysize`, to remove any sequences that were only present once. While this will exclude any true “singletons” (creating false negatives), a single sequencing error could result in a false positive, which is more likely, so we choose this approach. We then used the `usearch` clustering command, `cluster_otus`, to group the sequences into similar units (OTUs), within which sequences have at least 97% identity from the chosen centroid sequence. The command is a “greedy clustering algorithm”, which starts with the most abundant sequence (predicted to be more likely correct sequences than very rare sequences) as centroids. Remaining sequences are compared to the centroid, and if they are more than 97% identical, they are clustered within that OTU. If they are less than 97% identical, they start a new centroid (OTU). This method allows for the detection of chimeras (hybrid artifact sequences), which are discarded. We then used the `parallel_assign_taxonomy_uclust` command and the `Silva_111` representative set of sequences to assign rough taxonomy to the selected OTUs. This was sufficient for us to then remove any sequences returning chloroplast, *Eukarya*, unassigned, *Archaea* or mitochondria identities (leaving only *Bacteria*), using `remove.seqs` in `mothur`. Having removed non-bacterial sequences, we then used the `usearch` command, `usearch_global`,

to select our final OTUs. We used the usearch script, `uc2otutab.py`, to create an OTU table, which we converted into a `.biom` format. This process left us with 8,330,257 sequences, 7,700 of which were unique. One sample (one of the day 65, soil-only treatment plots) was left with only 8 sequences, so it was excluded from further analyses. Remaining samples contained from 8,830 to 194,356 total sequences.

#### *4.2.11.4 Community analysis*

We aligned the remaining sequences, with SSU-ALIGN (Nawrocki, 2009). We then used `ssu-mask` to remove (ignore) columns that did not align well (had low posterior probabilities that a nucleotide belongs in a given column). We then used the `make_phylogeny.py` script from QIIME (Caporaso *et al.*, 2010), using the `fasttree` method. Using this phylogeny, and the OTU table, we ran the `beta_diversity.py` script using weighted UniFrac as the diversity metric. UniFrac compares pairs of samples, determining the percent of branch length that is unique to one of them, rather than shared (Lozupone *et al.*, 2011). Weighted UniFrac accounts for the relative abundance of each OTU, not just considering its presence/absence. This resulted in a distance matrix, which we then used to run a principal coordinates analysis (PCoA) using `principal_coordinates.py`. We tested whether there were significant differences between amendment types with an ANOSIM, using the `compare_categories.py` command in QIIME. We performed this analysis (beta diversity using weighted UniFrac, PCoA, and ANOSIM) separately for each day. We assigned taxonomy to the OTUs using the QIIME `assign_taxonomy.py` command, and the QIIME GreenGenes 97% OTUs database as a reference.

## 4.3 Results

### 4.3.1 Soil C dynamics

Soil CO<sub>2</sub> fluxes from plots that received stover additions were significantly higher than all other plots for almost the whole first month (Figure 4.2). Plots with PyOM additions experienced significantly higher CO<sub>2</sub> fluxes than plots with no additions on days 0 and 12, after which there were no significant differences (Figure 4.2).

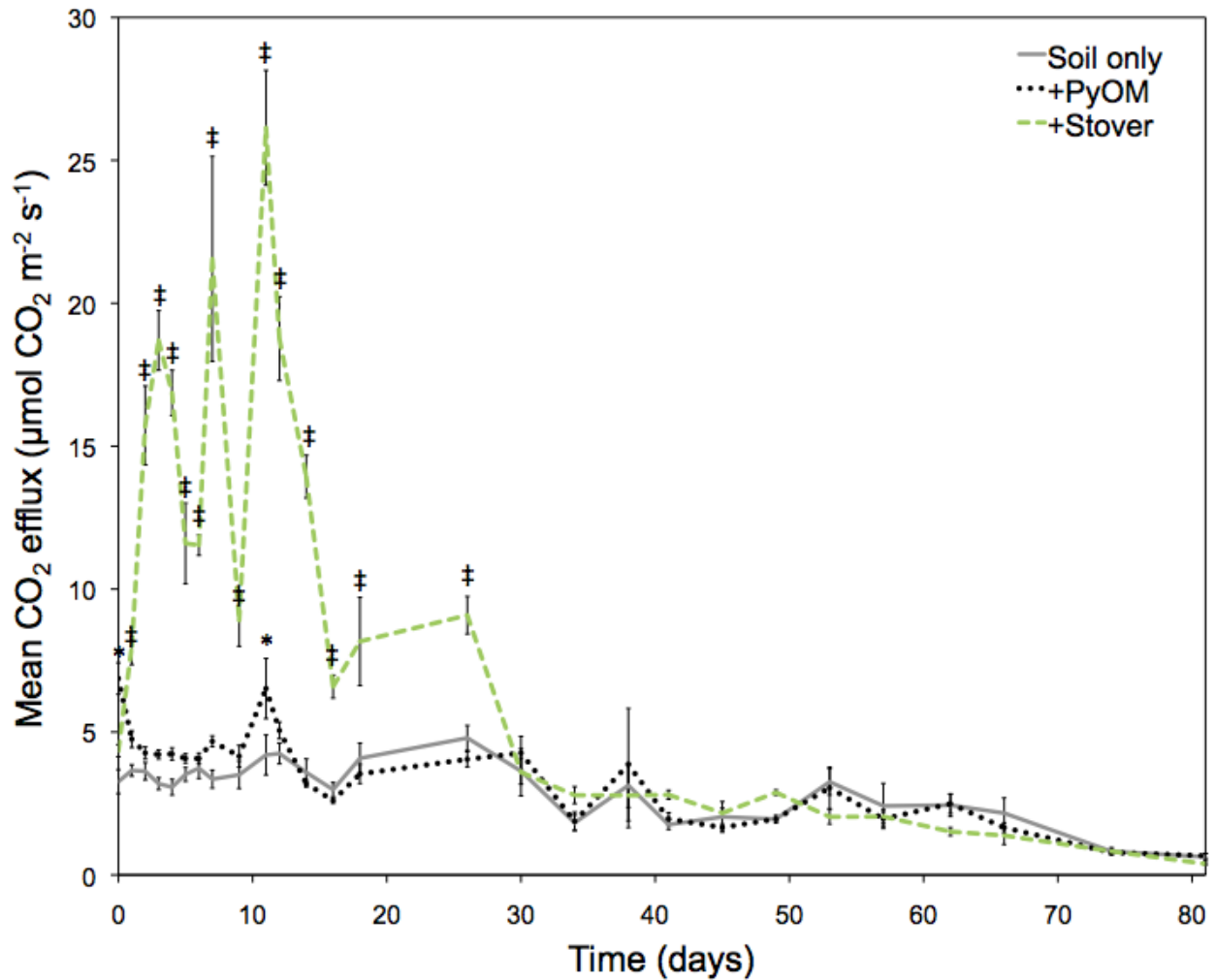


**Figure 4.2** Mean CO<sub>2</sub> flux rates. Error bars ±1SE, n=8-16. \* indicates significant differences between plots with PyOM additions and stover or no-addition plots, while ‡ indicates significant

differences between plots that received fresh stover additions and PyOM or no-addition plots (mixed model repeated measures design, Tukey-adjusted post-hoc comparisons,  $p < 0.05$ ).

The final cumulative  $\text{CO}_2\text{-C}$  emissions from the plots with stover were significantly greater than the sum of the total C in the added stover plus the final cumulative  $\text{CO}_2\text{-C}$  emissions from the plots with no additions (indicated by the star in Figure 4.3) ( $t$ -test,  $p < 0.05$ ).

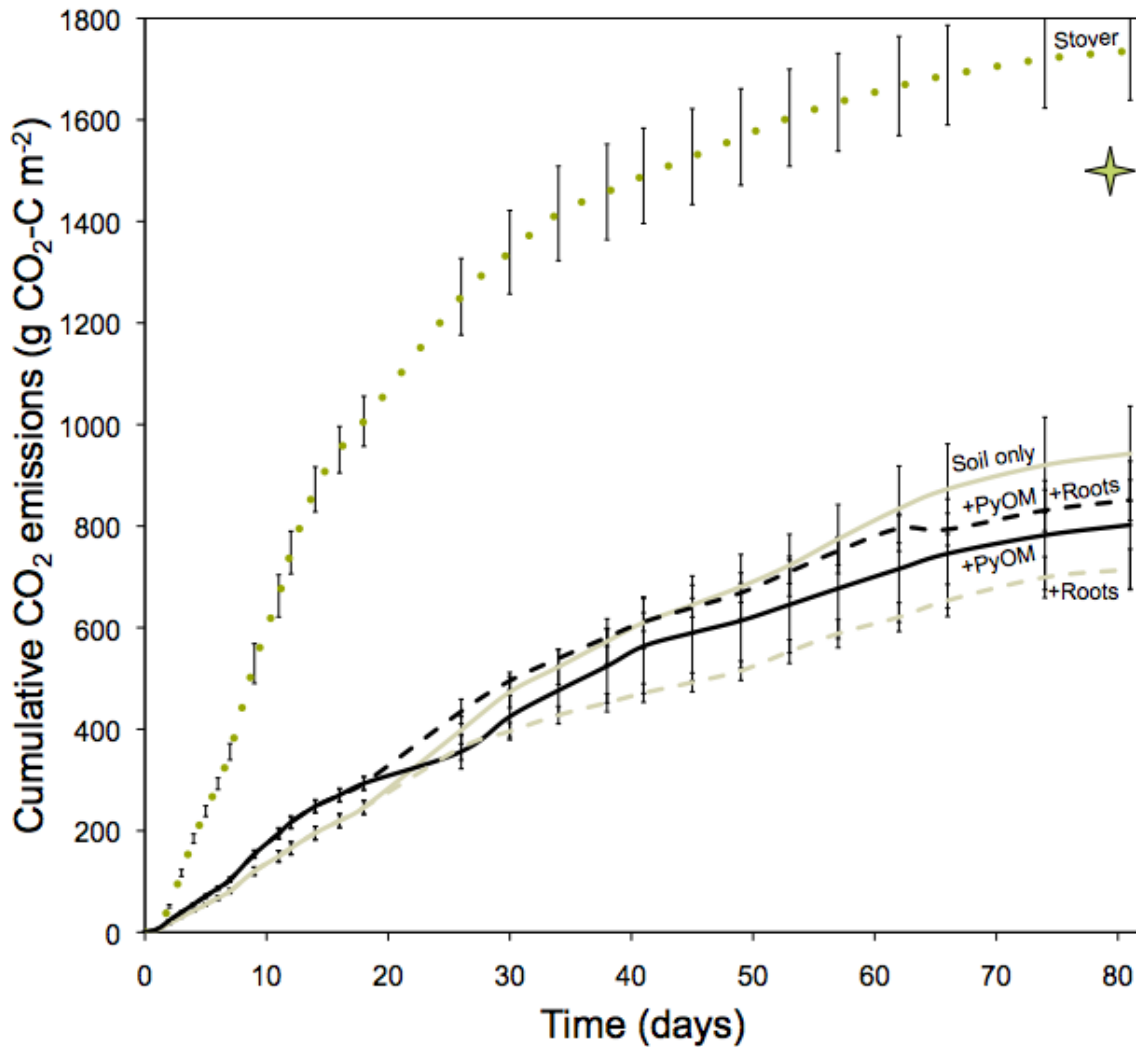


**Figure 4.3** Estimated cumulative mean evolved  $\text{CO}_2$ , assuming constant flux rates between sampling intervals. Dotted line indicates plots that received fresh stover additions. Black lines indicate plots that received PyOM additions. Dashed lines after day 18 indicate plots that had plants present. Error bars indicate  $\pm\text{SE}$ ,  $n=8-16$ . Star indicates expected cumulative  $\text{CO}_2$  emissions for the stover plots if all stover C had been mineralized and there was no increase in SOC mineralization.

On day 12, SOC-derived CO<sub>2</sub> fluxes were significantly greater in the plots that received corn stover additions, but not in the plots that received PyOM additions, while on day 65, there were significantly lower SOC-derived CO<sub>2</sub> fluxes from the plots that received corn stover additions, although overall fluxes were much lower on this date. Three-part partitioning revealed 334% greater root-C derived CO<sub>2</sub> emissions in the plots with PyOM additions than the plots with no additions and significantly lower PyOM-C derived CO<sub>2</sub> emissions than the plots with no plants (Figure 4.4).

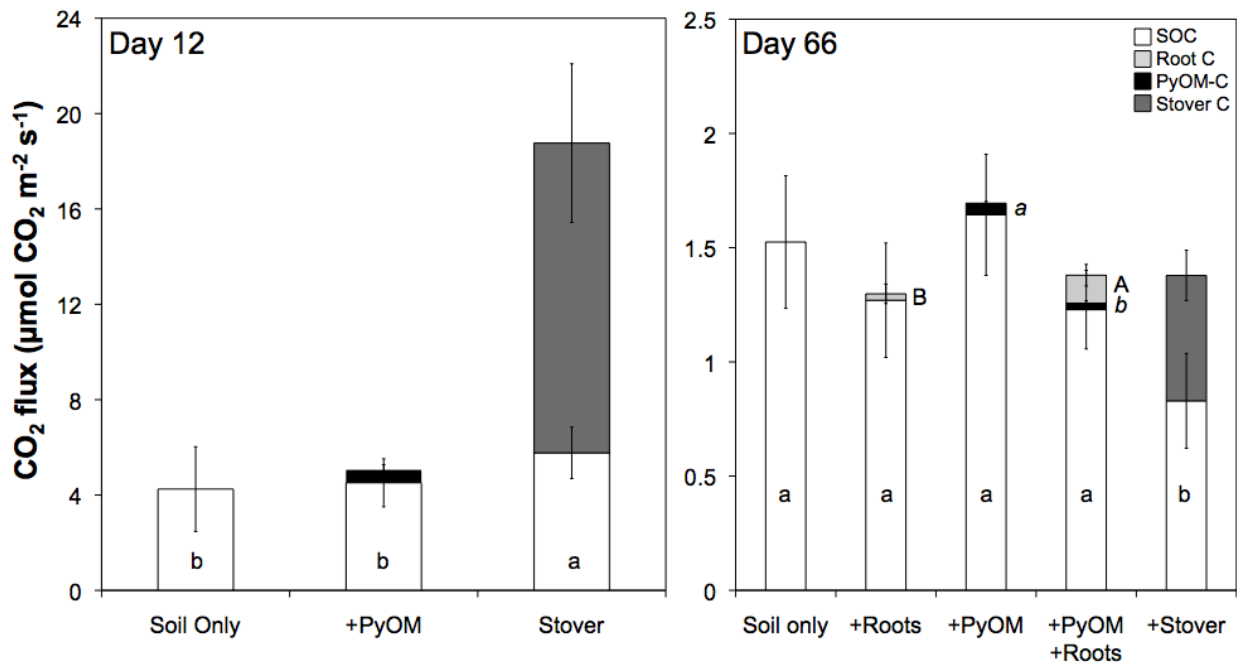


**Figure 4.4** Partitioned CO<sub>2</sub> fluxes on days 12 and 66. Note different scales on y-axis. Error bars  $\pm$ SE, n=8-16. Letters indicate significant differences within each fraction (SOC: ANOVA, Tukey's HSD,  $p < 0.05$ ; Root C and PyOM-C: one-tailed  $t$ -tests,  $p < 0.05$ ).

There were no significant changes in total SOC stocks over time within or between treatments. Both PyOM-C and stover C decreased significantly over time, showing major C losses, of 72% and 81%, respectively (Figure 4.5). Additionally, there was significantly less total C in stover than in PyOM at both timepoints ( $p < 0.007$ ).

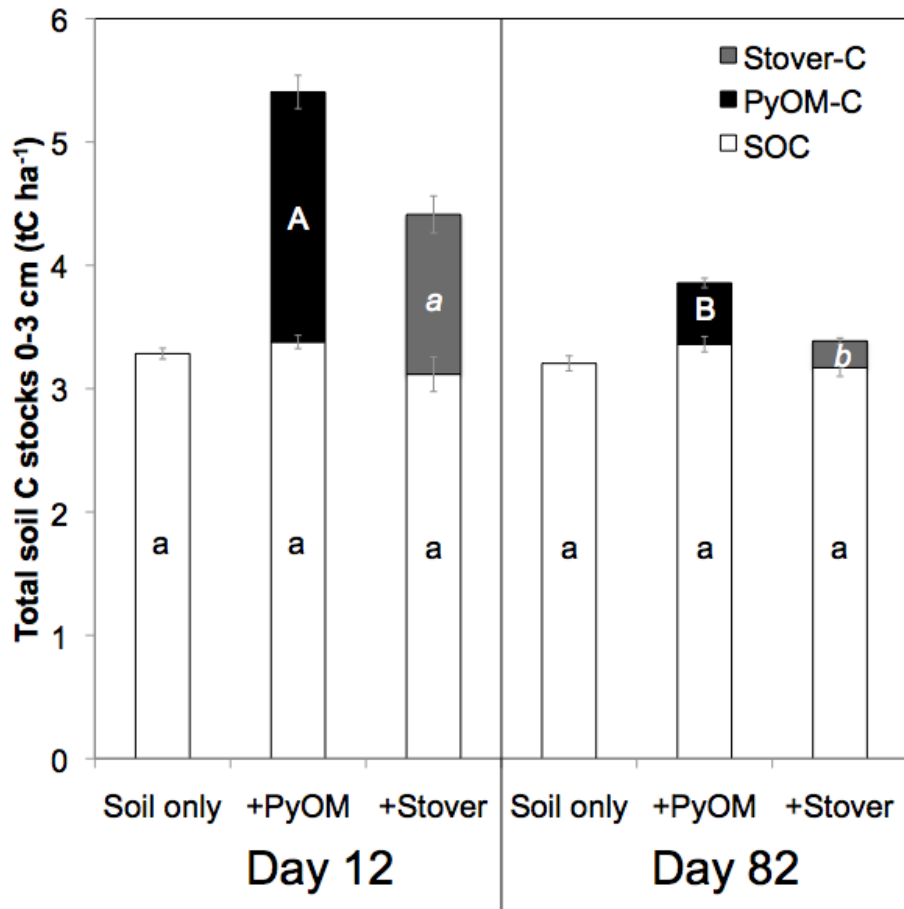


**Figure 4.5** Partitioned final soil C stocks near the beginning (Day 12) and end (Day 82) of trial. Error bars  $\pm 1$ SE,  $n=8-16$ . Letters indicate significant differences within each fraction (ANOVA, Tukey's HSD,  $p<0.05$ ).

#### 4.3.2 Biomass and pH

Plants from plots with PyOM additions had significantly greater aboveground biomass than the plots with no additions (Figure 4.6).

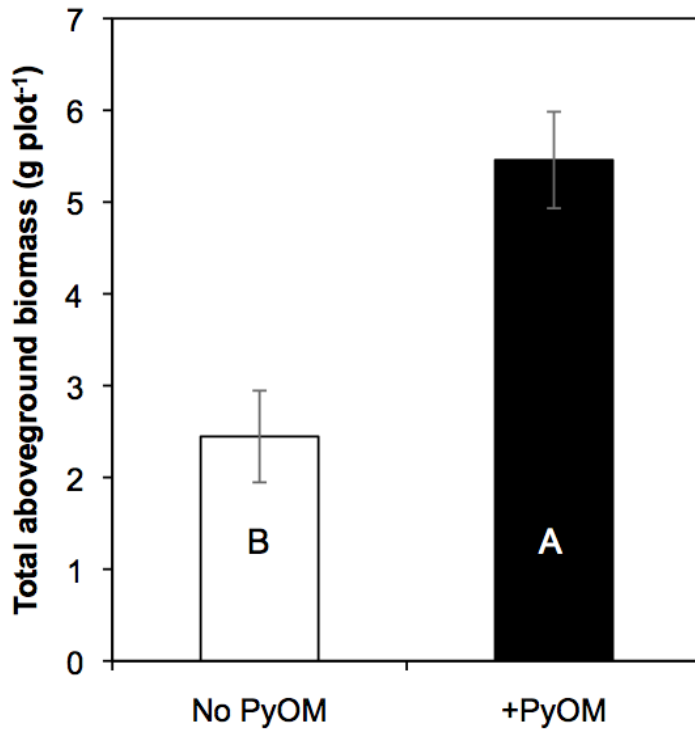


**Figure 4.6** Final mean above-ground dry biomass. Error bars  $\pm 1$ SE,  $n=8-16$ . Letters indicate significant differences ( $t$ -test,  $p<0.05$ ).

PyOM additions significantly increased soil pH by 0.85 initially, with an increase of 0.75 persisting at the end of the field trial (Figure 4.7). Stover additions did not significantly change the soil pH.

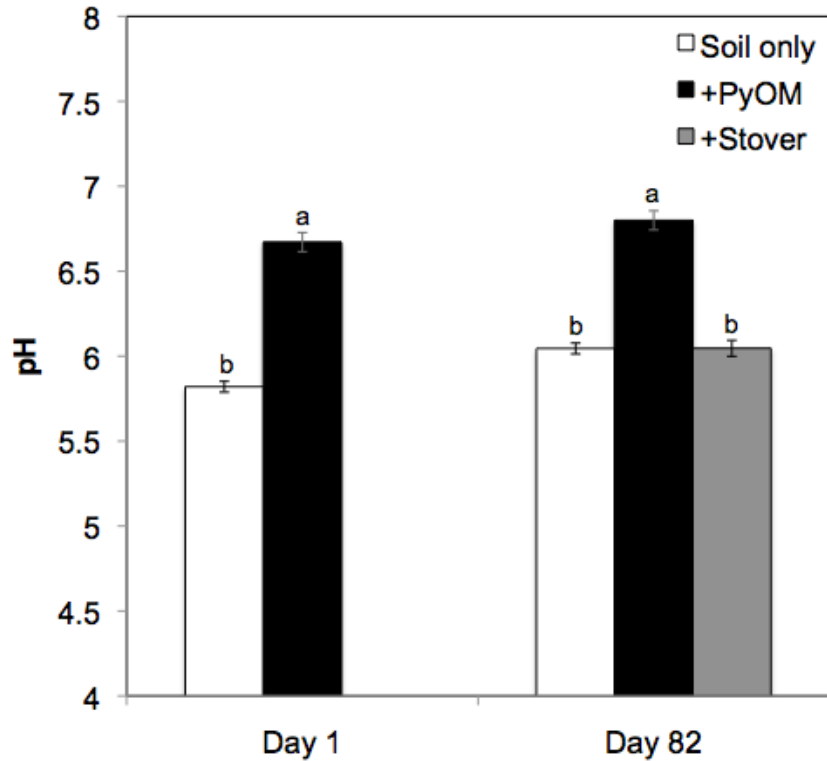


**Figure 4.7** Soil pH in DIW at the start and end of the trial with PyOM and stover amendments. Error bars  $\pm 1SE$ ,  $n=8-16$ , letters indicate significant differences (ANOVA, Tukey's HSD,  $p<0.05$ ).

#### 4.3.3 Microbial Community Analyses

Quantities of DNA extracted from the soil on day 1 did not change as a result of the additions, but on days 12 and 82, more DNA was extracted from the plots with fresh organic matter additions than those with PyOM or no additions, and this result was significant (ANOVA, Tukey's HSD,  $p<0.05$ ; supplementary information Table 4.S1). Additionally, significantly less DNA was extracted on the final day than on the first two sampling dates (ANOVA, Tukey's HSD,  $p<0.05$ ). The results from Day 1 indicate that the presence of PyOM likely did not substantially interfere with DNA extraction.

The PCoA plots are shown in Figure 4.8, with the fraction of variation explained by each component described in Table 3. On day 1, there are not clear differences between communities. By day 12, the corn stover-amended plots are clearly distinct from the other plots, and there appear to be some differences emerging between the plots with vs. without PyOM additions. By day 82, all three amendment types appear distinct.

**Table 4.3** Percent variation explained by each component for PCoA of weighted UniFrac matrices

<b>PCo</b>	<b>Day 1</b>	<b>Day 12</b>	<b>Day 82</b>
1	30	74	40
2	20	8	16
3	10	4	9

These trends are supported by the ANOSIM analyses, which report significant differences across amendment types for days 12 ( $p=0.001$ ) and 82 ( $p=0.001$ ). Testing only the PyOM or no PyOM plots showed a significant difference on day 82 ( $p=0.001$ ), as well as a difference on day 12, although this result was not significant ( $p=0.06$ ). There were no significant effects of plants on day 1, 12, or 82 ( $p$ -values 0.456, 0.708, 0.660, respectively).

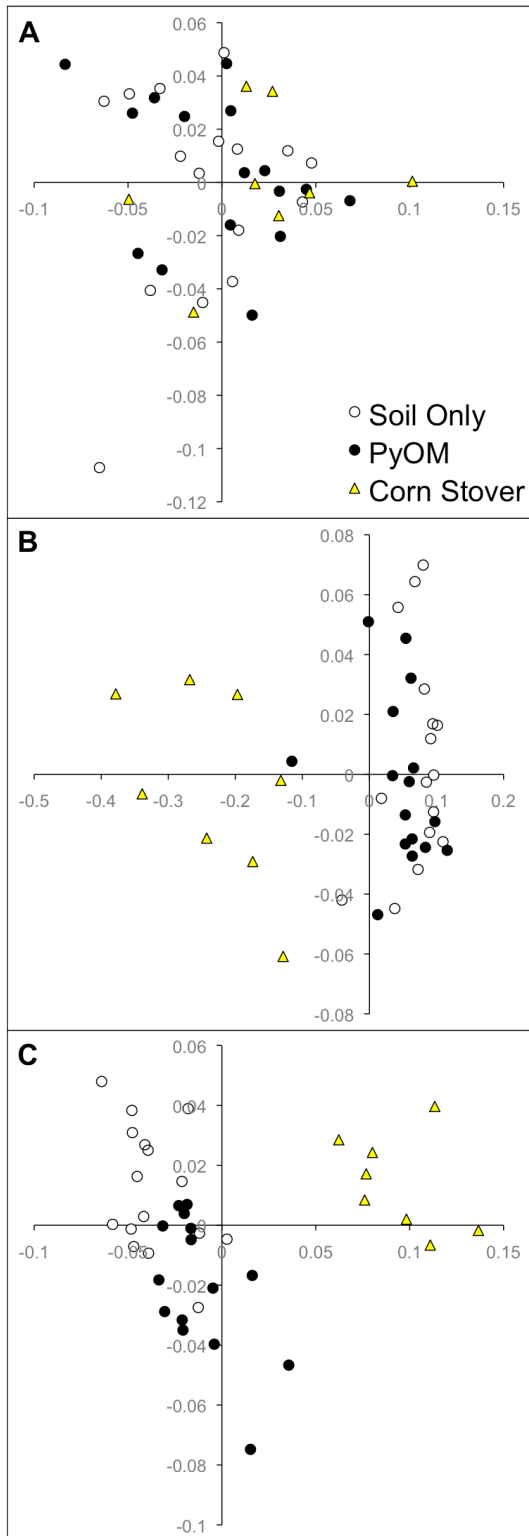


**Figure 4.8** PCoA components 1 (x-axis) and 3 (y-axis) from weighted UniFrac distances between bacterial communities on days 1 (A), 12 (B) and 82 (C). Open circles represent plots with no amendments, black circles plots with PyOM additions, and yellow triangles plots with stover additions (plots with and without plants were pooled by amendment treatment).

The relative fractions of a number of phyla were significantly higher (*Proteobacteria*, *Bacteroidetes*, and *Firmicutes*) or lower (*Acidobacteria*, *Planctomyces*, *Chloroflexi*, *Gemmatimonadetes*, *Armatimonadetes*, and *Nitrospirae*) in the plots that received stover than those with no amendments on days 12 and 82 (Figures 4.9 and 4.10). PyOM additions significantly decreased the fraction of taxa associated with the *Planctomyces* phylum on day 12 (Figure 4.9). On day 82, PyOM additions had significantly decreased the fraction of taxa associated with *Acidobacteria* or *Armatimonadetes* phyla, and increased the fraction associated with *Bacteroidetes* (Figure 4.10).

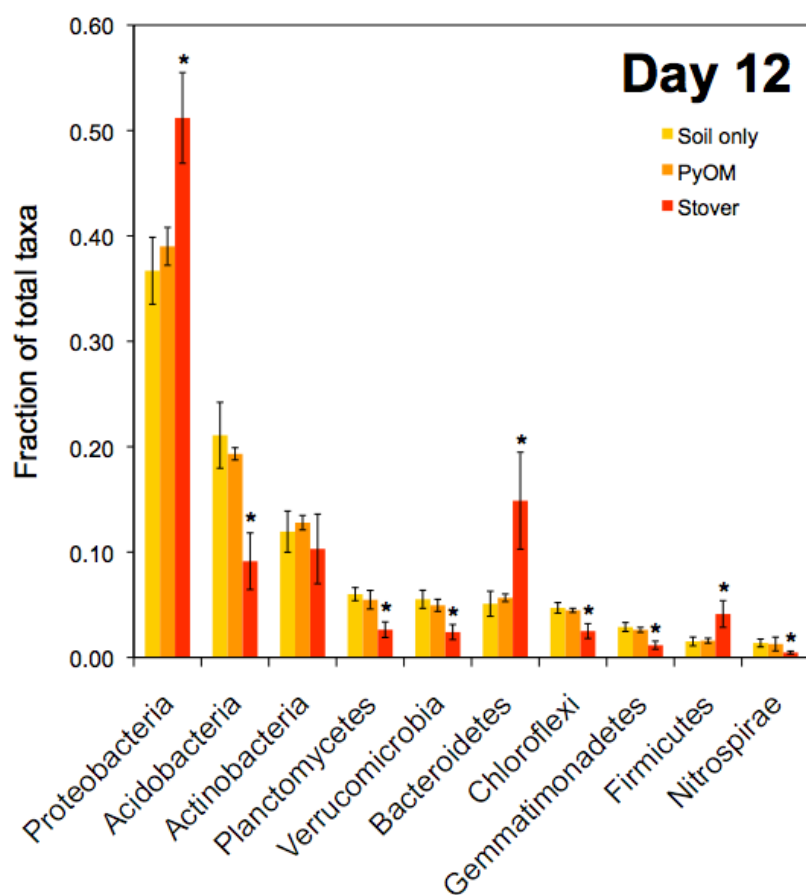


**Figure 4.9** Fraction of total taxa for top 10 phyla on Day 12. Error bars  $\pm 1SD$ ,  $n=8-16$ , \* indicates significant difference from soil-only treatment ( $t$ -test,  $p < 0.005$ , Bonferroni-corrected for 10 comparisons).

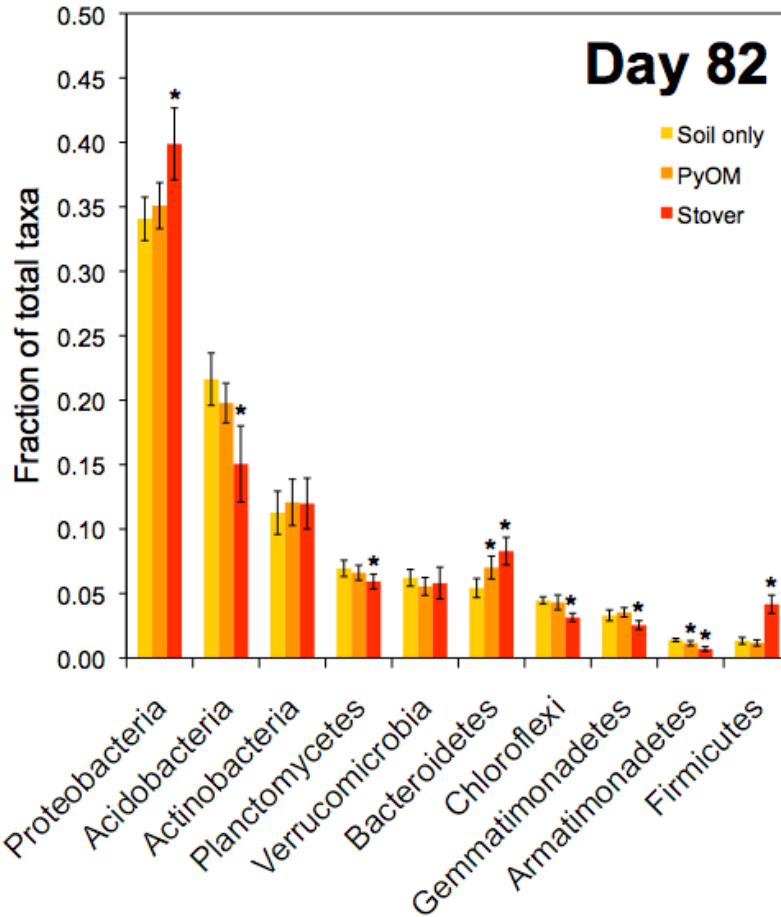


**Figure 4.10** Fraction of total taxa for top 10 phyla on Day 82. Error bars  $\pm 1SD$ ,  $n=8-16$ , \* indicates significant difference from soil-only treatment ( $t$ -test,  $p < 0.005$ , Bonferroni-corrected for 10 comparisons).

## 4.4 Discussion

### 4.4.1 Soil $CO_2$ dynamics

The significant increase in soil  $CO_2$  emissions on 5 of the first 6 days measured after PyOM additions (Figure 4.2) was likely due at least in part to the mineralization of PyOM. Because the PyOM was produced at the relatively low temperature of  $350^\circ C$ , there is likely a substantial fraction of relatively easily mineralizable C (Whitman *et al.*, 2013; Zimmerman, 2010).

Additionally, because the basic PyOM was added to a somewhat acidic soil, it is possible that some of the C losses are due to the dissolution of carbonates.

It is possible that some increase in SOC emissions occurred along with emissions of added PyOM-C, but on Day 12, when we partitioned CO<sub>2</sub> emission fluxes, SOC-derived CO<sub>2</sub> was not higher in the plots with PyOM additions (Figure 4.4). In contrast, the addition of stover significantly increased plot-level CO<sub>2</sub> emissions over a longer period of time (up to 49 days later) (Figure 4.2), and resulted in significantly greater SOC-derived CO<sub>2</sub> emissions on Day 12 (Figure 4.4). However, by day 66, there were significantly lower SOC-derived CO<sub>2</sub> emissions in the plots with stover (Figure 4.4). Thus, we might ask what the net effect of stover applications on SOC stocks likely was. Total final SOC stocks do not reflect significant changes for any of the treatments (Figure 4.5), likely indicating any net C losses were smaller than the precision with which we can measure the SOC stocks. However, the rough cumulative CO<sub>2</sub> emissions data (Figure 4.3) suggest that net SOC losses must have been greater in the plots with stover additions than those with no additions, in order to account for the total increase in CO<sub>2</sub> emissions with stover additions, because total CO<sub>2</sub> emissions exceeded the total amount of stover C added (value indicated by the star symbol in Figure 4.3), this would not be sufficient to account for total CO<sub>2</sub> emissions. The limitations to this assumption, of course, are that emission rates were measured intermittently, not constantly, so the calculation of cumulative emissions is only a rough estimate. Still, it is consistent with the partitioned data from Day 12 and the fact that total emissions early in the trial were substantially higher than later on, when decreased SOC emissions occurred in the plots with stover additions. Because significant differences in SOC-derived CO<sub>2</sub> emissions between plots with and without PyOM additions were not detected on

Day 12 or Day 66, and total estimated cumulative emissions in the plots with PyOM additions were not significantly different at the end of the trial, even if there was a short-term increase in SOC-derived CO<sub>2</sub> emissions with PyOM additions in the first few days, the cumulative emissions data would indicate that this was counteracted by decreased SOC mineralization over the course of the trial.

The lack of a detectable net “priming effect”(Bingeman *et al.*, 1953) on SOC from PyOM additions is reasonable. As reviewed in Chapter 1, specific combinations of PyOM materials and soils have been found to produce a wide range of effects. We found a net decrease in SOC mineralization in the same soil type under a different management history (Chapter 3) over a slightly shorter timeline (but under “optimal” conditions), with PyOM produced from maple twigs (*Acer saccharum*) rather than corn, but both at 350°C. Because we could not detect significant decreases in the field plots even with no amendments (but would expect them, since we measured CO<sub>2</sub> losses and there were no C inputs over the course of the trial), it would not necessarily be possible to detect a change in these losses using bulk SOC measurements.

There were significant losses of both PyOM and stover over the course of the experiment. While efforts were made to reduce wind and water erosion by mixing the amendments into the top layer of soil and by installing plastic guides to direct runoff water away from the plots, we predict that the bulk of these losses was due to physical losses, not mineralization. From a systems perspective, because significantly less stover-C remained than PyOM-C and it is possible that stover additions increased net SOC mineralization while PyOM additions did not, in this case, it

appears that producing and applying PyOM from corn stover resulted in slightly greater soil C storage than directly applying the same initial amount of corn stover to the soil.

#### *4.4.2 Three-part partitioning of CO<sub>2</sub> emissions flux*

We demonstrated the successful application of three-part partitioning of soil CO<sub>2</sub> emissions between three separate components for the fluxes on day 66. This approach allowed us to conclusively demonstrate that PyOM mineralization may be affected by the presence of plant roots, and that plant root respiration may be affected by the presence of PyOM. The significantly higher root-derived CO<sub>2</sub> emissions from plots with PyOM additions on Day 66 are consistent with the greater final aboveground biomass in those plots (Figure 4.6). A first explanation might be that these effects could be due to a pH increase (< 1 pH unit) in the soils with the addition of PyOM, which could have improved growth conditions and plant productivity. Dunavin (1969) found dry forage yield of sudangrass increased significantly with a pH increase from 5.4/5.8 to 6.4/6.9 in a fine sandy soil, and was accompanied by increased Ca and Mg concentrations. However, Fernandes and Coutinho (1999) found that increasing pH above 5.5 in two loamy sand Dystric Cambisols did not increase dry matter production in sudangrass, so pH effects may not be the full explanation. It is possible that the minerals added along with PyOM also provided nutrients to the plants, allowing for improved growth. Additionally, physical factors, such as improved water holding capacity, could have potentially had an effect, although the PyOM was only mixed into the top 1-2 cm. Another possibility is that the albedo effect played a role in plant growth and soil respiration in general, with the dark PyOM plots being warmer. However, we did not detect significant increases in soil temperature in the plots that received PyOM additions

(data not shown), so we argue that this is not likely an important factor. Additionally, these findings are only for a single time point - a “snapshot”. It would be ideal to have continuous  $^{13}\text{CO}_2$  measurements, so that conclusions could be made with regard to the net effect of PyOM and plants on soil C dynamics in the system.

While this partitioning approach could just as easily be applied to bulk samples as well as gas samples, in this trial, the amount of root-derived C in the bulk soil was likely very low, and not detectable within the margin of error. There was not a detectable effect of the sudangrass plants on the bulk soil  $^{13}\text{C}$  signature in the plots without PyOM additions, and in the greenhouse trial described in Chapter 2, even fully-grown corn plants contributed only a marginal amount of C to the total soil C. Thus, we did not apply three-part partitioning to the final total soil C stocks.

This partitioning approach would be applicable to a wide range of three-part systems - anywhere where one component could be produced with two different  $^{13}\text{C}$  labels. For example, one could use this approach with any  $\text{C}_3/\text{C}_4$  plant/soil pairing and a  $^{13}\text{C}$ -labelled organic amendment. It is an additional option to the method applied by Kuzyakov and Bol (2004), who partition the multiple C sources by creating a series of three combinations of components, where each separate source has a different  $^{13}\text{C}$  signature to the other two. Their approach is appealing in that it can work with only natural abundance  $^{13}\text{C}$  sources, and does not require isotopic labelling. Our approach is appealing in that it does not require that multiple components have “identical” isotopic signatures, which can be hard to achieve for some components, and that it requires only two “treatments”. For future applications, we would make a few recommendations: because of the high error often associated with isotopic partitioning methods due to the high multi-level

heterogeneity of natural systems, designing experiments with large numbers of replicates is ideal. Additionally, while we created the different  $^{13}\text{C}$  signatures in the added PyOM by combining different ratios of highly enriched and natural abundance PyOM, we would recommend that, if possible, the entire mass of the two sets of PyOM materials be uniformly enriched at the two different rates. This would protect against potential issues of sample heterogeneity, particularly for analyses that require only very small masses of material, such as solid C/N elemental and isotopic analyses.

#### *4.4.3 Soil microbial community shifts*

The magnitude of the shifts in soil bacterial communities correspond roughly to the soil  $\text{CO}_2$  fluxes. The plots that received corn stover amendments showed dramatic increases in  $\text{CO}_2$  emissions almost immediately, and significant shifts in those plots' communities were already detectable by day 12. While the plots that received PyOM additions began to show signs of divergence from the soil-only plots by day 12, their soil bacterial community differences were not significant until the final sampling date. This observation may indicate that the less dramatic short-term response to labile PyOM additions was not sufficient to cause significant community-level changes, although it may have caused significant changes at the level of the individual taxa. Indeed, we do see a trend toward increases in the same taxa that increase significantly with stover additions in the short term.

One possible explanation for the longer-term emergence of differences in the soil communities in the plots with PyOM additions is that it indicates a slower-to-emerge response to shifts in soil

pH. Soil microbial communities are highly sensitive to pH changes (Bartram *et al.*, 2013; Rousk *et al.*, 2010). In particular, the aptly named phylum *Acidobacteria* has been shown to be particularly sensitive to pH shifts, although its subgroups show variable responses to acidity: subgroups 1, 2, and 3 have been shown to increase at lower pHs, while subgroups 4, 5, 6, 7, and 17 have been shown to decrease at lower pHs (Bartram *et al.*, 2013; Rousk *et al.*, 2010). Both Bartram *et al.* (2013) and Rousk *et al.* (2010) characterized soils from long-term (50+ and 100+ years, respectively) liming trials, so it is not possible to predict from those studies the expected timescale of a soil microbial community response to pH changes. Still, we note that there was no change in the relative frequency of the *Acidobacteria*-5 order with PyOM additions on day 12, which is not what we would expect if driven by an increase in pH, and by day 82, there were still no significant differences in the frequency of the top 8 *Acidobacteria* orders (supplementary Figures 4.S2 and 4.S3). Thus, we might argue that the differences driving the shift in the bacterial community of plots with PyOM additions is likely not purely driven by an increased pH.

The positive response to stover additions of taxa from the *Proteobacteria*, *Bacteroidetes*, and *Firmicutes* phyla is consistent with previous analyses of soil microbial communities after the addition of easily-mineralizable C. Fierer *et al.* (2007) found a positive correlation between *Bacteroidetes* and  $\beta$ -*Proteobacteria* and increasing additions of sucrose. Although Fierer *et al.* (2007) did not observe a clear response from *Firmicutes*, Pascault *et al.* (2013) found taxa from the *Firmicutes* phylum were stimulated by wheat residue additions, while *Proteobacteria*, *Firmicutes*, and *Bacteroidetes* all responded positively and rapidly to alfalfa additions. However, phylum is a very coarse level at which to consider microbial function - there is likely high

functional diversity within a given phylum. The next steps in analyzing this dataset will include investigations at a finer taxonomic resolution to determine specifically which taxa responded to the additions of stover and PyOM.

#### *4.4.4 Conclusions*

PyOM additions did not increase net SOC mineralization over the course of the experiment, while stover additions likely did. However, the presence of PyOM affected plant growth, likely including plant root respiration. This effect may have been due to a pH shift, as well as mineral nutrient additions. Three-part stable C isotopic partitioning was demonstrated as one way to detect such three-way interactions. The added corn stover was readily available to microbes as a C substrate, and significantly impacted the soil microbial community, while added PyOM induced a smaller increase in total CO<sub>2</sub> emissions, and a smaller shift in the soil microbial community.

SUPPLEMENTARY INFORMATION FOR CHAPTER FOUR - PYROGENIC ORGANIC  
MATTER, SOIL ORGANIC MATTER, AND PLANT ROOT INTERACTIONS  
DETERMINED USING THREE-PART PARTITIONING WITH STABLE C ISOTOPES AND  
MICROBIAL COMMUNITY ANALYSIS

*4.S1 Iso-FD chambers*

Isotopic forced diffusion semi-static chambers were designed (Figure 4.S1) based on Nickerson *et al.* (2013) to allow for a simple estimate of the  $\delta^{13}\text{C}$  signature of soil  $\text{CO}_2$  fluxes. Chambers were machined out of aluminum and a Gore-Tex membrane was used to allow partial diffusion. Chambers were deployed in pairs, with one chamber top placed on the PVC soil collar, and the atmospheric reference chamber placed on a directly adjacent plugged PVC collar with the same volume as the chamber connected to the soil. The Gore-Tex material was sealed to the chamber with a rubber O-ring held tight with screws between the top and the sides of the metal chamber top (not pictured).

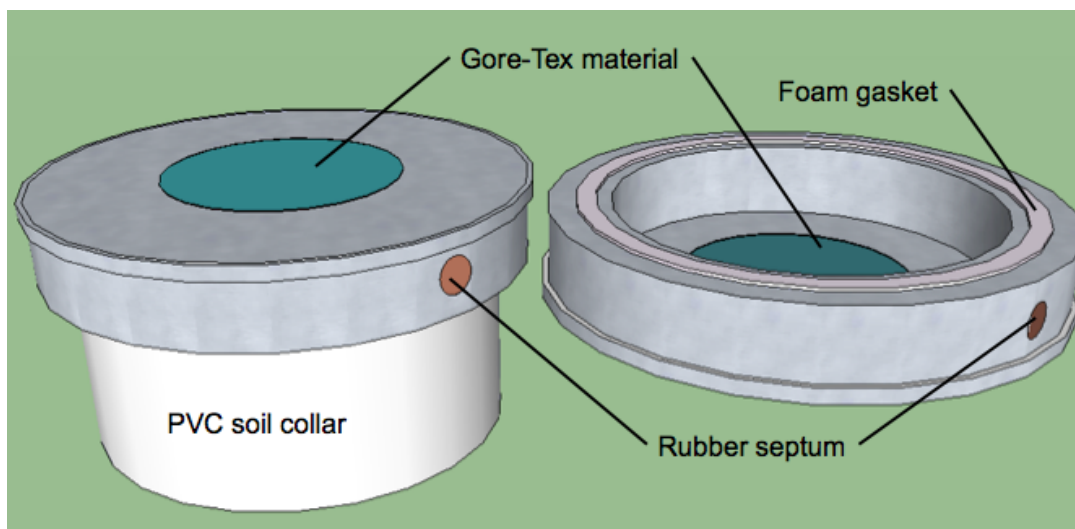


**Figure 4.S1** Sketch of isotopic forced diffusion chambers from above (left) and below (right).

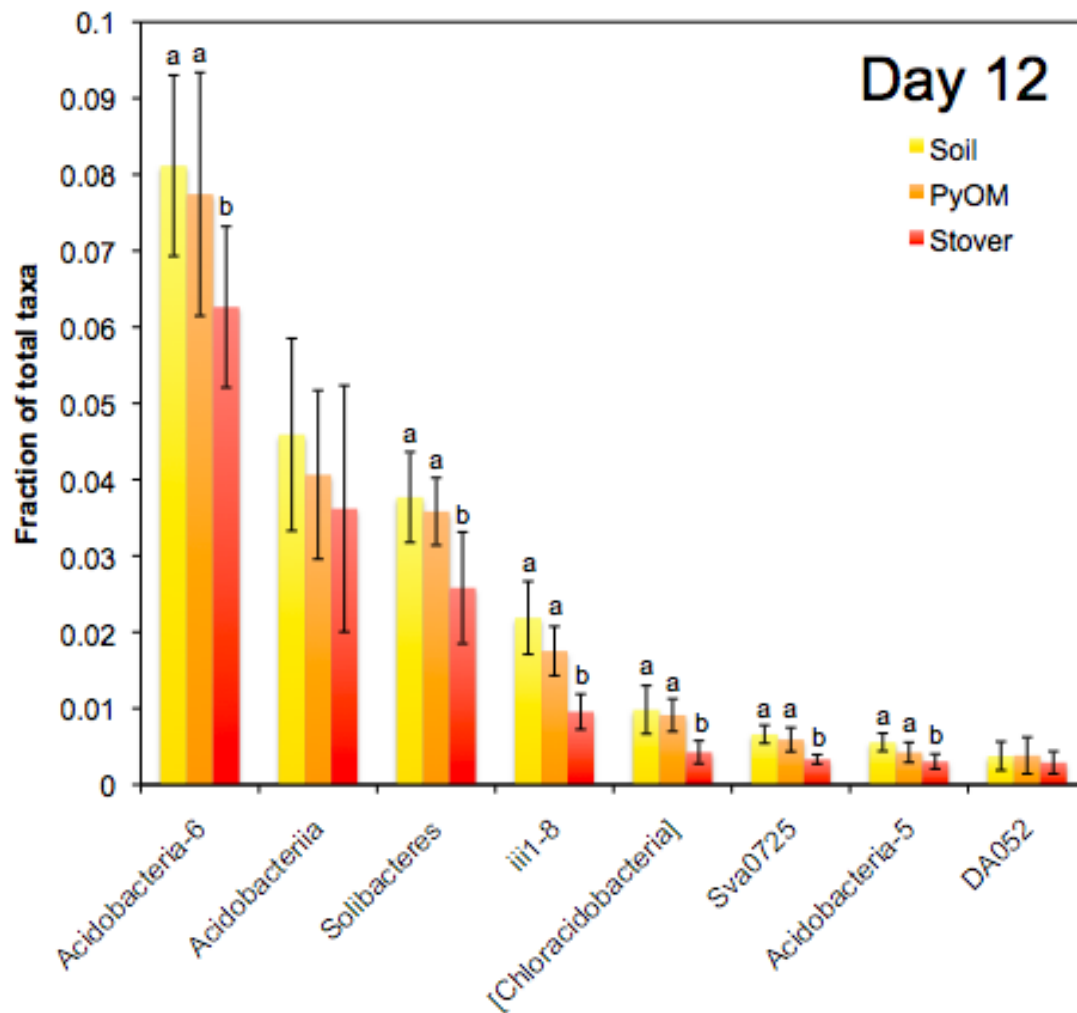


**Figure 4.S2** Relative abundance of the top 8 orders in the Acidobacteria phylum on day 12. Error bars  $\pm 1SD$ ,  $n=8-16$ , different letters indicate significant differences within an order (ANOVA, Tukey's HSD,  $p < 0.00625$ ).

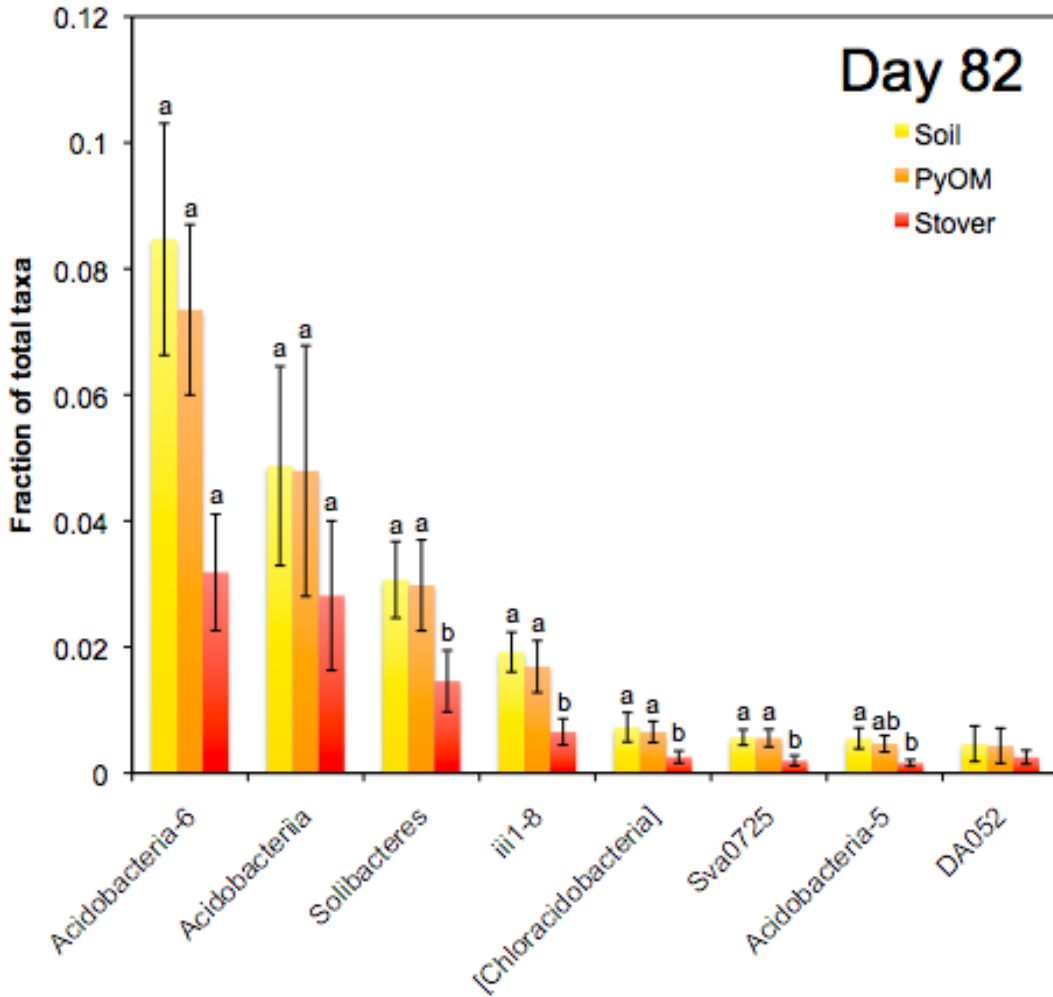


**Figure 4.S3** Relative abundance of the top 8 orders in the Acidobacteria phylum on day 82. Error bars  $\pm 1SD$ ,  $n=8-16$ , different letters indicate significant differences within an order (ANOVA, Tukey's HSD,  $p < 0.00625$ ).

**Table 4.S1** Mean total DNA extracted from soils ( $\mu\text{g DNA g}^{-1}$  dry soil)  $\pm$  SD, letters indicate significant differences between amendment types within days (ANOVA, Tukey's HSD,  $p < 0.05$ )

Amendment	Day 1	Day 12	Day 82
Soil only (n=16)	21.9 $\pm$ 1.6 a	20.1 $\pm$ 0.8 b	16.2 $\pm$ 0.6 b
+PyOM (n=16)	21.8 $\pm$ 1.0 a	18.9 $\pm$ 0.6 b	17.3 $\pm$ 0.7 b
+Stover (n=8)	24.8 $\pm$ 1.4 a	27.9 $\pm$ 1.2 a	22.4 $\pm$ 0.8 a

**Table 4.S2** Forward primer (full) sequences (adapterbarcodepad&link16Sfwdprimer)

AATGATACGGCGACCACCGAGATCTACACATCGTACGAATGTTTAAATGGTGYCAGCMGCMGCGGTRA  
AATGATACGGCGACCACCGAGATCTACACACTATCTGAATGTTTAAATGGTGYCAGCMGCMGCGGTRA  
AATGATACGGCGACCACCGAGATCTACACTAGCGAGTAATGTTTAAATGGTGYCAGCMGCMGCGGTRA  
AATGATACGGCGACCACCGAGATCTACACCTGCGTGTAATGTTTAAATGGTGYCAGCMGCMGCGGTRA  
AATGATACGGCGACCACCGAGATCTACACTCATCGAGAATGTTTAAATGGTGYCAGCMGCMGCGGTRA  
AATGATACGGCGACCACCGAGATCTACACCGTGAGTGAATGTTTAAATGGTGYCAGCMGCMGCGGTRA  
AATGATACGGCGACCACCGAGATCTACACGGATATCTAATGTTTAAATGGTGYCAGCMGCMGCGGTRA  
AATGATACGGCGACCACCGAGATCTACACGACACCGTAATGTTTAAATGGTGYCAGCMGCMGCGGTRA

**Table 4.S3** Reverse primer (full) sequences (adapterbarcodepad&link16Srevprimer)

CAAGCAGAAGACGGCATAACGAGATAACTCTCGCAACCCAACAGGCCGYCCAATTYMTTTRAGTTT  
CAAGCAGAAGACGGCATAACGAGATACTATGTCCAACCCAACAGGCCGYCCAATTYMTTTRAGTTT  
CAAGCAGAAGACGGCATAACGAGATAGTAGCGTCAACCCAACAGGCCGYCCAATTYMTTTRAGTTT  
CAAGCAGAAGACGGCATAACGAGATCAGTGAGTCAACCCAACAGGCCGYCCAATTYMTTTRAGTTT  
CAAGCAGAAGACGGCATAACGAGATCGTACTACAACCCAACAGGCCGYCCAATTYMTTTRAGTTT  
CAAGCAGAAGACGGCATAACGAGATCTACGCAGCAACCCAACAGGCCGYCCAATTYMTTTRAGTTT  
CAAGCAGAAGACGGCATAACGAGATGGAGACTACAACCCAACAGGCCGYCCAATTYMTTTRAGTTT  
CAAGCAGAAGACGGCATAACGAGATGTCGCTCGCAACCCAACAGGCCGYCCAATTYMTTTRAGTTT  
CAAGCAGAAGACGGCATAACGAGATGTCGTAGTCAACCCAACAGGCCGYCCAATTYMTTTRAGTTT  
CAAGCAGAAGACGGCATAACGAGATTAGCAGACCAACCCAACAGGCCGYCCAATTYMTTTRAGTTT  
CAAGCAGAAGACGGCATAACGAGATTCATAGACCAACCCAACAGGCCGYCCAATTYMTTTRAGTTT  
CAAGCAGAAGACGGCATAACGAGATTCGCTATACAACCCAACAGGCCGYCCAATTYMTTTRAGTTT

## REFERENCES

- Ameloot, N., Graber, E.R., Verheijen, F.G.A., De Neve, S., 2013. Interactions between biochar stability and soil organisms: review and research needs. *European Journal of Soil Science* 64, 379–390.
- Bartram, A.K., Jiang, X., Lynch, M.D., Masella, A.P., Nicol, G.W., Dushoff, J., Neufeld, J.D., 2013. Exploring links between pH and bacterial community composition in soils from the Craibstone Experimental Farm. *FEMS Microbiology Ecology*.
- Bates, D., Maechler, M., Bolker, B., Walker, S., 2014. lme4: Linear mixed-effects models using Eigen and S4. R package version 1.1-6. <http://CRAN.R-project.org/package=lme4>
- Bingeman, C.W., Varner, J.E., Martin, W.P., 1953. The effect of the addition of organic materials on the decomposition of an organic soil. *Soil Science Society of America Journal* 17, 34–38.
- Caporaso, J.G., Kuczynski, J., Stombaugh, J., Bittinger, K., Bushman, F.D., Costello, E.K., Fierer, N., Pena, A.G., Goodrich, J.K., Gordon, J.I., Huttley, G.A., Kelley, S.T., Knights, D., Koenig, J.E., Ley, R.E., Lozupone, C.A., McDonald, D., Muegge, B.D., Pirrung, M., Reeder, J., Sevinsky, J.R., Turnbaugh, P.J., Walters, W.A., Widmann, J., Yatsunencko, T., Zaneveld J., Knight, R., 2010. QIIME allows analysis of high-throughput community sequencing data. *Nature Methods* 7, 335–336.
- Chen, J., Liu, X., Zheng, J., Zhang, B., Lu, H., Chi, Z., Pan, G., Li, L., Zheng, J., Zhang, X., Wang, J., Yu, X., 2013. Biochar soil amendment increased bacterial but decreased fungal gene abundance with shifts in community structure in a slightly acid rice paddy from Southwest China. *Applied Soil Ecology* 71, 33–44.
- Czimczik, C.I., Masiello, C.A., 2007. Controls on black carbon storage in soils. *Global Biogeochemical Cycles* 21.
- de Mendiburu, F., 2013. agricolae: Statistical Procedures for Agricultural Research. R package version 1.1-4. <http://CRAN.R-project.org/package=agricolae>
- Dunavin, L.S., 1969. A comparison of Gahi-1 millet and Grazer A sorghum x sudangrass at several pH levels., *Proceedings of the Soil and Crop Science Society of Florida*, 163–168.
- Edgar, R.C., 2013. UPARSE: Highly accurate OTU sequences from microbial amplicon reads, *Nature Methods* 10, 996–998.
- Fernandes, M., Coutinho, J.F., 1999. Effect of liming and phosphate application on sudangrass growth and phosphorus availability in two temperate acid soils. *Communications in Soil Science and Plant Analysis* 30, 855–871.
- Fierer, N., Bradford, M.A., Jackson, R.B., 2007. Toward an ecological classification of soil bacteria. *Ecology* 88, 1354–1364.
- Flouri, T., Zhang, J., 2014. PEAR: a fast and accurate Illumina Paired-End reAd merger. *Bioinformatics* 30, 614–620.
- Gomez, J.D., Deneff, K., Stewart, C.E., Zheng, J., Cotrufo, M.F., 2014. Biochar addition rate influences soil microbial abundance and activity in temperate soils. *European Journal of Soil Science* 65, 28–39.
- Jeffery, S., Verheijen, F.G.A., van der Velde, M., Bastos, A.C., 2011. A quantitative review of the effects of biochar application to soils on crop productivity using meta-analysis. *“Agriculture, Ecosystems and Environment”* 144, 175–187.
- Jin, H., 2010. Characterization of microbial life colonizing biochar and biochar-amended soils. Cornell University, Ithaca, NY.

- Jindo, K., Sánchez-Monedero, M.A., Hernández, T., García, C., Furukawa, T., Matsumoto, K., Sonoki, T., Bastida, F., 2012. Biochar influences the microbial community structure during manure composting with agricultural wastes. *Science of The Total Environment* 416, 476–481.
- Kuzyakov, Y., Bol, R., 2004. Using natural  $^{13}\text{C}$  abundances to differentiate between three  $\text{CO}_2$  sources during incubation of a grassland soil amended with slurry and sugar. *Journal of Plant Nutrition and Soil Science* 167, 669–677.
- Laird, D.A., 2008. The charcoal vision: A win–win–win scenario for simultaneously producing bioenergy, permanently sequestering carbon, while improving soil and water quality. *Agronomy Journal* 100, 178–181.
- Lehmann, J., 2007. A handful of carbon. *Nature* 447, 143–144.
- Lehmann, J., Rillig, M.C., Thies, J., Masiello, C.A., Hockaday, W.C., Crowley, D., 2011. Biochar effects on soil biota - A review. *Soil Biology and Biochemistry* 43, 1812–1836.
- Lenth, R.V., 2014. lsmeans: Least-Squares Means. R package version 2.05. <http://CRAN.R-project.org/package=lsmeans>.
- Lozupone, C., Lladser, M.E., Knights, D., Stombaugh, J., Knight, R., 2011. UniFrac: an effective distance metric for microbial community comparison. *The ISME Journal* 5, 169–172.
- Maestrini, B., Nannipieri, P., Abiven, S., 2014. A meta-analysis on pyrogenic organic matter induced priming effect. *GCB Bioenergy*.
- Major, J., Lehmann, J., Rondon, M., Goodale, C., 2010. Fate of soil-applied black carbon: downward migration, leaching and soil respiration. *Global Change Biology* 16, 1366–1379.
- Masiello, C.A., Chen, Y., Gao, X., Liu, S., Cheng, H.-Y., Bennett, M.R., Rudgers, J.A., Wagner, D.S., Zygourakis, K., Silberg, J.J., 2013. Biochar and microbial signaling: Production conditions determine effects on microbial communication. *Environmental Science & Technology* 47, 11496–11503.
- Nawrocki, E.P., 2009. Structural RNA homology search and alignment using covariance models, Ph.D. thesis, Washington University in Saint Louis, School of Medicine.
- Nickerson, N., Egan, J., Risk, D., 2013. Iso-FD: A novel method for measuring the isotopic signature of surface flux. *Soil Biology and Biochemistry* 62, 99–106.
- Nolley, A., Brown, C.T., 2012. Screed - short read sequence utils. Michigan State University. <http://screed.readthedocs.org>.
- Pascual, N., Ranjard, L., Kaisermann, A., Bachar, D., Christen, R., Terrat, S., Mathieu, O., Lévêque, J., Mougél, C., Henault, C., Lemanceau, P., Péan, M., Boiry, S., Fontaine, S., Maron, P.-A., 2013. Stimulation of different functional groups of bacteria by various plant residues as a driver of soil priming effect. *Ecosystems* 16, 810–822.
- R Core Team, 2012. R: A language and environment for statistical computing. R Foundation for Statistical Computing, Vienna, Austria. ISBN 3-900051-07-0, URL <http://www.R-project.org/>.
- Rousk, J., Bååth, E., Brookes, P.C., Lauber, C.L., Lozupone, C., Caporaso, J.G., Knight, R., Fierer, N., 2010. Soil bacterial and fungal communities across a pH gradient in an arable soil. *The ISME Journal*, 1–12.
- Schloss, P.D., Westcott, S.L., Ryabin, T., Hall, J.R., Hartmann, M., Hollister, E.B., Lesniewski, R.A., Oakley, B.B., Parks, D.H., Robinson, C.J., Sahl, J.W., Stres, B., Thallinger, G.G., Van Horn, D.J., Weber, C.F., 2009. Introducing mothur: Open-source, platform-independent, community-supported software for describing and comparing microbial communities. *Applied Environmental Microbiology* 75, 7537–7541.

- Slavich, P.G., Sinclair, K., Morris, S.G., Kimber, S.W.L., Downie, A., Zwieten, L., 2013. Contrasting effects of manure and green waste biochars on the properties of an acidic ferralsol and productivity of a subtropical pasture. *Plant and Soil* 366, 213–227.
- Taketani, R.G., Lima, A.B., Conceição Jesus, E., Teixeira, W.G., Tiedje, J.M., Tsai, S.M., 2013. Bacterial community composition of anthropogenic biochar and Amazonian anthrosols assessed by 16S rRNA gene 454 pyrosequencing. *Antonie van Leeuwenhoek* 104, 233–242.
- van Es, H.M., Gomes, C.P., Sellmann, M., van Es, C.L., 2007. Spatially-balanced complete block designs for field experiments. *Geoderma* 140, 346–352.
- Vance, E.D., Brookes, P.C., Jenkinson, D.S., 1987. An extraction method for measuring soil microbial biomass C. *Soil Biology and Biochemistry* 19, 703–707.
- Watzinger, A., Feichtmair, S., Kitzler, B., Zehetner, F., Kloss, S., Wimmer, B., Zechmeister-Boltenstern, S., Soja, G., 2013. Soil microbial communities responded to biochar application in temperate soils and slowly metabolized  $^{13}\text{C}$ -labelled biochar as revealed by  $^{13}\text{C}$  PLFA analyses: results from a short-term incubation and pot experiment. *European Journal of Soil Science* 65, 40–51.
- Werth, M., Kuzyakov, Y., 2010.  $^{13}\text{C}$  fractionation at the root-microorganisms-soil interface: A review and outlook for partitioning studies. *Soil Biology and Biochemistry* 42, 1372–1384.
- Whitman, T., Enders, A., Lehmann, J., 2014. Pyrogenic carbon additions to soil counteract positive priming of soil carbon mineralization by plants. *Soil Biology and Biochemistry* 73, 33–41.
- Whitman, T., Hanley, K., Enders, A., Lehmann, J., 2013. Predicting pyrogenic organic matter mineralization from its initial properties and implications for carbon management. *Organic Geochemistry* 64, 76–83.
- Whitman, T., Scholz, S.M., Lehmann, J., 2010. Biochar projects for mitigating climate change: an investigation of critical methodology issues for carbon accounting. *Carbon Management*
- Zimmerman, A.R., 2010. Abiotic and microbial oxidation of laboratory-produced black carbon (biochar). *Environmental Science & Technology* 44, 1295–1301.

## APPENDIX 1.1

### PRIMARY DATA FOR CHAPTER TWO

Throughout this section treatment IDs are as follows:

A - no additions

B - biochar additions

C - corn plant

D - biochar additions + corn plant

**Table A1.1.1 Final Total Soil C Stocks**

Trtmt	Pot ID	Total %C final	$\delta^{13}\text{C}$ final (‰)
A	1	1.11	-26.09
A	5	1.08	-26.06
A	6	1.08	-25.93
A	16	1.06	-25.80
A	18	1.11	-26.01
A	20	1.13	-26.02
B	4	1.33	-17.54
B	8	1.39	-16.63
B	9	1.31	-16.20
B	14	1.33	-15.81
B	19	1.35	-16.38
B	21	1.44	-15.36
C	2	1.03	-26.02
C	7	1.09	-25.93
C	11	1.06	-25.99
C	17	1.06	-25.85
C	22	1.09	-25.95
C	24	1.08	-25.85
D	3	1.38	-16.08
D	10	1.35	-17.58
D	12	1.32	-16.09
D	15	1.42	-16.31
D	23	1.40	-17.02

**Table A1.1.2 Final Total Biomass Stocks**

Trtmt	Pot ID	Shoot or Root	%C	d13C (‰)	Dry biomass per pot (g)
C	2	Root	41.35	-13.99	20.89
C	7	Root	38.11	-13.62	20.84
C	11	Root	39.94	-14.02	20.46
C	17	Root	37.56	-14.08	39.94
C	22	Root	38.83	-13.91	16
C	24	Root	39.91	-13.88	8.58
D	3	Root	38.73	-14.01	28.54
D	10	Root	39.61	-13.60	17.76
D	12	Root	40.21	-13.94	35.1
D	15	Root	37.86	-14.02	30.72
D	23	Root	41.91	-13.81	36.87
C	2	Shoot	41.40	-14.15	41.62
C	7	Shoot	42.09	-13.61	54.8
C	11	Shoot	42.45	-13.89	56.51
C	17	Shoot	42.17	-13.95	76.75
C	22	Shoot	41.35	-13.92	38.8
C	24	Shoot	41.34	-13.81	40.76
D	3	Shoot	41.20	-14.03	62.64
D	10	Shoot	41.84	-13.70	47.68
D	12	Shoot	42.16	-13.88	61.1
D	15	Shoot	42.19	-13.96	64.18
D	23	Shoot	41.78	-14.19	66.36

**Table A1.1.3.1 CO<sub>2</sub> flux rates over the course of the trial and mean temperature (Days 1-21)**

Pot ID	Trtmt	Flux rate (mgCO <sub>2</sub> /minute/pot)				
		Day 1	Day 4	Day 8	Day 14	Day 21
1	A	0.091	0.039	0.018	0.056	0.023
5	A	0.075	0.087	0.085	0.081	-0.053
6	A	0.104	0.077	0.058	0.055	0.003
16	A	0.099	0.083	0.041	0.028	-0.018
18	A	0.089	0.053	0.099	0.067	0.018
20	A	0.134	0.103	0.160	0.060	0.029
4	B	0.170	0.086	0.044	0.062	0.010
8	B	0.154	0.114	0.012	0.072	-0.006
9	B	0.258	0.099	0.050	0.051	0.025
14	B	0.192	0.113	0.087	0.081	0.019
19	B	0.168	0.073	0.091	0.037	0.021
21	B	0.225	0.109	0.021	0.028	0.031
2	C	0.082	0.009	0.036	0.102	0.108
7	C	0.081	0.071	0.034	0.051	-0.038
11	C	0.103	0.108	0.074	0.079	0.046
17	C	0.133	0.090	0.046	0.054	0.034
22	C	0.098	0.079	0.166	0.084	0.147
24	C	0.112	0.089	0.059	0.067	0.037
3	D	0.119	0.061	0.091	0.122	0.026
10	D	0.140	0.100	0.087	0.083	0.032
12	D	0.186	0.183	0.062	0.103	0.156
13*	D	0.272	0.084	0.047	0.064	0.004
15	D	0.216	0.088	0.128	0.086	0.000
23	D	0.226	0.141	0.066	0.055	0.054
Temp (°C)		26.69	30.03	28.23	27.38	34.92

**Table A1.1.3.2 CO<sub>2</sub> flux rates over the course of the trial and mean temperature (Days 28-94)**

Pot ID	Trtmt	Flux rate (mgCO <sub>2</sub> /minute/pot)					
		Day 28	Day 36	Day 50	Day 61	Day 70	Day 94
1	A	-0.002	-0.009	-0.021	-0.020	-0.001	-0.023
5	A	0.036	-0.003	-0.017	-0.009	0.007	-0.005
6	A	0.003	-0.007	-0.017	-0.024	0.016	-0.013
16	A	0.010	-0.004	-0.009	-0.020	0.016	-0.019
18	A	0.013	-0.006	-0.013	-0.022	-0.008	0.021
20	A	-0.007	-0.007	-0.009	-0.008	0.016	0.022
4	B	0.002	-0.004	-0.016	-0.007	-0.005	-0.004
8	B	0.057	-0.008	-0.004	-0.014	0.017	-0.024
9	B	0.040	-0.010	-0.011	-0.013	0.007	-0.023
14	B	-0.015	-0.008	-0.022	-0.014	0.014	-0.011
19	B	0.004	-0.007	-0.021	-0.018	0.006	-0.004
21	B	-0.005	-0.005	-0.009	-0.011	0.027	0.004
2	C	0.037	0.016	0.102	0.277	0.269	0.053
7	C	-0.002	0.032	0.089	0.285	0.193	0.084
11	C	0.014	0.027	0.151	0.338	0.209	0.029
17	C	0.003	0.048	0.190	0.289	0.428	0.068
22	C	0.033	0.022	0.065	0.134	0.119	0.056
24	C	0.001	0.013	0.061	0.195	0.162	0.111
3	D	0.010	0.049	0.149	0.232	0.336	0.006
10	D	0.011	0.010	0.057	0.139	0.173	0.056
12	D	0.037	0.045	0.163	0.260	0.219	0.049
13*	D	0.007	0.008	-0.022	-0.033	-0.002	-0.030
15	D	0.011	0.039	0.138	0.343	0.215	0.088
23	D	0.003	0.000	0.314	0.208	0.350	0.029
Temp (°C)		36.77	29.11	27.41	31.50	25.67	30.32

\* The plant in Pot 13 was killed part way through the experiment, when one of the overhead greenhouse lights exploded one day during a sampling session, dripping something oily and, apparently, toxic, on the corn.

**Table A1.1.4 Gas samples and information for  $^{13}\text{CO}_2$  determination of fluxes, Day 1**

Treatment/Rep	Pot ID	Sampling Time (min)	[CO <sub>2</sub> ] (ppm)	$\delta^{13}\text{C}$ (‰)	Chamber volume (cm <sup>3</sup> )	
A1		1	15	892.5	-16.54	1997
A2		5	25	889.9	-15.74	1997
A3		6	35	1278.6	-19.76	1997
A4		16	45	1255.2	-18.81	1997
A5		18	55	1410.7	-19.90	1997
A6		20	65	1792.8	-21.92	1997
B1		4	15	1055.8	-3.06	1997
B2		8	25	1413.3	0.54	1997
B3		9	35	2076.5	4.45	1997
B4		14	45	2175.0	0.25	1997
B5		19	55	2529.9	2.83	1997
B6		21	65	2665.9	2.20	1997
C1		2	15	800.6	-15.66	1997
C2		7	25	1097.2	-17.75	1997
C3		11	35	1273.4	-19.17	1997
C4		17	45	1493.6	-20.04	1997
C5		22	55	1500.1	-20.72	1997
C6		24	65	1467.7	-20.20	1997
D1		3	15	952.1	-1.91	1997
D2		10	25	1327.8	-2.76	1997
D3		12	35	1803.2	-1.37	1997
D4		13	45	2432.8	1.68	1997
D5		15	55	2462.6	1.13	1997
D6		23	65	2886.2	1.82	1997
GH1	Greenhouse air		0	524.6	-9.41	
GH2	Greenhouse air		0	518.2	-9.33	
GH3	Greenhouse air		0	522.0	-8.95	

**Table A1.1.5 Gas samples and information for <sup>13</sup>CO<sub>2</sub> determination of fluxes, Day 8**

Treatment/Rep	Pot ID	Sampling Time (min)	[CO <sub>2</sub> ] (ppm)	δ <sup>13</sup> C (‰)	Chamber volume (cm <sup>3</sup> )	
A1 day2		6	20	1063.5	-18.07	2095
A2 day2		20	40	1581.7	-19.89	2144
A3 day2		1	60	2260.5	-20.55	2105
A4 day2		5	80	2435.4	-22.09	2071
A5 day2		16	100	2577.8	-21.50	2100
A6 day2		18	121	3706.1	-23.18	2115
B1 day2		9	20	934.0	-11.68	2124
B2 day2		21	40	1567.4	-15.01	2061
B3 day2		4	60	2554.5	-16.43	2051
B4 day2		8	80	2096.0	-14.20	2207
B5 day2		14	100	3054.6	-19.04	2061
B6 day2		19	120	3361.6	-16.45	2110
C1 day2		11	20	1287.6	-18.51	2056
C2 day2		24	40	1787.7	-17.89	2080
C3 day2		2	60	2675.0	-19.09	2061
C4 day2		7	80	2307.1	-18.23	2066
C5 day2		17	100	3286.4	-21.86	2051
C6 day2		22	120	3998.9	-21.80	2100
D1 day2		12	20	1340.7	-14.89	2022
D2 day2		23	40	2364.1	-15.72	1958
D3 day2		3	60	2254.0	-15.07	2115
D4 day2		10	80	2770.9	-15.76	2012
D5 day2		13	100	3922.5	-16.81	2066
D6 day2		15	120	4026.1	-15.93	2041
GH1 day2	Greenhouse air		0	484.5	-8.55	
GH2 day2	Greenhouse air		0	454.7	-7.32	

APPENDIX 1.2

PRIMARY DATA FOR CHAPTER THREE

Throughout this section treatment IDs are as follows:

O - 6-month pre-incubated soil

Y - 24-hour pre-incubated soil

+ - Increased DPyOM

0 - Unchanged DPyOM

-- Depleted DPyOM

\* indicates excluded or missing data, as described in the body of this dissertation

**Table A1.2.1 Partitioned CO<sub>2</sub> emissions: SOC-derived CO<sub>2</sub>**

Jar ID	Trtmt	SOC-derived CO <sub>2</sub> accumulated since last measurement (mL CO <sub>2</sub> )					
		Day 1	Day 2	Day 5	Day 10	Day 25	Day 47
5	O+	0.62	0.39	0.88	1.61	3.36	4.65
17	O+	0.69	0.41	0.97	1.66	3.62	4.77
29	O+	0.81	0.29	1.05	1.63	3.70	4.66
41	O+	0.66	0.35	1.08	1.68	4.53	4.87
53	O+	0.60	0.43	0.90	1.74	3.63	4.84
65	O+	0.58	0.46	1.63	1.69	3.84	5.11
77	O+	0.62	0.35	0.94	1.74	4.03	4.69
89	O+	0.65	0.36	0.80	1.71	3.86	4.82
6	00	0.63	0.43	0.91	1.66	3.59	4.88
18	00	0.58	0.39	0.94	1.83	3.72	4.95
30	00	0.71	0.33	1.26	*	5.18	*
42	00	0.66	0.31	1.10	1.76	4.09	5.03
54	00	0.70	0.40	0.91	1.72	3.95	5.19
66	00	0.63	0.39	1.00	1.66	3.94	4.94
78	00	0.76	0.43	0.94	1.73	4.01	5.06
90	00	0.73	0.30	0.77	1.67	4.04	4.86
7	O-	0.63	0.51	1.00	1.81	3.86	5.24
19	O-	0.81	0.33	0.87	1.79	3.72	4.71
31	O-	0.72	0.33	1.11	1.67	3.93	4.78
43	O-	0.60	0.37	1.08	1.75	4.09	4.81
55	O-	0.46	0.37	0.96	1.76	3.94	5.14
67	O-	0.63	0.36	1.04	1.69	4.08	4.99
79	O-	0.58	0.43	0.92	1.79	4.12	5.03
91	O-	0.62	0.32	0.87	1.65	4.07	4.80
8	OX	0.53	0.37	1.20	2.27	4.47	5.50
20	OX	0.57	0.33	1.10	2.01	4.39	5.54
32	OX	0.45	0.36	1.30	1.92	4.59	5.18
44	OX	0.51	0.40	1.14	1.92	4.82	5.68
56	OX	0.51	0.53	0.96	1.96	4.49	5.64

68	OX	0.53	0.44	1.10	1.92	4.59	5.63
80	OX	0.56	0.14	0.99	1.88	4.82	5.61
92	OX	0.54	0.31	1.17	1.95	4.99	5.95
1	Y+	2.28	1.58	2.88	3.75	6.04	5.83
13	Y+	2.45	1.49	3.17	3.53	6.14	5.80
25	Y+	2.31	1.47	3.09	3.45	5.84	5.36
37	Y+	2.41	1.55	3.31	3.51	6.32	6.28
49	Y+	2.11	1.67	3.01	*	5.98	5.53
61	Y+	2.45	1.58	3.10	3.45	6.34	5.90
73	Y+	2.41	1.55	2.92	3.59	5.96	5.50
85	Y+	2.55	1.53	3.06	3.50	6.01	5.45
2	Y0	2.43	1.61	2.97	3.73	6.00	5.79
14	Y0	2.46	*	3.19	3.54	6.26	5.78
26	Y0	2.47	1.54	3.37	*	*	*
38	Y0	2.36	1.62	3.28	3.40	6.38	5.98
50	Y0	2.28	1.55	2.95	3.58	6.20	6.14
62	Y0	2.51	1.59	3.13	3.53	6.50	6.58
74	Y0	2.35	1.47	2.70	3.53	6.17	5.69
86	Y0	2.48	1.58	3.18	3.58	6.46	5.73
3	Y-	2.40	1.57	2.93	3.63	5.85	5.53
15	Y-	2.29	*	3.07	3.64	6.42	6.12
27	Y-	2.41	1.41	3.12	3.58	5.96	5.66
39	Y-	2.40	1.48	3.25	3.50	6.03	5.69
51	Y-	2.37	1.46	2.89	3.52	5.99	6.01
63	Y-	2.51	1.52	2.99	3.69	6.43	6.83
75	Y-	2.45	1.51	2.81	3.61	6.41	5.86
87	Y-	2.32	1.30	2.94	3.48	6.23	6.04
4	YX	*	*	3.11	3.83	6.52	7.55
16	YX	2.39	1.38	3.06	3.64	6.42	7.78
28	YX	2.34	1.43	3.31	3.46	6.28	7.06
40	YX	2.44	1.50	3.17	3.51	6.73	7.92
52	YX	2.23	1.48	2.96	3.64	6.61	7.60
64	YX	2.31	1.50	2.95	3.65	6.13	7.64
76	YX	2.49	1.57	3.04	3.77	6.87	7.74
88	YX	2.17	1.26	3.03	3.49	6.49	7.44

**Table A1.2.2 Partitioned CO<sub>2</sub> emissions: PyOM-derived CO<sub>2</sub>**

Jar ID	Trtmnt	SOC-derived CO <sub>2</sub> accumulated since last measurement (mL CO <sub>2</sub> )					
		Day 1	Day 2	Day 5	Day 10	Day 25	Day 47
5	O+	1.03	0.71	0.74	0.59	0.70	0.74
17	O+	0.95	0.72	0.80	0.61	0.72	0.61
29	O+	1.11	0.59	0.84	0.61	0.79	0.71
41	O+	0.81	0.59	0.78	0.60	0.18	0.81
53	O+	0.92	0.68	0.74	0.64	0.64	0.76
65	O+	0.83	0.66	0.18	0.62	0.77	0.66
77	O+	0.87	0.48	0.69	0.64	0.88	0.73
89	O+	0.98	0.63	0.67	0.64	0.82	0.77
6	O0	0.73	0.54	0.64	0.55	0.64	0.71
18	O0	0.58	0.44	0.60	0.57	0.72	0.64

30	O0	0.77	0.46	0.71	*	0.74	*
42	O0	0.53	0.36	0.65	0.55	0.71	0.73
54	O0	0.62	0.42	0.58	0.57	0.81	0.74
66	O0	0.61	0.45	0.65	0.58	0.84	0.56
78	O0	0.67	0.53	0.68	0.60	0.85	0.68
90	O0	0.57	0.34	0.49	0.56	0.70	0.75
7	O-	0.43	0.41	0.57	0.54	0.63	0.46
19	O-	0.63	0.43	0.53	0.56	0.67	0.70
31	O-	0.58	0.41	0.71	0.57	0.67	0.63
43	O-	0.43	0.35	0.56	0.52	0.74	0.66
55	O-	0.33	0.34	0.56	0.53	0.58	0.67
67	O-	0.47	0.39	0.63	0.54	0.77	0.55
79	O-	0.45	0.37	0.52	0.52	0.80	0.54
91	O-	0.57	0.37	0.55	0.56	0.63	0.76
1	Y+	0.53	0.39	0.85	0.69	0.57	0.57
13	Y+	0.54	0.43	0.98	0.54	0.59	0.74
25	Y+	0.63	0.36	0.89	0.64	0.65	0.77
37	Y+	0.64	0.43	0.93	0.57	0.58	0.64
49	Y+	0.55	0.44	0.98	*	0.51	0.80
61	Y+	0.62	0.39	0.90	0.69	0.44	0.68
73	Y+	0.60	0.40	0.87	0.66	0.56	0.66
85	Y+	0.58	0.37	0.86	0.67	0.46	0.81
2	Y0	0.40	0.33	0.71	0.67	0.61	0.66
14	Y0	0.44	*	0.80	0.63	0.35	0.58
26	Y0	0.38	0.27	0.75	*	*	*
38	Y0	0.41	0.32	0.73	0.50	0.52	0.67
50	Y0	0.38	0.29	0.65	0.61	0.60	0.64
62	Y0	0.24	0.24	0.63	0.58	0.52	0.62
74	Y0	0.38	0.25	0.58	0.55	0.50	0.60
86	Y0	0.42	0.26	0.65	0.59	0.51	0.62
3	Y-	0.26	0.32	0.80	0.54	0.68	0.74
15	Y-	0.37	*	0.87	0.53	0.38	0.52
27	Y-	0.28	0.28	0.66	0.51	0.51	0.76
39	Y-	0.26	0.32	0.85	0.56	0.61	0.64
51	Y-	0.25	0.29	0.72	0.62	0.59	0.57
63	Y-	0.21	0.29	0.70	0.56	0.51	0.47
75	Y-	0.24	0.26	0.64	0.51	0.49	0.71
87	Y-	0.23	0.26	0.72	0.60	0.66	0.57

**Table A1.2.3 Total CO<sub>2</sub> emissions**

Jar ID	Trtmt	Total CO <sub>2</sub> accumulated since last measurement (mL CO <sub>2</sub> )					
		Day 1	Day 2	Day 5	Day 10	Day 25	Day 47
5	O+	1.65	1.10	1.62	2.21	4.06	5.39
17	O+	1.63	1.13	1.78	2.27	4.34	5.38
29	O+	1.92	0.88	1.89	2.24	4.49	5.38
41	O+	1.47	0.94	1.86	2.29	4.71	5.68
53	O+	1.52	1.10	1.65	2.38	4.27	5.61
65	O+	1.41	1.12	1.81	2.32	4.61	5.77
77	O+	1.49	0.83	1.63	2.38	4.90	5.43
89	O+	1.63	0.99	1.47	2.35	4.68	5.59
6	O0	1.36	0.97	1.55	2.21	4.23	5.59
18	O0	1.16	0.83	1.54	2.40	4.44	5.59
30	O0	1.49	0.78	1.97	3.01	5.92	7.24
42	O0	1.19	0.67	1.74	2.32	4.80	5.75
54	O0	1.32	0.82	1.49	2.29	4.77	5.93
66	O0	1.24	0.85	1.65	2.24	4.78	5.50
78	O0	1.43	0.96	1.62	2.33	4.85	5.73
90	O0	1.30	0.64	1.26	2.24	4.73	5.61
7	O-	1.06	0.93	1.57	2.35	4.49	5.70
19	O-	1.44	0.75	1.41	2.35	4.39	5.41
31	O-	1.30	0.74	1.82	2.24	4.59	5.41
43	O-	1.03	0.72	1.65	2.27	4.84	5.47
55	O-	0.79	0.71	1.52	2.29	4.53	5.81
67	O-	1.09	0.75	1.66	2.22	4.85	5.54
79	O-	1.03	0.80	1.44	2.30	4.92	5.57
91	O-	1.19	0.69	1.42	2.21	4.70	5.56
8	OX	0.53	0.37	1.20	2.27	4.47	5.50
20	OX	0.57	0.33	1.10	2.01	4.39	5.54
32	OX	0.45	0.36	1.30	1.92	4.59	5.18
44	OX	0.51	0.40	1.14	1.92	4.82	5.68
56	OX	0.51	0.53	0.96	1.96	4.49	5.64
68	OX	0.53	0.44	1.10	1.92	4.59	5.63
80	OX	0.56	0.14	0.99	1.88	4.82	5.61
92	OX	0.54	0.31	1.17	1.95	4.99	5.95
1	Y+	2.82	1.97	3.73	4.44	6.61	6.40
13	Y+	2.99	1.92	4.15	4.07	6.73	6.54
25	Y+	2.94	1.83	3.99	4.09	6.49	6.13
37	Y+	3.05	1.99	4.24	4.07	6.90	6.92
49	Y+	2.66	2.11	3.99	4.23	6.49	6.33
61	Y+	3.07	1.97	4.00	4.14	6.78	6.58
73	Y+	3.01	1.95	3.79	4.25	6.52	6.17
85	Y+	3.13	1.91	3.92	4.17	6.47	6.26
2	Y0	2.83	1.94	3.68	4.40	6.61	6.45
14	Y0	2.90	2.68	3.99	4.17	6.61	6.36
26	Y0	2.85	1.81	4.11	5.04	8.70	9.34
38	Y0	2.77	1.94	4.02	3.90	6.90	6.65
50	Y0	2.66	1.84	3.60	4.19	6.80	6.78
62	Y0	2.75	1.83	3.76	4.11	7.02	7.21

74	Y0	2.72	1.72	3.28	4.07	6.68	6.29
86	Y0	2.90	1.84	3.83	4.17	6.97	6.34
3	Y-	2.66	1.89	3.73	4.17	6.52	6.27
15	Y-	2.66	2.49	3.94	4.17	6.80	6.63
27	Y-	2.69	1.69	3.78	4.09	6.47	6.42
39	Y-	2.66	1.80	4.10	4.06	6.64	6.33
51	Y-	2.61	1.75	3.60	4.14	6.58	6.58
63	Y-	2.72	1.81	3.70	4.25	6.94	7.30
75	Y-	2.69	1.76	3.46	4.12	6.90	6.58
87	Y-	2.55	1.56	3.67	4.07	6.89	6.61
4	YX	0.90	1.04	3.11	3.83	6.52	7.55
16	YX	2.39	1.38	3.06	3.64	6.42	7.78
28	YX	2.34	1.43	3.31	3.46	6.28	7.06
40	YX	2.44	1.50	3.17	3.51	6.73	7.92
52	YX	2.23	1.48	2.96	3.64	6.61	7.60
64	YX	2.31	1.50	2.95	3.65	6.13	7.64
76	YX	2.49	1.57	3.04	3.77	6.87	7.74
88	YX	2.17	1.26	3.03	3.49	6.49	7.44

**Table A1.2.4  $\delta^{13}\text{C}$  values corresponding to total  $\text{CO}_2$  emissions in Table A1.2.3**

Jar ID	Trtmt	$\delta^{13}\text{C}$ (‰) with blank subtracted ( <i>i.e.</i> , only from sample)					
		Day 1	Day 2	Day 5	Day 10	Day 25	Day 47
5	O+	31.34	26.47	8.91	-4.09	-9.21	-12.25
17	O+	27.38	26.32	8.63	-4.03	-9.69	-13.99
29	O+	27.27	28.92	7.97	-3.94	-9.00	-12.63
41	O+	24.65	25.05	6.28	-4.42	-18.58	-11.93
53	O+	29.61	24.26	8.63	-4.05	-10.83	-12.35
65	O+	28.06	22.30	-17.41	-4.06	-9.61	-13.88
77	O+	27.69	21.78	6.65	-4.15	-8.74	-12.42
89	O+	29.52	25.91	8.85	-3.71	-9.00	-12.21
6	O0	21.55	19.55	5.64	-5.58	-10.68	-12.98
18	O0	18.00	17.51	3.91	-6.30	-9.99	-13.89
30	O0	20.01	21.67	2.05	-9.81	-12.53	-16.96
42	O0	13.67	18.24	2.68	-6.29	-10.92	-13.06
54	O0	15.77	16.38	3.92	-5.60	-9.32	-13.15
66	O0	17.76	18.01	4.21	-4.91	-8.95	-14.81
78	O0	15.52	19.11	6.18	-4.81	-9.07	-13.62
90	O0	13.20	18.00	3.94	-5.32	-10.98	-12.49
7	O-	9.89	10.52	2.03	-7.01	-11.42	-16.31
19	O-	12.63	19.78	3.29	-6.30	-10.62	-12.88
31	O-	13.07	19.22	4.06	-5.08	-11.14	-13.78
43	O-	10.77	13.86	0.57	-7.00	-10.54	-13.47
55	O-	11.08	13.14	2.33	-6.81	-12.28	-13.89
67	O-	11.57	16.13	3.12	-6.11	-10.17	-14.99
79	O-	12.07	11.75	2.13	-7.35	-9.86	-15.10
91	O-	16.00	17.25	3.84	-5.31	-11.87	-12.33
8	OX	-24.92	-24.86	-23.41	-22.04	-20.07	-21.89
20	OX	-24.43	-21.01	-24.70	-22.89	-20.44	-21.81
32	OX	-25.27	-25.12	-25.05	-24.27	-19.74	-22.08
44	OX	-24.65	-24.12	-25.00	-24.07	-20.52	-22.65
56	OX	-25.16	-23.96	-24.56	-23.18	-22.62	-22.65
68	OX	-24.71	-24.67	-23.58	-23.34	-23.14	-22.62
80	OX	-25.22	-32.79	-25.93	-24.38	-21.99	-21.89
92	OX	-25.03	-27.06	-24.63	-24.59	-22.06	-20.58
1	Y+	-6.35	-4.76	-5.30	-10.65	-13.95	-17.28
13	Y+	-7.08	-2.70	-4.67	-12.28	-13.89	-15.53
25	Y+	-3.96	-4.80	-5.56	-10.68	-13.06	*
37	Y+	-4.51	-3.02	-5.86	-11.88	-14.15	-14.68
49	Y+	-4.83	-3.71	-3.97	*	-14.55	-17.08
61	Y+	-5.11	-4.75	-5.45	-9.97	-15.43	-14.60
73	Y+	-5.38	-3.99	-5.11	-10.65	-14.01	-16.32
85	Y+	-6.61	-4.93	-5.92	-10.25	-15.06	-15.96
2	Y0	-11.48	-7.48	-7.80	-10.94	-13.56	-14.42
14	Y0	-10.52	-8.23	-7.23	-11.09	-16.26	-16.32
26	Y0	-12.23	-8.96	-8.65	-13.02	-15.80	-17.18
38	Y0	-10.81	-7.94	-8.55	-12.61	-14.76	-19.70
50	Y0	-11.13	-8.21	-8.77	-11.39	-13.82	-16.52
62	Y0	-15.96	-10.54	-9.67	-11.79	-14.80	-16.97

74	Y0	-11.67	-9.42	-8.92	-12.18	-14.73	-17.50
86	Y0	-11.10	-9.79	-9.58	-11.65	-14.87	-16.85
3	Y-	-15.37	-7.58	-7.07	-12.47	-12.77	-16.72
15	Y-	-11.73	-8.28	-6.48	-12.73	-16.09	-15.21
27	Y-	-14.78	-7.92	-9.81	-12.93	-14.50	-18.13
39	Y-	-15.21	-6.91	-7.48	-11.99	-13.59	-15.18
51	Y-	-15.57	-8.05	-8.13	-11.18	-13.81	-16.46
63	Y-	-16.91	-8.49	-8.71	-12.31	-14.90	-17.52
75	Y-	-15.84	-9.42	-8.99	-12.94	-15.00	-19.15
87	Y-	-15.99	-7.95	-8.23	-11.30	-13.38	-15.90
4	YX	-9.33	-26.53	-21.84	-21.49	-18.40	-17.50
16	YX	-23.68	-20.67	-21.35	-21.21	-19.86	-23.68
28	YX	-23.76	-22.57	-22.85	-21.78	-19.72	-24.20
40	YX	-23.12	-21.66	-23.14	-22.49	-19.51	-21.37
52	YX	-23.79	-19.93	-23.31	-21.53	-22.98	-23.05
64	YX	-23.56	-20.19	-20.31	-22.08	-19.31	-25.84
76	YX	-23.77	-21.18	-23.12	-22.18	-20.42	-25.45
88	YX	-23.93	-20.62	-22.22	-20.71	-19.31	-23.13

APPENDIX 1.3

PRIMARY DATA FOR CHAPTER FOUR

Throughout this section treatment IDs are as follows:

A - no additions

B - PyOM additions

C - sorghum-sudangrass plants

D - PyOM additions + sorghum-sudangrass plants

E - PyOM additions + sorghum-sudangrass plants (extra-<sup>13</sup>C-enriched)

F - fresh corn stover additions

\* indicates excluded or missing data, as described in the body of this dissertation

Plot ID	1	6	11	16	21	26	31	36
Block	1	2	3	4	5	6	7	8
Trtmt	A	A	A	A	A	A	A	A
BC	0	0	0	0	0	0	0	0
Day								
D0	3.69	4.83	2.83	3.09	2.48	4.04	8.53	3.38
D1	4.77	3.17	3.38	2.83	4.57	4.74	4.43	4.34
D2	6.06	3.05	4.18	2.70	5.46	4.77	5.40	3.72
D3	3.44	2.90	2.93	2.16	2.03	3.89	4.91	3.91
D4	3.87	2.90	2.33	2.31	2.23	3.44	4.32	3.38
D5	3.88	3.05	5.77	2.71	5.40	3.63	3.63	3.70
D6	3.58	2.98	4.00	2.13	7.53	4.26	4.68	4.39
D7	3.19	3.69	5.48	2.53	2.46	3.45	3.39	3.10
D9	2.54	3.21	2.15	2.05	6.03	3.11	7.64	3.87
D11	4.67	7.74	10.20	2.24	4.79	3.39	7.93	3.03
D12	4.00	3.62	3.91	3.78	5.06	3.14	8.71	3.99
D14	3.02	2.73	3.34	3.15	7.93	6.45	3.34	2.89
D16	3.20	2.27	3.54	2.01	3.60	2.64	*	2.99
D18	3.83	2.72	3.31	2.64	4.87	2.39	3.95	2.10
D26	6.77	4.08	5.86	3.24	6.87	8.06	4.26	5.32
D30	5.01	3.13	3.50	2.14	2.41	7.12	3.21	8.00
D34	1.26	1.21	1.88	1.60	4.03	4.61	1.65	1.33
D38	1.56	1.27	1.99	1.51	9.57	7.78	1.96	9.83
D41	1.80	1.61	1.22	2.37	3.90	1.77	1.53	2.05
D45	1.23	1.14	1.47	1.91	9.87	1.65	1.70	1.47
D49	1.89	1.49	1.62	2.57	3.20	2.39	2.01	2.15
D53	2.32	2.92	2.69	8.50	1.15	3.89	2.95	2.68
D57	2.06	1.24	1.54	1.16	14.03	2.84	2.94	1.40
D62	2.15	1.39	1.60	4.03	3.64	7.03	1.53	1.78
D66	1.16	0.73	1.35	1.21	1.70	6.74	3.14	1.39
D74	0.60	0.79	0.85	1.67	0.42	1.48	0.75	0.82
D81	0.28	0.37	1.47	1.62	0.40	0.85	0.52	0.72

<b>Table A1.3.2 CO<sub>2</sub> Fluxes for “B” plots - PyOM additions - over time (μmol CO<sub>2</sub> m<sup>-2</sup> s<sup>-1</sup>)</b>								
<b>Plot ID</b>	2	7	12	17	22	27	32	37
<b>Block</b>	1	2	3	4	5	6	7	8
<b>Trtmt</b>	B	B	B	B	B	B	B	B
<b>BC</b>	1	1	1	1	1	1	1	1
<b>Day</b>								
<b>D0</b>	5.92	4.92	3.75	5.18	8.26	4.62	8.06	8.03
<b>D1</b>	4.96	4.29	3.98	2.97	4.87	3.61	4.67	4.25
<b>D2</b>	4.14	5.26	3.22	2.61	5.55	3.48	4.30	4.65
<b>D3</b>	5.26	4.16	3.17	2.40	4.60	3.10	4.15	4.82
<b>D4</b>	4.91	5.27	3.29	2.17	4.76	3.63	3.19	4.17
<b>D5</b>	4.60	4.39	3.19	2.37	4.93	3.60	3.41	3.60
<b>D6</b>	6.08	3.67	2.89	2.44	4.15	3.73	3.43	4.57
<b>D7</b>	4.40	3.71	4.00	3.55	4.30	3.55	4.95	4.51
<b>D9</b>	4.21	3.20	3.00	2.48	3.73	3.30	2.88	3.65
<b>D11</b>	2.13	19.90	1.84	1.28	5.85	3.61	3.25	3.85
<b>D12</b>	4.08	5.11	5.08	7.11	3.73	3.24	5.19	5.41
<b>D14</b>	2.76	3.02	2.49	2.57	2.78	2.53	2.90	3.63
<b>D16</b>	2.84	2.86	1.75	1.69	2.77	2.22	2.13	2.55
<b>D18</b>	2.05	5.37	1.70	1.61	2.22	2.46	3.18	3.04
<b>D26</b>	3.73	7.39	2.25	2.02	2.86	4.07	3.28	4.04
<b>D30</b>	14.27	7.17	2.38	6.78	1.31	5.01	3.28	2.74
<b>D34</b>	2.34	1.36	1.12	1.13	1.33	1.47	1.12	1.47
<b>D38</b>	-3.13	32.51	2.52	1.94	0.99	1.23	1.48	1.42
<b>D41</b>	5.94	1.66	1.29	1.47	1.52	1.54	1.27	1.44
<b>D45</b>	1.87	1.11	1.11	1.21	1.38	1.60	1.07	2.05
<b>D49</b>	2.11	1.63	1.40	1.67	1.75	1.66	1.53	2.17
<b>D53</b>	3.43	3.00	1.94	3.38	0.59	1.83	2.86	2.16
<b>D57</b>	2.18	4.17	1.18	0.81	1.33	1.72	1.10	1.94
<b>D62</b>	6.48	2.73	1.33	0.66	1.07	1.84	1.78	2.11
<b>D66</b>	1.17	1.44	0.93	1.98	2.41	1.54	1.01	3.07
<b>D74</b>	1.08	0.81	0.65	0.58	0.49	0.58	0.65	0.73
<b>D81</b>	0.74	1.07	0.15	1.29	0.58	0.32	0.42	*

<b>Table A1.3.3 CO<sub>2</sub> Fluxes for “C” plots - sorghum-sudangrass - over time (<math>\mu\text{mol CO}_2 \text{ m}^{-2} \text{ s}^{-1}</math>)</b>								
<b>Plot ID</b>	3	8	13	18	23	28	33	38
<b>Block</b>	1	2	3	4	5	6	7	8
<b>Trtmt</b>	C	C	C	C	C	C	C	C
<b>BC</b>	0	0	0	0	0	0	0	0
<b>Day</b>								
<b>D0</b>	2.80	2.27	0.61	2.48	2.61	2.97	2.80	2.80
<b>D1</b>	3.86	2.24	3.11	2.30	3.71	3.59	3.66	3.78
<b>D2</b>	3.14	1.93	2.45	2.60	2.97	3.37	2.93	3.32
<b>D3</b>	3.08	2.39	2.21	2.59	3.47	3.07	4.45	3.64
<b>D4</b>	2.57	2.26	0.84	2.58	3.53	3.51	5.73	3.32
<b>D5</b>	3.40	2.56	1.79	2.91	3.48	3.22	3.85	3.32
<b>D6</b>	3.29	2.06	2.39	1.93	4.37	3.95	5.22	2.99
<b>D7</b>	3.61	1.51	0.89	2.90	4.34	2.95	4.51	5.61
<b>D9</b>	2.64	2.15	2.17	2.00	3.04	3.09	7.79	2.57
<b>D11</b>	2.36	0.89	0.99	2.49	7.11	2.80	5.38	1.15
<b>D12</b>	3.14	2.97	5.17	4.14	2.42	4.56	3.91	5.46
<b>D14</b>	2.49	2.57	7.38	2.40	2.47	1.92	3.00	2.31
<b>D16</b>	2.47	1.89	2.62	2.33	2.69	3.98	2.78	5.74
<b>D18</b>	2.29	2.29	6.17	9.23	2.03	7.49	4.78	5.21
<b>D26</b>	5.66	4.91	3.03	3.68	4.03	1.20	6.14	3.55
<b>D30</b>	2.44	3.21	1.91	3.19	3.90	2.86	*	2.47
<b>D34</b>	1.32	1.26	1.19	1.10	1.29	0.84	2.38	2.28
<b>D38</b>	1.38	2.47	1.29	0.38	0.86	3.40	1.42	3.45
<b>D41</b>	1.98	1.46	1.13	1.23	1.69	1.12	1.66	1.61
<b>D45</b>	1.33	1.14	1.19	1.38	1.49	0.84	3.01	1.72
<b>D49</b>	2.03	2.12	1.48	1.55	1.81	0.82	1.88	2.24
<b>D53</b>	2.23	2.45	2.09	5.29	2.42	2.41	2.28	5.82
<b>D57</b>	1.45	1.19	1.18	1.19	2.01	1.25	1.60	1.54
<b>D62</b>	1.49	1.23	1.71	1.51	1.74	4.43	1.80	2.01
<b>D66</b>	0.86	1.24	1.02	3.08	0.97	7.80	1.12	1.11
<b>D74</b>	0.68	0.75	0.53	0.83	0.68	0.50	0.90	0.92
<b>D81</b>	0.50	0.51	0.34	0.88	0.82	-0.17	0.64	0.42

<b>Table A1.3.4 CO<sub>2</sub> Fluxes for “D” plots - PyOM+sorghum-sudangrass - over time (μmol CO<sub>2</sub> m<sup>-2</sup> s<sup>-1</sup>)</b>								
<b>Plot ID</b>	4	9	14	19	24	29	34	39
<b>Block</b>	1	2	3	4	5	6	7	8
<b>Trtmt</b>	D	D	D	D	D	D	D	D
<b>BC</b>	1	1	1	1	1	1	1	1
<b>Day</b>								
<b>D0</b>	3.71	3.97	5.80	16.50	6.15	6.79	5.10	9.88
<b>D1</b>	3.07	3.29	5.14	7.75	4.46	6.11	4.57	5.45
<b>D2</b>	3.03	2.80	4.12	5.27	3.96	6.93	4.53	5.13
<b>D3</b>	3.55	2.88	4.25	5.00	4.61	5.48	4.73	4.48
<b>D4</b>	3.31	3.15	4.07	5.29	4.18	5.91	3.74	4.16
<b>D5</b>	2.87	4.22	3.58	4.57	5.43	4.92	3.80	3.98
<b>D6</b>	3.29	3.26	3.35	4.73	5.66	5.08	3.80	4.13
<b>D7</b>	4.53	4.87	4.95	4.55	4.96	5.67	5.10	5.54
<b>D9</b>	2.15	2.89	3.62	5.49	3.79	6.05	4.65	4.14
<b>D11</b>	2.30	4.01	1.87	9.93	5.04	8.24	8.89	11.20
<b>D12</b>	3.63	2.91	5.57	5.72	4.04	4.17	3.73	6.27
<b>D14</b>	3.67	3.15	3.31	4.04	2.30	3.76	3.21	4.36
<b>D16</b>	2.27	2.48	2.39	2.84	2.64	2.99	2.49	3.57
<b>D18</b>	1.53	4.22	2.27	7.36	7.20	3.78	2.84	5.41
<b>D26</b>	3.55	3.93	3.29	4.51	3.79	7.57	3.77	4.02
<b>D30</b>	8.05	2.32	1.97	3.18	2.03	7.47	2.56	4.95
<b>D34</b>	1.29	1.55	1.32	1.58	3.94	1.36	1.49	2.05
<b>D38</b>	0.88	2.91	0.57	36.28	-5.82	1.55	1.10	0.74
<b>D41</b>	1.87	1.36	1.27	1.47	2.09	1.79	1.61	2.18
<b>D45</b>	1.26	1.06	1.20	1.95	1.45	3.38	1.64	1.74
<b>D49</b>	1.85	1.31	1.58	2.43	2.48	2.55	1.88	1.83
<b>D53</b>	1.43	1.17	2.12	1.54	3.11	2.74	5.03	1.91
<b>D57</b>	1.20	1.04	1.12	1.58	1.82	6.30	3.11	1.43
<b>D62</b>	1.80	1.37	1.78	2.23	1.92	3.63	1.73	1.86
<b>D66</b>	1.07	2.58	0.99	*	1.24	1.92	1.00	1.17
<b>D74</b>	0.52	0.64	0.69	0.78	0.65	0.84	0.78	0.86
<b>D81</b>	0.38	0.40	1.26	0.65	0.62	0.30	0.94	0.43

<b>Table A1.3.5 CO<sub>2</sub> Fluxes for “E” plots - PyOM+sorghum-sudangrass - over time (μmol CO<sub>2</sub> m<sup>-2</sup> s<sup>-1</sup>)</b>								
<b>Plot ID</b>	5	10	15	20	25	30	35	40
<b>Block</b>	1	2	3	4	5	6	7	8
<b>Trtmt</b>	E	E	E	E	E	E	E	E
<b>BC</b>	1	1	1	1	1	1	1	1
<b>Day</b>								
<b>D0</b>	5.89	6.61	9.48	6.93	9.00	6.60	5.74	8.02
<b>D1</b>	3.67	3.77	6.17	5.65	9.10	3.82	3.95	4.43
<b>D2</b>	3.68	3.00	4.31	3.71	5.42	3.82	4.02	5.45
<b>D3</b>	5.17	3.84	4.30	3.84	4.91	3.92	4.21	4.24
<b>D4</b>	5.19	3.84	4.25	3.80	7.18	4.25	4.19	3.70
<b>D5</b>	5.92	4.04	4.05	3.57	5.05	3.95	4.05	3.73
<b>D6</b>	5.79	4.06	3.35	3.70	5.10	3.94	3.55	4.00
<b>D7</b>	7.33	3.19	3.90	4.80	6.42	4.29	4.44	4.69
<b>D9</b>	3.61	3.17	10.70	5.78	7.41	3.61	3.00	3.18
<b>D11</b>	10.10	6.91	5.98	21.10	5.02	2.31	7.15	4.76
<b>D12</b>	4.86	3.30	8.13	7.21	4.39	4.93	7.05	6.46
<b>D14</b>	4.45	2.41	3.48	3.41	2.86	3.10	2.80	3.85
<b>D16</b>	3.06	2.21	3.05	2.34	3.17	2.57	2.32	3.12
<b>D18</b>	2.13	2.15	3.46	3.71	3.57	4.98	3.58	4.98
<b>D26</b>	4.97	3.67	3.68	2.94	4.87	4.25	3.76	4.90
<b>D30</b>	2.60	2.32	2.81	4.68	4.18	3.90	3.73	2.68
<b>D34</b>	8.80	1.56	1.44	1.35	0.90	1.40	1.57	2.04
<b>D38</b>	0.73	1.83	3.32	1.92	1.73	1.33	4.18	0.43
<b>D41</b>	4.64	1.93	1.79	1.69	2.09	1.76	1.59	1.74
<b>D45</b>	1.73	1.47	1.52	1.36	2.55	2.66	1.56	1.98
<b>D49</b>	2.17	2.20	1.85	1.91	2.28	2.25	2.06	2.41
<b>D53</b>	0.60	3.24	19.03	1.03	3.24	2.82	2.35	2.55
<b>D57</b>	1.71	1.71	2.50	1.28	2.58	1.58	2.31	1.34
<b>D62</b>	6.34	2.23	6.80	1.42	2.51	2.17	1.75	2.20
<b>D66</b>	1.81	1.31	1.23	1.57	1.27	1.27	1.66	4.39
<b>D74</b>	0.62	0.76	0.89	0.97	0.91	0.64	0.74	1.99
<b>D81</b>	0.51	1.24	0.48	0.51	1.67	0.38	0.66	0.39

<b>Table A1.3.6 CO<sub>2</sub> Fluxes for “F” plots - fresh corn stover additions - over time (μmol CO<sub>2</sub> m<sup>-2</sup> s<sup>-1</sup>)</b>								
<b>Plot ID</b>	41	42	43	44	45	46	47	48
<b>Block</b>	1	2	3	4	5	6	7	8
<b>Trtmt</b>	F	F	F	F	F	F	F	F
<b>BC</b>	2	2	2	2	2	2	2	2
<b>Day</b>								
<b>D0</b>	5.01	3.44	5.24	4.53	4.26	3.76	4.45	4.07
<b>D1</b>	8.99	6.94	7.85	5.95	11.50	8.52	8.42	5.87
<b>D2</b>	16.80	12.60	23.60	12.90	14.40	13.50	12.90	19.10
<b>D3</b>	24.30	17.70	20.70	16.40	20.20	18.50	15.10	16.70
<b>D4</b>	19.70	16.30	18.50	18.20	14.10	13.90	15.40	18.80
<b>D5</b>	15.27	11.17	10.23	10.20	11.12	19.47	7.09	8.24
<b>D6</b>	12.70	12.10	9.79	12.90	11.10	11.20	11.20	11.30
<b>D7</b>	41.30	18.80	15.50	32.10	22.60	15.60	13.00	13.50
<b>D9</b>	13.60	8.76	7.13	10.00	11.30	7.16	5.97	7.34
<b>D11</b>	22.20	33.20	36.60	24.00	24.60	20.50	25.30	22.70
<b>D12</b>	18.60	18.30	24.40	21.73	11.63	14.60	18.70	22.13
<b>D14</b>	14.27	13.33	16.53	12.27	15.67	10.51	12.72	16.20
<b>D16</b>	8.05	6.98	6.91	6.19	4.11	6.78	6.62	7.07
<b>D18</b>	17.73	8.85	4.68	5.53	3.88	6.90	9.65	8.13
<b>D26</b>	12.26	9.88	9.69	*	7.80	7.99	7.05	8.93
<b>D30</b>	4.67	3.25	2.35	8.61	1.07	2.43	2.16	4.21
<b>D34</b>	4.20	3.49	2.66	2.59	1.89	*	2.24	2.46
<b>D38</b>	1.44	1.29	1.25	2.49	1.57	*	1.99	9.45
<b>D41</b>	2.65	3.41	2.09	2.98	2.77	3.16	2.33	3.05
<b>D45</b>	2.21	2.06	3.00	2.41	1.45	1.78	1.89	2.52
<b>D49</b>	3.09	2.77	2.97	3.07	2.49	2.91	3.21	2.55
<b>D53</b>	2.14	2.08	3.40	2.04	1.01	1.51	2.45	1.63
<b>D57</b>	2.10	1.54	1.83	1.83	0.99	3.10	2.82	2.12
<b>D62</b>	2.18	1.42	1.50	1.21	0.99	1.75	1.90	1.19
<b>D66</b>	0.83	1.01	1.47	3.41	0.70	1.73	0.82	1.06
<b>D74</b>	0.73	0.62	0.52	1.46	0.66	1.10	1.11	0.41
<b>D81</b>	0.44	0.37	0.43	0.27	0.21	0.40	0.43	0.55

**Table A1.3.7 <sup>13</sup>C signature of fluxes on selected days**

Plot ID	Trtmt	$\delta^{13}\text{C}$ of flux (‰)	
		Aug. 28	Nov. 6
1	A	-28.44	-29.69
6	A	-28.82	-29.79
11	A	-28.86	-29.28
16	A	-28.05	-27.33
21	A	-28.81	-29.97
26	A	-26.86	-28.23
31	A	-28.71	-29.62
36	A	-27.13	-29.48
2	B	-21.46	-27.06
7	B	-20.62	-25.93
12	B	-19.32	-27.22
17	B	-19.76	-26.43
22	B	-21.58	-28.05
27	B	-22.51	-26.95
32	B	-16.04	-26.04
37	B	-23.48	-28.66
3	C	-28.98	-28.77
8	C	-28.51	-27.76
13	C	-28.57	-29.02
18	C	-29.35	-28.81
23	C	-29.36	-29.37
28	C	-29.38	-29.09
33	C	-29.31	-28.69
38	C	-30.21	-29.35
4	D	-22.68	-26.17
9	D	-23.29	-27.51
14	D	-20.35	-26.81
19	D	-23.00	-27.59
24	D	-23.22	-25.91
29	D	-23.10	-26.19
34	D	-23.26	-28.84
39	D	-21.29	-28.15
5	E	-15.07	-24.30
10	E	-17.42	-25.04
15	E	-14.20	-24.41
20	E	-15.74	-26.81
25	E	-15.96	-26.12
30	E	-13.66	-25.40
35	E	-16.80	-25.21
40	E	-17.12	-27.55
41	F	-8.34	-15.40
42	F	-6.59	-15.20
43	F	-4.79	-14.86
44	F	-8.79	-18.04
45	F	-8.00	-16.01
46	F	-8.01	-17.65

47	F	-7.82	-18.89
48	F	-8.40	-16.49

**Table A1.3.8 Final biomass**

Plot ID	Trtmt	Dry (65°C) above-ground biomass (g)	
3	C	1.892	
8	C	1.168	
13	C	3.507	
18	C	0.428	
23	C	3.597	
28	C	2.564	
33	C	1.728	
38	C	4.68	
4	D	3.95	
9	D	0.506	
14	D	3.846	
19	D	6.169	
24	D	7.326	
29	D	4.541	
34	D	5.05	
39	D	2.38	
5	E	4.49	
10	E	6.108	
15	E	7.512	
20	E	6.927	
25	E	8.191	
30	E	5.99	
35	E	6.412	
40	E	7.93	

**Table A1.3.9 Early and late soil C stocks and associated <sup>13</sup>C**

Plot ID	Trtmt	Total %C		δ13C (‰)	
		Aug. 28	Nov. 6	Aug. 28	Nov. 6
1	A	1.52	1.52	-25.47	-25.57
6	A	1.49	1.66	-25.55	-25.03
11	A	1.48	1.35	-25.46	-24.68
16	A	1.41	1.37	-25.15	-25.23
21	A	1.40	1.42	-25.62	-25.39
26	A	1.67	1.41	-25.62	-25.41
31	A	1.45	1.34	-25.17	-25.50
36	A	1.40	1.38	-25.87	-25.71
2	B	2.12	2.04	-0.25	-12.70
7	B	1.95	2.31	-9.50	-0.62
12	B	2.27	2.74	-6.25	5.59
17	B	2.40	2.43	-6.24	-1.05
22	B	2.41	2.74	-8.07	-0.88
27	B	2.58	2.38	-4.65	-11.80
32	B	1.96	3.43	-13.88	6.00

37	B	2.40	1.96	-3.11	-7.48
3	C	1.50	1.48	-24.97	-24.05
8	C	1.47	1.43	-25.28	-25.22
13	C	1.45	1.42	-25.22	-24.98
18	C	1.34	1.33	-25.34	-25.18
23	C	1.46	1.48	-25.58	-25.35
28	C	1.60	1.64	-25.37	-25.21
33	C	1.51	1.56	-25.74	-25.69
38	C	1.46	1.42	-25.62	-25.32
4	D	2.39	2.05	-3.56	-10.84
9	D	2.52	2.02	-4.35	-11.79
14	D	2.31	2.15	-1.15	-2.59
19	D	1.96	2.73	-9.94	0.54
24	D	2.58	2.59	-1.31	-3.19
29	D	2.63	2.32	-1.34	-7.87
34	D	3.30	2.49	2.33	-5.64
39	D	2.74	3.12	-0.44	3.46
5	E	2.24	2.57	7.69	17.26
10	E	2.29	2.14	16.86	14.76
15	E	2.09	2.04	11.75	19.41
20	E	1.91	2.35	6.61	25.11
25	E	1.85	2.49	-3.18	22.76
30	E	2.17	2.27	12.18	19.46
35	E	2.23	2.01	22.43	10.92
40	E	2.07	2.05	14.30	13.32
41	F	2.76	1.73	-12.84	-20.95
42	F	2.91	1.84	-12.72	-20.07
43	F	2.42	1.87	-14.39	-19.11
44	F	2.71	1.62	-11.24	-20.76
45	F	2.25	1.70	-11.22	-19.98
46	F	2.08	1.94	-17.62	-20.42
47	F	2.23	1.65	-6.43	-21.43
48	F	1.93	1.91	-19.63	-16.86